2014

Host and Bacterial Determinants of Staphylococcus aureus Nasal Colonization in Humans

Gowrishankar Muthukrishnan
University of Central Florida

HOST AND BACTERIAL DETERMINANTS OF *STAPHYLOCOCCUS AUREUS* NASAL COLONIZATION IN HUMANS

by

GOWRISHANKAR MUTHUKRISHNAN
M.E. Birla Institute of Technology and Science, Pilani, India, 2007
M.S. University of Central Florida, United States of America, 2010

A dissertation submitted in partial fulfillment of the requirements
for the degree of Doctor of Philosophy
in the Burnett School of Biomedical Sciences
in the College of Medicine
at the University of Central Florida
Orlando, Florida

Summer Term
2014
Major Professor: Alexander M. Cole

ABSTRACT

Staphylococcus aureus (*SA*), an opportunistic pathogen colonizing the anterior nares in approximately 30% of the human population, causes severe hospital-associated and community-acquired infections. *SA* nasal carriage plays a critical role in the pathogenesis of staphylococcal infections and *SA* eradication from the nares has proven to be effective in reducing endogenous infections. To understand *SA* nasal colonization and its relation with consequent disease, assessment of nasal carriage dynamics among a diverse population and determining factors responsible for *SA* nasal carriage have become major imperatives.

Here, we report on an extensive longitudinal monitoring of *SA* nasal carriage in 109 healthy individuals over a period of up to three years to assess nasal carriage dynamics. Phylogenetic analyses of *SA* housekeeping genes and hypervariable virulence genes revealed that not only were *SA* strains colonizing intermittent and persistent nasal carriers genetically similar, but no preferential colonization of specific *SA* strains in these carriers was observed over time. These results indicated that other non-*SA* factors could be involved in determining specific carriage states. Therefore, to elucidate host responses during *SA* nasal carriage, we performed human *SA* nasal recolonization in a subset of *SA* nasal carriers within our cohort. In these studies, *SA* colonization levels were determined, and nasal secretions were collected and analyzed for host immune factors responsible for *SA* nasal carriage. Interestingly, we observed that stimulation of host immune responses lead to clearance of *SA* while sustained *SA* colonization was observed in hosts that did not mount a response during carriage. Further,

analysis of nasal secretions from hosts revealed that proinflammatory cytokines and chemokines were significantly induced during *SA* nasal clearance suggesting that innate immune effectors influence carriage.

SA utilizes a repertoire of surface and secreted proteins to evade host immune response and successfully colonize the nose. Analysis of the most abundant immunoevasive proteins in the exoproteome of *SA* nasal carrier strains revealed that expression levels of Staphylococcal protein A (SPA) produced by *SA* nasal carrier strains *in vitro* corresponded to the level of persistence of *SA* in the human nose. To determine if SPA is involved in modulating the host's response to *SA* colonization, a subset of participants in our cohort was nasally recolonized with equal concentrations of both wild-type (WT) and *spa*-disrupted (*Δspa*) autologous strains of *SA.* Interestingly, *Δspa* strains were eliminated from the nares significantly faster than WT when the host mounted an immune response, suggesting that the immunoevasive role of SPA is a determinant of carriage persistence. Collectively, this report augments our understanding of *SA* nasal carriage dynamics, in addition to identifying important host and microbial determinants that influence *SA* nasal colonization in humans. Better understanding of this phenomenon can lead to improved preventative strategies to thwart carriage-associated *SA* infections.

Dedicated to my parents

ACKNOWLEDGMENTS

I wish to express my sincere gratitude to numerous people who supported me throughout my graduate school. First and foremost, I would like to thank my dissertation mentor Dr. Alexander Cole for his excellent guidance and constant encouragement. His patience, mentoring and constant support has enabled me to mature as a scientist and changed the way I think about scientific problems and approach research. I will always remember and cherish the long scientific discussions with him and I value the life lessons that he has taught me.

I would like to thank my dissertation committee members Dr. William Self, Dr. Sean Moore and Dr. Christopher Parkinson for their tremendous help throughout the dissertation. I am indebted to them for their invaluable suggestions and advice at committee meetings and otherwise. I would also like to extend a special thank you to Dr. Amy Cole. In addition to giving me hands-on training at the bench, she also provided valuable guidance to improve my experimental design and trouble-shooting skills.

My fulfilling graduate school experience is filled wonderful memories that I will always cherish for the rest of my life. Thanks to the following people that made it possible:

- My labmates past and present. Specifically Matthew Wood, Ryan Lamers, Colleen Eade, Nicole Cowan, Christine Chong, Nitya Venkataraman, Karthikeyan Sivaraman, Todd Penberthy, and Vanathy Paramanandam. I can never forget all the scientific and non-

scientific bantering that we did in WackaTues, Natura, and other hangout places near UCF.

- My non-Biomed UCF friends Apurva Jain, Devendra Salvi, Simranjeet Singh, Meghal Parikh, Karthika Nair and Jyoti Katoch.
- Gerry Quinn (Dr. G) for his guidance and constant support that he extended during the initial years of my graduate school. I will fondly remember all the 2D PAGE and adhesion assays that we did together.
- Thank you to all the undergraduate students that worked on my project – Austin Ellis, Allen Seba, Alana Persaud and John Deichen.

Lastly, my heartfelt thanks to my family - Amma, Appa, Bala, Swetha, Naveen, Venkat, Shivani, Swati and Shruti. I would also like to extend a special thank you to the love of my life, my wife Anusha Naganathan. Without the constant support of my family especially during difficult times, this long and arduous graduate school journey would not have been possible.

My acknowledgments would not be complete without this quote by Peter Griffin from Family Guy "*I want to thank God and I want to thank the devil too because you know that is why God is there. He is minding the fence to make sure that guy never comes back. You know if it weren't for the devil God would have probably gone insane, blowing he's brains out from boredom.*"

TABLE OF CONTENTS

LIST OF FIGURES

LIST OF TABLES

LIST OF ABBREVIATIONS

2D-PAGE	Two-dimensional polyacrylamide gel electrophoresis
BHI	Brain heart infusion media
CA-MRSA	Community–acquired MRSA
CFU	Colony forming unit
ClfB	Clumping factor B
iTRAQ	Isobaric tags for relative and absolute quantitation
MLST	Multilocus sequence typing
MRSA	Methicillin-resistant *Staphylococcus aureus*
SA	*Staphylococcus aureus*
SPA	Staphylococcal protein A
ST	Sequence Type
TSB	Tryptic Soy Broth
VRSA	Vancomycin-resistant *Staphylococcus aureus*
WT	Wild-type *SA*

CHAPTER 1: INTRODUCTION

Staphylococcus aureus nasal carriage

Staphylococcus aureus (*SA*), first isolated by Alexander Ogstein in the1880s, is a gram-positive cocci that can colonize a number of mammalian hosts including humans [1-3]. *SA* has emerged to be an important human pathogen that causes a plethora of community-acquired and nosocomial infections, leading to high levels of mortality and morbidity. Staphylococcal infections range from mild skin and soft tissue infections (SSTIs) like boils, furuncles, impetigo etc., to more severe infections such as endocarditis, toxic shock syndrome, osteomyelitis, septic arthritis and pneumonia [2]. Increasing worldwide emergence of multidrug-resistant *SA* such as methicillin-resistant *SA* (MRSA) has made *SA* the world's leading cause of nosocomial infections [4]. In the United States, there are 80,500 invasive MRSA infections each year, leading to approximately 11,500 deaths; approximately 78% of these infections are healthcare-associated while 22% are community-associated [5]. According to recent estimates, the fatality rate due to MRSA infections annually in the United States is more than that attributed to HIV/AIDS [4].

Although *SA* colonizes multiple body sites in humans, the most frequent carriage site is the anterior nares [6]. Specifically, the moist squamous epithelium on the septum adjacent to nasal ostium is the main colonization site for *SA* in nasal carriers [7]. In most *SA* nasal carriage studies single nasal cultures were performed to determine if a healthy individual is *SA* carrier or not. However, by utilizing longitudinal sampling over time, *SA* nasal carriers can be further classified as persistent, intermittent or non-carriers [2,8,9]. Persistent carriers are individuals carrying *SA* in their nares at all times, intermittent carriers are colonized *SA* transiently and non-

carriers do not carry *SA* in their noses. Approximately 20% of healthy individuals are persistently colonized with *SA* in their nares, while the reminder are colonized either intermittently or never [2,3]. Recently, van Belkum and colleagues proposed a reclassification of *SA* nasal carriage types as persistent and non-persistent carriers [10]. Using experimental human *SA* nasal inoculations, they showed that nasal elimination kinetics of intermittent and non-carriers were similar and significantly higher than that of persistent carriers. Moreover, anti-staphylococcal antibody titers within intermittent and non-carriers were significantly lower than persistent carriers suggesting that persistent carriage type is distinctly different from other types of carriage [10].

The distinction between persistent and non-persistent carriage patterns is critical as *SA* nasal carriage is a major risk factor for staphylococcal infections and bacterial load of persistent carriers is much higher than non-persistent carriers [11]. Clinical studies have indicated a greater risk of bacteremia in *SA* nasal carriers compared to non-carriers. Greater than 80% of hospital-associated bacteremia is caused by invasion of endogenous colonizing *SA* strains [12,13]. Community- associated *SA* infections, especially skin and soft tissue infections (SSTIs), in carriers are also reportedly caused due to endogenously colonized *SA* [14]. Expectedly nasal carriage of antibiotic resistant MRSA strains in the community (CA-MRSA) is associated with higher risks of SSTIs than methicillin-susceptible *SA* (MSSA) nasal carriage [15-17].

Epidemiology and population dynamics of *Staphylococcus aureus* nasal carriage

The prevalence of *SA* nasal carriage in the healthy adult population is approximately 30%. However, certain patient populations are associated with higher rates of *SA* nasal carriage

compared to healthy adults. Greater than 90% of patients with atopic dermatitis are *SA* nasal carriers and patients with granulomatosis with polyangiitis also have higher rates of *SA* nasal carriage [18,19]. Additionally, higher *SA* nasal carriage rates are observed in diabetic, renal replacement therapy patients and HIV-positive individuals, though underlying mechanisms for increased rates are unclear [3,20,21].

To better understand prevalence of *SA* nasal carriage and its relation with host colonization or staphylococcal disease, the genetic diversity and population structure of colonizing *SA* strains needs to be properly defined and detailed. Several genotyping methods with varying levels of discriminatory power and reproducibility have been used to analyze the population structure of *SA* nasal carriage strains [22-24]. Multilocus sequence typing (MLST) is one of most common frequently used genotyping methodology to define the population structure of *SA* nasal carriage strains in great phylogenetic detail [22,25,26]. Using MLST, a majority of the *SA* isolates have been classified into 5 major clusters (clonal complexes (CC)) – CC5, CC8, CC30, CC45 and CC22 [2,27,28]. These CCs contain clinically relevant MRSA strains including the CA-MRSA clone USA300 (CC8), which is responsible for the majority of *SA*-related hospital bacteremia [29,30]. To characterize and segregate the subtypes of CA-MRSA clones in epidemiological studies, genotyping of Staphylococcal Cassette Chromosome mec (SCC*mec*) element has become a vital tool. Presence of SCC*mec* element carrying the *mec*A gene confers resistance to methicillin in *SA* and so far six main *SCCmec* types have been described for MRSA strains [31-34]. Recently, genotyping of hypervariable virulence genes such as Clumping factor B (*clfB*) and staphylococcal protein A (*spa*) have been employed in epidemiological studies to augment *SA* strain resolution [35-38].

Host and microbial determinants that influence *Staphylococcus aureus* nasal carriage

Given the association between *SA* nasal carriage and invasive disease, it is critical to understand host and microbial factors that influence carriage. For *SA* to successfully to colonize the human nares, the bacterium has to establish initial attachment or contact with the nasal niche through certain receptors, overcome host immune defenses and be able to successfully propagate in the nasal milieu [2]. Therefore, *SA* nasal carriage involves a complex interplay of *SA* factors expressed to overcome innate host defenses, establish attachment and a permissible host that is deficient in certain factors to allow for colonization [2,39,40].

Host-related factors that determine Staphylococcus aureus nasal carriage

Host factors are increasingly being implicated as major determinants of *SA* nasal carriage. Genetic studies have identified that polymorphisms in host genes such as human interleukin 4 (IL-4), glucocorticoid receptor, complement cascade protein (C-reactive protein), mannose-binding lectin (MBL), toll-like receptor 2 (TLR2) and vitamin D receptor are all linked to *SA* nasal carriage [41-46]. More importantly, the local immune environment and antimicrobial defense mechanisms at the nasal epithelial site plays a critical role in host's permissibility of *SA* to colonize the nose. Host defense lipids, peptides and proteins produced by nasal epithelia and immune cells recruited to the colonization site contribute to host antimicrobial defense [47]. Such host defense machineries encompassing antimicrobial peptides (AMPs) usually exhibit broad-spectrum antimicrobial activity and directly modulate innate immune responses and cause direct killing of the pathogen [48].

Antimicrobial peptides (AMPs) like secretory leukoprotease inhibitor (SLPI), defensins and cathelicidins, are small proteins used by the innate immune system to combat bacterial and viral infections in multicellular eukaryotes. Several AMPs and proteins including defensins, lysozyme, lactoferrin, hemoglobin have been identified in human nasal secretions and secretions from *SA* nasal carriers, but not noncarriers, support *SA* growth *in vitro* [7,49,50]. Interestingly, expression levels of Human β-defensins (HBD) HBD-2 and HBD-3 are up regulated during an inflammatory host response to *S. aureus* colonization. Compared to HBD-1 and HBD-2, HBD-3 is more effective against *S. aureus in vitro* [51-54]. Unsurprisingly, individuals with deficient induction of HBD-3 in keratinocytes have higher instances of persistent *SA* nasal carriage [55]. Polymorphisms in defensin gene promoter region DEFB1, that lead to impaired HBD expression were also associated with persistent *SA* colonization [56]. Down-regulation of HBD-3 expression and delaying pathogen recognition receptor (PRR), TLR2 expression and inhibiting the production of Interleukin-1 (IL-1) on nasal epithelia *in vitro* are likely an important evasion strategy of *S. aureus* against host innate immunity leading to better nasal colonization by carrier strains [57,58]. Moreover, TLR2 in combination with TLR1/TLR6, CD36 and CD14 as well as NOD-like receptors (NOD2) are also known to be involved in recognizing *SA* by innate immune cells [59-61]. Recognition of *SA* peptidoglycans by NOD2 causes increased expression of HBD-2, activation of inflammasomes causing IL-6 production and increased neutrophil-mediated *SA* phagocytosis and killing [62-64]. Expectedly NOD2-deficient mice are more prone to *SA* infections and NOD2 mutations in humans are associated with increased neutrophil dysfunction and reduced ability to clear *SA* infections [64,65]. Further, ficollins or MBL can also bind to *SA* thus activating complement system for opsonization and phagocytosis of *SA* [66].

Despite the importance of ficollins and NOD2-mediated inflammatory signaling cascade in combatting *SA* infections, their relevance with *SA* nasal colonization remains to be investigated.

In addition to innate immunity, adaptive immune responses may also influence *SA* nasal carriage. Several studies have revealed that IgG and IgA antibody levels against *SA* antigens were significantly higher in carriers compared to non-carriers, thus potentially offering greater protection for carriers against *SA*-related fatalities [12,67-69]. Whether *SA* nasal carriage is responsible for elevated anti-*SA* antibody levels was only recently addressed. Burian and colleagues reported that eventhough *SA* expresses certain non-enterotoxin superantigens during nasal colonization, these *SA* antigens were insufficient to induce a strong antibody response [70]. Moreover, experimental nasal inoculation of a laboratory *SA* strain did not significantly alter the antibody repertoire in healthy volunteers and high degree of inter-individual variation in antibody responses were observed [71,72]. These studies indicate that heightened anti-*SA* antibody levels in *SA* carriers may not be due to nasal colonization. Therefore, innate and cellular adaptive immune responses could be playing a more important role in determining *SA* nasal carriage.

Bacterial determinants of Staphylococcus aureus nasal carriage

In order to persistently colonize the nose, *SA* must successfully attach and overcome local immune defenses within the nose and numerous bacterial factors aid *SA* with these processes. Invading *SA* successfully adheres to nasal epithelial cells primarily through wall teichoic acid (WTA) and sortase-anchored family of proteins known as microbial surface components recognizing adhesive matrix molecules (MSCRAMMs) [73-75]. MSCRAMM-host protein

interaction studies *in vitro* and *in vivo* have detailed that clumping factor B (ClfB) adheres to cytokeratin K10, K8 and contributes to nasal carriage of *SA* [76-79]. Fibrinogen binding proteins (FnBPA and FnBPB) that interact with host molecules such as fibrinogen and fibronectin also play a crucial role in *SA* adhesion to host cells [80,81]. Other MSCRAMMs that have been shown to interact with human desquamated epithelia such as iron-regulated surface determinant proteins IsdA and IsdH, are also expressed during human nasal colonization of *SA* [11,82]. *SA* proteins such as serine-aspartic acid repeat proteins SdrC, SdrH and surface protein G (SasG) are also associated with adhesion of *SA* to host epithelial proteins; however, the exact mechanism of their interaction during nasal colonization remains to be determined [83].

In addition to adhesion, *SA* utilizes numerous proteins to successfully defend against host immune responses by inhibiting neutrophil chemotaxis, killing leukocytes using toxins, developing resistance to phagocytosis, resistance to killing by AMPs and survival in neutrophil phagosomes [84]. To inhibit neutrophil chemotaxis, *SA* secretes chemotaxis inhibitory protein of staphylococci (CHIPS) that binds to formyl peptide receptor (FPR) and C5a receptor and inhibit the signaling cascade that causes neutrophil migration to the site of inflammation[85-89]. In addition to impeding neutrophil chemostaxis, *SA* utilizes several surface proteins to interfere with complement formation and opsonization thereby preventing neutrophil phagocytosis [84]. These surface proteins include capsular polysaccharide, the extracellular staphylokinase (Sak), SPA, fibrinogen-binding protein Efb, and clumping factor A [84,90-93]. SPA, a surface protein involved in preventing *SA* opsonophagocytosis, is critical for the pathogenesis of staphylococcal infections and will be discussed in greater detail here.

Staphylococcal protein A (SPA)

SPA, a 40-60 KDa protein is crucial for evasion of human immune responses and pathogenesis of staphylococcal infections. It encompasses five immunoglobulin G-binding domains (A-E) and a polymorphic cell wall binding region (X), which is comprised of short 24 base pair sequence repeats (X_r) and cell wall attachment sequence (X_c) consisting of a LPXTG motif (Figure 1). This motif is important for the covalent anchoring of SPA to the staphylococcal cell wall [94]. SPA's IgG domains, which are approximately 58 amino acids in length each bind tightly with the Fc regions of IgG in a conformation not recognizable by neutrophils, therefore preventing opsonization and phagocytosis [95,96]. Independent of Fc binding, each IgG binding domain can also bind to Fab regions of B-cell receptors, which causes B-cell apoptosis and prevents the production of antistaphylococcal antibodies [97,98].

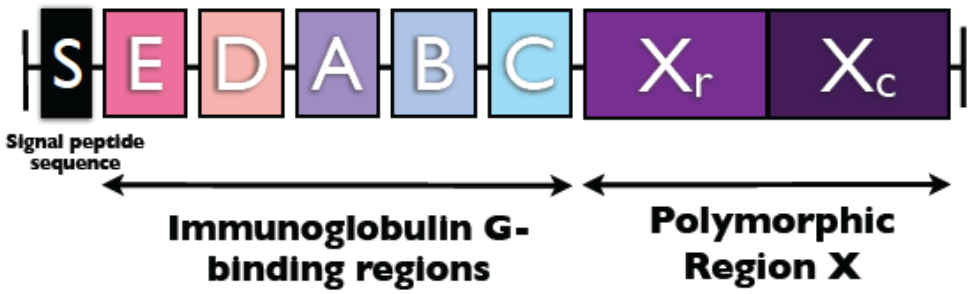

Figure 1: Functional domains of Staphylococcal protein A

The protein consists of signal peptide sequence (S), five immunoglobulin G-binding domains (A-E) and polymorphic cell wall binding region (X), which is comprised of short sequence repeats (X_r) and cell wall attachment sequence (X_c).

In addition to anti-complement functions, other binding properties of SPA contribute to its virulence. It's IgG binding domains recognize tumor necrosis factor α (TNFα) receptor 1 (TNFR1) and activate subsequent proinflammatory signaling cascade resulting in the

pathogenesis of pneumonia [99,100]. IgG domains also bind to EGFR and activate EGFR signaling and ADAM17 all leading to activation of proinflammatory signaling cascade [101]. SPA expression levels are regulated by panton-valentine leukocidin, which is closely associated with CA-MRSA pneumonia outbreaks in the hospitals [102]. Furthermore, SPA has also shown to promote *SA* biofilm formation and development of biofilm-associated infections in a murine catheter infection model [103]. Interestingly, SPA was detected at the RNA level during *SA* nasal colonization indicating a potential association with nasal carriage [11]. Therefore, we hypothesize that SPA, which is involved in immune evasion, is a co-determinant of *SA* nasal colonization.

Staphylococcus aureus nasal colonization models to study determinants of carriage

Nasal colonization models are essential to determine whether a bacterial or host factor contributes to *SA* nasal carriage and such studies have been predominantly performed utilizing murine models of colonization. The cotton rat model of nasal colonization has been the most popular model used for *SA* nasal carriage studies [104]. Studies performed using such models have helped define bacterial determinants of carriage, including wall teichoic acid (WTA), sortase, iron-regulated surface proteins IsdA and IsdH [74,82,105-107]. Recently, a murine-model based colonization study observed *SA* nasal clearance to be dependent on host neutrophil influx and T-cell mediated [108]. Though rodent models are helpful in defining molecular mechanisms leading to nasal carriage, these animals neither adequately mimic human colonization by *SA* nor do they naturally carry in *SA* in their nares and immune mediators are different. Therefore, it is essential to perform carriage studies utilizing the

physiologically relevant human nares, which would account for the dynamic interaction between host and bacteria. Recent human experimental carriage studies have been useful in determining the role of ClfB as a determinant of nasal carriage [77]. Utilizing such models, van Belkum and colleagues provided crucial insights into *SA* nasal carriage patterns in humans and reported that natural *SA* nasal survival among intermittent carriers was 14 days, while *SA* survival was greater than 154 days among persistent carriers [10]. Until now, few experimental nasal colonization studies have been performed utilizing relevant human nares and more such studies are necessary to better identify and elucidate *SA* nasal carriage determinants.

We sought to better understand *SA* nasal carriage dynamics, its relation with staphylococcal infections, and elucidate critical host and bacterial determinants that are responsible for *SA* nasal carriage in humans. To this aim, we assessed the population structure of *SA* nasal carriage strains in a diverse population of 109 healthy individuals for a period of up to three years and determined whether preferential colonization by certain genotypic *SA* strains occurs within persistent versus intermittent carriers. We observed that colonizing strains of *SA* are not specific to a particular host or carriage type and both carriage types change strains over time suggesting that other non-*SA* factors could be contributing to specific carriage states. Therefore, to elucidate host responses during carriage, we performed autologous human *SA* nasal recolonization in a subset of participants from our cohort of 109 health individuals. Interestingly, we observed nasal clearance of *SA* occurred within 9 days when host immune responses were stimulated, while *SA* persisted in the absence of a response. These results suggested that local inflammatory responses influence *SA* nasal carriage. To confirm the involvement of host immune responses, we hypothesized that disruption of immunoevasive

SPA would alter the host inflammatory responses and affect *SA* carriage. Interestingly, autologous recolonization with WT and an isogenic mutant *SA* lacking SPA (*Δspa*) revealed that *Δspa SA* were eliminated from the nares significantly faster than WT *SA* when the host mounted an immune response. These results provide first direct *in vivo* evidence of a potential role for human immune responses and SPA in nasal carriage. Collectively, our findings add to the growing evidence that host immune responses play a significant role in *SA* nasal colonization in humans.

CHAPTER 2: LONGITUDINAL GENETIC ANALYSES OF *STAPHYLOCOCCUS AUREUS* NASAL CARRIAGE DYNAMICS IN A DIVERSE POPULATION

Introduction

Staphylococcus aureus (SA) is a leading cause of community-acquired and nosocomial bacterial infections in humans. *SA* infections can range from mild skin infections to severe, highly invasive and necrotizing diseases [109]. With the spread of community-acquired methicillin-resistant *SA* (CA-MRSA) and vancomycin-resistant *SA* (VRSA) strains around the world, it has become even more pertinent to conduct *SA* epidemiological studies to monitor its dissemination [4,110].

The most common niche of *SA* in humans is the anterior nares [111-113] and *SA* nasal colonization is thought to be a major source of bacterial transmission with *SA* colonizing approximately 25% of the human population asymptomatically [2,39,114]. *Staphylococcus aureus* nasal colonization has been attributed to an amenable host, and numerous epidemiological studies have been conducted to identify nasal carriers and non-carriers of *SA* [2,3,12]. However, to understand better the dynamics of *SA* nasal carriage over time, longitudinal studies are required. Nasal carriage patterns amongst healthy individuals can be broadly classified as persistent (always colonized by *SA* in their nares), intermittent or non-carriers [2,8,9]. This distinction is important as persistent carriers are at a higher risk of developing active auto-infections than intermittent and non-carriers [2,12,13,115].

To understand better the genetic diversity of *SA* strains that colonize nasal carriers, the population structure of *SA* strains obtained from healthy individuals must be defined and

detailed. Multi locus sequence typing (MLST) is one of the most common means by which population structure of *SA* strains have been analyzed [22,26,27]. More recently, genotyping of hypervariable virulence genes (staphylococcal protein A (*spa*) [37,38] and clumping factor B (*clfB*) [116]) have also been employed to enhance strain resolution and thus offer better characterization of genetic relatedness between *SA* strains. Moreover, with the increasing prevalence of CA-MRSA, it is critical to understand the origin and the dissemination of major MRSA clones within the healthy population [33,117-119]. SCC*mec* typing, the most common means by which to identify MRSA has become a vital tool for the characterization of CA-MRSA clones in epidemiological studies [31,34].

Several studies including ours [49,120] have shown that *SA* nasal colonization is multifactorial, involving not only bacterial determinants but also host factors that predispose individuals to *SA* carriage [39,41,74,77,105,121,122]. However, the exact mechanisms leading to persistent versus intermittent or non-carriage remain unclear. It is also unknown whether persistent and intermittent hosts preferentially carry a specific genotype of *SA* strains. Therefore, understanding the patterns of nasal carriage and the preferential colonization by certain genotypes of *SA* strains in persistent and intermittent carriers will greatly augment our understanding of *SA* nasal carriage.

Recently, we revealed genetic associations between nasal carriage strains and clinical isolates in a cross-sectional survey of healthy individuals [36]. In the current study, we extended these analyses and longitudinally assessed the population structure of *SA* nasal carriage strains in a diverse population for a period of up to three years to gain a better understanding of nasal carriage dynamics, in addition to assessing whether preferential colonization by certain

genotypic *SA* strains occurs within persistent versus intermittent carriers. Interestingly, MLST analyses revealed that both intermittent and persistent carriers harbor genotypically similar strains that cluster into the same clonal complexes. Furthermore, these strains exhibited similarity to *SA* isolates of clinical significance. Genotyping studies using housekeeping (MLST) and hypervariable virulence genes (*spa* and *clfB*) revealed that both persistent and intermittent carriers change strains over time with no difference in the frequency of strain change between the two carrier groups. The current study contrasts previous findings that have stated that persistent carriers carry the same *SA* strain over long periods of time while intermittent carriers carry different strains during *SA* nasal carriage [2,123]. Overall, this study indicates that colonizing strains of *SA* are not specific to a particular host or carriage type (i.e., persistent versus intermittent carriers) and both carriage type change strains over time, suggesting that other non-*SA* factors could be contributing to specific carriage states.

Materials and Methods

Ethics statement for collection of bacterial strains from donors

The current study was approved by the University of Central Florida's Institutional Review Board (UCF IRB). All donors provided informed written consent to participate in the current study. Nasal swab sample collection for the current study was undertaken in the University of Central Florida (UCF) campus. UCF is a diverse community of nearly 60,000 students and approximately 8000 faculty and staff members of various ages, ethnic and racial backgrounds. All procedures and investigators involved in the sample collection process were Institutional

Review Board (IRB)-approved with Collaborative Institutional Training Initiative (CITI) certification.

Study population, design and bacterial strains

A total of 329 healthy individuals at UCF were screened for the presence of *SA* in their anterior nares. Specifically, the donor population (58.35% - Female, 40. 72% - Male and 0.93% - Unreported) consists of participants from various racial and ethnic backgrounds (White - 56.84%, Asian – 13.07%, Black – 17.63%, Pacific Islanders – 1.22%, Hispanic/Latino – 13.07%). Of the 329 individuals screened, 96 (29.2%) tested positive for *SA* nasal colonization at least once while the remaining 233 (70.8%) donors were classified as non-carriers because *SA* was never isolated from their nares. Of the 329 total individuals enrolled in our study, 109 participants – comprised of 61 carriers and 48 non-carriers – were monitored longitudinally (i.e., multiple nasal swab samples were collected from these individuals). Among the 96 *SA* positive carriers, 61 were monitored longitudinally while the remaining 35 carriers were screened for nasal colonization only once. In total, a median of four (range 2-18) nasal samples were obtained from each of 109 healthy individuals (including individuals that tested negative for *SA*) for a varying period of up to three years, with duration and frequency of collections dependent on donor availability. Following screening, donors were classified into persistent (if all nasal cultures tested *SA* positive for the duration of the study), intermittent (if at least one nasal culture tested negative for *SA* over the course of the study), and non-carriers (no cultures tested positive for *SA*) of *SA*.

Following nasal sample collection, *SA* strains were isolated as previously described [36]. Briefly, the anterior nares of the donors were swabbed with sterile, unflocked polyester-tipped swabs (Fisher Scientific, Pittsburgh, Pennsylvania, USA) and nasal samples were grown overnight on nutrient rich Tryptic Soy Agar (TSA) supplemented with 5% sheep's blood (Becton, Dickinson and Company, Franklin Lakes, New Jersey, USA). Bacterial colonies were identified as *SA* using Staphyloslide™ Latex Test reagent (Becton, Dickinson and Company, Franklin Lakes, New Jersey, USA) and sub-cultured in Trypticase Soy Broth (TSB; Becton, Dickinson and Company, Franklin Lakes, New Jersey, USA) overnight at 37°C and 250 rpm. Overnight cultures were subsequently used for isolation of genomic DNA.

Multilocus sequence typing

Genomic DNA from *SA* isolates was extracted using GenElute™ Bacterial Genomic DNA kit (Sigma-Aldrich Co., St. Louis, Missouri, USA), according to the manufacturer's instructions. Following extraction, multi locus sequence typing (MLST) of seven housekeeping genes *(arcC, aroE, glpF, gmk, pta, tpi, and yqiL)* was performed using primers and PCR conditions as previously described [26,36]. Sequence types (STs) for each *SA* strain were obtained based on the alleles identified at each of the seven loci using the *SA* MLST database (http:// www.mlst.net). New alleles and STs were submitted to the MLST database curator and subsequently added to the database.

Phylogenetic analyses of MLST data

Phylogenetic analysis of the concatenated MLST data of all isolates was performed as previously described [36] using the Metropolis-Hastings coupled Markov chain Monte Carlo method (MCMC) implemented in MrBayes v3.1.2 [124-126]. Triplicate MCMC analyses were performed in parallel [126] using the STOKES IBM High Performance Computing Cluster at UCF. Bayesian MCMC analyses were carried out using both partitioned and unpartitioned concatenated MLST data. Best-fit evolutionary models for each individual gene fragment (in the partitioned dataset) as well as unpartitioned dataset were selected based on Akaike Information Criterion implemented in jModelTest v0.1.1 [124,127]. For the concatenated unpartitioned MLST dataset, a generalized time-reversible (GTR) evolutionary model with inverse-gamma distribution was selected as the best-fit model. For loci *glpF*, *pta* and *yqiL* in the partitioned dataset, the Hasegawa, Kishino and Yano (HKY) substitution model was chosen while a HKY model with a gamma distribution was chosen for the *arcC* gene [128]. Additionally, the HKY model including invariable sites (HKY+I) was selected for locus *gmk*. For the *tpi* locus, a GTR substitution was the chosen model while a GTR+I model was identified as the best-fit substitution model for the *aroE* locus. Within each replicate MCMC analysis two independent Bayesian runs were performed with random starting trees and default settings. Each run consisted of 5 million generations with every 100 steps being sampled. For each analysis, a steady stationary state of the run was verified using Tracer v1.5 and a burn-in of 25% of the generations was performed. A final run consisting of 20 million generations was also performed to verify the likelihood scores from the shorter runs were consistent with the longer runs.

eBURST analyses of MLST data

The different Sequence types (STs) that were identified for each *SA* strain were classified into different groups using the eBURST v3 analysis software [28,129]. Each ST was assigned to a cluster group requiring six of the seven loci between members of the group to be identical [129]. eBURST analysis was also used to assess relatedness of nasal carriage strains to nosocomial epidemic strains.

spa typing and eBURP analysis of spa types

SA isolates were *spa* genotyped using primers and PCR conditions described previously [37,38] and sanger sequenced [130] at Eton Bioscience Inc. DNA sequencing facility (Durham, North Carolina, USA). *spa* types were determined using the Ridom StaphType (Ridom GmbH) software (http://www.spaserver.ridom.de/). All *spa* types including those newly identified were synchronized with the global *spa* type database via the StaphType server. To partition the intermittent and persistent carriers, eBURP-clustering analysis using the Ridom StaphType software was performed using default settings. *SA* isolates having less than 5 repeat units were excluded from the clustering analysis, as it is difficult to infer evolutionary history of a *SA* strain from spa type with less than five repeat units [38].

clfB typing and sequence analysis

For all *SA* isolates, the hypervariable region of the *clfB* gene was amplified and sequenced using the protocols and primers described previously [35,36]. Subsequently, sequence analyses of the hypervariable repeat region was performed using the in-house sequence analysis software

described previously [36]. Briefly, the nucleotide sequence of the R region of *clfB* gene was converted into a numeric profile based on the unique repeat units (Appendix A; Table 10). Subsequently, each unique repeat unit was assigned a specific color-coded box and the numeric output profile of clfB R region was converted into a color-coded representation (Appendix A; Figure 21) [36].

SCCmec typing

SA isolates were also screened for the presence of the *SCCmec* gene cassette that confers resistance to the antibiotic methicillin. Phenotypic screens for MRSA strains were performed by streaking single *SA* colonies on selective chromogenic MRSASelect™ agar plates (Bio-Rad, Hercules, CA, USA) and identified following the manufacturer's instructions. Following the phenotypic screening, a multiplex PCR reaction amplifying eight different loci of the *SCCmec* gene cassette was performed on the MRSA strains to determine the type assignment of the *mec* gene. The primers, protocols, and analyses used for multiplex PCR were performed as previously described [31,34].

Statistical Analysis

Student's t-tests for the differences in the length of *clfB* R region and X domain repeat region of *spa* gene were conducted using GraphPad Prism 4 software (GraphPad Software, La Jolla, CA, USA). A 2 x 2 contingency table was constructed and a G-test was performed to analyze the distribution of persistent and intermittent carriers among males and females within the cohort. Similarly, a 2 x 2 contingency table was constructed to evaluate the trend of *SA* strain change

between persistent and intermittent carriers and a G-test was performed to assess the differences in strain change in persistent and intermittent carriers. G-tests were performed using JMP Pro software (SAS Institute Inc., Cary, NC, USA) [131].

Results

Longitudinal assessment of SA nasal colonization in a healthy population identified persistent and intermittent carriers

To assess nasal colonization state over time, extensive longitudinal monitoring was performed in which multiple nasal samples were obtained from 109 healthy individuals for a period of up to three years. Following longitudinal sampling, donors were classified into persistent, intermittent, and non-carriers of *SA* based on their carrier indices (defined as the number of *SA* positive nasal swabs over the total number of swabs for each individual; Figure 2) such that all non-carriers and persistent carriers have carrier indices of exactly 0 and 1 respectively, while intermittent carriers have scores *between* 0 and 1. In total, sixty-one (56%) individuals were *SA* nasal carriers (23.8% persistent and 32.1% intermittent) and 48 (44.0%) were non-carriers. Within the study population, 23.8% of all female donors were persistent carriers while 30.1% were intermittent and 23.9% of all male participants were persistent carriers while 34.7% were intermittent (Likelihood ratio χ^2 = 0. 070, N=61, degrees of freedom (df =1), p= 0.7911, Table 1). Our comprehensive longitudinal monitoring for *SA* nasal colonization revealed true persistent and intermittent carriers and subsequently, genotyping studies were conducted on the isolated *SA* strains to assess genetic relatedness among them.

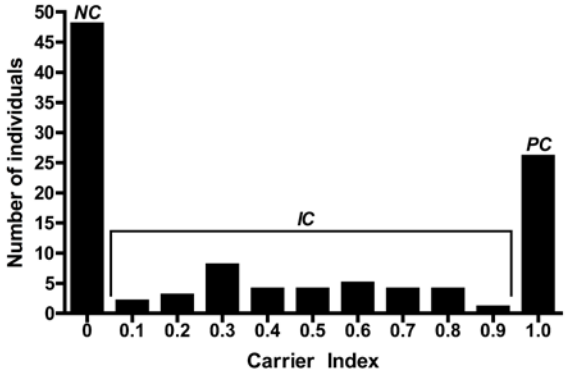

Figure 2: Distribution of *SA* nasal carrier indices among 109 healthy individuals monitored longitudinally.

Carrier index is defined as the number of *SA* positive nasal swabs over number of total swabs for each individual person. A total of 61 *SA* nasal carriers and 48 non-carriers were monitored longitudinally and their respective carrier indices are represented here. (*NC*) indicates *SA* non-carrier state, (*IC*) indicates *SA* intermittent carriage and (*PC*) indicates *SA* persistent carriage.

Table 1: Distribution of persistent and intermittent carriers among males and females.

Sex	Carriers (% carriage distribution across sex)[#]			Total[a]
	Persistent	Intermittent	Non-carriers	
Male	11 (23.9)	16 (34.7)	19 (41.4)	**46**
Female	15 (23.8)	19 (30.1)	29 (46.1)	**63**
Total[b]	**26**	**35**	**48**	**109**

[#] Only nasal swabs from carriers sampled 2 or more times were only included
[a] Total number of nasal carriers distributed across each sex
[b] Total number persistent, intermittent and non-carriers monitored during the study

SA strains isolated from persistent and intermittent carriers belong to the same genetic clusters as nosocomial strains

We have recently revealed genetic associations between nasal carriage strains and clinical isolates [36]; however, this initial study was a static cross-sectional survey that did not account for the nasal carrier class of donors (i.e. persistent vs. intermittent). In the current study, we have extended these analyses to a larger cohort of donors, including persistent and intermittent carrier strains that were monitored longitudinally for a period of up to three years.

To determine the genetic relatedness among *SA* strains, MLST analyses were performed on 297 *SA* nasal carriage strains obtained from 96 individuals. A total of 42 different sequence types (STs) were observed with 10 being newly identified (refer to Appendix A; Table 8 for genotyping details of all *SA* strains used in this study). Three novel alleles were also identified in this study at loci *glpF*, *gmk* and *pta.* Sequence types 5 (21.3% of all carriers), 30 (18% of all carriers) and 8 (16.4% of all carriers) were the most prevalent STs observed within the cohort (Table 2). *Staphylococcus aureus* strains belonging to ST15 were only isolated from persistent carriers. However, only one of these persistent carriers was monitored for more than one year and as such, elaborate longitudinal monitoring of a larger cohort of donors containing ST15 *SA* strains is required to determine if there is any preferential colonization of persistent carriers by ST15 *SA* strains.

Table 2: Predominant STs in persistent and intermittent carriers

Sequence type (ST) of *S. aureus* strains[#]	**Number of donors carrying each ST (% of donors carrying each ST)[a]**		**Total[b]**
	Persistent	**Intermittent**	
ST5	5 (19.2)	8 (22.8)	**13 (21.3)**
ST30	5 (19.2)	6 (17)	**11 (18)**
ST8	4 (15.4)	6 (17)	**10 (16.4)**
ST45	1 (3.8)	2 (5.7)	**3 (4.9)**
ST15	4 (15.4)	0	**4 (6.5)**
ST59	1 (3.8)	2 (5.7)	**3 (4.9)**
ST188	1 (3.8)	3 (8.5)	**4 (6.5)**

[#] Only nasal swabs from carriers sampled 2 or more times were included and only the most prominent STs prevalent in North America are presented here

[a] Percentage calculated using the total number of persistent and intermittent carriers in the cohort

[b] Total number persistent and intermittent carriers that carried one or more strains in their noses

Bayesian MCMC analysis of the concatenated MLST data revealed that *SA* strains isolated from persistent and intermittent carriers are closely related. Persistent and

intermittent carriers as well as strains isolated from clinical studies all group within the same clades (Figure 3A). Since the cohort included healthy individuals that were singly sampled (cross-sectional), phylogenetic analyses incorporating *SA* MLST data from these individuals were also performed (Appendix A; Figure 19) and the analyses reveal that all *SA* carrier strains within the cohort are highly similar to strains of clinical origin.

In addition to identifying phylogenetic relationships, eBURST clustering of the MLST data confirmed that persistent and intermittent carrier strains belong to the same clonal complexes as that of epidemic strains. As observed in Figure 3B, eBURST delineated nasal carriage and clinical strains into 10 groups and 11 singletons. Of these, five groups contained both clinical and nasal carriage strains and groups identified by eBURST also contained STs from both persistent and intermittent carrier strains (data not shown). Collectively, the phylogenetic analyses revealed genetic relatedness between persistent and intermittent carrier strains, in addition to genetic similarities with strains isolated from clinical settings.

SA strains from the nares of both persistent and intermittent carriers change over time

To date, few studies longitudinally assessed whether nasal carriage strains of *SA* in the nares of persistent and intermittent carriers change over time. Longitudinal monitoring of 61 carriers (both persistent and intermittent) revealed variations in the STs of *SA* nasal carriage strains over time. A representative set of persistent and intermittent carriers that were monitored between one and three years is depicted in Figure 4, revealing the patterns of strain change. In addition, 48 healthy individuals were monitored over time and identified as true non-carriers (Appendix A; Figure 20).

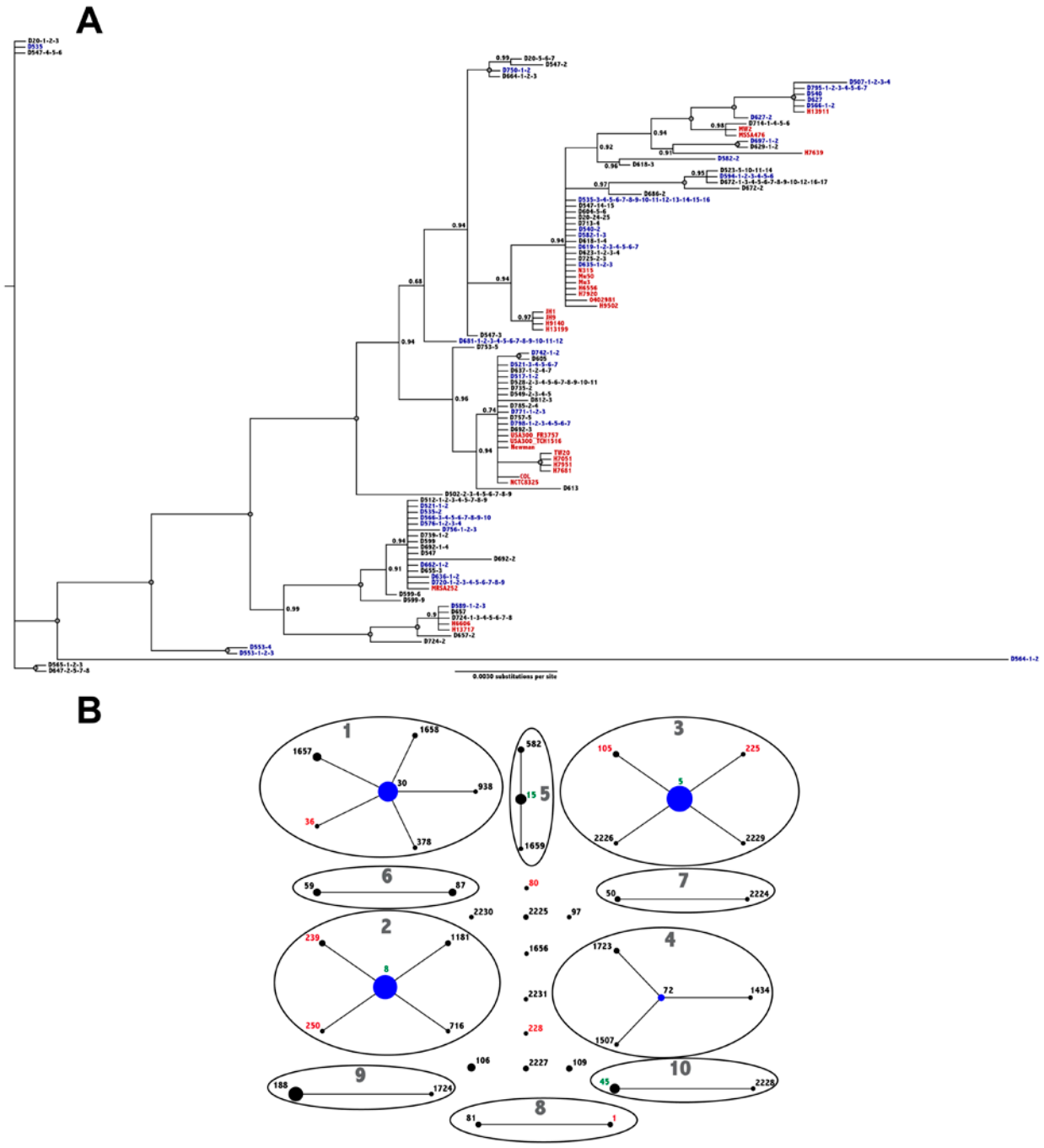

Figure 3: *SA* strains from persistent and intermittent nasal carriers are genetically related to nosocomial epidemic strains.

(A) Bayesian MCMC analysis of persistent carrier strains (colored in **blue**), intermittent carrier strains (colored in **black**) and nosocomial epidemic strains (colored in **red**). Numbers at each

node indicate posterior probability support and grey-filled circles represent 100% posterior probability. (B) eBURST analysis of the MLST data clusters STs from intermittent and persistent carriers into same clonal complexes and into groups that are represented by numbers in **grey**. STs colored in **black** are nasal carrier strains, STs colored in **red** are epidemic strains and those in **green** contain both carrier and epidemic strains. Circle sizes in each cluster are proportional to the number of isolates and **blue** circles are founders of that particular cluster.

Notably, it was observed that individuals who share households (such as spouses, siblings, roommates, etc.) tended to carry genetically similar strains (Appendix A; Table 9). For example, family members and individuals living in the same households (D528-D549, D523-D594, D618-D619 and D20-D547-D604 (Figure 4)) carried genetically similar strains at one or more sampling times. Interestingly, we observed that intermittent carriers D523 and D618 harbored genetically similar strains as that of their living partners D594 and D619, respectively. Additionally, it was observed that persistent carriers D619 and D635, who are identical twins, carried genetically similar strains during the entire study period. Though additional correlative studies are required, interesting trends of *SA* transmission over time among individuals living in the same household were observed within the cohort.

Previous reports have indicated that a single strain of *SA* colonizes the nose for long periods of time in persistent carriers while strains colonizing intermittent carriers tend to exhibit more extensive genotypic diversity [2,123]. In contrast, within our cohort, we observed that over time, 27% of persistent carriers and 23% of intermittent carriers changed the ST of their *SA* strain (Likelihood ratio $\chi^2 = 0.132$, N=61, df =1, $p= 0.7160$, Table 3). Additionally, phylogenetic analyses of the MLST data revealed that *SA* strains from these carriers clustered into the same genetic clades exhibiting a high degree of relatedness. Taken together, these

results indicate similar genotypic diversities of colonizing strains in persistent and intermittent carriers.

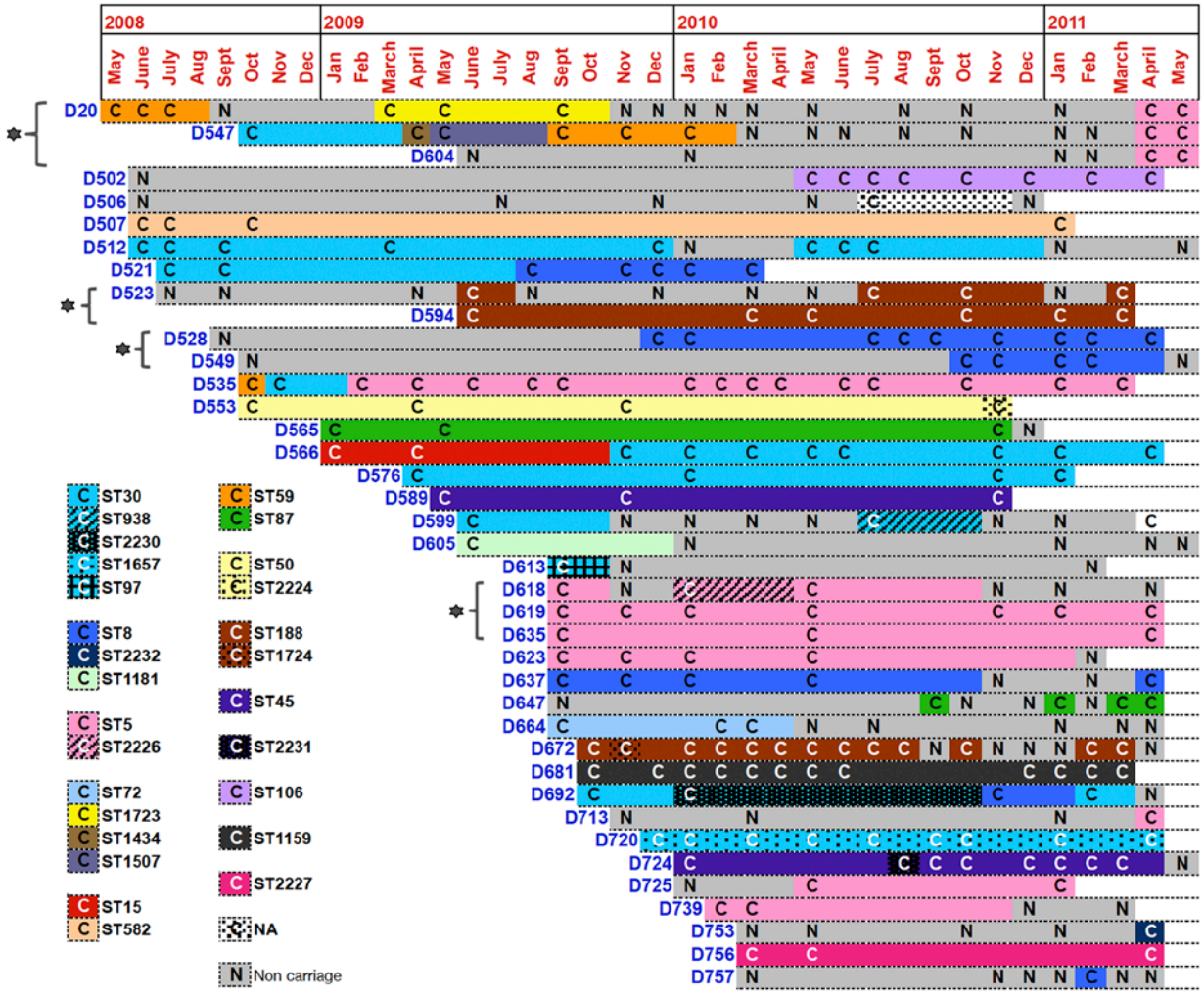

Figure 4: Longitudinal monitoring reveals that *SA* strains from both persistent and intermittent nasal carriers change over time.

A representative set of persistent and intermittent carriers that have been monitored for at least one year is depicted here. (C) indicates *SA* nasal carriage at the time of swabbing and (N) indicates *SA* non-carrier state. Colors represented in the figure correspond to different Sequence Types (STs) identified by MLST. STs are segregated into different cluster groups by eBURST analysis. Carriers within the same household are grouped next to each other (indicated by * and flower bracket). (NA) corresponds to ST not available.

Table 3: Persistent and intermittent carriers carrying more than one unique *SA* lineage in their noses during the study period

Number of different *S. aureus* strains[#]	Carriers (% of total in the carrier group)		Total[a]
	Persistent	Intermittent	
1	19 (73)	27 (77)	**46 (75.4)**
2	6 (23)	4 (11.5)	**10 (16.4)**
3	1 (4)	3 (8.5)	**4 (6.6)**
4	0	0	**0**
5	0	1 (3)	**1 (1.6)**
Total[b]	**26**	**35**	**61**

[#] Nasal swabs from carriers monitored 2 or more times were only included

[a] Percentage calculated using the total number of persistent and intermittent carriers in the cohort

[b] Total number persistent and intermittent carriers that carried one or more strains in their noses

Genotyping of hypervariable virulence genes revealed no preferential colonization of either persistent or intermittent carriers by specific SA strain genotypes

As MLST is based on housekeeping genes that evolve slowly [22], we also genotyped hypervariable virulence genes (spa and clfB) in order to obtain higher levels of strain resolution and further characterize the relatedness among strains obtained from persistent and intermittent carriers. Genotyping of the virulence gene spa was performed on 242 *SA* strains isolated from persistent and intermittent carriers. A total of 41 unique spa types were obtained, nine of which were newly identified in this study. Interestingly, high sub-ST strain resolution was obtained at the spa locus (discriminatory index of 0.957), and 11 (26.83%) of the 41 spa types identified contained persistent and intermittent carrier strains exhibiting identical X domain repeats. eBURP-clustering analysis performed on the SA strains grouped them into seven clonal complexes (spa-CC) and 13 singletons (refer to Appendix A; Table 8 for spa typing details of all *SA* strains used in this study). Interestingly, eBURP revealed that spa types from

both persistent and intermittent carriers clustered into the same clonal complexes, confirming the high degree of genetic relatedness observed in MLST phylogenetic analyses (Figure 5A).

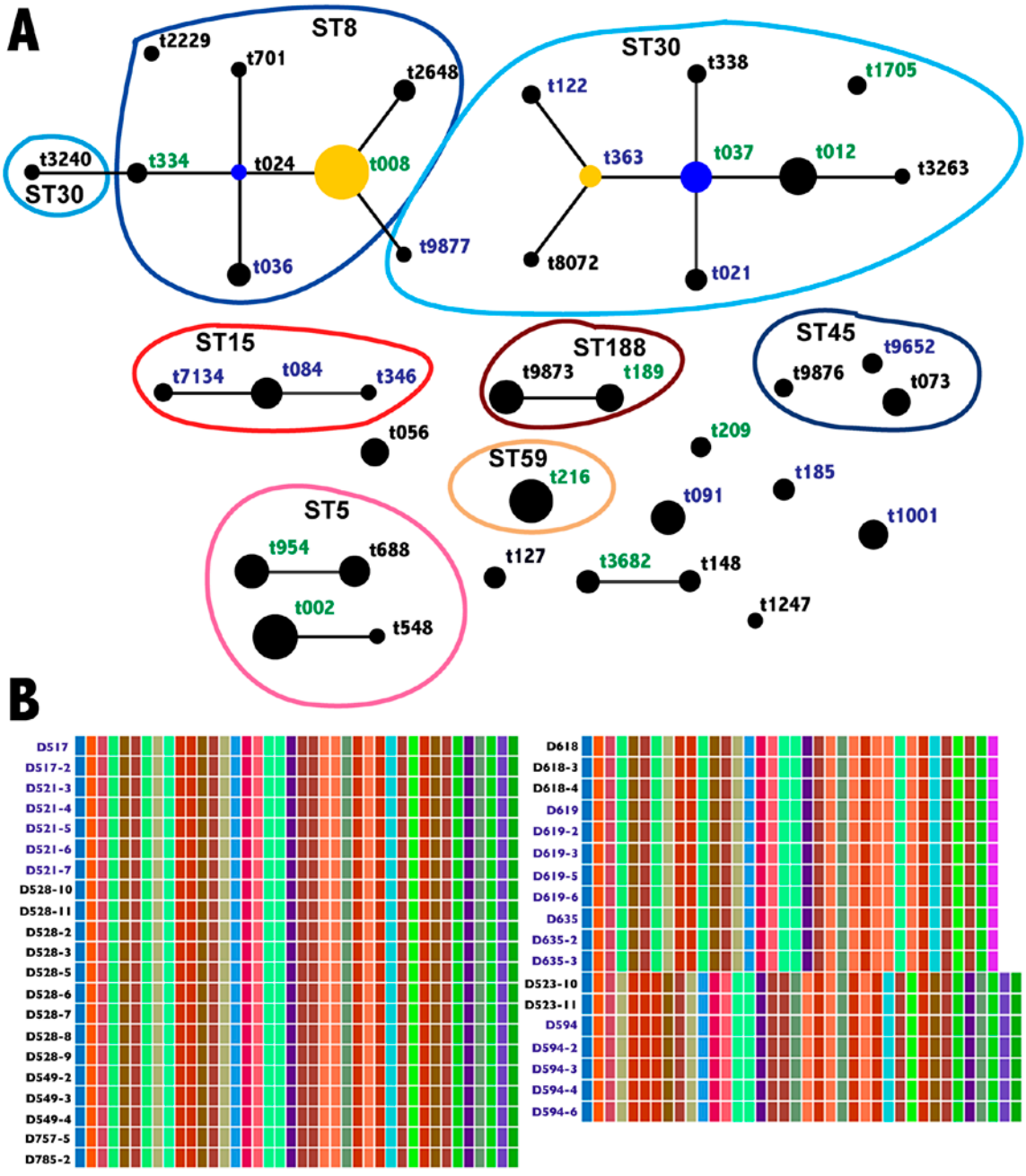

Figure 5: Genoytping of hypervariable virulence genes revealed no preferential colonization of specific genotypes of *SA* strains in persistent and intermittent carriers.

(A) eBURP clustering analysis based on *spa* types revealed that both persistent and intermittent carrier strains belonged to same clonal complexes. *spa* types colored in **blue** contain only

persistent carriers while those in **black** contain only intermittent carriers. *spa* types colored in **green** contain both intermittent and persistent carriers. Circle sizes in each cluster are proportional to the number of isolates and inferred founders (**blue** circles) and sub-founders (**yellow** circles) of each cluster are also represented here. *spa* types with less than 5 repeats were excluded from the eBURP analysis. (B) A representative set of *SA* persistent (colored in **blue**) and intermittent (colored in **black**) carrier strains having indistinguishable clfB R domain repeat region sequences. Like-colored boxes indicate 100% sequence similarity between *SA* strains.

Table 4: Classification of MRSA strains from persistent and intermittent carriers using *SCCmec* typing

Donor	MLST Sequence type (ST)	*SCCmec* type
D535-2[a]	ST30	I
D535-3-4-5-6-7-8-10-11-12-13-14-15-16	ST5	IV
D547[b]	ST30	I
D565-1-3	ST87	III
D618	ST30	IV
D795-2	ST15	II
D798-1-2-3-4-5-6	ST8	IV

[a] **Bold** indicates persistent MRSA carrier strains
[b] *Italics* indicates intermittent MRSA carrier strains

In addition to spa typing, we also performed genotyping of the hypervariable R region of clfB. This region determines the length of the extracellular ligand binding domain of ClfB protein, which is thought to influence bacterial adherence to host epithelia [132]. A previously developed in-house software was used to analyze this clfB R region [36]. Nucleotide analysis of the clfB R region was performed on 244 SA strains isolated longitudinally, and a total of 109 unique repeat units were observed (Appendix A; Table 10). Though variability was observed in the clfB gene fragments, 34.15% of all persistent carrier strains analyzed in our study contained identical sequence repeats to strains isolated from intermittent carriers, revealing relatedness between the SA strains. Figure 5B depicts the sequence similarity of the clfB repeat regions in a

representative sampling of nasal carriage strains isolated from persistent and intermittent carriers. Refer to Appendix A; Figure 21 for clfB typing details of all *SA* strains analyzed in this study.

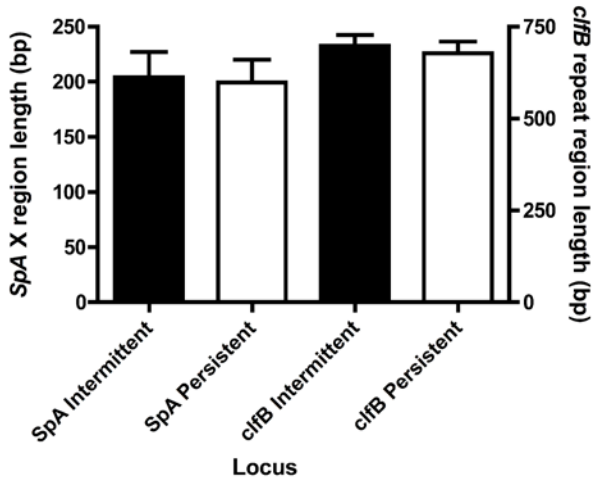

Figure 6: *spa* and *clfB* repeat domain lengths are indistinguishable between persistent and intermittent carriers.

Plots comparing X domain repeat region of *spa* and R region lengths of *clfB* between persistent and intermittent carrier *SA* strains.

Recently, human *in vivo* nasal colonization studies revealed ClfB exhibits a crucial function in bacterial adherence to the nares [77]. Therefore, we assessed whether differences in the length of *clfB* R region would correlate to intermittent or persistent carriage. Persistent carrier strains contained nearly identical R region lengths compared to intermittent carrier strains (p= 0.6646, Figure 6), suggesting that strains from these groups exhibit a high degree of relatedness. A similar analysis of the X domain repeat region of *spa* also revealed no significant difference in length between these two groups (p= 0.7797, Figure 6).

Collectively, longitudinal monitoring of *SA* nasal carriage strains followed by MLST and genotyping of hypervariable virulence genes (*spa* and *clfB*) revealed a high degree of genetic

relatedness between *SA* strains colonizing persistent and intermittent carriers. These results indicate no preferential colonization of either persistent or intermittent carriers by certain genotypes of *SA*.

Persistent and intermittent carriers harbor epidemic MRSA strains in their nares longitudinally over time

All 297 *SA* strains analyzed in this study were subjected to phenotypic screening to identify MRSA strains, and 11.78% of all *SA* carriers (sampled once or multiple times) carried MRSA strains in their nares. A subset of persistent and intermittent carriers harbored strains that were similar to CA-MRSA strains in their nares longitudinally over time (Table 4). Both occurrences of losing and acquiring MRSA strains were observed in these carriers throughout the colonization study period. Persistent carrier D798 carried an ST8-*SCCmec* type IV strain, which is genetically similar to the widely disseminated epidemic CA-MRSA strain USA300. Additionally, the persistent carrier D535 acquired and carried ST5-*SCCmec* type II MRSA strain for over two years. This strain is genotypically similar to another widespread nosocomial epidemic MRSA strain N315. These results indicate that some persistent and intermittent carriers carry epidemic MRSA strains in their nares over variable periods of time.

Discussion

There is considerable evidence indicating that *SA* carriage is an important risk factor for endogenous infection, and recent studies have substantiated that *SA* nasal carriage is multi-

factorial, involving both host and bacterial factors [2,7,39,43,49,120,133]. However, little is known about the extent to which the colonizing strains' factors contribute to persistent versus intermittent carriage of *SA* in the human nose. Therefore, as one of our goals, we set out to investigate whether there is preferential colonization by particular genotypes of *SA* strains among persistent and intermittent carriers. We observed no preferential colonization by particular genotypes of *SA* strains during colonization of either persistent or intermittent carriers. These findings reveal the close genetic relatedness of *SA* strains carried by the carriers in our cohort and raise additional questions about other factors that are responsible for determining persistent versus intermittent carriage states. Previous studies suggest that host factors are crucial determinants of *SA* carriage [42,133] and the fact that this study could not find any genetic differences between strains colonizing persistent and intermittent carriers, collectively may imply as yet unknown factors (including host, microbiome and environment [134]) could primarily be responsible in determining carriage state.

The definition of persistent carriage varies between studies, and one study defined persistent carriage based on a semi-quantitative approach, called the "culture rule" where nasal swabs were collected one week apart to determine persistent or intermittent carriage [135]. However, it is arguable that a more comprehensive longitudinal sampling over longer periods of time is required to identify true persistent carriers. In the current study, extensive longitudinal monitoring of healthy individuals was performed for a period of up to three years to differentiate true persistent carriers from intermittent carriers and non-carriers. This distinction is crucial because bacterial loads between persistent and intermittent carriers vary widely (about 1000 fold more CFUs in persistent carriers [135]), which puts persistent carriers

at a higher risk of acquiring *SA* infections [12,13]. Interestingly, we observed that some persistent carriers carry highly virulent epidemic CA-MRSA strains like USA300 in their nares longitudinally over time, potentially putting them at greater risks of acquiring MRSA infections. CA-MRSA clone USA300 is a widely disseminated virulent strain that is responsible for majority of community associated soft tissue and skin infections [136,137]. Though *SA* nasal carriage itself is seemingly benign to the host's nose, carriers in general are known to require the use of antibiotics more than non-carriers (Rotterdam ERGO cohort [138]). More frequent antibiotic usage could lead to the emergence of multidrug resistant *SA* strains, in addition to affecting the equilibrium of the host's commensal flora.

Previous studies have suggested that a single *SA* strain often colonizes the nose for long periods of time in persistent carriers while strains colonizing intermittent carriers tend to exhibit more genotypic diversity as periods of decolonization and recolonization occur [2,123]. In contrast, our longitudinal sampling and genotyping studies (using MLST, *spa* and *clfB*) revealed that *SA* strains carried by both persistent and intermittent carriers clustered into the same clades exhibiting high degree of genetic relatedness and *SA* strains carried in their nares change over varying periods of time. It is likely, however, that these changes are due to the acquisition of distinct strains—that are genetically similar to the one being replaced—as opposed to the same strain undergoing mutational events. While high sub-ST strain resolution and genotypic analyses of relatedness were obtained in this study, large scale whole genome sequencing of *SA* strains isolated from intermittent and persistent carriers may be the most accurate technique in discerning the genetic relatedness in these *SA* strains. Next generation sequencing technologies could surely assist with such large-scale genome studies [139].

Several hypervariable virulence genes like *spa* and *clfB* have been postulated to be involved in *SA* nasal carriage [39,74,77,105,120-122,140]. However, it is unclear whether polymorphisms in these genes and differences in their repeat lengths would affect the ability of *SA* to bind nasal epithelia and hence, contribute to persistent or intermittent carriage. Our longitudinal analyses revealed that strains isolated from persistent and intermittent carriers showed a high degree of genetic relatedness with respect to polymorphic changes in *spa* and *clfB* genes. These findings echo the findings of a previous study, which demonstrated that polymorphisms in repeat regions of virulent genes *spa* and *coa* (coagulase) do not contribute to persistent carriage [141]. In fact, no studies to date have been able to detect any bacterial factors involved in distinguishing persistent versus intermittent carriage states, suggesting a greater role for other factors in carriage type.

It has been previously speculated that the carriage state can be imposed on members of the same household [142,143]. The current study, though limited, also observed patterns of *SA* transmission among individuals living in the same household in which persistent and intermittent carriers cohabitating in the household harbored genetically similar *SA* strains. In a similar fashion, studies among the institutionalized elderly population observed that both persistent and intermittent carriage strains are shared among household members and the transmitted *SA* strains exhibited genotypic similarities [142]. However, additional correlative studies using a larger cohort of individuals living in the same household are necessary.

Bacterial interference has been hypothesized to be involved in determining *SA* non-carriage state rather than carriage state. Commensal flora of the body are known to protect the host against acquisition of new *SA* strains [144]. The phenomenon of bacterial interference

contributing to *SA* nasal colonization was elegantly demonstrated in a recent study by Iwase and colleagues in which *Staphylococcus epidermidis*, a resident bacterium of the human nares, was shown to inhibit both nasal colonization and biofilm formation of *SA*. Specifically, they demonstrated that a serine protease (Esp) secreting *S. epidermidis* eliminated *SA* colonizing the nasal cavities of healthy individuals [145]. Perhaps, the absence of Esp-expressing *S. epidermidis* in the nasal niche could potentially contribute to persistent *SA* carriage. Additionally, competitive bacterial interference between *SA* and *Streptococcus pneumoniae* have also been studied extensively. Several studies have confirmed an inverse relationship between *SA* and *S. pneumoniae* colonization in the nasopharyngeal niche [143,146]. This inverse relationship between *SA* and *S. pneumoniae* could influence *SA* carriage.

While we have achieved our goal of assessing the genotypic diversity between *SA* strains from persistent and intermittent carriers, we find it pertinent to note that some inherent limitations complicate data interpretation. This study focused only on nasal carriage strains, although *SA* is known to colonize other extra-nasal regions in humans [2]. Regarding the labeling of persistent and intermittent carriers it is important to note that the success rate for isolating *SA* from swab samples never reaches 100%. Moreover, the sample collection was dependent largely on the willingness of donors participating in the study, which lead to gaps in periodicity of sample collection.

In conclusion, the current study illustrates the lack of genotypic differences in *SA* colonizing persistent and intermittent carriers, and the strain relatedness between these carriers observed within the study may be higher than previously thought. Assessment of nasal carriage dynamics between strains colonizing persistent and intermittent carriers and

understanding complex host-pathogen interactions during carriage are crucial for developing effective intervention strategies for nasal carriage and subsequent prevention of community-associated and nosocomial *SA* infections.

CHAPTER 3: EXOPROTEOME OF *STAPHYLOCOCCUS AUREUS* REVEALS PUTATIVE DETERMINANTS OF NASAL CARRIAGE

Introduction

Staphylococcus aureus is one of the most common causes of community-acquired and nosocomial infections throughout the world [2]. These infections have become even more pertinent with the global spread of community-acquired Methicillin-resistant *SA* (CA-MRSA)[4] and the emergence of Vancomycin-resistant *SA* (VRSA) [110]. In the US alone, the mortality rate from *SA* infections surpasses those attributed to HIV/AIDS [4]. Many community-acquired and nosocomial *SA* infections are disseminated through nasal carriage, which occurs in approximately one quarter of the population [2], thus identifying determinants of nasal carriage is a priority for successful amelioration of this condition.

Although nasal carrier strains of *SA* have evolved diverse strategies to ensure their survival and carriage in nasal passages, colonization can also be attributed to amenable hosts that carry *SA* persistently or intermittently [7,43,147]. In an immunologically robust host, nasal secretions contain a plethora of defensive antibacterial proteins and peptides such as lysozyme, lactoferrin, secretory leukoprotease inhibitor (SLPI), cathelicidins, α-defensins and β-defensins including human β-defensin 3 (HBD-3), the most effective of the β-defensins against *SA* infections [51,53,147,148]. However, a key determinant for the nasal carriage of *SA* is the failure of these secretions to prevent colonization. Carrier strains, and not non-carrier strains of *SA*, have been reported to persist and replicate within nasal fluids from carrier donors and on the surface of organotypic nasal epithelia, indicating that carriers have factors that aid in nasal

colonization of *SA* [49,57]. Likewise, investigations by several groups have indicated that colonization of the human nose by *SA* is influenced by bacterial determinants including sortase A (SrtA) [74,122], clumping factor B (ClfB) [77,149], tagX [105], and enterotoxins [140,150,151]. However, this may not represent the complete repertoire of bacterial factors necessary for nasal colonization in humans [114,152].

Our previous studies on a nasal carrier strain of *SA* indicate that it possesses several colonization advantages in comparison to its genetically similar non-carrier counterpart [57]. These advantages included downregulation of host HBD-2, HBD-3 and interleukin-1 (IL-1), along with the ability to form biofilms [57,153]. Biofilm-producing strains of *SA* exhibit higher survival rates against not only antibiotic drugs, but also against natural AMPs present in the host's nasal mucosa [153,154]. Interestingly, the formation of protective biofilms was not evident in the non-carrier strain [153]. Collectively, these findings led us to postulate that the origin of factors, which facilitated nasal colonization by *SA* carrier strains, are present at the primary interface between the host and the pathogen, namely the bacterial surface and freely secreted proteins collectively termed the exoproteome.

Using high throughput gel-free proteomics in concert with 2D-PAGE, we determined the repertoire of proteins contained within the exoproteome of a successful nasal carrier strain of *SA* in comparison to its genetically similar non-carrier counterpart. Analysis of these differences revealed putative determinants of nasal carriage. For the first time, we also compared the exoproteome of the biofilm form of the carrier strain of *SA* with its planktonic counterpart to assess its contribution to successful nasal carriage. Exoproteome analysis by 2D-PAGE revealed a marked difference in the distribution of proteins between carrier and non-carrier *SA* strains.

Subsequent isobaric tagging for relative and absolute quantification (iTRAQ) [155] confirmed these findings, revealing that the carrier strain of *SA* expressed a greater number of proteins involved in cell attachment and immunoevasion than the non-carrier strain. On closer examination of the most abundant immunomodulatory proteins, we found that Staphylococcal protein A (SPA), known to be involved in *SA* virulence and biofilm formation [100,103,156], was secreted in significantly greater amounts by *SA* nasal carrier strains compared to the non-carrier strain. This may indicate a relationship between SPA and the carriage status of *SA*. By comparing the exoproteomes between a successful carrier strain of *SA* and a non-carrier strain, we have identified individual proteins and functional classes of proteins that may determine the nasal carriage status of *SA*.

Materials and Methods

Bacterial strains and culture conditions

SA strain D30 that has been extensively characterized [7,57,152], was originally isolated from the anterior nares of a healthy donor, and served as the carrier strain for the experiments herein. *SA* strain 930918-3, (from Ian Holder, Shriners Burn Hospital, Cincinnati, Ohio, USA), which is genetically similar to the carrier strain D30, and has been extensively characterized [152], served as the non-carrier strain of *SA* in these experiments. Additionally, persistent *SA* carrier strains D20, D98, D39 and intermittent carrier strain D37 were used in this study [7], *SA* was cultivated on Tryptic Soy Agar (TSA; Bacto™, Becton, Dickinson and Company, MD, USA) and subcultured in Trypticase Soy Broth (TSB; Bacto™, Becton, Dickinson and Company, MD,

USA), from which stocks were prepared. For all experiments, snap-frozen (-80°C) stocks of SA were thawed rapidly and cultured at 37°C. Levels of inocula were estimated by measuring the absorbance of a washed bacterial suspension in PBS (Mediatech Inc., VA, USA) at 625 nm. An OD at 625 nm of 0.1 approximated 2.0 x 10^7 CFU/ml. Inocula were quantitated by spreading 10µl aliquots of the liquid culture on TSA and enumerating CFU following 18 hours incubation at 37°C [57,153].

Preparation of carrier strain biofilms

SA carrier strain snap-frozen culture was incubated in TSB media and allowed to grow until stationary phase (6-8 h). The stationary culture was transferred to flasks containing 50 ml TSB at a 1:100 dilution and incubated without shaking at 25°C for 3 days to promote biofilm formation. Biofilms were subsequently washed three times with 0.85% NaCl and incubated overnight in ambient PBS. The supernatant was then centrifuged and used for exoproteome purification [153].

Preparation of protein extracts and 2D-PAGE

2D-PAGE was used to analyze exoproteomes from the carrier strain D30 and non-carrier strain 930918-3. Based on the growth kinetics of our *SA* strains, a modified approach from Dreisbach and colleagues was utilized for *SA* exoproteome preparation [157]. Briefly, one liter of bacterial culture was grown for 24 hours at 250 rpm, 37°C, centrifuged and resuspended in 40 ml of PBS. Protease and phosphatase inhibitors (Halt™ protease and phosphatase single-use inhibitor, Pierce, IL, USA) were added to the culture and shaken overnight and the resulting supernatant

was collected and filter (0.2µm) sterilized. The extract was further purified by a C18 SepPak (Waters Corporation, MA, USA) column according to the manufacturer's instructions, except that the final elution was in 80% acetonitrile/ 20% HPLC grade water. The sample was dehydrated to 10µl and diluted with 100µl of HPLC grade water. The total protein concentration of the sample was estimated using Micro BCA^{TM} Protein Assay Kit (Thermo Scientific, Pierce, IL, USA) according to the manufacturer's instructions [158-161]. Approximately 400µg of total protein was subjected to 2D-PAGE analysis as per the manufacturer's protocol (BioRad, CA, USA). The sample was prepared in rehydration sample buffer I (8 M urea, 2% CHAPS, 50 mM DTT (dithiothreitol) 1x ReadyStrip buffer 0.1–0.4% (w/v) Bio-Lyte ampholytes) and absorbed onto a ReadyStrip IPG gel strip, pH 4-7 (BioRad, CA, USA). The strip was then subjected to isoelectric focusing (IEF) at 50 VµA per strip, initially at 250V for 15 minutes and then ramping to 10,000V in 3 hours followed by an additional focusing for 12–16 hrs at 20°C until 60,000 volt-hours was reached. Strips were rinsed in glycine gel running buffer and soaked in Equilibration Buffer I (6 M urea, 0.375 M Tris, pH 8.8, 2% SDS, 20% glycerol, 2% (w/v) DTT) for 5 minutes followed by Equilibration Buffer II (6 M urea, 0.375 M Tris, pH 8.8, 2% SDS, 20% glycerol, and 2.5% (w/v) iodoacetamide) for 5 minutes. The gel strips were then rinsed in SDS gel buffer and resolved by a 2nd dimension using a precast BioRad Ready Gel Tris-HCl, 4–20% linear gradient at 40 mA for 5 hrs. The gels were subsequently stained using silver nitrate.

Protein digestion, labeling with iTRAQ reagents and On-Line 2D NanoLC-MS/MS

Approximately 120 µg of the exoproteome sample from the planktonic *SA* carrier strain D30, the planktonic non-carrier strain 930918-3 and the carrier strain D30 biofilm were subjected to overnight acetone precipitation at -20°C. Samples were resuspended in dissolution buffer, alkylated, trypsin-digested at 37°C overnight and labeled with iTRAQ 4plex Reagents kit as per the manufacturer's instruction (AB Sciex Inc., CA, USA). iTRAQ tags were applied as follows: iTRAQ 114 = Carrier strain D30 biofilm, iTRAQ 115 = planktonic non-carrier strain 930919-3, iTRAQ 116 = planktonic carrier strain D30, iTRAQ 117 = planktonic carrier strain D30. The four iTRAQ samples were mixed, lyophilized, resuspended in Strong Cation Exchange (SCX) solvent, and subjected to LC-MS/MS analysis of each peak fraction by QSTAR ESI quadrupole time-of-flight tandem MS system (Applied Biosystems, CA, USA) [155,162,163]. Complete iTRAQ analyses were performed three independent times for each sample tested.

iTRAQ Data Analysis

Raw MS data processing, protein identification, quantification and subsequent statistical analyses were performed using the Paragon^{TM} algorithm [164] of ProteinPilot version 2.0.1 software (AB Sciex Inc., CA, USA). Comprehensive searches against the National Center for Biotechnology Information (NCBI) bacterial database with biological modifications and amino acid substitutions were performed to identify the proteins. Additionally, parameters such as cysteine alkylation by MMTS, iTRAQ modification of N-terminal peptide residues, modifications of lysine and tyrosine residues were considered during the analyses, as well as other default parameters were considered by the software. Further classification and analyses of the

identified proteins were performed using the ProGroup™ algorithm. This algorithm enabled confident protein identification using the least set of identified peptides based on total protein scores that is generated from peptide confidence scores. Scores higher than a 95% confidence level were used for identifying proteins. Mean, Standard Deviation (S.D) and p values generated by the ProGroup algorithm were used for relative protein quantification between the samples. iTRAQ fold-ratio >1.2 and <0.8 combined with a *p* value < 0.05 was used to determine differential protein expression between the samples. These cutoff values for variation in the expression, recommended by the Paragon™ algorithm, are a widely accepted fold-ratio [163,165-171]. Proteins identified with one distinct contributing peptide were subjected to manual validation by the assessment and confirmation of their MS/MS spectra (data not shown) [155,162,164,172].

Anti-SPA ELISA

The expression of protein A (SPA) was quantified using the Assay Designs™ protein A Enzyme Immunometric Assay (EIA) kit (Enzo Life Sciences International, PA, USA) as per the manufacturer's instructions with minor modifications. Briefly, exoproteome samples from 1L of stationary phase cultures (~2.0 x 10^{10} CFU/ml) of nasal carrier, non-carrier and epidemic strains were prepared as mentioned previously and equal volumes (25µl) at dilutions 1/1x10^5, 1/2 x10^5, 1/4 x10^5 and 1/16 x10^5 were subjected to assay analysis. The concentration of SPA was calculated against standards according to manufacturer's instructions and represented as µg/ml of total protein. A one-tailed Student's *t*-test was used to measure the significance of SPA expression between *SA* strains.

Results

Comparative analyses of SA exoproteomes reveal differences in the distribution pattern of proteins between nasal carrier and non-carrier strains

Since the first interface between host and pathogen is the bacterial exoproteome, we hypothesized that a comparison between a carrier and a genetically similar non-carrier SA strain exoproteome would reveal key differences that could be important in nasal colonization of SA. To screen initially for these differences we used 2D-PAGE and observed significant differences in the distribution of secreted proteins between nasal carrier and non-carrier strains as typified by the distribution of MS/MS-verified SPA, (49.5 kDa). Additionally, multiple isoforms of SPA were exclusively detected in the carrier strain (Figure 7)

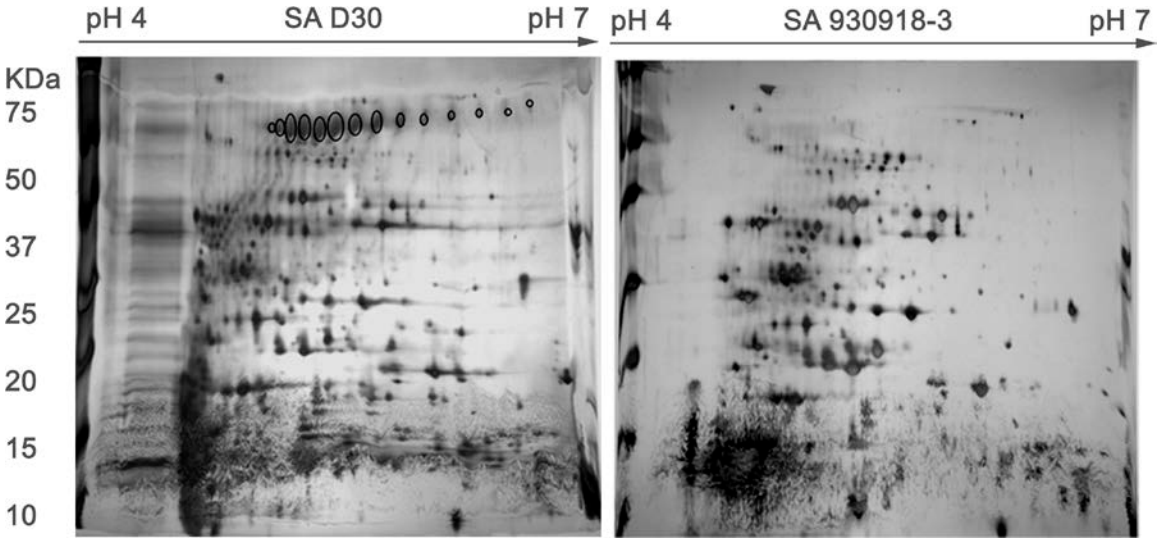

Figure 7: Comparative exoproteome analysis of carrier (D30) and non-carrier (930918-3) strains of *SA* reveals significant differences in protein distribution.

The distribution pattern of the exoproteomes of genetically similar strains of *SA* differed from the carrier to the non-carrier strain as evidenced by the distribution of Staphylococcal protein A (SPA) 49.5 KDa (circled). SPA spots were confirmed using ELISA and mass spectrometry.

iTRAQ-coupled LC-MS/MS analyses of identified a total of 488 proteins in the aggregate SA exoproteome

An experimental workflow for the analysis of *SA* exoproteomes by iTRAQ is described in Figure 8A. Briefly, purified proteins were subjected to trypsin-digestion and labeled with iTRAQ reagents. Peptides from *SA* carrier strain (D30) exoproteome were labeled with iTRAQ reagents 116 and 117 whilst peptides from the non-carrier strain (930918-3) and carrier strain (D30) biofilm exoproteomes were labeled with iTRAQ reagents 115 and 114, respectively. These iTRAQ-labeled samples were then mixed, lyophilized and fractionated using Strong Cation Exchange (SCX) chromatography. Subsequently, SCX fractions were subjected to LC-MS/MS analysis (Figure 8). The entire set of experiments from the collection of the exoproteome to LC-MS/MS analysis was performed 3 independent times (N=3). LC-MS/MS analysis of 21 SCX fractions identified a total of 488 proteins (95% confidence, unused score >1.3) from 5970 distinct peptides (Appendix B; Table 12 and Table 13). In addition, the identified proteins' expression levels were significantly different between carrier strain, non-carrier strain and carrier strain biofilm ($p<0.05$) conditions as depicted by the volcano plot illustration of iTRAQ data (Figure 8).

Representative iTRAQ ion spectra and MS/MS spectra showing protein identification and quantification of selected proteins from carrier and non-carrier strains are illustrated in Figure 9**.** Figure 9A reveals representative MS/MS and iTRAQ ion spectra of a uniquely identified peptide (99% confidence) from immunoglobulin G binding protein A precursor. iTRAQ analysis revealed a >2.2 fold increase in expression of this protein between carrier D30 (iTRAQ label 116) and non-carrier 930918-3 (iTRAQ label 115) strains. Figure 9A&B illustrate the

iTRAQ ion spectra and MS/MS spectra for the proteins ABC transporter substrate-binding protein and autolysin revealing lower and equal expression levels, respectively, between carrier strain D30 (iTRAQ label 116) and non-carrier strain 930918-3 (iTRAQ label 115). The corresponding amino acid sequences of the peptides depicted in Figure 9 are given in supplemental information (Appendix B; Table 11).

The nasal carrier strain of SA expresses a greater number of proteins implicated in colonization than its non-carrier counterpart

The proteins identified in the exoproteomes were categorized with reference to their potential contribution to nasal carriage as conceived by Burian and colleagues [11]. These included proteins involved in metabolism, protein synthesis and trafficking, stress, pathogenesis and immunomodulation, cell adhesion, cell division and cycle, transport and unknown functions (Appendix B; Table 12**)**. iTRAQ analyses revealed that the carrier strain of *SA* expressed a markedly different repertoire of proteins in comparison to the non-carrier strain (Figure 10). We observed that 131 proteins were differentially expressed between carrier and non-carrier strain exoproteomes. Of these 131 proteins, 66 were expressed in higher amounts in the carrier strain of *SA* compared to the non-carrier strain, and 25 of these proteins exhibited a >2-fold increase in expression levels (see Table 5 for a partial list of proteins and Appendix B; Table 12 for the complete list).

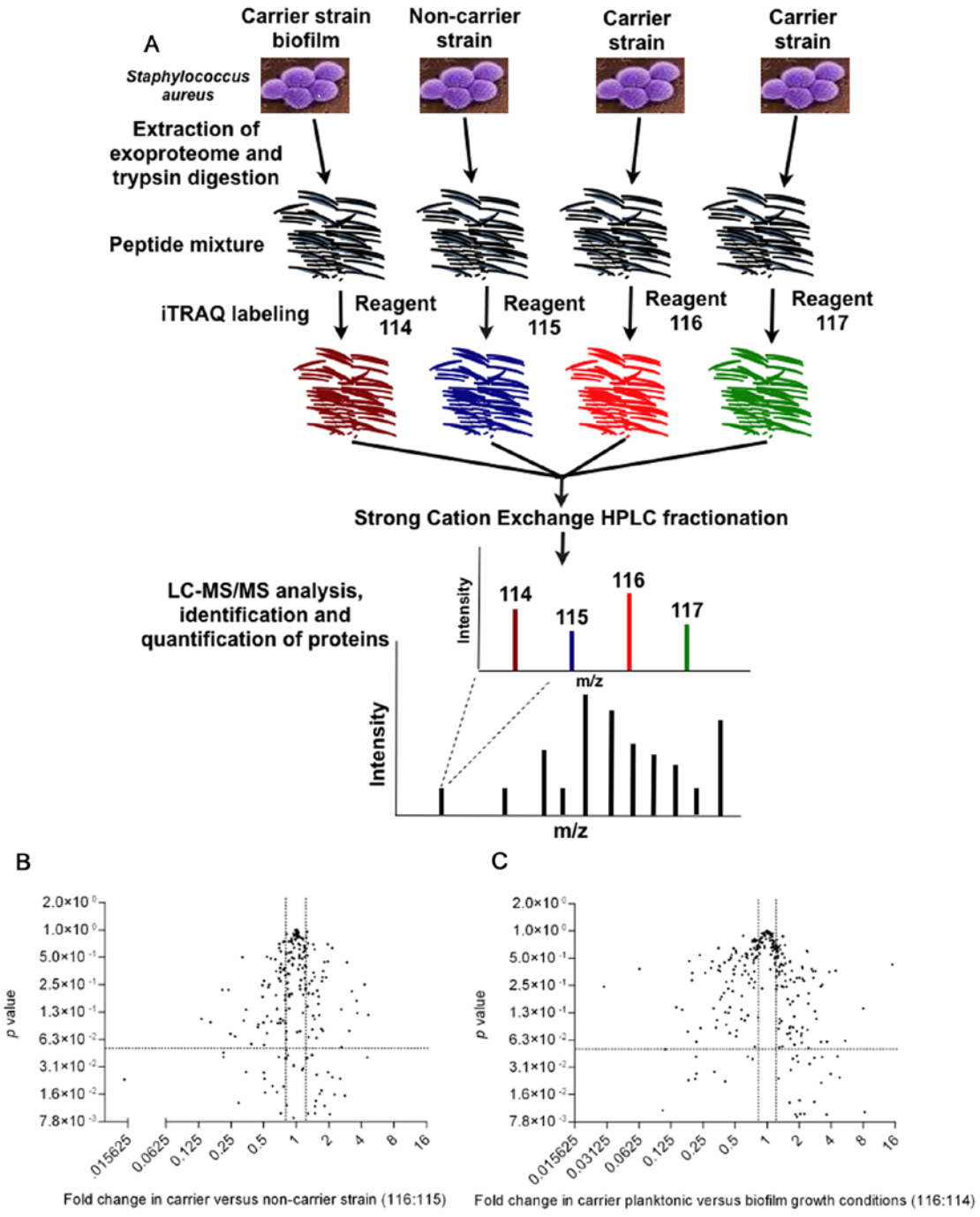

Figure 8: Integrated experimental workflow for the analysis of *SA* exoproteome by iTRAQ and volcano plot illustration of iTRAQ data

(A) The exoproteome of the carrier strain, the non-carrier strain and a carrier strain biofilm (growth media free) were extracted, purified and concentrated with the aid of C18 solid phase extraction cartridges. Proteins were subject to trypsin-digestion and labeled with iTRAQ reagents. Digests from the carrier strain (D30) exoproteome were labeled with iTRAQ reagents

116 and 117 whilst digests from the non-carrier strain (930918-3) exoproteome and carrier strain (D30) biofilm were labeled with iTRAQ reagents115 and 114 respectively. Labeled samples were mixed, lyophilized and fractionated using Strong Cation Exchange (SCX) chromatography. The HPLC fractions were analyzed by LC-MS/MS on a QSTAR ESI quadruple time-of-flight tandem MS system. The entire set of experiments from the collection of the exoproteome to LC MS/MS analysis was performed 3 times (N=3) and the raw MS/MS data were collated together for further analysis. (B) Protein expression fold change in SA carrier strain as compared to non-carrier strain. (C) Protein expression fold change in SA carrier strain under planktonic and biofilm growth conditions. Fold differences of protein expression are plotted against their respective p values. All proteins identified by at least one peptide with greater than 95% confidence are represented here. Horizontal dashed lines identify fold changes with p values of 0.05. Vertical dashed lines delineate a 2-fold change in the ratio of protein expression.

Our exoproteomic analyses revealed that additional adhesive proteins might play critical roles in colonizing the human nasal mucosa (Table 5). We observed that the *SA* carrier exoproteome contained a markedly larger number of adhesive proteins than the non-carrier strain (Figure 10C). One of the major proteins involved in host attachment, the cell wall surface anchor family protein (SasD), demonstrated nearly 4-fold higher expression in the carrier compared to the non-carrier strain (Table 5). iTRAQ analysis also detected significantly higher levels of two proteins in the carrier strain that have previously been implicated in nasal colonization: serine-aspartate repeat family protein (SrdH) and sortase (Srt) (Table 5). SasD and SrdH are two cell wall-anchored proteins containing host attachment domains (MSCRAMMs) [73,173]. These MSCRAMM proteins are covalently anchored to the host adhesive matrix molecules via the LPXTG motif recognized by sortase [74]. SasD contains a slightly modified LPXAG anchor to host matrix molecules.

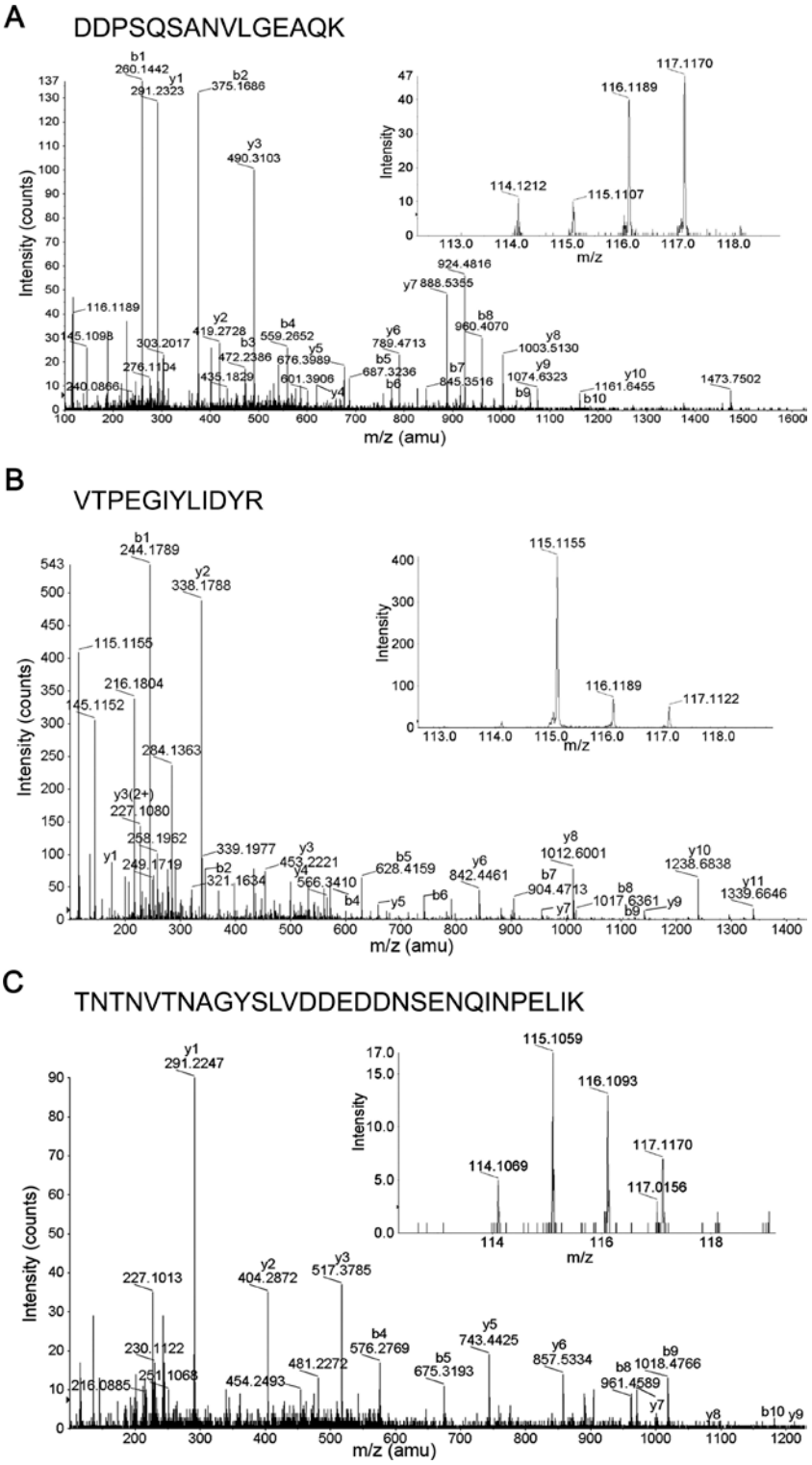

Figure 9: Representative iTRAQ MS/MS spectra showing protein identification in carrier and non-carrier strains from selected proteins.

Representative MS/MS spectra of uniquely identified peptides (confidence, 99%) from (A) Immunoglobulin G binding protein A precursor (B) ABC transporter, substrate-binding protein

and (C) Autolysin are represented here. The inset reveals the iTRAQ reagent peaks for relative quantitation in the *SA* strains. Illustrations for higher, lower and equal expression levels between carrier strain D30 (iTRAQ label 116) and non-carrier strain 930918-3 (iTRAQ label 115) have been provided.

Immunomodulatory Proteins And Toxins

Immunomodulatory proteins play critical roles in *SA* infection of the host and subsequent nasal carriage [84]. Based on a comprehensive literature survey of the functions of these proteins, our results indicated that the carrier strains of *SA* contained a greater number of proteins which downregulate immunity, whereas the non-carrier strains contained a greater number of proteins which upregulate host immunity. Some of the most noticeable immunomodulatory proteins detected in greater abundance in the carrier strain were SPA and surface elastin binding protein (EbpS) (Table 5). On the other hand, penicillin binding protein (PBP) 2, and cold shock protein (Csp) that makes *SA* susceptible to antibiotics and antimicrobial peptide human cathepsin G respectively [174,175], were found in higher levels in the non-carrier strain.

Immunoevasive proteins including cell surface elastin binding protein (EbpS), SPA, PBP1, immunodominant staphylococcal antigen A precursor and α-hemolysin precursor identified in our study have also been independently observed in other studies [157,172,176-178]. However, their roles with relevance to nasal colonization have not been elucidated. Notably, we observed that the expression levels of immunomodulatory toxins such as α-hemolysin precursor that are responsible for bacterial invasion of the host, were elevated in the carrier strain. Interestingly, leukocidin/hemolysin toxin family protein that helps in the formation of pores during *SA* pathogenesis of host was dominant in the non-carrier strain (Table 5).

Transport Proteins

SA carrier strains can resist the host's antimicrobial agents by active efflux of the agents using translocation machineries [179]. This phenomenon is mirrored in our results in which the nasal carrier strain produced substantially more transport proteins compared to its non-carrier counterpart (Figure 10C, Table 5). These included several proteins from the ATP-binding cassette (ABC) transporter super family and one from the common protein translocation machinery, Sec translocon (Table 5). Sec translocon proteins are implicated in bacterial pathogenesis and in the secretion of virulence proteins [178]. We observed that a key member of this translocon, protein-export membrane protein SecF that is part of the bifunctional translocase SecDF, was found in higher levels in the carrier strain indicating the likely involvement of these transport proteins in nasal colonization.

Stress

SA, when subjected to osmotic shock, heat, oxidative stress, starvation, alkaline shock etc, triggers a stress response [180]. Our iTRAQ data revealed that the carrier strain of *SA* secreted fewer stress response proteins in comparison to its non-carrier counterpart. Specifically, stress proteins such as CsbD-like superfamily and alkaline shock protein 23 (ASP23) were expressed in lower levels in the carrier strain (Table 5). However, not all stress proteins were downregulated in the carrier strain. Some stress proteins that are normally expressed when *SA* is exposed to environmental stress such as superoxide dismtase (SOD) and thioredoxin-disulphide reductase were expressed at similar levels by both strains (Table 5).

Table 5: Proteins from the exoproteome of the nasal carrier strain of SA and the non-carrier strains are assigned into functional categories as identified and quantified by iTRAQ.

Accession No.	Protein name	Number of peptides[a]	Fold ratio[b]			
			carrier/ non-carrier	*p* value	Planktonic carrier/ Biofilm carrier	*p* value
	Stress related proteins					
gi|87162409	CsbD-like superfamily	34	*0.4565*[c]	*0*	**1.3708**[d]	**0.0058**
gi|87162159	Hypothetical protein SAUSA300_1582, similar to CsbD-like family protein	13	*0.6747*	*0*	2.0123	0.0135
gi|87162200	Alkyl hydroperoxide reductase subunit C	27	**1.1686**[d]	**0.0002**	**1.6239**	**0.0128**
gi|87161642	Alkyl hydroperoxide reductase subunit F	1	0.4971	0.0957	0.3723	0.188
gi|87160786	Hypothetical protein SAUSA300_1652, putative universal stress protein	24	*0.862*	*0.0006*	0.8978	0.2323
gi|87162087	Universal stress protein family	18	**2.9027**	**0.0004**	**3.0664**	**0**
gi|70726220[e]	Hypothetical protein SH1219, putative universal stress protein	7				
gi|894289	Alkaline shock protein 23 (ASP23)	20	*0.5771*	*0*	1.1024	0.6569
gi|87160079	Peptide methionine sulfoxide reductase regulator (MsrR)	10	0.8648	0.1957	1.7545	0.0863
gi|87161086	Methionine-R-sulfoxide reductase	1	1.238	0.8192	15.0177	0.4261
gi|87161236	Thioredoxin*	12	**1.3978**	**0.0003**	*0.7305*	*0.0387*
gi|87161001	Thioredoxin-disulfide reductase	9	0.792	0.169	1.1776	0.6298
gi|87161687	Thiol peroxidase	8	*0.756*	*0*	1.4239	0.2404
gi|21282513	Hypothetical protein MW0784, similar to thioredoxin-fold containing protein family	5	*0.8983*	*0.0001*	1.2352	0.3626
gi|87160477	Putative thioredoxin	5	1.218	0.2208	1.2503	0.6608
gi|87160405	Hypothetical protein SAUSA300_1909, similar to thioredoxin family of proteins	4	0.987	0.9858	0.7007	0.628
gi|87160511	Catalase	5	*0.5021*	*0.027*	**4.7999**	**0.0241**
gi|87161707	Superoxide dismutase (Mn/Fe family)	5	0.9286	0.4111	0.7623	0.7832
gi|88195790	Putative ferritin	4	0.7199	0.5798	0.4058	0.1265
gi|87162273	Osmc/Ohr family protein	1	2.1538	0.6357	2.8528	0.3618
gi|87160980[e]	Hypothetical protein SAUSA300_0725, similar to putative Oxidoreductase	1	0.5794		1.3866	
	Pathogenesis and immunomodulatory proteins					
gi|87160749	Cell surface elastin binding protein	200	**1.7517**[d]	**0**	1.3029	0.0961
gi|133853458	Immunoglobulin G binding protein A precursor	138	**2.2282**	**0**	1.0756	0.3757
gi|56749001	Immunodominant staphylococcal antigen A precursor	57	**1.4061**	**0**	0.9476	0.656
gi|15926764	Penicillin-binding protein 1	43	**1.3495**	**0.0004**	**1.4429**	**0.0048**
gi|87162077	Penicillin binding protein 2	32	*0.6419*	*0.0001*	0.6655	0.1167
gi|87161157	Penicillin-binding protein 4	6	1.6283	0.1152	**2.7796**	**0.013**
gi|70726765	Beta-lactamase	10	0.0849	0	*0.1207*	*0.0022*
gi|87161577	Cold shock protein, CSD family	36	*0.7651*[c]	*0*	*0.7602*	*0.0001*
gi|87160015	Staphylococcal tandem lipoprotein	14	*0.4398*	*0.0002*	1.1702	0.4995
gi|47169194[e]	Chain A, staphylococcal protein A, B-domain, Y15W mutant, Nmr, 25 structures	12	0.9803			
gi|87160380	Alpha-hemolysin precursor	10	**2.6865**	**0**	1.1949	0.4484
gi|87160982	Leukocidin/hemolysin toxin family protein	10	*0.3131*	*0*	0.7128	0.2953

Accession No.	Protein name	Number of peptides[a]	Fold ratio[b]			
			carrier/ non-carrier	*p* value	Planktonic carrier/ Biofilm carrier	*p* value
gi|87161881	Antibacterial protein	7	*0.5416*	*0*	0.8559	0.5626
gi|15927581	Hypothetical protein SA1813 similar to leukocidin-like protein 2	5	*0.3607*	*0*	1.1987	0.519
gi|87162162	Hypothetical protein SAUSA300_1018 similar to SCP/PR1-like extracellular protein	8	1.0669	0.5321	0.6697	0.3322
gi|87160365	Antibacterial protein	4	0.9121	0.1981	*0.2771*	*0*
gi|87162347	Hypothetical protein SAUSA300_2164 similar to extracelluar adherence protein	4	0.3271	0.1009	*0.1106*	*0.0494*
gi|87160217	Secretory Antigen Precursor (SsaA)	4	0.9951	0.9764	0.5127	0.069
gi|88194063	Hypothetical protein SAOUHSC_00257 similar to EsxA virulent protein	4	0.384	0.0557	2.158	0.2965
gi|68565538	Protein esaA	2	0.2372	0.2204	0.197	0.2859
gi|87160905[e]	Hypothetical protein SAUSA300_0282 similar to virulence protein EssB	1	0.2942		0.4179	
gi|87162375	Hypothetical protein SAUSA300_1323 similar to conserved virulence factor C	2	0.809	0.5491	0.1985	0.3431
gi|87160520	Acetyltransferase family protein in Oat A family	3	**2.0482**	**0.0094**	0.8063	0.7857
gi|87161173	Teicoplanin Resistance Associated Membrane Protein (TcaA)	3	0.8209	0.9069	1.4697	0.7023
gi|88195687	Hypothetical protein SAOUHSC_01999 similar to peroxiredoxin Q/BCP	3	**2.9885**	**0.0002**	**1.9644**	**0.0359**
gi|87162379[e]	Ferredoxin	1	1.1786		1.8553	
gi|87161897	IgG-binding protein SBI	2	3.6719	0.1219	5.4157	0.0616
gi|87160565[e]	Immunodominant antigen B	1	29.6467		2.0875	
gi|62391257[e]	Secreted penicillin binding protein [*Corynebacterium glutamicum* ATCC 13032]	1	1.6876		2.2857	
	Cell adhesion proteins					
gi|87160939	Cell wall surface anchor family protein	57	**3.6116[d]**	**0**	1.2777	0.0838
gi|151222604	Hypothetical protein NWMN_2392 similar to cell wall surface anchor family protein	40	*0.0911[c]*	*0*	*0.2444*	*0*
gi|87162315	Putative cell wall binding lipoprotein	16	1.2742	0.1446	1.1145	0.7887
gi|87162026	Autolysin	31	1.0742	0.6135	0.7695	0.2717
gi|87160697	D-alanine-activating enzyme/D-alanine-D-alanyl protein (dltD)	18	1.2272	0.2515	**1.9912**	**0.0001**
gi|87160121	D-alanine-activating enzyme/D-alanine-D-alanyl protein (dltC)	1	0.6864	0.533	16.1543	
gi|61213890	77 kda outer membrane protein precursor	11	*0.2627*	*0*	0.6572	0.1167
gi|81781509	UPF0365 protein SAV1573	8	**1.8364**	**0.0005**	**2.9173**	**0.0019**
gi|87160285	Rod shape-determining protein MreC	8	0.8103	0.0767	**2.9577**	**0**
gi|87160775	N-acetylmuramoyl-L-alanine amidase	8	1.5402	0.0651	**2.0519**	**0.0096**
gi|87161887	N-acetylmuramoyl-L-alanine amidase domain protein	7	1.893	0.3018	1.3838	0.4234
gi|88196468	Putative sortase	5	**2.0829**	**0.001**	1.2683	0.5337
gi|87161790	5'-nucleotidase family protein	3	3.6218	0.1664	1.5688	0.1773
gi|87160715	Fmt protein	2	1.1273	0.8064	1.1849	0.6709
gi|81673756	Phosphoglucosamine mutase	1	0.7583	0.739	3.3119	0.2556
gi|87160798	Serine-aspartate repeat family protein (SdrH)	1	**1.49**	**0.0115**	1.3251	0.4213
gi|116694144[e]	Flp pilus assembly protein TadC	1	1.3693		2.585	
gi|81781921	Extracellular matrix protein-binding protein EMP precursor	1	0.5809	0.4841	1.4533	0.5086
gi|91211353[e]	AsmA suppressor of OmpF assembly mutants	1				
	Transport proteins					

Accession No.	Protein name	Number of peptides[a]	Fold ratio[b]			
			carrier/ non-carrier	*p* value	Planktonic carrier/ Biofilm carrier	*p* value
gi|87162197	Amino acid ABC transporter, amino acid-binding protein	34	0.9535	0.4842	1.3001	0.0518
gi|87162140	Oligopeptide ABC transporter, substrate-binding protein	30	**1.1547**[d]	**0.0301**	1.3918	0.0533
gi|87161352	ABC transporter, substrate-binding protein	12	*0.2931*	*0.0126*	0.4137	0.092
gi|21282147	Hypothetical protein MW0418 similar to ABC transporter, substrate-binding protein	6	1.0242	0.8594	1.2602	0.507
gi|87161864	ABC transporter, substrate-binding protein	3	**2.8266**	**0.0151**	2.1079	0.0742
gi|87160588	Molybdenum ABC transporter, molybdenum-binding protein (ModA)	17	**1.5245**	**0.0005**	1.8056	0.0558
gi|87161641	Amino acid ABC transporter, permease/substrate-binding protein	7	**6.1167**	**0**	**2.5162**	**0.0341**
gi|21284120	Oligopeptide transporter putative substrate binding domain	6	**2.4913**	**0.0004**	1.9632	0.1937
gi|87161764	Putative iron compound ABC transporter, iron compound-binding protein	5	1.4063	0.0805	0.7301	0.561
gi|87160849	Iron compound ABC transporter, iron compound-binding protein	4	0.5869	0.0986	0.6344	0.5184
gi|87161518	Glycine betaine/carnitine/choline ABC transporter	4	0.9366	0.6998	1.0605	0.8404
gi|87162224	Osmoprotectant ABC transporter, permease	2	0.6537		3.9979	
gi|126355053[e]	ABC transporter-related protein [*Pseudomonas putida* GB-1]	1	37.5193		6.929	0.0699
gi|149194563[e]	ABC transporter-related protein [*Caminibacter mediatlanticus* TB-2]	1	1.6215		0.0083	
gi|87162212[e]	Amino acid ABC transporter, ATP-binding protein	1	5.1042		0.571	
gi|87161315	Hypothetical protein SAUSA300_2378 similar to potassium efflux protein kefA	21	**1.4953**	**0**	1.6492	0.0873
gi|87160965	Phosphocarrier protein (HPr)	11	**1.1099**	**0.0026**	*0.4598*	*0*
gi|87162382	PTS system, glucose-specific IIA component	11	1.0668	0.4928	**2.9434**	**0.004**
gi|87162442	Transferrin receptor	8	**3.331**	**0**	**3.5596**	**0.0002**
gi|87160279	AcrB/AcrD/AcrF family protein	7	1.4716	0.1045	1.0728	0.9096
gi|87162284	Putative ferrichrome ABC transporter	1	0.2468	0.0722	0.5068	0.6105
gi|87161389	Putative iron compound ABC transporter, iron compound-binding protein	1	2.6052	0.134	1.4787	0.3341
gi|87160515	Protein-export membrane protein SecF	6	**1.4937**	**0.0097**	0.7504	0.4761
gi|87160369	Hypothetical protein SAUSA300_0833	3	0.5373	0.5051	0.4642	0.5479
gi|15925912	RGD-containing lipoprotein	3	1.2004	0.4097	1.0422	0.9709
gi|87161142	Ferric hydroxamate receptor	3	1.0332	0.8931	0.4321	0.2314
gi|87160674	Putative lipoprotein	41	*0.2959*[c]	*0*	*0.7197*	*0.0011*
gi|87161872	Putative lipoprotein	2	4.2798	0.2519	2.4403	0.1588
gi|87160414	Multidrug resistance protein A, drug resistance transporter	1	0.6934	0.2928	0.7756	0.7943
gi|23005821[e]	COG1131: ABC-type multidrug transport system, ATPase component	1			0.6174	
gi|149201149	Nitrate transport ATP-binding subunits C and D	1	1.5776		7.9917	0.1401
gi|151575108	Outer membrane efflux protein	1	1.1986	0.2951	3.8451	0.3525
gi|87161139	Iron transport associated domain protein	1	1.6828		0.1596	
gi|149910101	Hypothetical transport protein [*Moritella sp.* PE36]	1	**2.2325**	**0**	**4.2379**	**0**
gi|35211526[e]	gll0963 [*Gloeobacter violaceus* PCC 7421]	1				
gi|127512243[e]	Efflux transporter, RND family, MFP subunit	1				
gi|146301866[e]	RND efflux system, outer membrane lipoprotein, NodT family	1	0.9695	0.7073	0.4187	
gi|17131745[e]	all2652	1	1.7839		0.8275	

Accession No.	Protein name	Number of peptides[a]	Fold ratio[b]			
			carrier/ non-carrier	*p* value	Planktonic carrier/ Biofilm carrier	*p* value
gi|87162344	Phosphonate ABC transporter, phosphonate-binding protein	1	1.3653	0.3305	**6.3883**	**0.0356**
gi|51595518	Molybdenum transport regulatory (repressor) protein (ModE)	1	1.3022	0.3562	1.1322	0.9636
gi|152936446[e]	Flagellar motor switch protein fliG	1				

[a] The list contains quantitative information of the proteins (including the number of peptides) from the iTRAQ data set. These proteins have met the criteria (i.e., unused prot score >2.0, change in expression levels of at least 1.2-fold p-value <0.05 and EF < 1.4 for all ratios) as defined in the Experimental Procedures. [b] Relative change in protein levels between secretomes [c] italicized numbers= down-regulation. [d] **bold numbers =**up-regulation. [e] iTRAQ identified unique proteins not quantified. *Denotes a protein with multiple functions

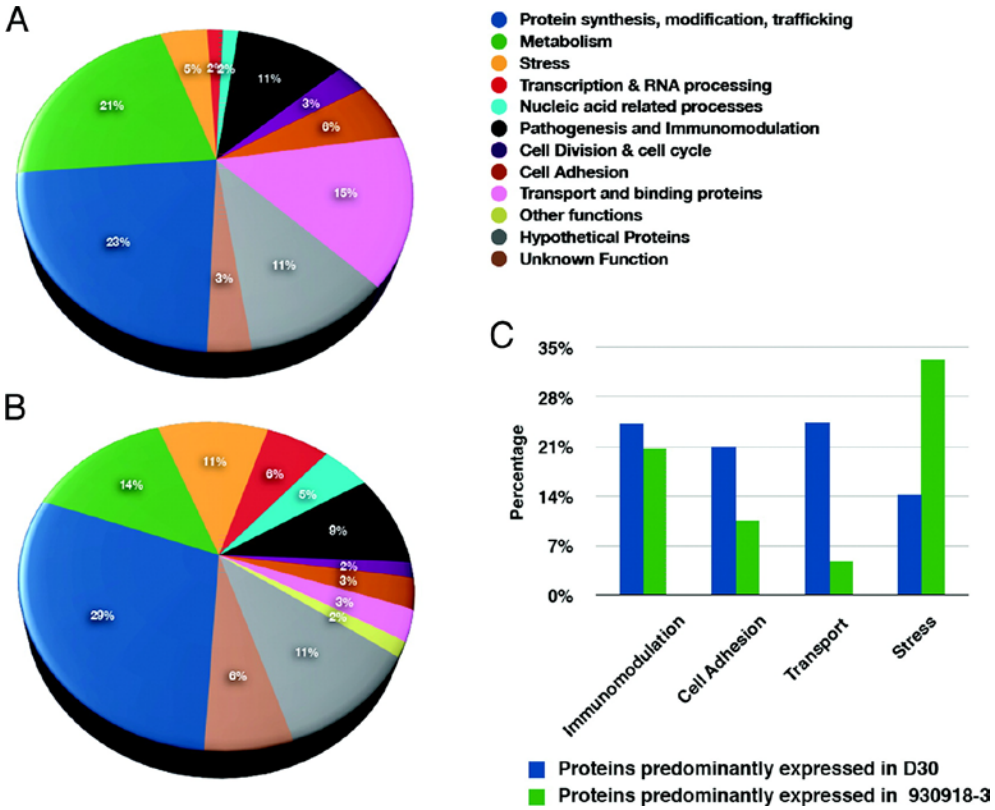

Figure 10: The nasal carrier strain of *SA* expresses a greater number of adhesion/ binding proteins in its exoproteome than its non-carrier counterpart.

A comparison of *SA* exoproteomes using iTRAQ has revealed that (A) the nasal carrier strain of *SA* (D30) expresses a different repertoire of proteins than (B) a genetically similar non-carrier strain (930918-3). (C) Percentage of proteins that were significantly up-regulated in that category in comparison to the other tested strain. The carrier strain of *SA* contains a greater

proportion of proteins related to binding and adhesion but less stress proteins. Proteins were identified with high confidence (p <0.05) in three independent experiments (N=3).

The SA nasal carrier biofilm exoproteome contains a greater number of stress and immunoevasion proteins than its planktonic counterpart

We previously reported that the carrier strain of *SA* (D30) adopted a biofilm mode of growth under ambient laboratory conditions [153]. We hypothesized that biofilm formation may facilitate nasal carriage, given the importance of this form of growth to colonization and defensive capabilities of *SA* [181]. We therefore compared the biofilm exoproteome of a carrier strain of *SA* with its planktonic counterpart. To our knowledge, this was the first time such a comparison has been reported for the respective exoproteomes. We observed that 84 proteins were differentially expressed between planktonic and biofilm growth forms of the carrier strain of *SA*. Of the 84 proteins, 46 were expressed at higher amounts in the biofilm exoproteome compared to its planktonic counterpart and 35 exhibited >2-fold expression (See Table 5 for partial list of proteins and supplemental Table 13 for the complete list).

It was observed that the exoproteome of the biofilm form of the nasal carrier strain of *SA* was markedly different in terms of stress and immunomodulatory proteins compared to its planktonic counterpart (Figure 11A and Figure 11B). Specifically, iTRAQ analyses revealed that the carrier strain biofilm had 4-fold fewer adhesive proteins as compared to the planktonic form (Figure 11C). Specifically, D-alanine-activating enzyme (DltD) protein, involved in D-alanylation of wall techoic acid (WTA) during cell wall synthesis, was significantly down-regulated in the biofilm exoproteome [182]. Another protein involved in cell wall peptidoglycan synthesis, N-acetylmuramoyl-L-alanine amidase, was also significantly down-

regulated in the biofilm form, perhaps indicating a lower cell wall turnover in the *SA* carrier strain when it adapts a biofilm mode of growth.

Adhesive proteins, together with immunomodulatory proteins, enable biofilms to resist the action of antibiotics and other antimicrobial agents [183,184]. Not surprisingly, our iTRAQ analyses revealed that the biofilm growth form of the carrier strain of *SA* secreted more immunomodulatory proteins than the planktonic form (Figure 11C). Curiously, penicillin binding proteins (PBPs), including PBP1 and PBP4 that enable *SA* to resist β-lactam antibiotics, were expressed in lower levels in the biofilm growth mode. Another mechanism that allows bacterial biofilms to evade antimicrobial agents is the use of efflux pumps and transporters [185]. Unexpectedly, the carrier strain biofilm secreted 3-fold fewer number of transport proteins compared to the planktonic form (Figure 11C).

Although the number of immunomodulatory proteins was only marginally greater in the carrier strain than the non-carrier strain based on the iTRAQ findings, these results did not concur with other analyses we conducted. We had observed that the resistance of the carrier strain to innate immune defense molecules (Reactive Oxygen Intermediates) is twice as much as the non-carrier strain (data not shown). Additionally, the resistance of biofilms to innate host molecules is 10-15 times greater than the planktonic variety (data not shown). Perhaps, the effectiveness of immune evasion by *SA* is not determined by the number of immunomodulatory proteins, but by the potency and quantity of individual proteins. To this end, we further analyzed one of the most abundant immunological *SA* proteins, Staphylococcal Protein A (SPA).

SPA from SA carrier strains is found in higher concentrations than the non-carrier strain

SPA, which can be found to be either cell-wall associated or secreted, is well known for its binding, immunological, and biofilm promoting properties [84,103,156]. Not surprisingly, we noticed throughout the *SA* exoproteomic analyses that levels of SPA were consistently higher in the carrier strain than the non-carrier strain (Figure 12). Using an SPA ELISA, we confirmed that the carrier strain had nearly 8-fold higher SPA levels than the non-carrier strain (Figure 12). This was verified in several other persistent carrier strains such as (D20, D39 and D98) and an intermittent carrier strain (D37). The levels of SPA were much higher in persistent carriers and comparatively lower in the intermittent carrier, although all carriers had significantly higher SPA levels compared to the non-carrier strain (Figure 12). These results suggest a possible correlation between increased SPA levels and nasal carriage.

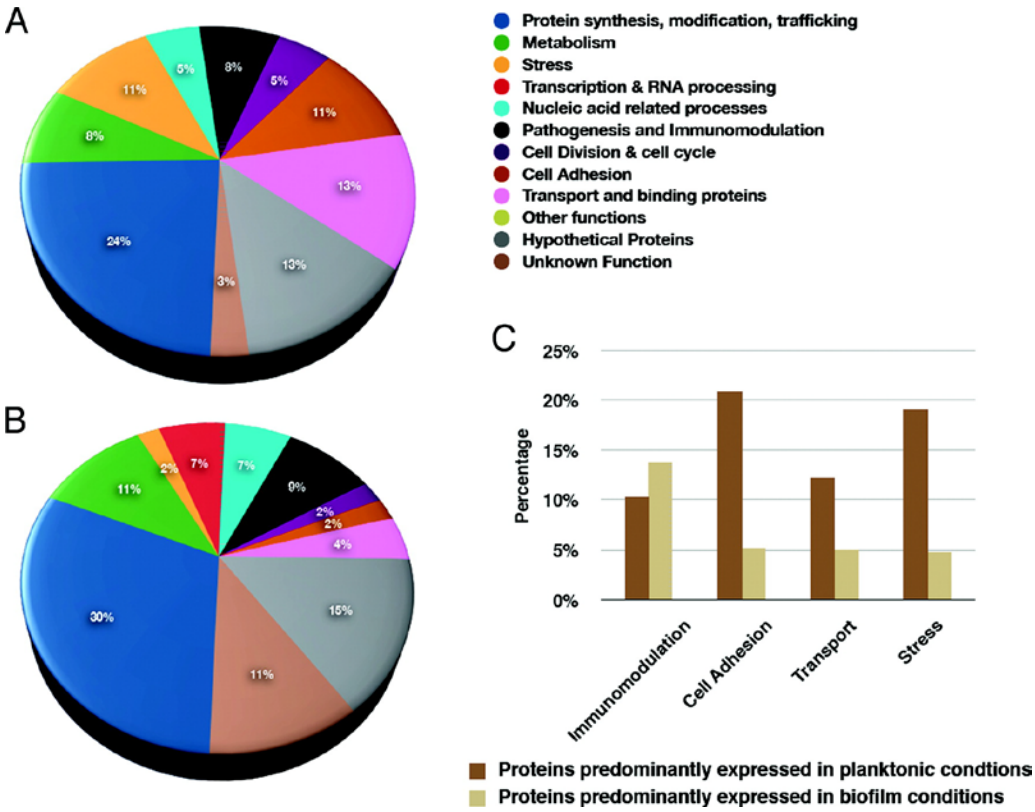

Figure 11: The biofilm growth form of nasal carrier strain of *SA*, in comparison to its planktonic counterpart contains marked differences in its exoproteome related to stress and immunoevasion.

The expression of proteins from the exoproteome of (A) the planktonic form of *SA* nasal carrier strain and (B) the biofilm form of the *SA* nasal carrier strain differ significantly in (C) proteins pertaining to stress, adhesion, immunomodulation and transport. Proteins were identified with high confidence (p <0.05) in three independent experiments (N=3).

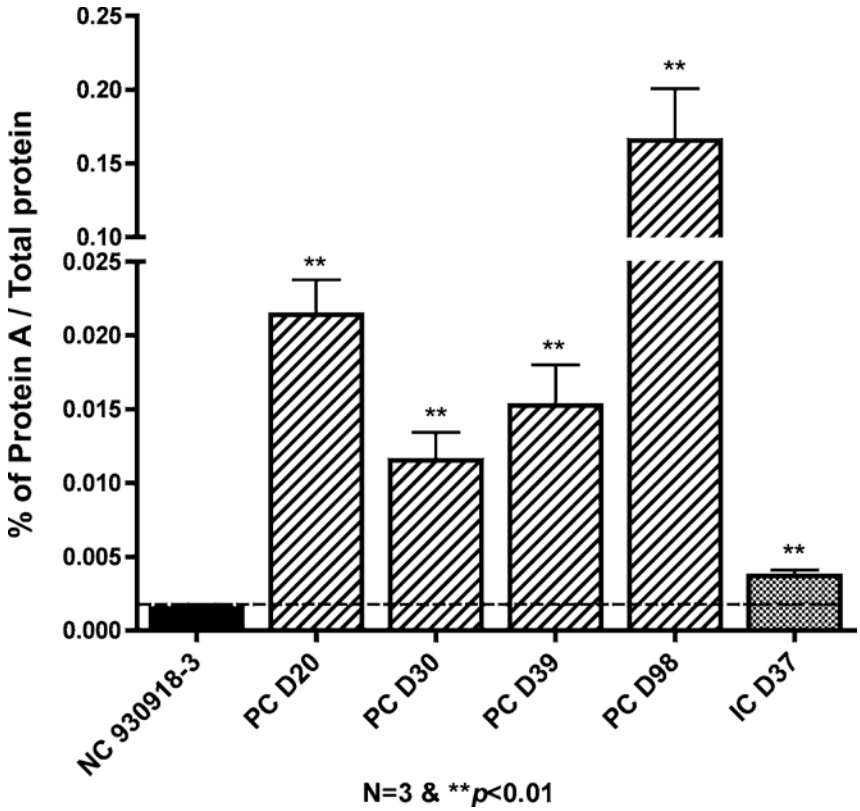

Figure 12: Immunomodulatory Staphylococcal protein A (SPA) is significantly up regulated in nasal carrier strains of *SA* compared to its non-carrier counterpart.

The expression of SPA was measured in the exoproteomes of one non-carrier and 4 persistent carrier strains (PC) D20 (**p =0.001), D30 (**p =0.006), D39 (**p =0.007), D98 (**p =0.009) and 1 intermittent carrier (IC) D37 (**p =0.008), strain using anti-SPA ELISA and compared to non-carrier strain 930918-3. Equal volumes of total exoproteome from nasal carrier and non-carrier strains were used for ELISA in three independent experiments (N=3) and the result was expressed as percentage of SPA concentration to total protein concentration.

Peptide mass fingerprinting of SPA from the carrier strain revealed that one of the isoforms of SPA was 49.5 kDa. Subsequent MS/MS and *in silico* analyses revealed that the protein contains three IgG binding domains as found in most species of *Staphylococcus* and also a cell wall localization motif LysM [186]. This motif is responsible for SPA interaction with cell wall components of the bacteria but is not consistently present in all species of *SA* [181,186]. Furthermore, MS/MS analysis also revealed the repeated occurrence of the LysM motif in other proteins such as cell wall binding autolysin, and cell surface elastin binding protein (data not

shown). This repeated occurrence of LysM motif in important cell attachment proteins may indicate its possible involvement in *SA* nasal colonization.

Discussion

Through a comprehensive analysis of the exoproteomes of a nasal carrier strain of *SA* and a genetically similar non-carrier strain, we have endeavored to analyze proteins or groups of proteins, which may contribute to nasal carriage. In tandem, we compared the exoproteomes of biofilm and planktonic carrier *SA* cultures in order to evaluate possible determinants of nasal carriage. Interestingly, our results indicated that the exoproteome of the carrier strain of *SA* (D30) contains a greater number of proteins related to adhesion, protein transport and immunoevasion, and fewer stress proteins than its genetically similar non-carrier counterpart (930918-3). Similarly, an analysis of the exoproteome of the biofilm growth form of *SA* carrier strain revealed a greater number of immunoevasive proteins in comparison to its planktonic counterpart but fewer stress, adherence, and transport proteins.

Other researchers have examined various aspects of the *SA* proteome, with reference to proteins that promote adherence [83,187], immunoevasive proteins [84,188], total proteome [177], secretome [176], exoproteome [189] and surfacome [157] in addition to mRNA levels during nasal colonization [11,190]. However, our studies have focused on the difference between proteins in the exoproteome of a carrier strain of *SA* and a non-carrier strain in order to elucidate putative determinants that might influence *SA*'s ability to colonize nasal mucosa.

Several proteomics studies have indicated that *SA* proteins present in the extracellular milieu such as secreted and cell surface exposed proteins are highly diverse [157,178,191]. However, no correlation between nasal carriage and heterogeneity of these proteins was discussed. In contrast, our study not only identified similar heterogeneity in cell surface and secreted proteins, but also deduced a marked difference in profile of cell surface and secreted proteins between nasal carrier and non-carrier strains.

The adherence of the *SA* carrier strain to host cells is an integral process in nasal carriage. Although several adhesive proteins have already been identified as important factors for nasal carriage [77,83,105] our exoproteome analysis has revealed that the carrier strain of *SA* contains twice as many adhesive proteins as a non-carrier strain. The results have highlighted the importance of SasD and SrdH, which have hitherto not been considered important in nasal carriage. Together with high expression levels of Srt, this seems to be indicative of high processing levels of membrane bound proteins, which is an important indicator in nasal carriage as considered by Burian and colleagues [11].

In contrast, *SA* carrier biofilm exoproteome secreted fewer adhesive proteins compared to the planktonic exoproteome. This may be expected as adhesion is already established once the carrier has formed a biofilm and subsequently the main function of the bacteria is survival and possibly ongoing detachment to aid in biofilm dissemination. Specifically, the adhesive D-alanine-activating enzyme (DltD) (responsible for D-alanylation of WTA during cell wall synthesis) was detected in the biofilm exoproteome [182]. It has been noted that inactivating the *dlt* operon in *SA* leads to increased susceptibility of *SA* to antimicrobial peptides including

defensins and protegrins [192]. Perhaps the presence of *dlt* operon in *SA* biofilms confers a multifunctional role of resistance to antimicrobial peptides, adhesion and biofilm formation.

Together with adhesion, immunomodulation is one of the key factors in the nasal carriage of *SA,* since it allows for long-term survival of the bacteria in the host [84,187]. Previously, we observed the ability of the carrier strain of *SA* (D30) to downregulate defensins and pathogen receptors [57], indicating the involvement of bacterial immunomodulatory proteins in *SA* nasal carriage. In support of this concept, the present results revealed that the nasal carrier isolates of *SA* contain a greater number of proteins that downregulate host immunity, whereas the non-carrier isolates contain a greater number of proteins that upregulate host immunity. This result is verified in Burian and colleagues' observations on nasal colonization [11]. A large proportion of these immunomodulatory proteins have also been corroborated in the surfacomes of the *SA* COL, Newman, RN6390 and USA300 [157]. Additionally, our proteomics approach revealed that the carrier strain biofilm revealed a similar trend with greater number of immunomodulatory proteins being found in the biofilm when contrasted with the planktonic growth form.

The high abundance of SPA, a versatile immunoevasive and binding molecule, may be linked to the carrier strains' overall immunoevasive strategy. Interestingly, differential SPA expression patterns even within persistent and intermittent carriers could advantageously be used as a diagnostic tool to differentiate them. Certainly, greater amounts of surface bound molecules with high levels of sortase could be associated with the observation that proteins involved in protein modification, secretion and trafficking are found in greater numbers in the carrier strain of *SA* in comparison to the non-carrier strain.

The rates of cell wall turnover found in *Staphylococcus* in general are quite high [193]. This constant turnover of the cell wall provides ample decoy material for *SA* to engage host innate defenses and is proportional to successful colonization of the human nasal passages [11]. This strategy can be seen in other pathogen/host dynamics such as *Schistosoma spp* and is referred to as sloughing [194].

Recently, researchers discovered that low concentrations of host chemokines, including CXCL9 and CXCL10, induce the release of SPA, while high concentrations of chemokines can also be antibacterial [195,196]. This echoes findings from our previous research on the effects of the cytokine IL-1α. We demonstrated that the carrier strain of *SA* downregulated the production of IL-1α during infection and IL-1α decreased the growth of *SA* carrier strain on nasal epithelial cells [153]. At this stage we have not assessed if the cytokine would also induce SPA. Since we detected multiple isoforms of SPA in the carrier strain of *SA* but not in the non-carrier, we suspect that it may be posttranslationally modified in sequential stages such as the glycosylation patterns observed in the Golgi apparatus [197]. Glycosylation of exoproteins such as SPA might play crucial roles in bacterial pathogenesis and immunoevasion [198]. We hypothesize that SPA is sequentially glycosylated in nasal carrier strains of *SA* and may be linked to nasal carriage.

One of the more surprising observations from our carrier strain exoproteome analysis was the low expression of stress proteins in comparison to the non-carrier strain. Perhaps, as observed by other authors, nasal colonization does not constitute a full-blown infection but rather a persistent sub-clinical infection [7,11]. Interestingly, transcript analysis of some key stress proteins also revealed that stress response stimuli are absent in the nasal milieu [11].

It has been postulated that *SA* develops resistance to nasal fluids by decreasing the uptake of antimicrobials or actively translocating them from the cell [179], and several bacterial transport proteins play vital roles in these processes. A greater number of transport proteins in the exoproteome of nasal carrier strain in comparison to the non-carrier strain could make it more resistant to antimicrobial agents in the nasal milieu. Specifically, several proteins from the ATP-binding cassette (ABC) transporter super family and the protein-export membrane protein SecF (part of the bifunctional translocase SecDF) were found in much higher levels in the carrier strain. Further investigation into the implications of these results and the role of these transport proteins in the nasal carriage of *SA* is currently being pursued.

Increasing evidence suggests that the phenomenon of *SA* nasal carriage is a complex host-pathogen interaction for which the bacteria have evolved numerous immunoevasion strategies for successful colonization of the host [7,57,153]. Our current exoproteomic study suggests that the *SA* nasal carrier strain is able to adapt itself to the human nasal passages by secreting a distinct repertoire of proteins in comparison to the non-carrier strain. Indeed, we have elicited the identities of several underreported proteins, which may be important in the nasal carriage of *SA*. Additionally, while it is not known if every carrier strain of *SA* adopts a biofilm mode of growth in the nose, it has become increasingly apparent that a biofilm mode of growth may be more representative of the *in vivo* condition [199,200]. This comparison can be a foundation for future studies to identify fully the state of *SA* in the nose and its contributing factors. In conclusion, this exoproteome analysis has elucidated important strategies adopted by the *SA* carrier strain in its dissemination through nasal carriage that further augments our understanding of nasal carriage of *SA*.

CHAPTER 4: ESSENTIAL ROLES PLAYED BY HOST IMMUNE RESPONSES AND STAPHYLOCOCCAL PROTEIN A DURING *STAPHYLOCOCCUS AUREUS* NASAL CARRIAGE

Introduction

Staphylococcus aureus (SA) causes many nosocomial and community-acquired infections in humans, ranging from mild skin and soft tissue infections to severe and often fatal pneumonia [109]. The anterior nasal region is the primary reservoir of *SA* in humans and approximately 30% of the normal population carries *SA* asymptomatically in their nares at any given time, with as much as 60% of the population carrying *SA* transiently when monitored longitudinally over time [2,9,110]. *SA* nasal carriers have an increased risk of being infected by their nasally carried *SA* [12,13] as well as transmitting infectious *SA* to others. A better understanding of factors that influence nasal carriage of *SA* will be necessary to reduce the risk of these infections.

SA nasal carriage is a multifactorial process involving the dynamic interplay between both host and bacterial factors in nares [2,39,40]. *SA* nasal carriage studies performed in rodent and human models have helped define bacterial determinants of carriage, including wall teichoic acid (WTA), clumping factor B, iron-regulated surface proteins IsdA and IsdH [77,82,105-107].

More recently, reports have increasingly implicated host processes as the major determinants of *SA* nasal carriage (reviewed in [2,40,147]). Human genetic studies have revealed an association between polymorphisms in host genes and persistent *SA* nasal carriage [41,42,44,45]. Human nasal secretions contain several components that are critical to innate mucosal defense. However, secretions from nasal carriers were defective in killing *SA* strains

and the presence of hemoglobin in nasal secretions promotes *SA* nasal colonization by inhibiting *agr* quorum sensing in *SA* [7,49,50]. Additionally, *SA* carrier strains subvert innate host defenses on nasal epithelia *in vitro* and a recent murine-model based colonization study observed *SA* clearance to be largely dependent on neutrophil influx and mediated by T-lymphocytes [57,108,153]. Collectively, these studies underscore the importance of host factors in influencing nasal carriage.

We surmised that *in vivo SA* nasal colonization, which accounts for the dynamic interaction between host and bacteria, would best determine factors that influence carriage [201]. Holtfreter and colleagues demonstrated that experimental nasal colonization in humans with avirulent NCTC 8325-4 did not boost humoral responses or elicit new antistaphylococcal antibodies and that anti-*SA* antibody profiles were highly variable among individuals [72]. Additionally, Burian and colleagues observed that long term *SA* nasal colonization on intact epithelium is insufficient to induce a strong antibody response [70] and such responses usually are triggered by *SA* infections [69,189,202]. These studies suggest that carriage is less controlled by differences in antibody response against *SA* and more by host innate immune responses during colonization.

Until now no studies have used human experimental colonization approaches to study host innate immune responses to *SA* nasal carriage or investigate how the host response influences nasal carriage of *SA* strains rendered deficient in putative determinants of carriage. In the current study, we autologously recolonized human noses with their own strains of *SA* to explore intranasal survival of *SA* and its relationship to host immune factors that mediate nasal carriage of *SA*. We observed that *SA* nasal carriage was dynamic and was influenced by

differences in global immune responses during carriage. We observed that proinflammatory cytokines and chemokines were significantly induced during nasal clearance of *SA*, while extended carriage of *SA* was observed in the absence of an immune response. To understand how the immunoevasive protein staphylococcal protein A (SPA) modulates the host response, a subset of participants were subjected to autologous nasal co-colonization with wild-type (WT) *SA* and its isogenic mutant lacking functional SPA (*Δspa*). Intriguingly, when the host mounted an immune response to colonization, autologous *Δspa* strains were cleared significantly faster compared to WT, indicating the role played by SPA in maintaining persistence of *SA* in the nares. Taken together, our studies demonstrate *in vivo*, the direct involvement of host immune responses in *SA* nasal survival and identify SPA as a likely determinant of *SA* nasal carriage.

Materials and Methods

Ethics statement

All participants were adults, >21 years of age, who provided informed consent to participate in the current study, which was performed at the University of Central Florida (UCF).
The *SA* recolonization protocol and all procedures involved in sample collection were approved by UCF's Institutional Review Board (IRB), which is fully accredited by the Association for the Accreditation of Human Research Protection Programs (AAHRPP). Per the request and approval of UCF's IRB, oral consent was obtained from each participant, which was documented by the study investigators. Participant names were associated with unique

identifier codes, and this confidential identifying information was kept under lock and key with access granted only to the study investigators.

Participant population and SA strains used in the study

A total of 20 different autologous human nasal recolonization studies in 40 nostrils were performed using each participant's own nasal *SA* strain isolated previously. See Table 6 for details about participants and their naturally colonizing *SA* strains. In total, 11 healthy individuals (6 males and 5 females, median age 38 years, range 22-47 years) participated in this study. These nasal *SA* carriers were selected from among 109 healthy individuals whose carriage status was monitored longitudinally for *SA* nasal carriage for a period of up to three years [203]. All participants adhered to the study protocol and none of the volunteers experienced any adverse effects during the study period.

Autologous recolonization of SA in human nares

The nasal carriage status of the participant was determined prior to decolonization treatment. For eradication of bacteria from nares, protocols described elsewhere were adapted with minor modifications [10,77]. All participants self-administered mupirocin nasal ointment (Bactroban, GlaxoSmithKline, Philadelphia, PA) topically twice a day for 5 days to decolonize microbial flora present in their anterior nares. One week after the final treatment, colonization status was assessed and nasal secretions were collected as described below. Subsequently, *SA* nasal inoculation was performed using protocols previously described [10,77]. Briefly, each participant's own previously isolated nasal *SA* strain was grown to log phase in Trypticase™ Soy

Broth (TSB; Becton, Dickinson and Company, Franklin Lakes, NJ) for 2.5 hours at 37 ^{o}C and 250 rpm, then harvested by centrifugation and washed with HBSS (Fisher Scientific, Pittsburgh, PA). Each nostril of the participant was inoculated with 2 X 10^{7} CFUs of *SA* on two consecutive days. All *SA* strains introduced into participants were confirmed for mupirocin sensitivity prior to experimental recolonization.

Nasal swabbing was performed every 2 to 3 days post inoculation for a period of up to 35 days using established protocols [203,204]. In summary, the anterior region of each nostril was swabbed with sterile unflocked polyester-tipped swabs (Fisher Scientific) and dipped in 2 mL of TSB to extract the microbial flora from the swab. 100 µL of this culture was plated on tryptic soy agar (TSA) containing 5% sheep's blood (Becton, Dickinson and Company) and incubated at 37 ^{o}C for 16 hours. Bacterial colonies were identified as *SA* using Staphyloslide^{TM} Latex Test reagent (Becton, Dickinson and Company) and enumerated for all days on which follow-up cultures were performed. *SA* colonies were also genotyped using *spa* typing and compared to that of the inoculated *SA* strain using primers and PCR conditions described previously [37,38,203].

Nasal fluid collection and processing

Nasal secretions were collected throughout the *in vivo* recolonization study at 7 days prior to *SA* nasal inoculation (Day -7) and multiple times every week post inoculation for a period of up to 35 days as described previously [7] using a vacuum-aided suction device. When required, brief microtip sonication was performed for 10 seconds on ice to homogenize nasal fluid samples.

Cell lines and culture conditions

Human nasal epithelial cells (RPMI 2650; American Type Culture Collection (ATCC), Manassas, VA) were grown at 37°C, 5% CO_2 and seeded on collagen-coated Transwell inserts (0.4-µm pore-size, both 12-mm and 24-mm diameter; Corning Inc., Corning, NY) for experiments as described previously [57,205,206]. Once confluent, Transwells were exposed to the air-liquid interface (ALI) at 37^{o}C and 5% CO_2, and treatments were performed within 4-7 days following ALI exposure, when each well exhibited a nasal cell layer capable of sealing the basal media away from the apical compartment of the Transwell.

Targeted genetic disruption of spa in SA nasal carrier strains

Site-directed disruption of staphylococcal protein A (*spa)* was performed using TargeTron-based insertion of mobile group II introns into *spa* (Sigma-Aldrich, St. Louis, MO), as per the *SA*-specific procedure described by Yao and colleagues [207]. Here, the TargeTron methodology was significantly modified, as the naturally colonizing nasal carrier *SA* strains were refractory to genetic transformations due to Type I and Type IV restriction barriers. To circumvent these restriction barriers and enable gene disruption in these natural isolates, *spa*-pNL9164 intron insertion plasmids were passaged through high-efficiency *E. coli* cloning strain DC10B [208] prior to electroporating into *SA*. Subsequently, site-specific intron-insertion in these natural isolates was confirmed by PCR and sequence analysis. A total of 4 different *spa*-disrupted (*Δspa*) *SA* nasal strains were generated. Table 6**,** Table 7 and supplemental Table 14 list all the *SA* strains, plasmids and oligonucleotides generated and used in this study.

Immunodetection of analytes from host nasal secretions and SA lysates

Processed nasal secretions collected from participants during nasal recolonization were analyzed using Bio-Rad multiplex cytokine array (Bio-Rad Laboratories Inc., Hercules, CA) to detect 27 different cytokines and growth factors (IL-1β, IL-1Ra, IL-2, IL-4, IL-5, IL-6, IL-7, IL-8, IL-9, IL-10, IFN-γ, IL-12, IL-13, IL-15, IL-17, IP-10, MCP-1, MIP-1α, MIP-1β, PDGF, RANTES, TNF-α, Eotaxin, FGF basic, G-CSF, GM-CSF, and VEGF) according to the manufacturer's instructions. For the detection of expressed SPA, cell wall and exoprotein fractions of WT and *Δspa SA* grown to exponential phase were prepared using protocols previously described with minor modifications [209,210]. Bacterial lysates equivalent to 5 million CFUs were resolved by SDS-PAGE alongside 100ng of recombinant staphylococcal protein A (Sigma-Aldrich), used as a standard. Gels were transferred on to PVDF membranes (Millipore Corporation, Bedford, MA) and blotted with either rabbit polyclonal antibody against SPA (catalogue # ab60206; Abcam, Cambridge, MA) or mouse monoclonal antibody against SPA (catalogue # ab49734-200; Abcam). In addition, SPA expression in WT and *Δspa* were quantified using the Assay Designs protein A Enzyme Immunometric Assay (EIA) kit (Enzo Life Sciences International, Plymouth, PA) as per the manufacturer's instructions. Protein sample preparation from WT and *Δspa SA* grown to exponential phase were prepared using protocols previously described with modifications [49,211]. Briefly, *SA* cells were lysed with 10% acetic acid and vortexed for 30 min at ambient temperature for protein extraction. The recovered soluble proteins extracts were concentrated and used for SPA ELISA.

Growth studies to determine the fitness of isogenic Δspa mutant SA in comparison to wild-type SA

In vitro growth studies in nutrient rich TSB, or minimal media (Dulbecco's Modified Eagle's Medium (DMEM; Mediatech, Inc., Manassas, VA) supplemented with 0.05% fetal bovine serum (FBS; Gemini Bioproducts, West Sacramento, CA), were performed for up to 24 hours using WT and isogenic mutant (*Δspa*) *SA* strains at 37^{o}C and 250 rpm, after which the samples or their dilutions were plated on TSA plates and incubated at 37^{o}C for 16 hours. CFUs were enumerated to determine the growth of these strains. Additionally, turbidity assays and micro-CFU assays were performed using WT and isogenic mutant *SA* strains using protocols described previously [205,212].

Growth studies on human nasal epithelial cells were performed as described previously [57,153,205]. Briefly, 50 to 100 CFUs of either WT or isogenic mutant *SA* were inoculated topically on confluent monolayers of nasal epithelial cells exposed to ALI. At each timepoint post *SA* treatment, non-adherent *SA* was collected by rinsing with PBS (termed "wash fraction") and adherent *SA* was collected by scraping the cells and subjecting them to mild sonication (termed "adhere fraction"). Dilutions of the wash and adhere fractions were plated on TSA, incubated at 37^{o}C for 16 hours and subsequently CFUs were enumerated to determine the growth of *SA* on nasal epithelial cells.

Autologous nasal co-colonization using WT and Δspa strains

The study design for the experimental nasal recolonization studies, using both WT and *Δspa* strains, is similar to the protocol described above, but with minor modifications. A total of 7 nasal colonization studies in 14 nostrils were performed (N= 4 strains, 3 participants, and 1-2 replicates each). Recolonization was performed by applying 10^7 CFUs per strain of WT and *Δspa* strains (1:1 mixture) in each nostril of the participant. Follow-up cultures and nasal fluid collection were performed, and comparative strain survival of WT and *Δspa* strains was determined using a combination of CFU enumeration and colony PCR with primers that detect intron integration in *Δspa* (primers described in supplemental Table 14).

Statistical analyses

All analyses were performed using Microsoft Excel (Microsoft Corporation, Redmond, WA) or GraphPad Prism 4 software (GraphPad Software, La Jolla, CA). For all growth studies either Student's t-test or two-way ANOVA with Bonferroni posttest was performed for comparisons. All *in vivo* experiments that were carried out for the complete term of the study (22 days or more) were included. For multiplex cytokine data obtained from nasal secretions, total picograms of each cytokine at each sampling time were calculated based on the volume of nasal fluid obtained. For comparing total cytokine expression levels pre (day -7) and post *SA* inoculation, non-parametric Man Whitney test, Wilcoxon rank test were performed where appropriate. For calculating aggregate fold change in cytokine expression (i.e. aggregate immune response), picograms/donor cytokine levels were log-transformed, converted to fold expression in comparison to mupirocin-treated, pre-inoculation timepoint (day -7) and summed

for all cytokines for each day of collection. Subsequently, aggregate fold changes in cytokine expression were compared between *in vivo* studies with *SA* nasal clearance and *SA* nasal survival. *SA* carriage patterns in competitive recolonization studies with WT and *Δspa* strains were analyzed using Kaplan-Meier survival curves with log rank tests and mean survival time calculations.

Results

Nasal carriage state depends on inflammatory host response to SA colonization

Previous studies have shown that nasal secretions collected from *SA* nasal carriers support the growth of *SA in vitro* and that *SA* carrier strains subvert innate host defenses to better attach to nasal epithelia in culture [7,49,57,153]. In the current study, we sought to identify human host factors that contribute to *SA* nasal carriage *in vivo*. We autologously colonized healthy participants, previously identified as *SA* nasal carriers and monitored for 1-3 years, with their previously characterized strains of *SA*. All participants were subjected to a five-day treatment with topical nasal mupirocin to decolonize the nose of *SA*. Each participant's own previously isolated *SA* strains were used in all experimental colonization studies to account for the specificity of host-bacterial associations during *SA* recolonization studies (see Table 6 for strain and participant details). Post inoculation, *SA* nasal survival was monitored at regular intervals for more than 3 weeks by nasal swabbing and CFU enumeration to determine *SA* clearance rates.

Interestingly, in the majority of the autologous inoculations, we observed complete

clearance of *SA* from the nares (Figure 13A**,** $p < 0.001$, N = 15), and at least a one log-reduction in *SA* load occurred within one-week of inoculation. The median survival of *SA* in participants during complete nasal clearance was 10 days (Figure 13A). We also observed that levels of non-*SA* commensal flora in the nose were not significantly affected due to mupirocin nasal treatment as commensal levels were restored within 10 days post mupirocin treatment, which immediately preceded the first autologous *SA* recolonization for each participant (Figure 13B). Moreover, non-*SA* commensal flora levels remained relatively unaffected throughout the duration of the study post *SA* inoculation (Figure 13B).

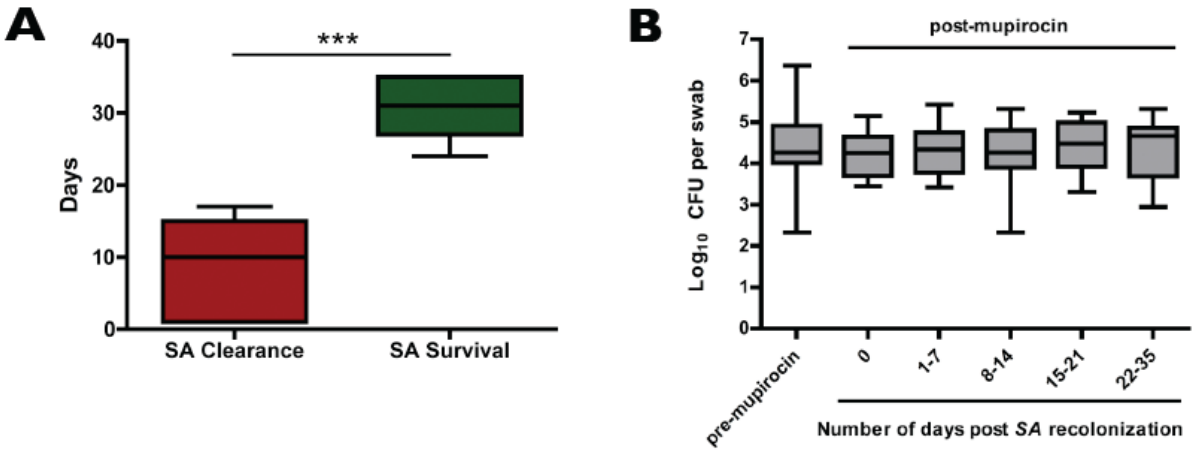

Figure 13: Human autologous recolonization using naturally colonizing nasal SA strains revealed distinct carriage patterns within our cohort.

(A) *SA* nasal survival rate in participants post inoculation is indicated in days (***$p < 0.001$, N=15). (B) Shown are matched comparisons of non-*SA* commensal CFU levels pre-mupirocin and post-mupirocin nasal treatment in a subset of participant's involved in recolonization studies.

To determine if host inflammatory factors influence carriage, whole nasal secretions were collected throughout the *SA* recolonization study period and analyzed for a diverse panel of 27

different cytokines, chemokines, and growth factors (list of analytes provided in Methods).

Table 6: Participants and *SA* strains isolated from nasal carriers used in this study

***Staphylococcus aureus* strains**	**Participants information**	**MLST**	**Spa type**	**Reference**
D20	Isolated from D20	ST30	t12255	[7]
D20-24	Isolated from D20	ST5	t688	[203]
D502-9	Isolated from D502	ST105	t056	[203]
D528-11	Isolated from D528	ST8	t008	[203]
D547-14	Isolated from D547	ST5	t688	[203]
D637-7	Isolated from D637	ST8	t2648	[203]
D713-4	Isolated from D713	ST5	t548	[203]
D720-7	Isolated from D720	ST1657	t1001	[203]
D756-3	Isolated from D756	ST2227	t012	[203]
D757-5	Isolated from D757	ST8	t008	[203]
D830	Isolated from D830	ST2233[#]	t12893[#]	This study
D831	Isolated from D83	ST22	t852	This study
D20 *Δspa* (with disrupted *spa* gene)	D20	ST30	t12255	This study
D20-24 *Δspa*	D20	ST5	t688	This study
D547-14 *Δspa*	D547	ST5	t688	This study
D830 *Δspa*	D830	ST2233[#]	t12893[#]	This study

[#] Previously unidentified MLST allele profiles and/or *spa* types

Analytes IL-2, IL-4, IL-5, IL-9, IL-10, IL-13, IL-15, IL-17, MIP-1α, RANTES and GM-CSF were expressed at very low concentrations (< 10 picograms/donor) and so were excluded for further analyses. Expression levels of these factors were compared to levels observed in donor-matched pre-inoculation nasal fluids (Supplemental Figure 22**,** N=15 experiments). Further,

aggregate fold change for each cytokine, which is based on whether analyte concentrations increased or decreased as compared to donor-matched pre-*SA* inoculation cytokine levels was calculated. Subsequently, fold change represented with distinct color assignments of red shades for increases in expression upregulation and green shades for decreases in expression (Supplemental Figure 22).

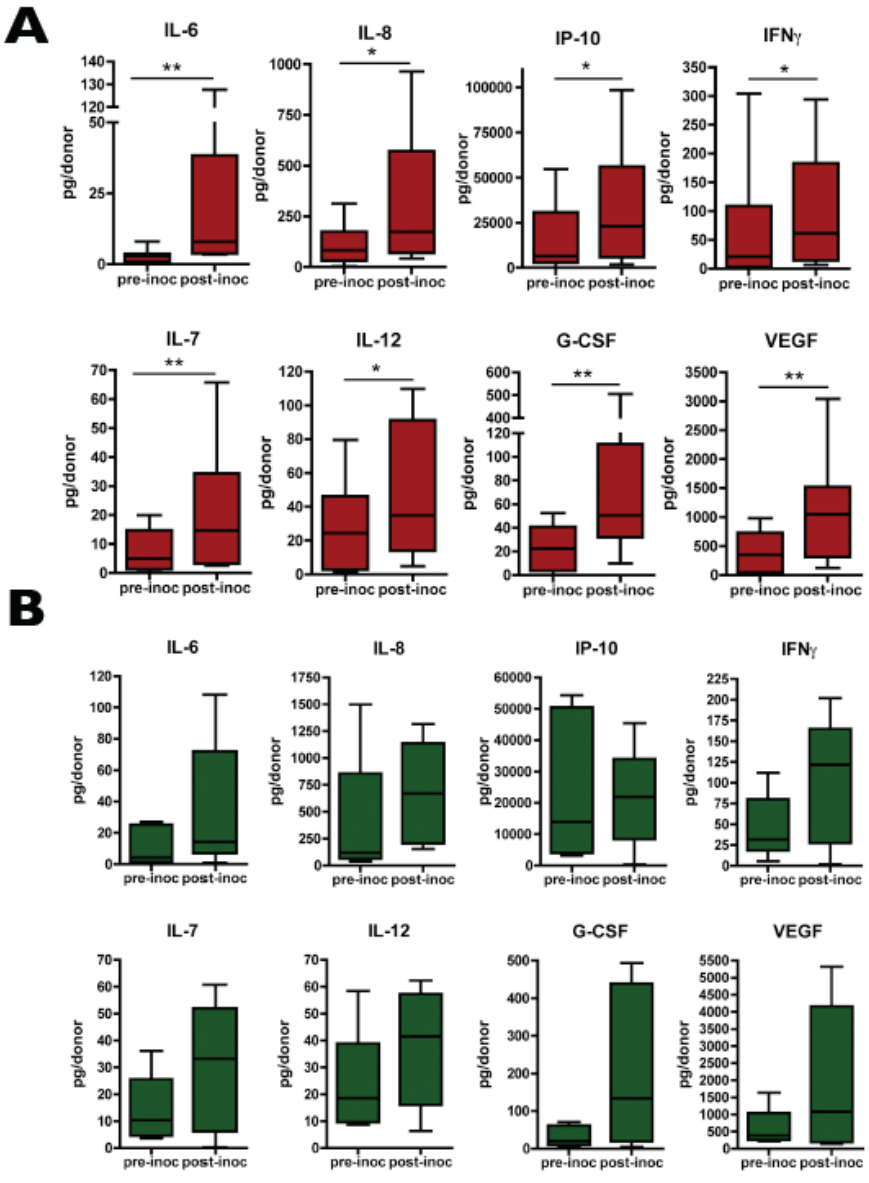

Figure 14: Significant induction of proinflammatory cytokines, chemokines and growth factors causes *SA* nasal clearance

Shown are matched pre-inoculation and post-inoculation expression levels of cytokines (picograms/donor, N=15) during **(A)** *SA* nasal clearance and **(B)** *SA* nasal survival. Cytokines IL-6 (**p= 0.004), IL-8 (*p= 0.048), IP-10 (*p= 0.027), IFNγ (*p= 0.037), IL-7 (**p= 0.002), IL-12 (*p= 0.019), G-CSF (**p= 0.004) and VEGF (**p= 0.002) were significantly induced post-inoculation only during *SA* nasal clearance.

Table 7: *E. coli* strains and plasmids used in this study

Bacterial strains or plasmids	Description	Source or Reference
***Escherichia coli* strains**		
Max efficiency DH5α	High transformation efficiency cloning strain	Life Technologies
DC10B	DNA cytosine methyltransferase mutant of an *E. coli* cloning strain. Passage of *SA* specific plasmids through DC10B enables genetic manipulation in refractory *SA* strains	[208]
Plasmids		
pNL9164	Temperature sensitive TargeTron Plasmid (*E. coli-SA* shuttle vector) for targeted insertion of group II intron in *SA*	Sigma
D20 *spa*-pNL9164	TargeTron plasmid to functionally disrupt *spa* gene in nasal carrier strain D20	This study
D547 *spa*-pNL9164	TargeTron plasmid to functionally disrupt *spa* gene in nasal carrier strains D20-24, D547-14 and D830	This study

Interestingly, proinflammatory cytokines, chemokines and growth factors including IL-6, IL-8, IP-10, and VEGF were significantly induced post-inoculation during *SA* nasal clearance (Figure 14A). Importantly, no significant induction of host inflammatory responses were observed during *SA* nasal survival (Figure 14B) suggesting that the immune state of a participant predisposes *SA* nasal carriage. Remaining cytokine data are included in supplemental Figure 23**.** In addition, overall host immune responses in participants during *SA* colonization were analyzed by computing cumulative expression levels (picograms/donor) of all 16 analyzed cytokines pre- and post-inoculation during *SA* nasal clearance and survival in participants (Figure 15A). We

observed that the total cytokine response was significantly upregulated post-inoculation only during nasal clearance of *SA* (Figure 15A, $p = 0.01$). Intriguingly, aggregate fold change in cytokine expression was significantly higher in participants during clearance than in participants during *SA* nasal survival (Figure 15B, $p = 0.046$). Moreover, aggregate fold change in participants calculated over the duration of the study period during *SA* clearance was also significantly higher than during *SA* survival (Figure 15B, $p = 0.041$). Collectively, these observations suggest that induction of robust inflammatory response to colonizing *SA* leads to nasal *SA* clearance.

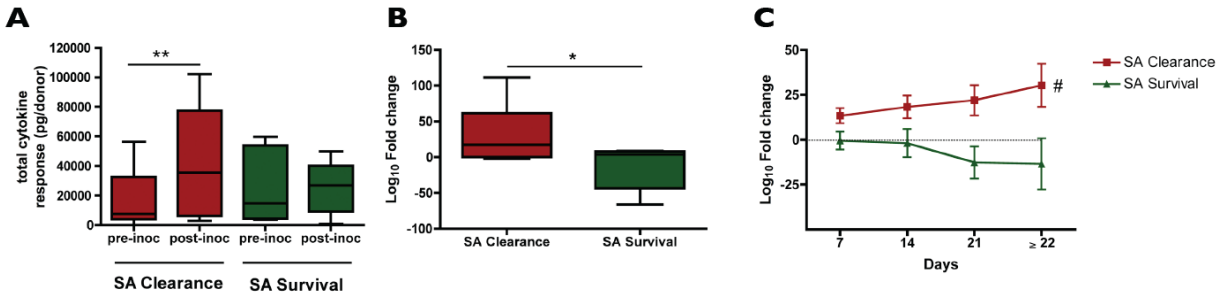

Figure 15: Host immune response during SA nasal colonization corresponds to persistence or clearance

(A) Shown are the cumulative expression levels (picograms/donor) of all 16 analyzed cytokines pre-inoculation and post-inoculation during *SA* nasal clearance and *SA* survival in participants. The total cytokine response was significantly upregulated post-inoculation only during *SA* nasal clearance (** $p = 0.01$, N=15). (B) Shown is the comparison of aggregate fold change in cytokine expression normalized to pre-inoculation levels in participants following > 21 days of monitoring and segregated by *SA* colonization. Aggregate fold change is significantly higher during *SA* nasal clearance (* $p = 0.046$, N=15). (C) Aggregate fold change in cytokine expression calculated over time in participants during *SA* clearance and survival. Aggregate fold change over time is significantly higher during clearance ($^{\#}p = 0.041$, N=15).

Isogenic SA mutants lacking SPA exhibited increased clearance rates compared to WT in human nares

From the recolonization studies with wild-type (WT) community-acquired *SA* isolates presented above, we observed that local inflammatory responses influence *SA* carriage. To confirm the involvement of host immune responses to nasal carriage, we hypothesized that disruption of an immunomodulatory bacterial protein would alter host inflammatory responses and affect carriage. Staphylococcal protein A (SPA) plays a key role in *SA* immune evasion by interfering with neutrophil phagocytosis and complement activation [84,96]. Recently, Falugi and colleagues demonstrated the role of SPA in subverting adaptive immune responses *in vivo* [213]. We postulated that SPA contributes to modulation of host nasal immune responses, and thus could affect the survival of *SA* in human nares. Toward this aim, in a subset of participants within our cohort, we sought to perform autologous recolonization studies with equal concentrations of WT and *spa*-disrupted (*Δspa*) *SA* nasal carrier strains.

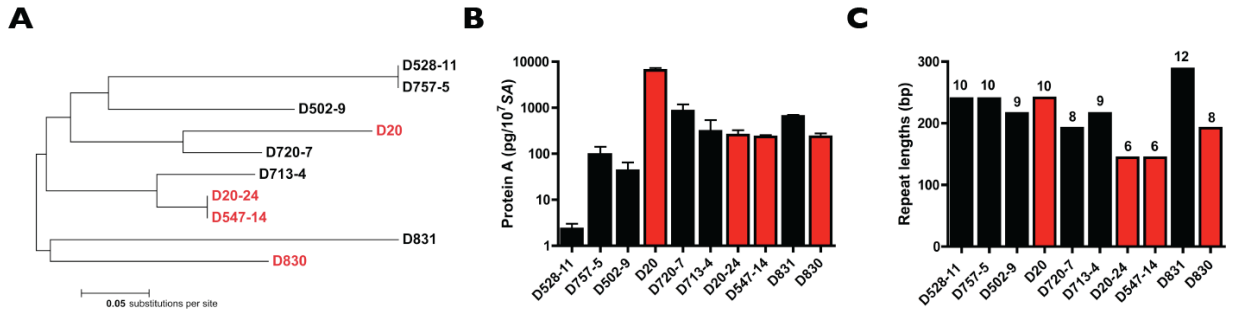

Figure 16: Evolutionary and expression analyses of SPA in SA nasal carrier strains within our cohort

(A) Evolutionary relationships of WT *SA* strains based on *spa* typing is depicted using the Neighbor-Joining method. The tree is drawn to scale, with branch lengths in the same units as those of the evolutionary distances used to infer the phylogenetic tree. (B) SPA expression in *SA* nasal carrier strains used in the autologous recolonization was measured using anti-SPA ELISA. (C) *spa* repeat domain lengths and number of short sequence repeats (number above each bar) of all *SA* nasal carrier strains are also represented. Taxa labels in (A) Bar graphs in (B), (C)

colored in **black** indicate *SA* carrier strains used in WT recolonization studies, those in **red** indicate strains used in competitive recolonization with WT, *Δspa* strains. Nasal carrier strains D547-14 and D830 were used in both types of recolonization studies.

We previously showed that expression levels of SPA produced by *SA* nasal carrier strains *in vitro* corresponded to the level of persistence of *SA* and type of carriage in the human nose [120]. Additionally, Garofalo and colleagues demonstrated that length of the polymorhphic region of SPA regulates inflammatory responses *in vivo* [214]. Our analyses of polymorphic regions of *spa* of *SA* strains used in WT *SA* recolonization and SPA expression levels revealed marked heterogeneity within the cohort (Figure 16). Therefore, a convenient subset of participants and *SA* strains based on number of *spa* repeat units and SPA expression levels were selected and *spa*-disruption and recolonization was performed.

To achieve isogenic mutants lacking SPA, we performed site-directed disruption of the gene using the TargeTron gene knockout system (Figure 17A; see Table 6 for all mutant *SA* strains). Unlike traditional allelic exchange gene knockout methods, the TargeTron methodology does not utilize antibiotic-selectable markers and thus eliminates the possibility of introducing *SA* strains, which are resistant to these antibiotics, into human participants during experimental *SA* recolonization. The absence of SPA expression in *Δspa* strains was confirmed by anti-SPA Western (Figure 17B) and ELISA (Figure 17C**)**. Next, we determined if gene-disruption affected the fitness of *SA* nasal carrier strains. *In vitro* growth studies carried out in nutrient rich media (Figure 17D**)** and minimal media (Figure 17E) revealed no significant growth difference between WT and *Δspa* strains. Further, no growth differences were observed between WT and *Δspa* strains when cultured on nasal epithelial cells at the air-liquid interphase (Figure 17F and G**;** all strains presented in Figure 24). These results suggest that *spa*-disruption

did not affect the fitness of *SA* nasal carrier strains.

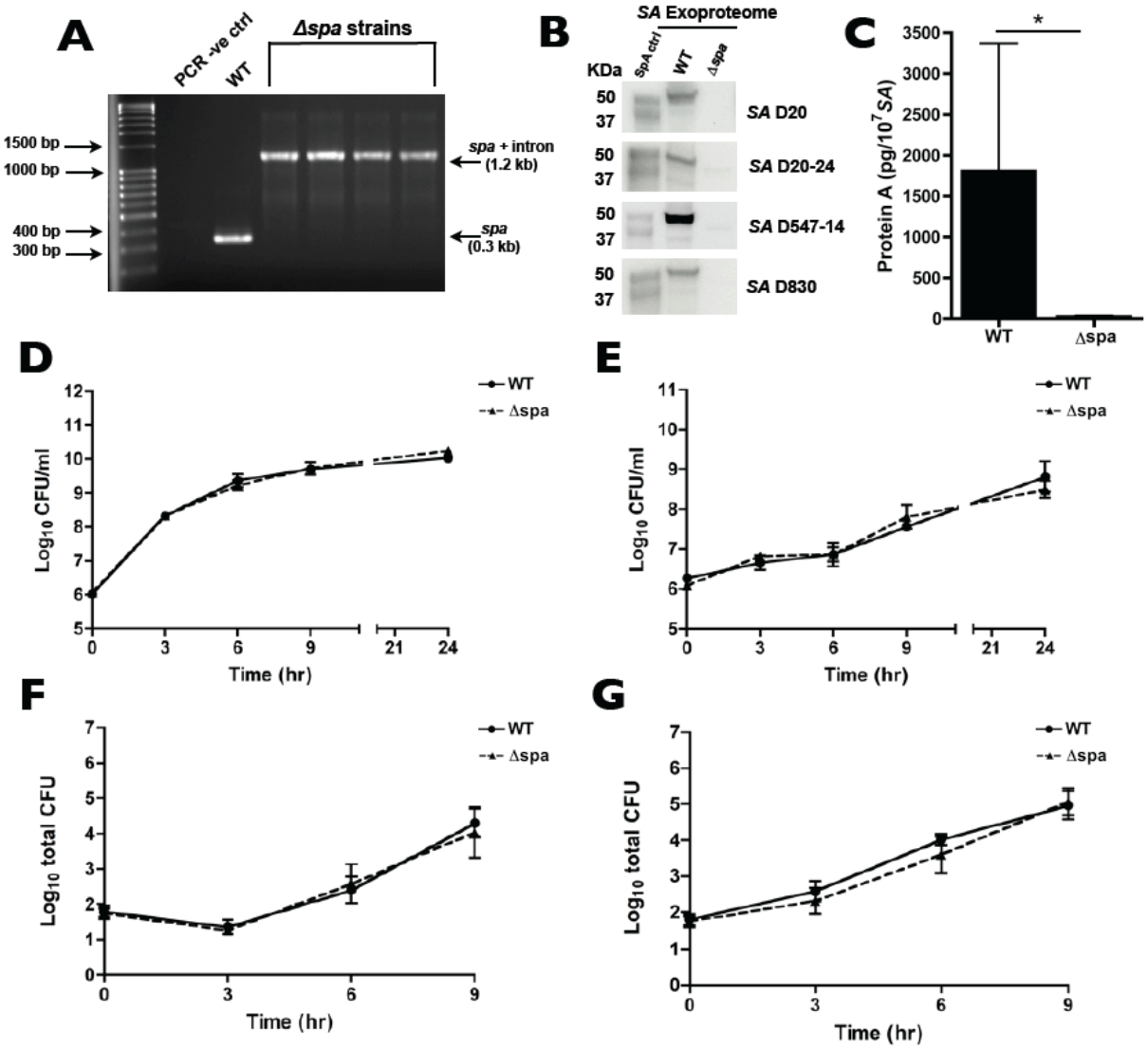

Figure 17: Functional disruption of *spa* did not affect the fitness of nasal carrier strains of *SA*

(A) Disruption of *spa* gene in *SA* nasal carrier strain D20. Shown is the PCR amplification of *spa* gene in WT and gene-disrupted *SA* strains. (B) Western immunoblot analysis of SPA expression in *SA* WT and *Δspa* strains. 100ng of recombinant protein A was used as a standard. (C) SPA detected by ELISA in WT and *Δspa* strains and concentration represented per 10 million CFUs of *SA* (N = 4, 3 replicates each, **p* = 0.014). Growth kinetics of D20 WT and *Δspa* strains in (D) nutrient rich media (TSB) and (E) minimal media (DMEM+0.05%FBS). (F) Wash and (G) adhere fractions from nasal epithelia inoculation with *SA* showed no growth difference between D20 WT and *Δspa* strains. No significant differences between WT and *Δspa* observed in panels D-G (N=3-4).

We next performed autologous recolonization with equal concentrations of WT and *Δspa* strains in human nares, and monitored host immune responses and nasal carriage of WT and *Δspa SA* strains. Because induction of robust inflammatory response determined nasal carriage with WT *SA*, the competitive recolonization studies were stratified based on aggregate fold changes in cytokine expression in the nasal secretions from participants. Interestingly, we observed that aggregate fold changes in cytokine expression from participants exhibiting an immune response were significantly higher than that of participants who induced any immune response (Figure 18A**,** $p = 0.019$). Intriguingly, in participants who mounted an immune response due to colonization, *Δspa SA* clearance rate was significantly higher than that of WT (Figure 18B; log rank: $\chi^2 = 4.051$, $p = 0.044$). Mean survival of *Δspa SA* (7.1 days) was significantly lower than that of WT *SA* (15.8 days) in participants that elicited a response (Figure 18C, $p = 0.035$). Conversely, in participants with low immune responses, no difference between WT and *Δspa SA* survival was observed (Figure 18D; log rank: $\chi^2 = 0.004$, $p = 0.948$). Likewise, no difference in mean survival was observed between WT (15.1 days) and *Δspa* (16.0 days) (Figure 18E, $p = 0.217$). Collectively, these studies strongly suggest that SPA is likely a co-determinant of *SA* nasal carriage in humans.

Discussion

SA primarily colonizes the anterior nares in humans and nasal carriage is established due to the complex interplay of bacterial factors and host factors during colonization [2,7,39,49]. How these factors lead to stable *SA* colonization in human noses is incompletely understood. Thus

acquiring knowledge about carriage factors is important for controlling carriage and dissemination of *SA*.

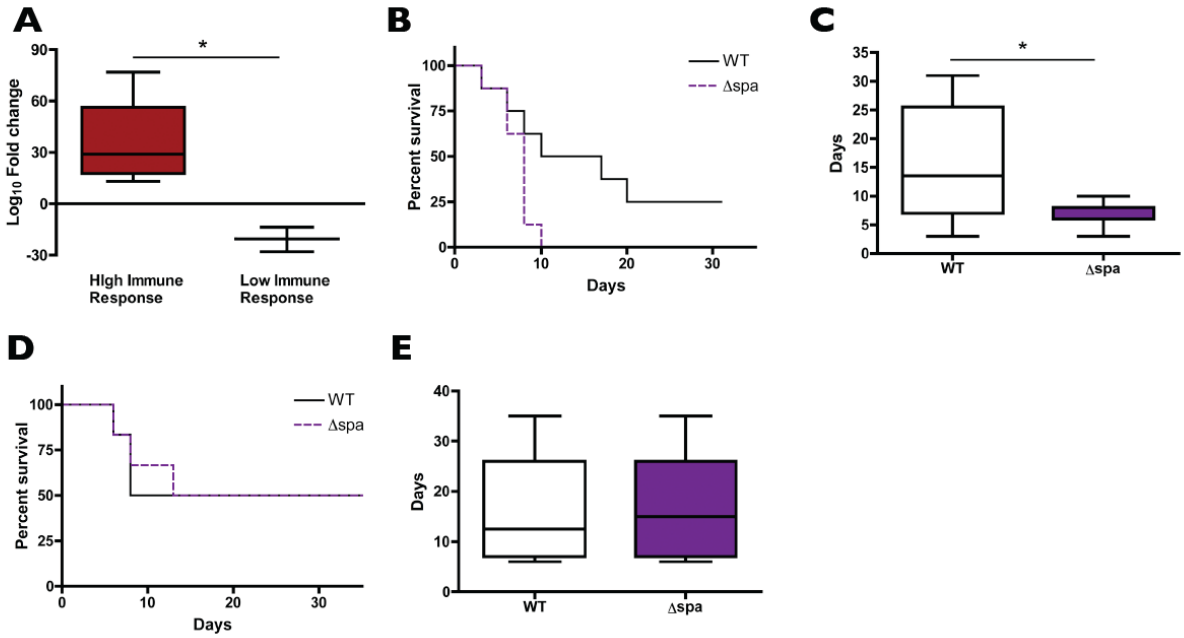

Figure 18: *Δspa SA* exhibits reduced persistence in human nasal colonization

(A) Aggregate fold change in cytokine expression levels (compared to day -7) of participants that produced high immune responses to *SA* compared to low response participants (**p= 0.006). Kaplan-Meier survival curves of WT (solid line) and *Δspa SA* (colored dashed line) in noses of participants mounting a (B) High or (D) Low immune response to colonization. *Δspa* strains' clearance rate was significantly higher than that of WT (*p= 0.0441) in studies with high immune responses only. (C) and (E) Median survival of *Δspa SA* compared to WT *SA* either in high and low immune response (*p = 0.035).

In the current study, we evaluated the role of host immune responses to *SA* nasal carriage by utilizing a controlled experimental recolonization model that heretofore is the most biologically relevant representation of intermittent *SA* nasal carriage in humans. Using this approach we revealed *in vivo* that the nasal carriage state is influenced by the host's inflammatory response to *SA* colonization. Interestingly, the majority of time the host elicited an immune response during nasal carriage, it led to rapid *SA* nasal clearance. Less frequently,

there was *SA* persistence, which was attributed to the host failing to elaborate any response following *SA* recolonization. Initially, this was surprising, as we had surmised that by reintroducing a participant's own *SA* isolate, nasal carriage would be easily restored. Moreover, since the *same* isolate of *SA* could persist in one recolonization experiment but not in the next, or vice versa, in the same participant, this points to a carriage state that is predominantly defined by the host's varied ability to respond to *SA*. van Belkum and colleagues reported that natural *SA* nasal survival was 14 days among intermittent carriers and greater than 154 days among persistent carriers [10]. Perhaps the attenuated immune responses to *SA* challenge that we observed in a subset of participants likely leads to persistent *SA* nasal carriage in certain humans.

Analysis of nasal secretions from autologous recolonization revealed that proinflammatory cytokines and chemokines secreted into nasal fluid were significantly induced during *SA* nasal clearance. We observed that cytokines IL-6 and IL-8 were significantly upregulated post inoculation during *SA* clearance. Epithelial cells respond to *SA* challenge, by producing IL-6 and IL-8, which are crucial for triggering host innate responses including trafficking of neutrophils to the site of infection to phagocytize *SA* and production of antimicrobial peptides that directly kill *SA* [100,215,216]. Neutrophil recruitment during infection is also tightly modulated by IFNγ and interestingly, this cytokine was significantly upregulated during clearance [217]. In addition, we observed that IP-10, a chemokine that binds to the receptor CXCR3 and recruits inflammatory cells to infection site was significantly upregulated during *SA* nasal clearance. Recently, IL-17-mediated T-helper 17 immune response was shown to play an important role in *SA* nasal clearance using murine models of colonization

[108]. Surprisingly, in our human colonization experiments, IL-17 was expressed in extremely low levels in nasal secretions. It is possible that IL-17 could be cell-associated and not secreted or that lower IL-17 expression is enough to activate T-lymphocytes. Nevertheless, it is clear that a predominantly epithelia-derived and neutrophil-mediated inflammatory host response likely causes *SA* nasal clearance *in vivo*.

Commensal flora of the nose, especially serine protease (ESP) secreting *S. epidermidis*, can reportedly protect the host from *SA* colonization [144,145]. Intriguingly, in *S. epidermidis* isolated from majority of participants during recolonization, presence of the *esp* gene was observed (103 of 124 *S. epidermidis* isolates from 8 participants; Table 15). Additionally, we observed that the overall levels of non-*SA* commensal flora in recolonization studies remained unaffected. However, the shift in nasal microbiome due to topical antibiotic use prior to autologous recolonization can influence host responses during *SA* nasal colonization. Nonetheless, the dynamic interaction between *SA* and resident commensals including ESP-secreting *S. epidermidis* in these recolonization studies and how they affect host defenses during colonization merits future investigations.

SA has evolved a repertoire of factors to evade the host's immunity and successfully colonize the nose [84]. SPA is important for *SA* immunoevasion [11,96,188] and interestingly, *in vivo,* we observed autologous *Δspa* strains being eliminated from the nares significantly faster than WT when the host elaborated an immune response to recolonization. The IgG domains of SPA bind to the Fc region of host immunoglobulins in a confirmation unrecognizable by neutrophils, thereby enabling to *SA* to evade neutrophil-mediated phagocytosis [84]. In our competitive recolonization studies, when the host elaborated an immune response, it is

possible that *SA* strains lacking SPA, or expressing significantly lower quantities of SPA were more efficiently phagocytized. Thus *Δspa* strains were more rapidly eliminated from the nares than WT strains. Additionally, expression studies both at transcript and protein levels revealed an association between SPA levels and persistence of *SA* carriage in the human nares [11,120]. Collectively, these results suggest that SPA is a likely co-determinant of human *SA* nasal carriage and a potential therapeutic target for developing novel *SA* nasal decolonization strategies.

SA virulence and host defense mechanisms during *SA* pathogenesis and infection have been described previously. However, comparatively little is known about the immune responses during asymptomatic nasal carriage of *SA*, which was surprising given the prevalence of carriage in humans. For the first time, by utilizing a highly relevant human autologous *SA* nasal recolonization model, we characterized the extent to which immune responses influence *SA* carriage. Given the association between risk of *SA* infections and nasal carriage, it is essential to completely understand the immune mechanisms underlying *SA* colonization in humans. This knowledge can aid in developing novel decolonization strategies to tackle carriage-associated *SA* infections.

GENERAL DISCUSSION, CONCLUSION AND FUTURE DIRECTIONS

SA nasal carriage occurs in approximately 30% human population asymptomatically and if *SA* breaches the physical and immunological barriers of the human host, it can invade the host resulting in systemic and often fatal infections. Importantly, it has been known that colonization by *SA* increases the risk of autoinfection [2,3,13,114]. *SA* nasal colonization is acknowledged to be multifactorial; however, our understanding of population structure, mechanism and factors responsible to *SA* nasal carriage is incomplete. In this dissertation, we sought to better understand *SA* nasal carriage dynamics in humans over time and elucidate critical host and bacterial determinants that are responsible for *SA* nasal carriage in humans.

Given that persistent nasal carriers of *SA* have higher risks for endogenous *SA* infection [12,115], it was necessary to investigate whether particular genotypes especially the more virulent *SA* (belonging to CC8, CC5, CC30 or CA-MRSA) preferentially colonize persistent carriers. In chapter two, we reported our findings of the population structure of *SA* nasal carriage strains from a cohort of persistent and intermittent carriers. Our comprehensive longitudinal sampling and discriminating genotyping studies (MLST, *spa* type, *clfB* type) revealed that *SA* carried by persistent and intermittent carriers exhibited high degree of genetic relatedness. This lack of genetic differences between *SA* strains colonizing persistent and intermittent carriers implies that host, nasal microbiome, and/or environmental factors could primarily determine carriage state in humans. But certain bacterial factors expressed in all *SA* (persistent and intermittent carrier *SA*) are critical for colonization [11,75,77]. Therefore, to better understand carriage, chapters three and four focused on determining host and bacterial

factors that are responsible for carriage. Towards this aim, we developed a highly relevant *SA* recolonization model in humans to study these factors that influence carriage.

Host factors are increasingly recognized to be major determinants of *SA* nasal carriage. Using *SA* recolonization, we provided first direct *in vivo* support for the essential role played by local inflammatory responses in the survival of *SA* in human nares. Importantly, analyses of nasal secretions during *SA* recolonization revealed that proinflammatory cytokines were induced during *SA* nasal clearance. This correlates well with *in vitro* studies on human nasal epithelial cells in which *SA* carrier strains was shown to subvert host innate immune responses by delaying TLR2 and suppressing the production of proinflammatory IL-1β [57,153]. Additionally, a recent study utilizing a rodent colonization model demonstrated that *SA* nasal clearance is dependent on IL-17 mediated T-helper 17 (Th17) immune response and subsequent neutrophil influx [108]. IL-17 is also a crucial regulator of antimicrobial peptide production including α defensins (Human neutrophil peptides (HNPs) 1-3 and Human β-Defensins (HBDs) 1-3 at mucosal surfaces [216,218]. Interestingly, presence of these antimicrobial peptides in nasal secretions from *SA* carriers indicates that a predominantly epithelially derived and neutrophil-mediated inflammatory host response influence nasal carriage outcome in humans [7,49]. It is not surprising that HIV-positive individuals with immune dysregulation or atopic dermatitis patients expressing lower levels of HBD-2 and cathelicidin (LL-37) have higher rates of *SA* persistent colonization than healthy individuals [18,20,21,219].

Secreted and surface proteins of *SA* including MSCRAMMs play a critical role in adhesion and immunoevasion of host during nasal colonization. Therefore, in chapter three, using quantitative proteomic approaches, we compared the exoproteins of nasal carrier *SA* strain and its genetically similar *SA* isolated from a skin of burnt of victim. Interestingly, we observed that greater number of proteins involved in immunoevasion and adhesion, which influence *SA*'s ability to colonize the nose, were expressed in *SA* nasal carrier strain exoproteome. In particular, high abundance of SPA, an important immunoevasive protein, was detected the *SA* nasal carrier strain. Additionally, we also observed that expression levels of SPA corresponded to the level of *SA* persistence in the nose. Therefore, we hypothesized that SPA is an important determinant of *SA* nasal carriage. Subsequently, in chapter four, we evaluated SPA's role in carriage, by creating *SA* nasal carrier strains lacking SPA and performed competitive *SA* recolonization studies in humans. Interestingly, we observed that isogenic mutants lacking SPA were eliminated from the nares significantly faster than WT when host was able to elicit an inflammatory response to recolonization. These findings provide strong *in vivo* support and shed new insights into role of SPA in nasal carriage of *SA*. Given the significant role for SPA in *SA* virulence, pathogenesis and immune evasion, the functional link between *SA* nasal clearance and role of SPA in modulating host immune responses during nasal colonization remains to be investigated. Preliminary studies by other members of our group revealed a correlation between absence of SPA in *SA* and activation of transcription factor NF-kB, which mediates the expression of proinflammatory signaling cytokines and chemokines in nasal epithelia. However, a recent study indicated that genotypic variability in *SA* nasal carriage strains caused variable host cell responses *ex vivo* [220]. Collectively, these results further confirm that host immune

responses play a predominant role in nasal colonization of *SA* in humans. Future investigations into the mechanism of nasal epithelial responses due to *SA* infection will be necessary to better decipher the functional link between carriage and inflammatory response during *SA* colonization.

For human *SA* recolonization studies, we utilized topical antibiotic mupirocin for clearance of *SA* and commensal flora from the nose prior to recolonization. Eradication of nasally colonized *SA* using the topical mupirocin has proven to be effective in reducing *SA* infections due to carriage [13,221,222]; however, such *SA* decolonization strategies are increasingly being threatened by the emergence antimicrobial resistance in *SA* including mupirocin-resistant *SA* [223]. Therefore, there is an urgent need for developing innovative therapeutics to combat resistant *SA* infections. A combinatorial approach involving drugs that affect host immune responses in concert with antibiotics can ameliorate the growing concern of antimicrobial resistance. For instance, a recent study demonstrated that inhibition of Tumor Necrosis Factor (TNF) in combination with antibiotic therapy greatly lessened staphylococcal arthritis and sepsis in mice [224]. Another study reported that treatments combining antibiotics with cytokines Granulocyte-Macrophage Colony-Stimulating Factor (GM-CSF) and TNFα improved survival of mice infected with *Klebsiella pneumoniae* [225]. Such combinatorial immunotherapeutics can be adapted for *SA* decolonization treatments.

In addition, development of novel *SA* decolonization treatments also requires conducting *SA* pathogenesis investigations where riskier interventions would be necessary. For such investigations, non-human primate models of *SA* nasal carriage would be better suited than human colonization models. Unlike rodents, primates such as rhesus macaques are natural

nasal carriers of *SA* [226]. A recent cross-sectional survey of 731 rhesus macaques revealed a 39% *SA* nasal carriage rate [226]. These primates could serve as useful *SA* nasal carriage models for studying colonization mechanisms in greater detail and developing new *SA* nasal eradication therapies.

Together, the studies conducted here advanced our understanding of nasal carriage dynamics and host immune responses during *SA* nasal colonization in humans. In addition, this work provided *in vivo* support for the essential role played by host immune responses in the survival of *SA* in human nares and importantly identifies the role of SPA as a co-determinant of *SA* nasal carriage. Improved understanding of *SA* nasal carriage can facilitate for development of effective intervention strategies for carriage and subsequently for preventing nosocomial and community-associated *SA* infections.

APPENDIX A: CHAPTER TWO SUPPLEMENT

Table 8: Complete genotyping details of *SA* strains analyzed in this study

Taxa label	MLST Sequence type (ST)	*spa* type	*spa* clonal complex as revealed by eBURP clustering analysis (*spa*-CC)[a]	*clfB* R region sequence obtained?[a]
D20	59	t216	#7 [b]	YES
D20-2	59	t216	#7	YES
D20-24	5	t688	5: no founder	YES
D20-25	5	t688	5: no founder	YES
D20-3	59	t216	#7	YES
D20-5	1723	t148	4: no founder	YES
D20-6	1723	t148	4: no founder	YES
D20-7	1723	t148	4: no founder	YES
D502-2	106	t056	#1	YES
D502-3	106	t056	#1	YES
D502-4	106	t056	#1	YES
D502-5	106	t056	#1	YES
D502-6	106	t056	#1	YES
D502-7	106	t056	#1	YES
D502-8	106	t056	#1	YES
D502-9	106	t056	#1	YES
D507	582	t084	6: no founder	YES
D507-2	582	t084	6: no founder	YES
D507-3	582	t084	6: no founder	YES
D507-4	582	t084	6: no founder	YES
D512	30	t012	2: *spa*-CC 037	YES
D512-2	30	t012	2: *spa*-CC 037	YES
D512-3	30	t1705	#10	YES
D512-4	30	t012	2: *spa*-CC 037	YES
D512-5	30	t012	2: *spa*-CC 037	YES
D512-7	30	t012	2: *spa*-CC 037	YES
D512-8	30	t012	2: *spa*-CC 037	YES
D512-9	30	t012	2: *spa*-CC 037	YES
D517	8	t012	2: *spa*-CC 037	YES
D517-2	8	t1705	#10	YES
D521	30	t122	2: *spa*-CC 037	YES
D521-2	30	t122	2: *spa*-CC 037	YES
D521-3	8	t036	1: *spa*-CC 024	YES
D521-4	8	t036	1: *spa*-CC 024	YES
D521-5	8	t036	1: *spa*-CC 024	YES
D521-6	8	t036	1: *spa*-CC 024	YES
D521-7	8	t036	1: *spa*-CC 024	YES
D523-10	188	t189	3: no founder	YES
D523-11	188	t189	3: no founder	YES
D523-14	188	t012	2: *spa*-CC 037	YES
D523-5	188	t189	3: no founder	YES
D524[c]	30	NA	NA	NA
D528-10	8	t008	1: *spa*-CC 024	YES
D528-11	8	t008	1: *spa*-CC 024	YES
D528-2	8	t024	1: *spa*-CC 024	YES
D528-3	8	t008	1: *spa*-CC 024	YES
D528-5	8	t008	1: *spa*-CC 024	YES
D528-6	8	t008	1: *spa*-CC 024	YES
D528-7	8	t008	1: *spa*-CC 024	YES

Taxa label	MLST Sequence type (ST)	*spa* type	*spa* clonal complex as revealed by eBURP clustering analysis (*spa*-CC)[a]	*clfB* R region sequence obtained?[a]
D528-8	8	t008	1: *spa*-CC 024	YES
D528-9	8	t008	1: *spa*-CC 024	YES
D531	30	NA	NA	NA
D535	59	t216	#7	YES
D535-10	5	t002	7: no founder	YES
D535-11	5	t002	7: no founder	YES
D535-12	5	t002	7: no founder	YES
D535-13	5	t002	7: no founder	YES
D535-14	5	t002	7: no founder	YES
D535-15	5	t002	7: no founder	YES
D535-16	5	t002	7: no founder	YES
D535-2	30	t216	#7	YES
D535-3	5	t002	7: no founder	YES
D535-4	5	t002	7: no founder	YES
D535-5	5	t002	7: no founder	YES
D535-6	5	t002	7: no founder	YES
D535-7	5	t002	7: no founder	YES
D535-8	5	t002	7: no founder	YES
D535-9	5	t002	7: no founder	YES
D540	15	t346	6:no founder	YES
D540-2	5	NA	NA	YES
D543	5	NA	NA	NA
D547	30	t3263	2: *spa*-CC 037	YES
D547-14	5	t688	5: no founder	YES
D547-15	5	t688	5: no founder	YES
D547-2	1434	t148	4: no founder	YES
D547-3	1507	t002	7: no founder	YES
D547-4	59	t216	#7	YES
D547-5	59	t216	#7	YES
D549-2	8	t008	1: *spa*-CC 024	YES
D549-3	8	t008	1: *spa*-CC 024	YES
D549-4	8	t008	1: *spa*-CC 024	YES
D549-5	8	t008	1: *spa*-CC 024	YES
D553	50	t185	#5	YES
D553-2	50	t185	#5	YES
D553-3	50	t185	#5	YES
D553-4	2224	t185	#5	YES
D554	8	NA	NA	NA
D558	45	NA	NA	NA
D560	508	NA	NA	NA
D563	30	NA	NA	NA
D564	2225	t216	#7	YES
D564-2	2225	t216	#7	YES
D565	87	t216	#7	YES
D565-2	87	t216	#7	YES
D565-3	87	t216	#7	YES
D566	15	t7134	6: no founder	YES
D566-10	30	t037	2: *spa*-CC 037	YES
D566-2	15	t7134	6: no founder	YES
D566-3	30	t037	2: *spa*-CC 037	YES
D566-4	30	t037	2: *spa*-CC 037	YES
D566-5	30	t037	2: *spa*-CC 037	YES

Taxa label	MLST Sequence type (ST)	*spa* type	*spa* clonal complex as revealed by eBURP clustering analysis (*spa*-CC)[a]	*clfB* R region sequence obtained?[a]
D566-6	30	t9877	1: *spa*-CC 024	YES
D566-7	30	t037	2: *spa*-CC 037	YES
D566-8	30	t037	2: *spa*-CC 037	YES
D566-9	30	t037	2: *spa*-CC 037	YES
D574	34	NA	NA	NA
D576	30	t363	2: *spa*-CC 037	YES
D576-2	30	t363	2: *spa*-CC 037	YES
D576-3	30	t363	2: *spa*-CC 037	YES
D576-4	30	t363	2: *spa*-CC 037	YES
D577	672	NA	NA	NA
D579	398	NA	NA	NA
D582	5	t002	7: no founder	YES
D582-2	1656	t216	#7	YES
D582-3	5	t002	7: no founder	YES
D584	45	NA	NA	NA
D589	45	t9652	#12	YES
D589-2	45	t9652	#12	YES
D589-3	45	t9652	#12	YES
D592	30	NA	NA	NA
D594	188	t189	3: no founder	YES
D594-2	188	t189	3: no founder	YES
D594-3	188	t189	3: no founder	YES
D594-4	188	t189	3: no founder	YES
D594-5	188	t037	2: *spa*-CC 037	YES
D594-6	188	t189	3: no founder	YES
D597	15	NA	NA	NA
D599	30	t037	2: *spa*-CC 037	YES
D599-9	398	t037	2: *spa*-CC 037	YES
D604-5	5	t688	5: no founder	YES
D604-6	5	t688	5: no founder	YES
D605	1181	t334	1: *spa*-CC 024	YES
D607	30	NA	NA	NA
D608	30	NA	NA	NA
D613	97	t1247	#9	YES
D618	5	t954	5: no founder	YES
D618-3	2226	t954	5: no founder	YES
D618-4	5	t954	5: no founder	YES
D619	5	t954	5: no founder	YES
D619-2	5	t954	5: no founder	YES
D619-3	5	t954	5: no founder	YES
D619-5	5	t954	5: no founder	YES
D619-6	5	t954	5: no founder	YES
D619-7	5	t954	5: no founder	YES
D623	5	t688	5: no founder	YES
D623-2	5	t688	5: no founder	YES
D623-3	5	t688	5: no founder	YES
D623-4	5	t688	5: no founder	YES
D627	15	t1509	Excluded	YES
D627-2	1659	t1509	Excluded	YES
D628	109	NA	NA	NA
D629	109	t3745	Excluded	YES
D629-2	109	t3745	Excluded	YES

Taxa label	MLST Sequence type (ST)	*spa* type	*spa* clonal complex as revealed by eBURP clustering analysis (*spa*-CC)[a]	*clfB* R region sequence obtained?[a]
D635	5	t954	5: no founder	YES
D635-2	5	t954	5: no founder	YES
D635-3	5	t954	5: no founder	YES
D636	1658	t021	2: *spa*-CC 037	YES
D636-2	1658	t021	2: *spa*-CC 037	YES
D637	8	t2648	1: *spa*-CC 024	YES
D637-2	8	t2648	1: *spa*-CC 024	YES
D637-4	8	t2648	1: *spa*-CC 024	YES
D637-7	8	t2648	1: *spa*-CC 024	YES
D643	508	NA	NA	NA
D647-2	87	t216	#7	YES
D647-5	87	t216	#7	YES
D647-7	87	t216	#7	YES
D647-8	87	t216	#7	YES
D651	30	t338	2: *spa*-CC 037	YES
D655-3	30	t338	2: *spa*-CC 037	YES
D657	45	t9876	#13	YES
D657-2	2228	t9876	#13	YES
D662	30	t021	2: *spa*-CC 037	YES
D662-2	30	t021	2: *spa*-CC 037	YES
D664	72	t3682	4: no founder	YES
D664-2	72	t3682	4: no founder	YES
D664-3	72	t3682	4: no founder	YES
D672	188	t9873	3: no founder	YES
D672-10	188	t9873	3: no founder	YES
D672-12	188	t9873	3: no founder	YES
D672-16	188	t9873	3: no founder	YES
D672-2	1724	t9873	3: no founder	YES
D672-3	188	t9873	3: no founder	YES
D672-4	188	t9873	3: no founder	YES
D672-5	188	t9873	3: no founder	YES
D672-6	188	t9873	3: no founder	YES
D672-7	188	t9873	3: no founder	YES
D672-8	188	t9873	3: no founder	YES
D672-9	188	t9873	3: no founder	YES
D678	109	NA	NA	NA
D681	1159	t091	#3	YES
D681-10	1159	t091	#3	YES
D681-11	1159	t091	#3	YES
D681-12	1159	t091	#3	YES
D681-2	1159	t091	#3	YES
D681-3	1159	t091	#3	YES
D681-4	1159	t091	#3	YES
D681-5	1159	t091	#3	YES
D681-6	1159	t091	#3	YES
D681-7	1159	t091	#3	YES
D681-8	1159	t091	#3	YES
D681-9	1159	t091	#3	YES
D686-2	2229	t701	1: *spa*-CC 024	YES
D691	30	NA	NA	NA
D692	30	t012	2: *spa*-CC 037	YES
D692-2	2230	t209	#6	YES

Taxa label	MLST Sequence type (ST)	*spa* type	*spa* clonal complex as revealed by eBURP clustering analysis (*spa*-CC)[a]	*clfB* R region sequence obtained?[a]
D692-3	8	t2229	#11	YES
D692-4	30	t012	2: *spa*-CC 037	YES
D697	109	t209	#6	YES
D697-2	109	t209	#6	YES
D710	30	NA	NA	NA
D713-4	5	t548	7: no founder	YES
D714	81	t127	#4	YES
D714-4	81	t127	#4	YES
D714-5	81	t127	#4	YES
D714-6	81	t127	#4	YES
D719	30	NA	NA	NA
D720	1657	t1001	#8	YES
D720-2	1657	t1001	#8	YES
D720-3	1657	t1001	#8	YES
D720-4	1657	t1001	#8	YES
D720-5	1657	t1001	#8	YES
D720-6	1657	t1001	#8	YES
D720-7	1657	t1001	#8	YES
D720-8	1657	t1001	#8	YES
D720-9	1657	t1001	#8	YES
D724	45	t073	#2	YES
D724-2	2231	t073	#2	YES
D724-3	45	t073	#2	YES
D724-4	45	t073	#2	YES
D724-5	45	t073	#2	YES
D724-6	45	t073	#2	YES
D724-7	45	t073	#2	YES
D724-8	45	t073	#2	YES
D725-2	5	t002	7: no founder	YES
D725-3	5	t002	7: no founder	YES
D729	5	NA	NA	NA
D732	5	NA	NA	NA
D733	5	NA	NA	NA
D735-2	8	t3240	1: *spa*-CC 024	YES
D739-2	30	t8072	2: *spa*-CC 037	YES
D742	1181	t334	1: *spa*-CC 024	YES
D742-2	1181	t334	1: *spa*-CC 024	YES
D750	72	t3682	4: no founder	YES
D750-2	72	t3682	4: no founder	YES
D752	8	NA	NA	NA
D753-5	2232	NA	NA	YES
D756	2227	t012	2: *spa*-CC 037	YES
D756-2	2227	t012	2: *spa*-CC 037	YES
D756-3	2227	t012	2: *spa*-CC 037	YES
D757-5	8	t008	1: *spa*-CC 024	YES
D758	15	NA	NA	NA
D771	8	t008	1: *spa*-CC 024	YES
D771-2	8	t008	1: *spa*-CC 024	YES
D771-3	8	t008	1: *spa*-CC 024	YES
D776	508	NA	NA	NA
D785-2	8	NA	NA	NA
D785-4	8	t008	1: *spa*-CC 024	YES

Taxa label	MLST Sequence type (ST)	*spa* type	*spa* clonal complex as revealed by eBURP clustering analysis (*spa*-CC)[a]	*clfB* R region sequence obtained?[a]
D795	15	t084	6: no founder	YES
D795-2	15	t084	6: no founder	YES
D795-4	15	t084	6: no founder	YES
D795-5	15	t084	6: no founder	YES
D795-6	15	t084	6: no founder	YES
D795-7	15	t084	6: no founder	YES
D798	8	t008	1: *spa*-CC 024	YES
D798-2	8	t008	1: *spa*-CC 024	YES
D798-3	8	t008	1: *spa*-CC 024	YES
D798-4	8	t008	1: *spa*-CC 024	YES
D798-5	8	t008	1: *spa*-CC 024	YES
D798-6	8	t008	1: *spa*-CC 024	YES
D798-7	8	t008	1: *spa*-CC 024	YES
D799	5	NA	NA	NA
D812-3	716	t008	1: *spa*-CC 024	YES
D819	30	NA	NA	NA
D506-5[#]	NA	NA	NA	NA

[#] No ST available.

[a] *spa* typing and *clfB* typing was performed on *S. aureus* strains isolated from carriers enrolled in longitudinal analysis study (i.e. nasal swabs from carriers monitored 2 or more times).

[b] Cluster number to which to the strain belongs as revealed by *spa* eBURP clustering analysis. Founder *spa* type, if present, for each *spa*-CC is also shown here.

[c] Italicized taxa = Cross sectional donors monitored only once to detect *S. aureus* in the nares. NA = sequence type or *spa* type or clfB typing information not available.

Table 9: *SA* nasal carriage pattern among closely related donors

Closely related donors	Type of donor relationship	Total *SA* strains	Identical *SA* strains as classified by MLST	Non-identical SA strains as classified by MLST
D528-D549	Spouse	13	13	0
D523-D594	Spouse	10	10	0
D618-D619	Living together	10	9	1
D619-D635	Twins	10	10	0
D20-D547-D604	Father-Mother-Child	18	12	6

Table 10: Nucleotide sequence of SD repeats generated for the gene *clfB*

Repeat numbers	Repeat sequences	Repeat numbers	Repeat sequences
1	TCGGATTCGGACAGTGAC	50	TCGGATTCAAACAGCGAT
2	TCAGGCTCAGACAGCGAC	51	TCGGACTCAGACAGTGAC
3	TCAGGTTCAGACAGTGAC	52	TCAAACTCAGATAGTGAC
4	TCGGACTCAGACAGCGAC	53	TCGGATTCAGATAGCGAT
5	TCAGATTCAGATAGTGAC	54	TCGGATTCAGATAGCGAC
6	TCAGACTCAGATAGTGAC	55	TCAGACCCAGACAGTGAG
7	TCAGATTCAGACAGCGAT	56	TCAGATTCAGACAGTGAG
8	TCGGATTTAGACAGCGAT	57	TCAGACTCGGATAGCGAT
9	TCGGATTCAGACAGCGAC	58	TCGGACTCAGACAGTTAC
10	TCAGATTCAGATAGTGAT	59	TCAGGTTCAGACAGTGAG
11	TCAGATTCAGACAGCGAC	60	TCGGGTTCAGATAGCGAC
12	TCAGACTCAGATAGTGAT	61	TCGGAATCAGACAGTGAT
13	TCAGACTCAGACAGTGAG	62	TCAGATTCCGACAGCGAC
14	TCAGATTCAGATAGCGAT	63	TCGGACTCAGATAGCAAC
15	TCAGACTCAGACAGTGAC	64	TCGGATTCGGACAGCGAC
16	TCCGATTCAGATAGCGAT	65	ACAGATTCAGATAGTGAC
17	TCGGACTCAGATAGCGAC	66	ACAGATTCAGACAGCGAC
18	TCCGATTCAGATAGCGAG	67	TCTGATTCAGACAGCGAC
19	TCAGACTCAGACAGTGAT	68	TCCGATTCAGATAGTGAT
20	TCGGATTCAGACAGCGAT	69	TCCGACACGGACAGCGAC
21	TCGGATTCAGACAGTGAC	70	TCAGATTCAGAAAGTGAC
22	TCAGGTTCAGATAGCGAC	71	TCCGATTCAGACAGCGAT
23	TCAGAATCAGATAGCGAT	72	TCTGATTCAGACAGCGAT
24	TCGGATTCAGACAGTGAT	73	TCAGATTCAGAGAGCGAT
25	TCAGAATCAGATAGCGAC	74	TCCGACTCAGACAGCGAC
26	TCAGAATCAGATAGTGAG	75	TCCGGTTCAGATAGTGAT
27	TCAGATTCAGACAGTGAC	76	TCAGATTCCGACAGCGAT
28	TCGGACTCAGACAGTGAT	77	TCGGATTCCGACAGCGAC
29	TCAGACTCAGATAGCGAT	78	TCAGATTCCGACAGTGAT
30	TCAGACTCAGACAGCGAT	79	TCCGACTCAGACAGCGAT
31	TCAGAATCAGACAGCGAC	80	TCCGATTCAGATAATGAC
32	TCAGACTCAGATAGCGAC	81	TCCGATTCTGATAGTGAC
33	TCAGACTCAGACAGCGAC	82	TCCGACTCTGATAGTGAC
34	TCGGACTCAGACAGCGAT	83	TCTGATTCAGATAGTGAT

Repeat numbers	Repeat sequences	Repeat numbers	Repeat sequences
35	TCAGACTCGGATAGCGAC	84	TCCGATTCAGACAGTGAC
36	TCGGATTCAGATAGTGAC	85	TCAGACTCAGAAAGCGAT
37	TCAGAATCAGACAGTGAT	86	TCACACTCAGATAGTGAC
38	TCAGGTTCAGATAGCGAT	87	TCGGACTCGGATAGTGAC
39	TCAGATTCAGATAGCGAC	88	TCAGACTCAGGTAGCGAT
40	TCAGAATCAGACAGTGAC	89	TCAGACTCAGATAGTGAG
41	TCAGACAGCGAT	90	TCAGATTCAGACAGCGAG
42	TCAGATTCAGATAGTGAG	91	TCGGATTCCGACAGTGAT
43	TCGGACTCAGATAGCGAT	92	TCAGATTCAGATAGCAAT
44	TCGGATTCAGACAACGAT	93	TCAGAGTCAGATAGTGAG
45	TCAGAATCAGACAGCGAT	94	TCAGATTCGGACAGCGAT
46	TCAGAATCAGACAGTGAG	95	TCAGATTCAGATAGCAAC
47	TCAAACTCAGACAGTGAG	96	TCGAATTCAGACAGTGAT
48	TCGGACTCAGATAGTGAC	97	TCAGACTCATACAGTGAT
49	TCGGACTCAGACAGTGAG	98	TCAGATTCAGGTAGTGAC
99	TCAGATTCCGATAGTGAC	114	TCGGACTCAGAGAGCGAT
100	TCCGACTCCGACAGCGAT	115	TCAGATTCAGACGGCGAT
101	TTAGATTCAGATAGCGAT	116	TCGGAGTCAGATAGCGAC
102	TCAGGCTCAGACAGCGAT	117	TCGGACTCAGACAGTGAA
103	TCGGATTCAGACAGTGAG	118	TCAGAATCAGACGGCGAT
104	TCAGGTTCCGATAGCGAT	119	TCAGACTCGTGTAGCGAT
105	TCGGATTCCGATAGTGAC	120	TCCGACTCAGGTAGCTGT
106	TCCGACTCAGATAGTGAC	121	TCAGACTCCGATAGTGAG
107	TCGGAGTCAGAGAGTGAC	122	TCAGATTCTTACAGCGAT
108	TCAGACTCTTATAGTGAC	123	TCCCACTCAGGTAGCAAT
109	TCGGACTCAGAAAGTGAC	124	TCAGACAGTGAC
110	TCGGACTCGGACTGTGAA	125	TCAGATTCAGACGGCGAC
111	TCGGATTCAAAGAGCGAT	126	TCCGATTCAGATAGCGAC
112	TCGGATTCAGACAGAGAC	127	TCAGACTCCGACAGCGAT
113	TCGGACGCAGATACCGAC		

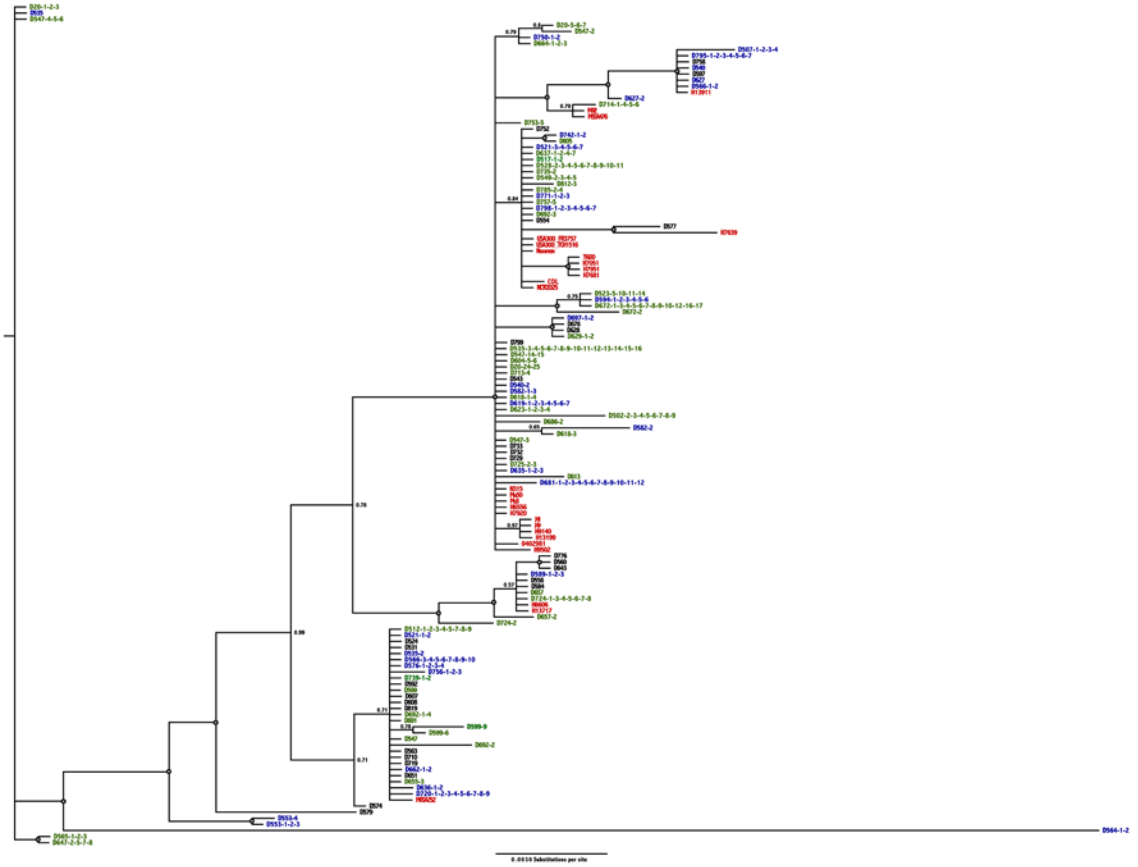

Figure 19: *SA* strains isolated from nasal carriers are genetically related to nosocomial epidemic strains.

Bayesian analyses of *SA* strains isolated from all nasal carriers enrolled in both cross-sectional (with only single nasal culture) and longitudinal studies (persistent carrier strains (**blue**), intermittent carrier strains (**green**)) are genetically similar to *SA* strains isolated from clinical settings (**red**). Numbers at each node indicate posterior probability support and grey-filled circles represent 100% posterior probability.

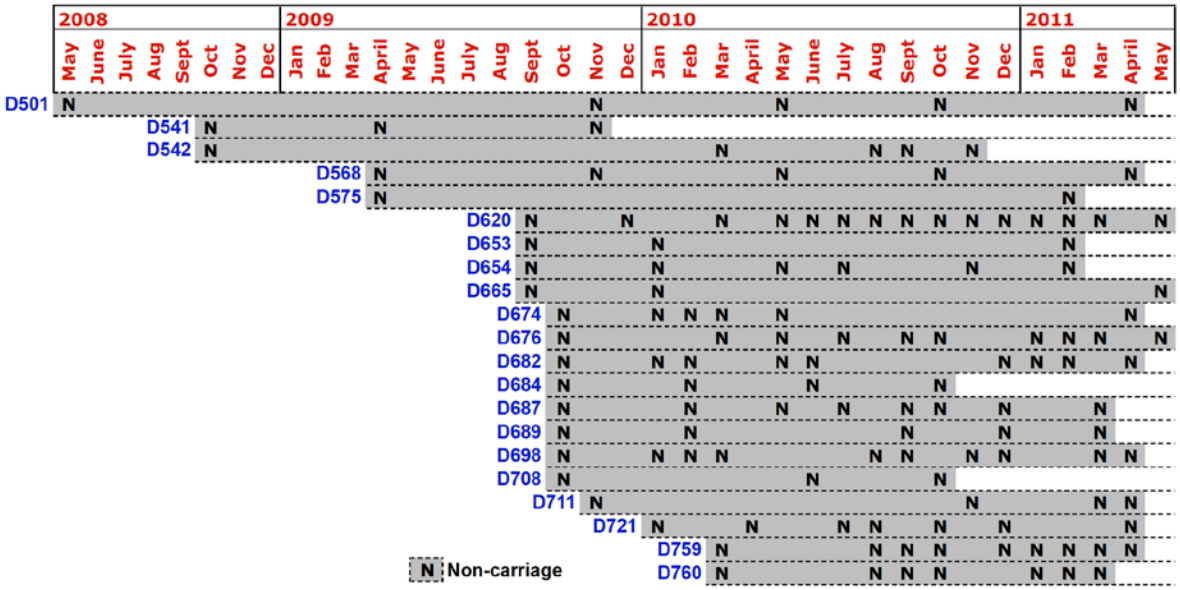

Figure 20: Longitudinal monitoring of healthy individuals for *SA* nasal carriage also identified true non-carriers of *SA*.

Shown here is a representative set of true non-carriers of *SA* that have been monitored for a year or more. (N) indicates *SA* non-carrier state.

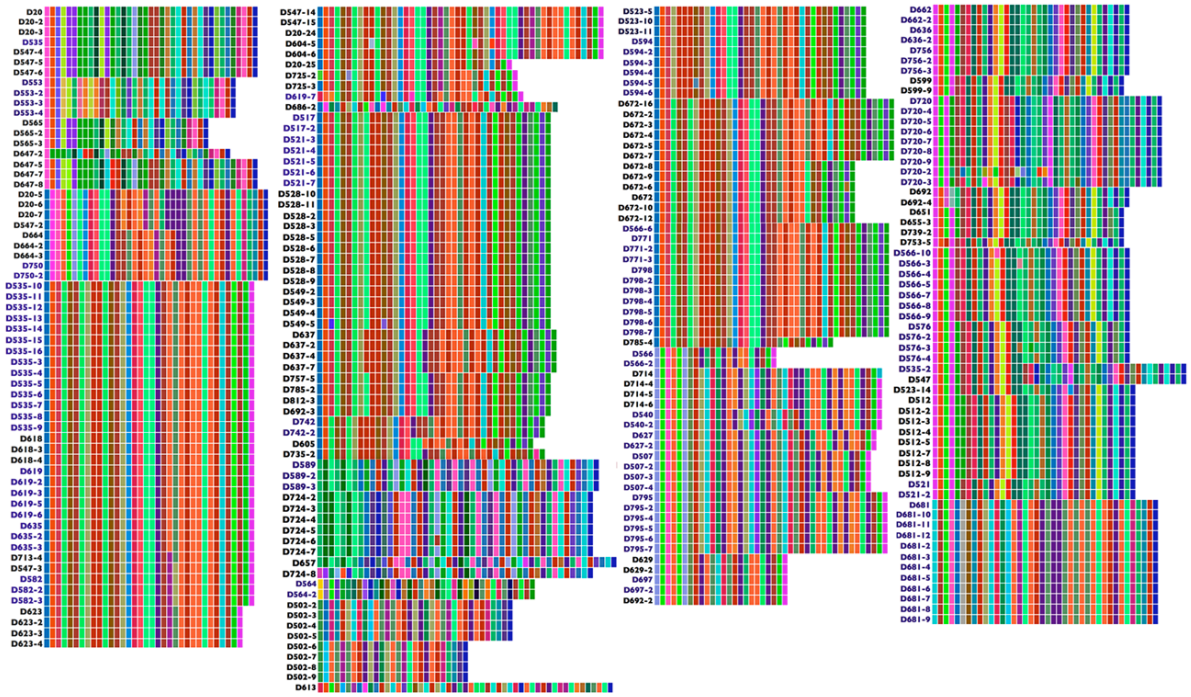

Figure 21: Color-coded repeat regions of R domains at the locus *clfB* of all *SA* strains isolated from persistent and intermittent carriers analyzed in this study.

Shown here is the nucleotide analysis of the c*lfB* R region on all *SA* strains isolated from persistent (colored in **blue**) and intermittent carriers (colored in **black**).

APPENDIX B: CHAPTER THREE SUPPLEMENT

Table 11: Peptide sequence of representative MS/MS spectra of uniquely identified proteins (Confidence, 99%) from D30 and 930918-3 depicted in Figure 9 with its multiple b and y series daughter ions, is shown here

I. Immunoglobulin G binding protein A precursor				
Peptide sequence: DDPSQSANVLGEAQK				
Residue	**b ions**	**b+2 ions**	**y ions**	**y+2 ions**
D	**260.1363**	130.5718	1847.9225	**924.4649**
D	**375.1632**	188.0853	1588.7935	794.9004
P	**472.2160**	236.6116	1473.7665	**737.3869**
S	**559.2480**	280.1276	1376.7138	688.8605
Q	**687.3066**	344.1569	**1289.6818**	**645.3445**
S	**774.3386**	387.6729	**1161.6232**	581.3152
A	**845.3757**	423.1915	**1074.5911**	537.7992
N	**960.4027**	480.7050	**1003.5540**	502.2807
V	**1059.4711**	530.2392	**888.5271**	444.7672
L	**1172.5552**	586.7812	**789.4587**	395.2330
G	1229.5766	615.2919	**676.3746**	338.6909
E	**1358.6192**	679.8132	**619.3532**	310.1802
A	1429.6563	**715.3318**	**490.3106**	245.6589
Q	1557.7149	779.3611	**419.2734**	210.1404
K	1829.9119	**915.4596**	**291.2149**	146.1111
II. ABC transporter, substrate-binding protein				
Peptide sequence: VTPEGIYLIDYR				
Residue	**b ions**	**b+2 ions**	**y ions**	**y+2 ions**
V	**244.1778**	122.5925	**1582.8597**	**791.9335**
T	**345.2254**	173.1164	**1339.6892**	670.3483

Residue	b ions	b+2 ions	y ions	y+2 ions
P	442.2782	221.6427	**1238.6416**	619.8244
E	**571.3208**	**286.1640**	**1141.5888**	**571.2980**
G	**628.3423**	314.6748	**1012.5462**	506.7767
I	**741.4263**	**371.2168**	**955.5247**	**478.2660**
Y	**904.4896**	452.7485	**842.4407**	421.7240
L	**1017.5737**	509.2905	**679.3774**	340.1923
I	1130.6578	565.8325	**566.2933**	283.6503
D	1245.6847	623.3460	**453.2092**	**227.1083**
Y	1408.7480	704.8777	**338.1823**	169.5948
R	**1564.8492**	782.9282	**175.1190**	88.0631
III. Autolysin				
Peptide sequence: TNTNVTNAGYSLVDDEDDNSENQINPELIK				
Residue	**b ions**	**b+2 ions**	**y ions**	**y+2 ions**
T	**246.1570**	123.5821	3612.6915	1806.8494
N	360.1999	180.6036	3367.5418	1684.2745
T	**461.2476**	231.1274	3253.4988	1627.2531
N	**576.2746**	288.6409	3152.4512	1576.7292
V	**675.3430**	**338.1751**	3037.4242	1519.2157
T	**776.3907**	**388.6990**	2938.3558	1469.6815
N	**890.4336**	445.7204	2837.3081	1419.1577
A	**961.4707**	**481.2390**	2723.2652	1362.1362
G	**1018.4922**	**509.7497**	2652.2281	1326.6177
Y	1181.5555	591.2814	2595.2066	1298.1069
S	**1268.5875**	634.7974	2432.1433	1216.5753
L	**1381.6716**	691.3394	2345.1113	1173.0593

Residue	b ions	b+2 ions	y ions	y+2 ions
V	1480.7400	740.8736	2232.0272	1116.5172
D	1595.7669	798.3871	2132.9588	1066.9830
D	1710.7939	855.9006	2017.9318	1009.4696
E	1839.8365	920.4219	1902.9049	951.9561
D	1954.8634	977.9353	1773.8623	887.4348
D	2069.8904	1035.4488	1658.8354	829.9213
N	2183.9333	1092.4703	1543.8084	772.4078
S	2270.9653	1135.9863	1429.7655	715.3864
E	2400.0079	1200.5076	1342.7335	671.8704
N	2515.0349	1258.0211	1213.6909	607.3491
Q	2643.0934	1322.0504	**1098.6639**	549.8356
I	2756.1775	1378.5924	**970.6053**	485.8063
N	2870.2204	1435.6139	**857.5213**	429.2643
P	2967.2732	1484.1402	**743.4784**	**372.2428**
E	3096.3158	1548.6615	646.4256	323.7164
L	3209.3998	1605.2036	**517.3830**	259.1951
I	3322.4839	1661.7456	**404.2989**	202.6531
K	3594.6809	1797.8441	**291.2149**	146.1111

Table 12: Functional classification of the total 488 identified exoproteome proteins of nasal carrier strain (D30) and non-carrier strain (930918-3) as identified by iTRAQ analysis in three independent experiments.

D30:930918-3 is the ratio of protein expression levels between the carrier and non-carrier strain. The p values and the error factor associated with the protein expression levels are also indicated here

Accession no.	Name	Number of peptides	Total score	Seq Coverage (%)	D30:930918-3	*p* value	Error factor
Amino Acid & Protein Synthesis							
gi|88194310	translation elongation factor Tu	109	63.62	85.8	0.756	0.0005	1.1671
gi|87161362	50S ribosomal protein L15	47	48.25	83.6	0.676	0	1.0548
gi|14586725	translation elongation factor Tu	35	26.26	70.4			
gi|87160058	cysteine synthase A	25	40.61	84.8	1.8127	0	1.1792
gi|73919121	30S ribosomal protein S7	25	18.57	68.6	0.562	0	1.1774
gi|87161596	30S ribosomal protein S16	23	22.1	52.7	0.7662	0	1.0403
gi|87160271	30S ribosomal protein S20	23	14	22.9	0.6794	0.0002	1.2112
gi|87161732	30S ribosomal protein S9	20	24.3	58.3	1.2431	0.0391	1.2293
gi|87160361	50S ribosomal protein L5	20	20.23	53.6	0.8123	0.0625	1.2449
gi|87160513	50S ribosomal protein L22	20	13.82	54.7	0.853	0.0052	1.1149
gi|56961930	elongation factor Tu [Bacillus clausii KSM-K16]	20	23.05	57.3	0.8654	0.464	1.9995
gi|90110058	50S ribosomal protein L3	19	4.01	18.4	1.0205	0.075	1.0225
gi|87161210	translation elongation factor Ts	18	26.16	73.4	1.0124	0.9176	1.2729
gi|87161455	ribosomal protein L7/L12	17	19.7	78.7	0.7709	0	1.0293
gi|87160153	ribosome recycling factor	17	14.48	64.1	1.8758	0.0001	1.3391
gi|87161079	translation initiation factor IF-1	17	10.02	77.8	0.6472	0	1.1701
gi|87162219	30S ribosomal protein S1	16	26.03	57.3	1.3052	0	1.1043
gi|87161718	50S ribosomal protein L9	15	21.91	63.5	1.1328	0.0289	1.118
gi|87160155	50S ribosomal protein L4	15	17.22	77.8	0.8015	0.1307	1.3381
gi|70725821	50S ribosomal protein L30	15	17.07	79.7	0.5375	0	1.2454
gi|87162334	50S ribosomal protein L2	13	19.76	41.5	1.0102	0.87	1.1294
gi|87161133	ribosomal protein L11	13	8.83	67.9	1.1874	0.0077	1.1282
gi|87161952	50S ribosomal protein L32	13	7.36	57.9	1.303	0.199	1.5092

Accession no.	Name	Number of peptides	Total score	Seq Coverage (%)	D30:930918-3	*p* value	Error factor
gi|11612404	elongation factor Tu [Enterococcus dispar]	13	21.05	74.5	1.3041	0.2037	1.8473
gi|82581599	50S ribosomal protein L7/L12	13	7.44	84.4			
gi|88909112	50S ribosomal protein L17	11	12.79	35.8	0.9462	0.0318	1.0514
gi|90101744	30S ribosomal protein S8	10	16.55	89.4	0.9522	0.9051	EF > 2
gi|91207380	50S ribosomal protein L1	9	11.57	47	0.8113	0.0474	1.2296
gi|151220721	translation elongation factor G (EF-G)	8	15.92	37.8	0.7577	0.1014	1.4088
gi|87161329	50S ribosomal protein L21	8	13.4	55.9	0.7865	0.007	1.1665
gi|91207792	30S ribosomal protein S6	8	10.34	60.2	0.9515	0.8625	1.8119
gi|97181999	50S ribosomal protein L10	7	12.54	66.9	0.9042	0.7366	1.8768
gi|87161988	50S ribosomal protein L3	7	9	46.4	0.8124	0.0387	1.2166
gi|87161367	threonyl-tRNA synthetase	6	13.25	28.2	0.7131	0.2741	1.9426
gi|91207680	30S ribosomal protein S11	6	10.43	41.9	1.7472	0.3033	EF > 2
gi|87160873	50S ribosomal protein L23	6	9.18	45.1	1.0434	0.3747	1.0991
gi|87161591	30S ribosomal protein S15	6	8.82	51.7	1.0212	0.8765	1.3915
gi|87160559	aspartyl/glutamyl-tRNA amidotransferase subunit C	6	8.68	67	1.1874	0.6344	EF > 2
gi|56749400	Seryl-tRNA synthetase (Seryl-tRNA(Ser/Sec) synthetase) (Serine--tRNA ligase) (SerRS)	6	8	29.9	1.7623	0.0777	1.9038
gi|87161370	50S ribosomal protein L31 type B	6	6.22	59.5	0.6056	0	1.141
gi|87161038	hypothetical protein SAUSA300_0916 [USA300]	5	10.92	60.9	0.6974	0.6352	EF > 2
gi|87160935	50S ribosomal protein L6	5	7.97	50.6	0.4875	0.2475	EF > 2
gi|73917907	30S ribosomal protein S10	5	6.9	62.7	1.1065	0.2812	1.2147
gi|91207889	30S ribosomal protein S5	4	8.59	58.4	0.9047	0.8043	EF > 2
gi|87161481	50S ribosomal protein L29	4	8.2	47.9	0.6737	0.0947	1.6135
gi|88195373	glycyl-tRNA synthetase	4	6.23	15.6	0.8245	0.2604	1.5584
gi|71153662	50S ribosomal protein L25 (General stress protein CTC)	4	6.13	36.4	0.8086	0.0064	1.1431
gi|59797753	Glutamine synthetase (Glutamate--ammonia ligase) (GS)	4	6.12	16.6	0.8982	0.5688	1.6173
gi|90101727	30S ribosomal protein S4	3	6	36	0.9035	0.7581	EF > 2

Accession no.	Name	Number of peptides	Total score	Seq Coverage (%)	D30:930918-3	*p* value	Error factor
gi|87161271	chorismate mutase/phospho-2-dehydro-3-deoxyheptonate aldolase	3	6	19.6	0.9876	0.8675	1.3299
gi|87160953	translation initiation factor IF-3	3	6	21.1	2.5237	0.0001	1.3993
gi|87162332	50S ribosomal protein L16	3	5.44	42.4	1.2673	0.5251	EF > 2
gi|153202305	ribosomal protein S21 [HPB2262]	3	5.3	38.2	0.2723	0.0673	EF > 2
gi|87161395	50S ribosomal protein L24 [USA300]	3	4.54	41	0.7638	0.0191	1.2467
gi|87161828	50S ribosomal protein L27	3	4.09	35.1	0.6052	0.0193	1.4154
gi|152937150	translation elongation factor Tu [Clostridium botulinum F str. Langeland]	3	5.28	30.7			
gi|38372424	30S ribosomal protein S8	3	6.04	55.3	0.3701		
gi|87161168	50S ribosomal protein L13	2	5.21	36.6	0.6392	0.4742	EF > 2
gi|91207727	30S ribosomal protein S13	2	5.03	52.1	1.6113	0.1853	EF > 2
gi|87162298	30S ribosomal protein S19 [USA300]	2	4.6	51.1	0.8359	0.2643	1.4279
gi|87160596	50S ribosomal protein L18 [USA300]	2	4.58	46.2	0.7592	0.3675	1.967
gi|151220702	glutamyl-tRNA synthetase	2	4	22.1	1.1302	0.4851	EF > 2
gi|87161400	phenylalanyl-tRNA synthetase (beta subunit)	2	3.7	33.3	1.2949	0.1985	EF > 2
gi|87162294	phosphoribosylaminoimidazole carboxylase, catalytic subunit	2	3.7	48.9	0.7044		
gi|90101380	Translation initiation factor IF-2	2	3.48	35.2	1.3228	0.256	1.7976
gi|90101385	Translation initiation factor IF-2	1	3.56	14.3	1.4791	0.3052	EF > 2
gi|87162006	tetrahydrodipicolinate acetyltransferase	1	3.05	33.1	0.2073	0.2206	EF > 2
gi|87160672	30S ribosomal protein S2	1	2.29	11	2.593		
gi|87162222	translation elongation factor P	1	2.19	12.4	3.0873	0.0778	EF > 2
gi|149122046	(Glutamate--ammonia-ligase) adenylyltransferase [Methylobacterium sp. 4-46]	1	2.15	38.3	1.7745	0.3525	EF > 2
gi|138896204	Valyl-tRNA synthetase [Geobacillus thermodenitrificans NG80-2]	1	2.13	9.1	0.9308		
gi|73662075	peptide chain release factor 1 [ATCC 15305]	1	2.11	13.1	0.9875		
gi|91207843	30S ribosomal protein S3	1	2.06	35.5	0.4789		

Accession no.	Name	Number of peptides	Total score	Seq Coverage (%)	D30:930918-3	*p* value	Error factor
gi|113476121	RNA binding S1 [Trichodesmium erythraeum IMS101]	1	2.05	22.7	1.5197		
gi|149376055	imidazole glycerol phosphate synthase subunit HisF [Marinobacter algicola DG893]	1	2.03	32.7			
gi|73918993	Dihydrodipicolinate synthase (DHDPS)	1	2.02	26.4	0.3177	0.5002	EF > 2
gi|92090969	Arginine biosynthesis bifunctional protein argJ [Includes: Glutamate N-acetyltransferase (Ornithine acetyltransferase) (Ornithine transacetylase) (OATase); Amino-acid acetyltransferase (N-acetylglutamate synthase) (AGS)] [Contains: Arginine biosynthesis b	1	2.01	21.1	1.4968		
gi|97051447	Serine hydroxymethyltransferase (Serine methylase) (SHMT)	1	2.01	14.1	0.4881		
gi|21284173	2-hydroxyacid dehydrogenase [MW2]	1	2.01	7.7	11.5272		
gi|90108439	Valyl-tRNA synthetase (Valine--tRNA ligase) (ValRS)	1	2.01	13.8	1.0338		
gi|87161786	1-pyrroline-5-carboxylate dehydrogenase	1	2	12.5	0.1948		
gi|145588242	ribosomal protein L3 [Polynucleobacter sp. QLW-P1DMWA-1]	1	2	39	1.1519		
gi|90101261	Dihydrodipicolinate reductase (DHPR)	1	2	16.7	0.2288		
gi|87160676	threonine synthase	1	2	15.9	1.4354		
gi|87161544	branched-chain amino acid aminotransferase	1	2	21.5	0.4505		
gi|87162399	50S ribosomal protein L20	1	1.8	16.1	0.9087	0.5969	1.4847
gi|38605460	50S ribosomal protein L11	1	2.84	23.4			
gi|121534747	ribosomal protein L11[Thermosinus carboxydivoransNor1]	1	2.01	22			
gi|116491401	Ribosomal protein L11 [Oenococcus oeni PSU-1]	1	2	15.3			
gi|126635115	non-ribosomal peptide synthetase A [Actinoplanes friuliensis]	1	1.54	22.7	1.6096	0.4126	EF > 2
gi|115502775	50S ribosomal protein L16	1	1.54	42.5	0.9457	0.7245	1.5067

Accession no.	Name	Number of peptides	Total score	Seq Coverage (%)	D30:930918-3	*p* value	Error factor
gi|15672583	serine hydroxymethyltransferase [Lactococcus lactis subsp. lactis Il1403]	1	1.52	16.4	1.3212	0.0016	1.1075
gi|148242083	L-asparaginase II [Synechococcus sp. RCC307]	1	1.52	15.9			
gi|58761240	elongation factor [Mycoplasma fermentans]	1	2.51	28.9	1.1529		
gi|89052742	Glutamate synthase (ferredoxin) [Jannaschia sp. CCS1]	1	1.31	13.4	1.3467	0.0291	1.2986
Energy Metabolism							
gi|87161989	quinol oxidase, subunit II	92	88.88	50.8	3.1872	0	1.095
gi|87161213	hypothetical protein SAUSA300_1720 [USA300]	19	21.88	35.6	0.5872	0.0013	1.3635
gi|70726902	hypothetical protein SH1901 [JCSC1435]	15	25.23	38.2	4.5461	0.0398	EF > 2
gi|87162272	triosephosphate isomerase	15	16.92	64.8	1.4153	0.0001	1.1749
gi|88196553	fructose-bisphosphate aldolase class-I, putative	14	24.51	64.2	1.9277	0.0004	1.3923
gi|87160110	phosphopyruvate hydratase	14	22.02	50	1.0846	0.077	1.0948
gi|87162014	fructose bisphosphate aldolase	13	14.13	55.9	1.9282	0	1.2112
gi|87161115	glyceraldehyde-3-phosphate dehydrogenase, type I	11	16.49	53.3	0.9238	0.4056	1.2517
gi|87162120	formate acetyltransferase	11	16.45	22.2	2.4393	0	1.3988
gi|87160940	phosphate acetyltransferase	10	17.3	59.8	1.2661	0.0394	1.2496
gi|87162024	pyruvate kinase	9	14.37	45	1.02	0.8745	1.3095
gi|87161439	hypothetical protein SAUSA300_0871 [USA300]	9	11.01	40.3	0.8634	0.137	1.2257
gi|81782064	3-hexulose-6-phosphate synthase (HPS) (D-arabino-3-hexulose-6-phosphate formaldehyde lyase)	8	11.53	64.8	0.49	0.0009	1.4616
gi|91206698	Glucose-6-phosphate isomerase (GPI) (Phosphoglucose isomerase) (PGI) (Phosphohexose isomerase) (PHI)	6	10.18	37.2	1.0904	0.2236	1.1689
gi|87159954	pyruvate dehydrogenase E1 component, beta subunit	5	10.84	41.5	0.5528	0.2345	EF > 2
gi|87160408	phosphoglycerate kinase	5	9.9	30.1	0.7908	0.1914	1.4523

Accession no.	Name	Number of peptides	Total score	Seq Coverage (%)	D30:930918-3	*p* value	Error factor
gi|87161599	malate:quinone-oxidoreductase	5	9.38	26.9	0.5397	0.1134	EF > 2
gi|73663225	glyceraldehyde-3-phosphate dehydrogenase [ATCC 15305]	5	9.64	44.2	0.4823		
gi|87161833	putative lipase/esterase [USA300]	5	8	30	1.396	0.0423	1.3764
gi|87162313	5'-nucleotidase, lipoprotein e(P4) family	4	8.82	16.2	1.6469	0.0158	1.4105
gi|87161068	formate-tetrahydrofolate ligase	4	8.03	32.4	1	1	1.3286
gi|87162359	aconitate hydratase [USA300]	4	8.01	18.1	0.2186	0	1.3832
gi|87161490	alcohol dehydrogenase	4	8	33.6	1.5432	0.0256	1.4152
gi|87161543	2,3-bisphosphoglycerate-independent phosphoglycerate mutase	4	8	17.4	1.0673	0.5116	1.3217
gi|87161186	deoxyribose-phosphate aldolase	4	8	54.1	0.9905	0.8801	1.1671
gi|87160632	hypothetical protein SAUSA300_1804 [USA300]	4	7.9	65.8	0.7123	0.3467	EF > 2
gi|81694562	Transketolase	4	7.84	21	0.7876	0.3804	1.9597
gi|90102247	6-phosphogluconate dehydrogenase, decarboxylating	4	6.32	19	0.6499	0.1914	EF > 2
gi|87161569	methylenetetrahydrofolate dehydrogenase/methenyltetrahydrofolate cyclohydrolase	4	6.2	44.4	0.5754	0.0004	1.2155
gi|87162047	Ornithine aminotransferase	4	6.01	23.7	2.631	0.0516	EF > 2
gi|87160754	pyruvate dehydrogenase E1 component, alpha subunit	4	6	17	0.5156	0.0163	1.586
gi|151221843	hypothetical protein NWMN_1631 [Newman]	3	6.34	45.1	1.6035	0.1536	1.9954
gi|87161332	succinyl-CoA synthetase, alpha subunit	3	6.09	39.7	1.302	0.0663	1.3363
gi|91206786	2,3-bisphosphoglycerate-dependent phosphoglycerate mutase (Phosphoglyceromutase) (PGAM) (BPG-dependent PGAM) (dPGM)	3	6	23.2	0.8166	0.0118	1.149
gi|81695276	Probable acetyl-CoA acyltransferase (Acetoacetyl-CoA thiolase)	3	6	32.3	0.3443	0.133	EF > 2
gi|70727178	hypothetical protein SH2179 [JCSC1435]	3	5.74	15.7	1.9715	0.0273	1.7609

Accession no.	Name	Number of peptides	Total score	Seq Coverage (%)	D30:930918-3	*p* value	Error factor
gi|73920841	L-lactate dehydrogenase 1 (L-LDH 1)	3	4.35	17.4	0.7067	0.1044	1.6896
gi|87162164	Acetoin(diacetyl) reductase [USA300]	3	4	21.7	1.2001	0.5029	1.991
gi|87161124	citrate synthase II [USA300]	2	4.62	11	0.213	0.0447	EF > 2
gi|61214622	Phosphoenolpyruvate-protein phosphotransferase (Phosphotransferase system, enzyme I)	2	4.23	22.9	5.1034	0	1.5376
gi|87161326	putative NADP-dependent malic enzyme [USA300]	2	4.08	23	0.7235	0.42	EF > 2
gi|77417488	Succinyl-CoA synthetase beta chain (SCS-beta)	2	4.02	18.6	0.7154	0.1054	EF > 2
gi|87161670	isocitrate dehydrogenase, NADP-dependent	2	4	19.7	0.2127	0.0402	EF > 2
gi|73663003	dihydrolipoamide S-acetyltransferase component of pyruvate dehydrogenase complex E2	2	4	16.6	0.8631	0.186	1.2922
gi|87162156	phosphoenolpyruvate carboxykinase (ATP)	2	4	11.3	0.7101	0.0953	1.9271
gi|87161885	transglycosylase [USA300]	2	4	11.3	2.726	0.0035	1.2924
gi|87160719	hypothetical protein SAUSA300_0844 [USA300]	2	2.02	14.9	0.4426	0.0854	EF > 2
gi|78101526	Chain A, Crystal Structure Of 3',5"-Aminoglycoside Phosphotransferase Type Iiia Adp Neomycin B Complex	1	2.5	18.6	0.0141	0.0227	EF > 2
gi|123548254	Putative aldehyde dehydrogenase SAB2006c	1	2.24	9.9	0.872		
gi|87161665	L-lactate dehydrogenase	1	2.18	25.1	0		
gi|87161078	4-oxalocrotonate tautomerase	1	2.03	37.7	1.8234	0.443	EF > 2
gi|23465821	polyphosphate kinase [Bifidobacterium longum NCC2705]	1	2.04	12.8	0.9744	0.7924	1.451
gi|87162105	glycerate dehydrogenase-like protein	1	2.01	20.5	1.0281	0.8218	EF > 2
gi|152976979	pyruvate kinase [Bacillus cereus subsp. cytotoxis NVH 391-98]	1	2.22	11.8			
gi|56748589	Acetate kinase (Acetokinase)	1	2	12.8	0.7315		
gi|87160338	6-phosphofructokinase [USA300]	1	2	31.9	0.4741		
gi|119717219	UDP-glucose/GDP-mannose dehydrogenase [Nocardioides sp. JS614]	1	2	13	0.6648		

Accession no.	Name	Number of peptides	Total score	Seq Coverage (%)	D30:930918-3	*p* value	Error factor
gi|87161715	hypothetical protein SAUSA300_1902 [USA300]	1	2	7.6	0.9099		
gi|87160639	hypothetical protein SAUSA300_0843 [USA300]	1	2	20.2	0.5712		
gi|152933808	L-serine dehydratase, iron-sulfur-dependent, beta subunit [Clostridium botulinum F str. Langeland]	1	1.72	19.2	1.0543	0.2593	1.1182
gi|110637666	urea amidohydrolase (urease) alpha subunit [Cytophaga hutchinsonii ATCC 33406]	1	1.52	18.6			
gi|78223411	Short-chain dehydrogenase/reductase SDR [Geobacter metallireducens GS-15]	1	1.52	15.4	0.7358		
gi|87161617	chaperone protein DnaK	30	32.79	60.5	1.7333	0.0006	1.3604
gi|87160551	trigger factor	17	21.26	58.2	1.0493	0.3682	1.1129
gi|88195151	hypothetical protein SAOUHSC_01427 [NCTC 8325]	16	30.82	54.2	1.8927	0.0006	1.4148
gi|87162356	foldase protein PrsA precursor	15	22.35	49.4	2.3495	0.0003	1.5348
gi|87161296	putative serine protease HtrA [USA300]	9	17.52	28.5	1.2062	0.3449	1.5089
gi|87161831	putative ATP-dependent Clp proteinase	7	12.11	37.5	1.0524	0.9183	EF > 2
gi|87160799	ornithine carbamoyltransferase	7	11.82	30.3	8.6761	0	1.3373
gi|87159917	urocanate hydratase	5	9.57	31.6	0.982	0.8025	1.1848
gi|87161225	copper chaperone copZ	5	2.04	64.7	0.7969	0.0951	1.3211
gi|87161349	dihydrolipoamide dehydrogenase	4	7.4	24.6	0.9476	0.889	EF > 2
gi|87161339	glycine cleavage system H protein	4	4.1	46	0.9478	0.0326	1.0498
gi|87160352	hypothetical protein SAUSA300_0857 [USA300]	3	7.61	50.3	1.0465	0.7076	1.3266
gi|87161328	hydrolase family protein	3	6.41	51.1	0.5022	0.0546	EF > 2
gi|116248102	Serine protease htrA-like	3	5.76	26.3	1.0002	0.9995	1.9869
gi|87161390	DJ-1/PfpI family protein	2	4.13	23.3	0.9854	0.9905	EF > 2
gi|87160700	60 kDa chaperonin	2	4.09	22.9			
gi|87162424	putative membrane-associated zinc metalloprotease [USA300]	2	4	25.4	0.4153	0.0033	1.3841
gi|87161475	NAD-specific glutamate dehydrogenase	2	4	15.7	0.8324	0.0419	1.166
gi|87160107	signal peptidase IB	2	4	43.9	0.7953	0.0077	1.0907
gi|87161613	co-chaperone GrpE	2	4	23.6	2.3294	0.0016	1.1554

Accession no.	Name	Number of peptides	Total score	Seq Coverage (%)	D30:930918-3	*p* value	Error factor
gi|87160848	peptidase, rhomboid family	2	2.03	9.4	1.5285	0.0132	1.32
gi|87162079	putative pyridoxal phosphate-dependent acyltransferase [USA300]	1	2.17	10.6	0.133	0.1049	EF > 2
gi|87161347	Peptidase family M20/M25/M40	1	2	19.6	0.4047		
gi|90183185	ATP-dependent Clp protease proteolytic subunit (Endopeptidase Clp)	1	2	34.9	0.6635	0.1336	EF > 2
gi|87161219	hypothetical protein SAUSA300_0207 [USA300]	1	2	12	0.8407		
gi|15672533	trigger factor [Lactococcus lactis subsp. lactis Il1403]	1	1.7	12.9	1.3292		
gi|152975536	amino acid adenylation domain [Bacillus cereus subsp. cytotoxis NVH 391-98]	1	1.31	6.8	1.4732		
Stress							
gi|87162409	CsbD-like superfamily	34	23.94	90.6	0.4565	0	1.0526
gi|87162200	Alkyl hydroperoxide reductase subunit C	27	17.18	51.9	1.1686	0.0002	1.0833
gi|87160786	hypothetical protein SAUSA300_1652 [USA300]	24	31.43	68.6	0.862	0.0006	1.087
gi|894289	alkaline shock protein 23; ASP23	20	19.57	69.8	0.5771	0	1.2652
gi|87162087	universal stress protein family	18	22.55	71.7	2.9027	0.0004	1.7367
gi|87162159	hypothetical protein SAUSA300_1582 [USA300]	13	8.33	75	0.6747	0	1.1266
gi|87161236	Thioredoxin	12	15.51	83.7	1.3978	0.0003	1.1934
gi|87160079	peptide methionine sulfoxide reductase regulator MsrR	10	10.51	33.9	0.8648	0.1957	1.2556
gi|87161001	thioredoxin-disulfide reductase	9	10	36	0.792	0.169	1.423
gi|87161687	thiol peroxidase	8	8	55.5	0.756	0	1.0849
gi|70726220	hypothetical protein SH1219 [JCSC1435]	7	13.15	54.7			
gi|87160477	putative thioredoxin [USA300]	5	10.3	58.3	1.218	0.2208	1.4236
gi|87160511	Catalase	5	7.43	20.2	0.5021	0.027	1.7724
gi|87161707	superoxide dismutase (Mn/Fe family)	5	6.01	40.2	0.9286	0.4111	1.2176
gi|21282513	hypothetical protein MW0784 [MW2]	5	4	41.5	0.8983	0.0001	1.0481
gi|88195790	ferritin, putative [NCTC 8325]	4	6.67	51.8	0.7199	0.5798	EF > 2

Accession no.	Name	Number of peptides	Total score	Seq Coverage (%)	D30:930918-3	*p* value	Error factor
gi|87160405	hypothetical protein SAUSA300_1909 [USA300]	4	4.21	27.8	0.987	0.9858	EF > 2
gi|87161642	alkyl hydroperoxide reductase subunit F	1	2.72	12.8	0.4971	0.0957	EF > 2
gi|87161086	methionine-R-sulfoxide reductase	1	2.33	16.2	1.238	0.8192	EF > 2
gi|87162273	OsmC/Ohr family protein	1	2	34.3	2.1538	0.6357	EF > 2
gi|87160980	hypothetical protein SAUSA300_0725 [USA300]	1	2	17.9	0.5794		
gi|87160505	DNA-binding protein HU	36	20	75.6	0.9424	0.0086	1.0451
gi|87161697	transcription elongation factor GreA [USA300]	9	12	60.1	0.7916	0.0003	1.1165
gi|87160906	putative transcriptional regulator [USA300]	9	12	39.7	0.7951	0.3188	1.6575
gi|90110870	DNA-directed RNA polymerase alpha chain (RNAP alpha subunit) (Transcriptase alpha chain) (RNA polymerase subunit alpha)	5	6.37	27.7	1.2309	0.3925	1.7145
gi|87161137	DNA-directed RNA polymerase, beta' subunit	3	6.01	23.4	1.1599	0.1932	1.3917
gi|87159899	transcriptional regulator, MarR family	3	6	46.3	0.3925	0.0037	1.2802
gi|81695152	DNA-directed RNA polymerase beta chain (RNAP beta subunit) (Transcriptase beta chain) (RNA polymerase subunit beta)	3	4.04	25.2	0.992	0.9968	EF > 2
gi|81651715	Putative septation protein spoVG	2	3.1	47	0.7076	0.3798	EF > 2
gi|148556982	Hydantoinase/oxoprolinase [Sphingomonas wittichii RW1]	1	2.23	29.2	1.0013		
gi|87161403	DNA-directed RNA polymerase, omega subunit	2	2.3	62.5	0.2764	0.0037	1.6419
gi|87161266	anti-sigma-B factor, antagonist	2	2	23.1	0.7145	0.3443	EF > 2
gi|87160104	hypothetical protein SAUSA300_2547 [USA300]	1	2.15	20.9	0.7023		
gi|87160250	hypothetical protein SAUSA300_0003 [USA300]	1	2.01	58	0.8638	0.3266	1.6311
gi|87159916	DNA-directed RNA polymerase, delta subunit	1	2	22.2	1.5688		
gi|87162043	lytic regulatory protein	1	2	8.8	0.2805		
gi|153095029	DeoR family transcriptional regulator [PHL213]	1	2	12.5	0.3202	0.0044	1.5926
gi|126433686	transcriptional regulator, MarR family [JLS]	1	2	25.7			
gi|88193109	Chain B, Crystal Structure Of Sara, A Transcription Regulator From Staphylococcus Aureus	1	1.94	21.3	65.0811		

Accession no.	Name	Number of peptides	Total score	Seq Coverage (%)	D30:930918-3	*p* value	Error factor
gi|149186684	transcription-repair coupling factor [Erythrobacter sp. SD-21]	1	1.62	19.3			
gi|94968840	response regulator receiver protein [Acidobacteria bacterium Ellin345]	1	1.52	21.8			
gi|87162130	triacylglycerol lipase precursor [USA300]	3	4.01	20.6	1.1518	0.8098	EF > 2
gi|87162021	acyl carrier protein	2	5.7	77.9	1.1794	0.6781	EF > 2
gi|87161805	3-oxoacyl-(acyl-carrier-protein) reductase	2	4	53.7	0.5628	0.2504	EF > 2
gi|87161662	hypothetical protein SAUSA300_1856 [USA300]	2	4	39.8	0.6643	0.1368	EF > 2
gi|99032669	Chain B, The Crystal Structure Of B-Ketoacyl-Acp Synthase Ii (Fabf) From Staphylococcus Aureus	1	2.18	17.2	0.4901	0.1839	EF > 2
gi|87161082	acetyl-CoA carboxylase, biotin carboxyl carrier protein	1	2.02	33.1	1.4737	0.6105	EF > 2
gi|70726948	enoyl-(acyl carrier protein) reductase [JCSC1435]	1	2.02	14.8	1.9673	0.6946	EF > 2
gi|87160287	fatty acid/phospholipid synthesis protein PlsX	1	2	10.4	0.821		
gi|119502734	acetyl-CoA carboxylase [marine gamma proteobacterium HTCC2080]	1	1.7	15.2	1.1261	0	1.0379
gi|148821476	PE-PGRS family protein [Mycobacterium tuberculosis F11]	1	1.4	34.8	0.7261	0.3413	EF > 2
gi|38604919	Inosine-5'-monophosphate dehydrogenase (IMP dehydrogenase) (IMPDH) (IMPD)	13	20	55.9	0.92	0.4233	1.2392
gi|87161595	phosphoribosylformylglycinamidine synthase	5	6.32	59.8	0.7704	0.3644	1.9166
gi|87161373	adenylate kinase [USA300]	4	8.04	53	0.7969	0.039	1.2338
gi|87161059	uracil phosphoribosyltransferase	3	6.37	31.6	1.1612	0.5693	1.7875
gi|81650637	Pyrimidine-nucleoside phosphorylase (PYNP)	3	6.05	24	0.3446	0.0274	EF > 2
gi|87161310	dihydroorotase [USA300]	3	6.02	22.2	1.4411	0.6933	EF > 2
gi|987497	nucleoside diphosphate kinase	3	6	53	5.5577		
gi|87160143	purine nucleoside phosphorylase	3	3.55	30.5	0.9905	0.8897	1.197
gi|87160876	adenylosuccinate synthetase	2	4.01	15.5	0.8506	0.4488	EF > 2
gi|87162294	phosphoribosylaminoimidazole carboxylase, catalytic subunit	2	3.7	48.9	0.7044		

Accession no.	Name	Number of peptides	Total score	Seq Coverage (%)	D30:930918-3	*p* value	Error factor
gi|87160186	polyribonucleotide nucleotidyltransferase	1	2.69	48.9	1.0208	0.9917	EF > 2
gi|91206761	[Protein-PII] uridylyltransferase (PII uridylyl-transferase) (Uridylyl-removing enzyme) (UTase)	1	2.38	15.4	1.4468	0.3403	EF > 2
gi|84366297	ATP-dependent RNA helicase [Xanthomonas oryzae pv. oryzae MAFF 311018]	1	2.22	33.5			
gi|87161299	hypoxanthine phosphoribosyltransferase	1	2.02	20.8	1.393	0.278	EF > 2
gi|87160831	dihydroorotate dehydrogenase	1	2	11.6	2.0693		
gi|70726884	phosphoribosylamine--glycine ligase [JCSC1435]	1	2	8.7	0.4665		
gi|91206832	GMP synthase [glutamine-hydrolyzing] (Glutamine amidotransferase) (GMP synthetase)	1	2	10.3	0.8728		
gi|150385859	carbamoyl-phosphate synthase, large subunit [Victivallis vadensis ATCC BAA-548]	1	1.42	17.7			
DNA Metabolism: replication, recombination and repair							
gi|88195046	hypothetical protein SAOUHSC_01316 [NCTC 8325]	6	10	23.7	1.1427	0.3803	1.3824
gi|134296873	DEAD/DEAH box helicase domain protein	3	7.7	21.2	1.1963	0.6546	EF > 2
gi|149125815	LigA [Methylobacterium sp. 4-46]	1	2.96	49.2	0.6642	0.0165	1.3457
gi|87160839	recombinase A protein	1	2.01	9.3	0.5374	0.0734	EF > 2
gi|88193844	hypothetical protein SAOUHSC_00023 [NCTC 8325]	1	2.01	26.7	1.0471		
gi|70725957	hypothetical protein SH0956 [JCSC1435]	1	2	15.5	0.5701		
gi|88193825	DNA polymerase III, beta subunit	1	2	10.1	0.5518		
gi|150005913	ATP-dependent exonuclease V, alpha subunit - helicase superfamily I member [Bacteroides vulgatus ATCC 8482]	1	2	6.8	1.0341		
gi|98311102	thermostable nuclease	1	2	6.9	3.0672		
gi|149189072	MshA, mannose-sensitive haemaglutinin [AK1]	1	2	10.8			
gi|149913440	NAD-dependent deacetylase [Roseobacter sp. AzwK-3b]	1	2	7.7			

Accession no.	Name	Number of peptides	Total score	Seq Coverage (%)	D30:930918-3	*p* value	Error factor
gi|109946687	ComB3 protein [Sheeba]	1	2	15.9	1.0007	0.9971	1.495
gi|121611662	DEAD/DEAH box helicase domain protein [Verminephrobacter eiseniae EF01-2]	1	1.91	21.5	0.5971		
gi|153006953	LigA [Anaeromyxobacter sp. Fw109-5]	1	1.82	44.1	0.6966	0.5254	EF > 2
gi|147676398	DNA polymerase III, gamma/tau subunits [Pelotomaculum thermopropionicum SI]	1	1.7	31.6	1.3459	0.0099	1.1953
gi|41409059	hypothetical protein MAP2961c [Mycobacterium avium subsp. paratuberculosis K-10]	1	1.54	46.9	0.8078	0.5586	EF > 2
gi|61215122	DNA repair protein recO (Recombination protein O)	1	1.52	17.7			
Pathogenesis and Immunomodulation							
gi|87160749	cell surface elastin binding protein	200	45.07	43.4	1.7517	0	1.2421
gi|133853458	immunoglobulin G binding protein A precursor	138	58.7	78.8	2.2282	0	1.171
gi|56749001	Immunodominant staphylococcal antigen A precursor	57	18.55	49.8	1.4061	0	1.0856
gi|15926764	penicillin-binding protein 1	43	61.62	38.4	1.3495	0.0004	1.1748
gi|87161577	cold shock protein, CSD family	36	16.74	65.2	0.7651	0	1.0296
gi|87162077	penicillin binding protein 2	32	52.49	66.6	0.6419	0.0001	1.2366
gi|87160015	staphylococcal tandem lipoprotein	14	21.24	48.9	0.4398	0.0002	1.4325
gi|47169194	Chain A, Staphylococcal Protein A, B-Domain, Y15w Mutant, Nmr, 25 Structures	12	12.14	82.3	0.9803		
gi|70726765	beta-lactamase	10	16.53	40.6	0.0849	0	EF > 2
gi|87160380	alpha-hemolysin precursor	10	14.14	36.7	2.6865	0	1.2524
gi|87160982	Leukocidin/Hemolysin toxin family protein	10	13.16	49.7	0.3131	0	1.414
gi|87162162	hypothetical protein SAUSA300_1018 [USA300]	8	16.29	24.9	1.0669	0.5321	1.2388
gi|87161881	antibacterial protein	7	4.08	50	0.5416	0	1.115
gi|87161157	penicillin-binding protein 4	6	7.74	23.4	1.6283	0.1152	1.8598
gi|15927581	hypothetical protein SA1813 [N315]	5	11.45	39.9	0.3607	0	1.4457
gi|87162347	hypothetical protein SAUSA300_2164 [USA300]	4	6.34	48.2	0.3271	0.1009	EF > 2

Accession no.	Name	Number of peptides	Total score	Seq Coverage (%)	D30:930918-3	*p* value	Error factor
gi|87160217	secretory antigen precursor SsaA	4	6.25	25.5	0.9951	0.9764	1.4636
gi|88194063	hypothetical protein SAOUHSC_00257 [NCTC 8325] - ESAT6 family virulence protein	4	6.01	53.6	0.384	0.0557	EF > 2
gi|87160365	antibacterial protein [USA300]	4	2	50	0.9121	0.1981	1.1578
gi|87160520	acetyltransferase family protein	3	4.09	51.1	2.0482	0.0094	1.5289
gi|87161173	teicoplanin resistance associated membrane protein TcaA protein [USA300]	3	4.02	11.3	0.8209	0.9069	EF > 2
gi|88195687	hypothetical protein SAOUHSC_01999 [NCTC 8325]	3	3.52	15.2	2.9885	0.0002	1.4259
gi|68565538	Protein esaA	2	4.01	23.2	0.2372	0.2204	EF > 2
gi|87162375	hypothetical protein SAUSA300_1323 [USA300]	2	2.01	38.6	0.809	0.5491	EF > 2
gi|87161897	IgG-binding protein SBI	1	2.7	10.6	3.6719	0.1219	EF > 2
gi|87160565	immunodominant antigen B	1	2.61	28	29.6467		
gi|87160905	hypothetical protein SAUSA300_0282 [USA300]-similar to essB,	1	2	12.6	0.2942		
gi|87162379	Ferredoxin	1	2	18.9	1.1786		
gi|62391257	secreted penicillin binding protein [Corynebacterium glutamicum ATCC 13032]	1	1.7	7	1.6876		
Cell Division and Cycle							
gi|87162194	cell division protein ftsZ	18	20.02	43.6	1.0579	0.704	1.3468
gi|87161534	putative cell division protein FtsH [USA300]	7	15.83	34.3	1.5338	0.0062	1.2998
gi|87161782	cell division protein	7	7.81	30.8	1.1558	0.778	EF > 2
gi|87162117	hypothetical protein SAUSA300_1337 [USA300]	5	9.29	58.8	0.9429	0.9174	EF > 2
gi|73662607	putative cell division initiation protein [ATCC 15305]	3	6.99	46.2	1.2227		
gi|87160736	cell-division initiation protein	3	3.16	51.5	0.7201	0.0097	1.1937
gi|87161457	HIT family protein	2	3.58	29.3	0.9705		
gi|24374683	hypothetical protein SO_3170 [MR-1]	1	2.01	17.1	2.5571	0.0232	1.871

Accession no.	Name	Number of peptides	Total score	Seq Coverage (%)	D30:930918-3	*p* value	Error factor
gi|151591524	cell divisionFtsK/SpoIIIE [Methylobacterium extorquens PA1]	1	1.7	22.1	1.1688	0.9016	EF > 2
Cell Adhesion							
gi|87160939	cell wall surface anchor family protein	57	42.04	60.2	3.6116	0	1.1326
gi|151222604	hypothetical protein NWMN_2392 [Newman]	40	59.98	69.5	0.0911	0	1.3616
gi|87162026	autolysin	31	42.59	49.3	1.0742	0.6135	1.3283
gi|87160697	D-alanine-activating enzyme/D-alanine-D-alanyl, dltD protein	18	24.96	49.4	1.2272	0.2515	1.4254
gi|87162315	putative lipoprotein [USA300]	16	14.26	40.4	1.2742	0.1446	1.3919
gi|61213890	77 kDa outer membrane protein precursor	11	22.71	36.1	0.2627	0	1.3683
gi|81781509	UPF0365 protein SAV1573	8	14.02	46.2	1.8364	0.0005	1.3046
gi|87160285	rod shape-determining protein MreC	8	11.59	51.8	0.8103	0.0767	1.2641
gi|87160775	N-acetylmuramoyl-L-alanine amidase	8	11.4	29.9	1.5402	0.0651	1.5923
gi|87161887	N-acetylmuramoyl-L-alanine amidase domain protein	7	14.01	25.4	1.893	0.3018	EF > 2
gi|88196468	sortase, putative [NCTC 8325]	5	10.01	25.7	2.0829	0.001	1.4021
gi|87161790	5'-nucleotidase family protein [USA300]	3	2.04	10.4	3.6218	0.1664	EF > 2
gi|87160715	fmt protein [USA300]	2	4.86	20.4	1.1273	0.8064	EF > 2
gi|81673756	Phosphoglucosamine mutase	1	2.8	20.4	0.7583	0.739	EF > 2
gi|87160798	serine-aspartate repeat family protein, SdrH	1	2.21	17.5	1.49	0.0115	1.3123
gi|116694144	flp pilus assembly protein TadC [Ralstonia eutropha H16]	1	2.19	22.9	1.3693		
gi|81781921	Extracellular matrix protein-binding protein emp precursor	1	2.12	12.9	0.5809	0.4841	EF > 2
gi|87160121	D-alanine-activating enzyme/D-alanine-D-alanyl, dltC protein	1	1.7	38.5	0.6864	0.533	EF > 2
gi|91211353	AsmA suppressor of OmpF assembly mutants [Escherichia coli UTI89]	1	1.7	19.9			

Accession no.	Name	Number of peptides	Total score	Seq Coverage (%)	D30:930918-3	*p* value	Error factor
Transport proteins							
gi|87160674	putative lipoprotein [USA300]	41	30.7	68.4	0.2959	0	1.1033
gi|87162197	amino acid ABC transporter, amino acid-binding protein	34	41.25	63.3	0.9535	0.4842	1.1423
gi|87162140	oligopeptide ABC transporter, substrate-binding protein	30	41.53	48.3	1.1547	0.0301	1.1385
gi|87161315	hypothetical protein SAUSA300_2378 [USA300]	21	21.34	58	1.4953	0	1.1373
gi|87160588	molybdenum ABC transporter, molybdenum-binding protein ModA	17	26.41	46.5	1.5245	0.0005	1.2498
gi|87161352	ABC transporter, substrate-binding protein	12	18.38	38.7	0.2931	0.0126	EF > 2
gi|87160965	phosphocarrier protein HPr	11	17	89.8	1.1099	0.0026	1.0687
gi|87162382	PTS system, glucose-specific IIA component	11	12	54.2	1.0668	0.4928	1.2135
gi|87162442	transferrin receptor	8	12.69	31.9	3.331	0	1.3395
gi|87160279	AcrB/AcrD/AcrF family protein	7	13.76	34	1.4716	0.1045	1.6227
gi|87161641	amino acid ABC transporter, permease/substrate-binding protein	7	10.49	30.7	6.1167	0	1.7179
gi|21284120	oligopeptide transporter putative substrate binding domain [MW2]	6	12.01	29.1	2.4913	0.0004	1.4168
gi|87160515	protein-export membrane protein SecF	6	10.63	16.2	1.4937	0.0097	1.3267
gi|21282147	hypothetical protein MW0418 [MW2]	6	8.69	49.3	1.0242	0.8594	1.3595
gi|87161764	putative iron compound ABC transporter, iron compound-binding protein [USA300]	5	10.17	36	1.4063	0.0805	1.4816
gi|87160849	iron compound ABC transporter, iron compound-binding protein	4	8	28.5	0.5869	0.0986	1.9934
gi|87161518	glycine betaine/carnitine/choline ABC transporter [USA300]	4	8	14.4	0.9366	0.6998	1.4703
gi|87161864	ABC transporter, substrate-binding protein	3	8.12	25.2	2.8266	0.0151	EF > 2
gi|87160369	hypothetical protein SAUSA300_0833 [USA300]	3	6.1	20.5	0.5373	0.5051	EF > 2
gi|15925912	RGD-containing lipoprotein [N315]	3	6.02	17.4	1.2004	0.4097	1.7354
gi|87161142	ferric hydroxamate receptor	3	4	8.9	1.0332	0.8931	EF > 2

Accession no.	Name	Number of peptides	Total score	Seq Coverage (%)	D30:930918-3	*p* value	Error factor
gi|87162224	osmoprotectant ABC transporter, permease	2	4	35.1	0.6537		
gi|87161872	putative lipoprotein [USA300]	2	4	16.4	4.2798	0.2519	EF > 2
gi|87160414	multidrug resistance protein A, drug resistance transporter	1	3.16	15.3	0.6934	0.2928	EF > 2
gi|87162284	putative ferrichrome ABC transporter [USA300]	1	3.05	22.3	0.2468	0.0722	EF > 2
gi|149201149	nitrate transport ATP-binding subunits C and D [TM1035]	1	2.4	16.3	1.5776		
gi|151575108	outer membrane efflux protein [Ralstonia pickettii 12D]	1	2.22	15.6	1.1986	0.2951	1.7416
gi|87161139	iron transport associated domain protein [USA300]	1	2.09	21.1	1.6828		
gi|149910101	Hypothetical transport protein [Moritella sp. PE36]	1	2.02	6.8	2.2325	0	1.1098
gi|87161389	putative iron compound A C transporter, iron compound-binding protein [USA300]	1	2.01	9.9	2.6052	0.134	EF > 2
gi|35211526	gll0963 [Gloeobacter violaceus PCC 7421]	1	2	14			
gi|87162212	amino acid ABC transporter, ATP-binding protein	1	2	25.6	5.1042		
gi|127512243	efflux transporter, RND family, MFP subunit [Shewanella loihica PV-4]	1	2	11.1			
gi|126355053	ABC transporter related [Pseudomonas putida GB-1]	1	1.71	6.4	37.5193		
gi|17131745	all2652 [Nostoc sp. PCC 7120]	1	1.7	37.6	1.7839		
gi|149194563	ABC transporter-related protein [Caminibacter mediatlanticus TB-2]	1	1.7	8.4	1.6215		
gi|87162344	phosphonate ABC transporter, phosphonate-binding protein	1	1.7	4.4	1.3653	0.3305	EF > 2
gi|51595518	molybdenum transport regulatory (repressor) protein ModE [Yersinia pseudotuberculosis IP 32953]	1	1.55	33.5	1.3022	0.3562	EF > 2

Accession no.	Name	Number of peptides	Total score	Seq Coverage (%)	D30:930918-3	*p* value	Error factor
gi|23005821	COG1131: ABC-type multidrug transport system, ATPase component [Magnetospirillum magnetotacticum MS-1]	1	1.52	17.5			
gi|152936446	flagellar motor switch protein fliG [Clostridium botulinum F str. Langeland]	1	1.52	7.7			
gi|146301866	RND efflux system, outer membrane lipoprotein, NodT family [Flavobacterium johnsoniae UW101]	1	1.46	14.1	0.9695	0.7073	EF > 2
Other functions							
gi|21283573	hypothetical protein MW1844 [MW2]	4	6.1	29.1	1.2273	0.2285	1.4175
gi|15928229	hypothetical protein SA2436 [N315]	2	4.14	12	0.9599	0.637	1.4175
gi|87161880	manganese-dependent inorganic pyrophosphatase	2	4	18.4	0.5097	0.0232	1.3771
gi|87161327	S-ribosylhomocysteinase	1	2.16	21.8			1.568
gi|116696021	signal transduction histidine kinase containing a receiver domain (hybrid) [Ralstonia eutropha H16]	1	2.01	23.6	1.4217	0.1981	
gi|62900222	HAM1 protein homolog	1	2	25.1	0.9614		EF > 2
gi|56749556	6,7-dimethyl-8-ribityllumazine synthase (DMRL synthase) (Lumazine synthase) (Riboflavin synthase beta chain)	1	2	30.5			
gi|87161407	hypothetical protein SAUSA300_1160 [USA300]	1	2	21.3	4.1631		
gi|29347076	hydrolase, haloacid dehalogenase-like hydrolase [Bacteroides thetaiotaomicron VPI-5482]	1	1.74	17.1	0.9924	0.9952	
gi|146292939	TonB-dependent siderophore receptor [Shewanella putrefaciens CN-32]	1	1.7	9.8	0.7143		EF > 2
Hypothetical proteins							

Accession no.	Name	Number of peptides	Total score	Seq Coverage (%)	D30:930918-3	*p* value	Error factor
gi|87160135	hypothetical protein SAUSA300_1581 [USA300)	23	8.04	72.9	0.3596	0	0
gi|87159943	hypothetical protein SAUSA300_1908 [USA300]	21	17.48	29.3	1.5549	0.0001	1.1148
gi|87160606	hypothetical protein SAUSA300_1698 [USA300]	20	14.73	64.3	0.387	0	1.2259
gi|87161419	hypothetical protein SAUSA300_1795 [USA300]	18	10.24	86	1.079	0.2432	1.1923
gi|15926079	hypothetical protein SA0363 [N315]	13	21.12	47.6	1.4849	0	1.1595
gi|87161713	hypothetical protein SAUSA300_0385 [USA300]	8	8	41.5	0.8594	0.5635	1.138
gi|88195776	hypothetical protein SAOUHSC_02093 [NCTC 8325]	8	6	71.2	0.9873	0.8789	1.7367
gi|87160537	hypothetical protein SAUSA300_2132 [USA300]	7	11.27	80.2	1.0867	0.6798	1.1881
gi|87161087	hypothetical protein SAUSA300_2144 [USA300]	7	8.59	28	0.2896	0	1.5006
gi|87160300	hypothetical protein SAUSA300_1440 [USA300]	6	10.54	27.7	0.1735	0.0003	1.2497
gi|87160039	hypothetical protein SAUSA300_2330 [USA300]	5	10.04	32.2	1.2051	0.593	1.9882
gi|87160421	hypothetical protein SAUSA300_0172 [USA300]	5	8	68.7	1.0018	0.9952	EF > 2
gi|87162221	hypothetical protein SAUSA300_0664 [USA300]	5	8	66.7	0.692	0.0402	EF > 2
gi|88196395	hypothetical protein SAOUHSC_02759 [NCTC 8325]	5	4.01	23.2	2.1631	0.0241	1.4103
gi|87161527	hypothetical protein SAUSA300_1572 [USA300]	5	2	34.3	1.0092	0.9387	1.8773
gi|88195426	hypothetical protein SAOUHSC_01721 [NCTC 8325]	4	5	53.5	0.8342	0.3307	1.323
gi|87161381	hypothetical protein SAUSA300_1857 [USA300]	2	4.03	50.9	1.0179	0.8885	1.5208
gi|15926825	hypothetical protein SA1085 [N315]	2	4.02	13.1	1.2371	0.6284	1.6169
gi|87160698	hypothetical protein SAUSA300_1906 [USA300]	2	4	13.6	3.2755	0.2111	EF > 2
gi|87159919	hypothetical protein SAUSA300_2527 [USA300]	2	4	49.5	0.3861		EF > 2
gi|87161111	hypothetical protein SAUSA300_2212 [USA300]	2	4	61.1	1.0786	0.412	
gi|87161468	hypothetical protein SAUSA300_1215 [USA300]	2	4	41.5	1.2885	0.0096	1.3728
gi|88195065	hypothetical protein SAOUHSC_01336 [NCTC 8325]	2	2.32	41.8	0.834	0.2239	1.2048
gi|87160907	hypothetical protein SAUSA300_0602 [USA300]	2	2.1	17.9	1.0512	0.9538	1.3997
gi|87161979	hypothetical protein SAUSA300_2560 [USA300]	2	2	47	0.161	0.0966	EF > 2
gi|87162360	hypothetical protein SAUSA300_1685 [USA300]	2	2	9.2	1.0751	0.8346	EF > 2

Accession no.	Name	Number of peptides	Total score	Seq Coverage (%)	D30:930918-3	*p* value	Error factor
gi|150393509	hypothetical protein SaurJH1_1041 [JH1]	2	2	25			EF > 2
gi|21284001	hypothetical protein MW2272 [MW2]	1	3.17	16.5	4.6526	0.1163	
gi|87162045	hypothetical protein SAUSA300_1788 [USA300]	1	2.68	47.9	1.0535	0.8698	EF > 2
gi|77465081	hypothetical protein RSP_3067 [Rhodobacter sphaeroides 2.4.1]	1	2.52	26	2.2694	0.0155	EF > 2
gi|87160235	hypothetical protein SAUSA300_1904 [USA300]	1	2.26	28.1	0.4473	0.0077	1.7548
gi|87161000	hypothetical protein SAUSA300_1606 [USA300]	1	2.24	47.1	1.5647	0.2156	1.4911
gi|93140725	Uncharacterized N-acetyltransferase SAB1040c	1	2.19	19.2	0.7824	0.7467	EF > 2
gi|87161220	hypothetical protein SAUSA300_0383 [USA300]	1	2.14	23.3	0.674		EF > 2
gi|87161658	hypothetical protein SAUSA300_2148 [USA300]	1	2.1	21.5	1.2192		
gi|87159886	hypothetical protein SAUSA300_2493 [USA300]	1	2.08	34.9	2.9543	0.4404	
gi|55773538	conserved hypothetical protein [HB8]	1	2.06	8.4	1.0904	0.8292	EF > 2
gi|119386105	hypothetical protein Pden_3391 [PD1222]	1	2.04	30.6	1.2549	0.9572	EF > 2
gi|87160533	hypothetical protein SAUSA300_1321 [USA300]	1	2.01	17.2	0.9115		EF > 2
gi|30262516	hypothetical protein BA2524 [Bacillus anthracis str. Ames]	1	2.01	30.1	0.7071		
gi|87160245	hypothetical protein SAUSA300_1864 [USA300]	1	2.01	6.9	0.5931		
gi|87160914	hypothetical protein SAUSA300_1223 [USA300]	1	2	18.3	2.0375		
gi|70726727	hypothetical protein SH1726 [JCSC1435]	1	2	8.6	1.968	0.4486	
gi|21283169	hypothetical protein MW1440 [MW2]	1	2	52.9	0.0267	0.0043	EF > 2
gi|87162265	hypothetical protein SAUSA300_1057 [USA300]	1	2	18.2	0.8927		EF > 2
gi|87160560	hypothetical protein SAUSA300_1335 [USA300]	1	2	9.1	0.4827		
gi|87160349	hypothetical protein SAUSA300_0982 [USA300]	1	2	6.1	1.2009		
gi|87160886	hypothetical protein SAUSA300_0990 [USA300]	1	1.84	40.3	1.3089	0.7278	
gi|116618724	hypothetical protein LEUM_1630 [ATCC 8293]	1	1.71	22	2.0837	0.0014	EF > 2
gi|15595185	Hypothetical protein BB0840 [B31]	1	1.7	7.8	1.9176	0.2845	EF > 2
gi|145299288	hypothetical protein ASA_2332 [Aeromonas salmonicida subsp. salmonicida A449]	1	1.7	18.2	0.5493		1.2273
gi|148556846	hypothetical protein Swit_3945 [RW1]	1	1.7	31.8	1.3657	0.0256	

Accession no.	Name	Number of peptides	Total score	Seq Coverage (%)	D30:930918-3	*p* value	Error factor
gi|118602465	hypothetical protein Rmag_0450 [Candidatus Ruthia magnifica str. Cm (Calyptogena magnifica)]	1	1.7	10.1	1.0723	0.6071	1.2906
gi|83647697	hypothetical protein HCH_05022 [Hahella chejuensis KCTC 2396]	1	1.53	8.4	1.3081		1.6444
gi|89070338	hypothetical protein OG2516_12764 [Oceanicola granulosus HTCC2516]	1	1.53	23.8			
gi|86136324	hypothetical protein MED193_19414 [Roseobacter sp. MED193]	1	1.53	38.3	1.1649		
gi|88194234	hypothetical protein SAOUHSC_00444 [NCTC 8325]	1	1.52	41.9	1.0288		
gi|149191551	hypothetical protein VSAK1_15442 [Vibrio shilonii AK1]	1	1.52	11.9	1.791		
gi|145220937	hypothetical protein Mflv_0333 [Mycobacterium gilvum PYR-GCK]	1	1.52	5.8			
gi|88194796	hypothetical protein SAOUHSC_01044 [NCTC 8325]	1	1.52	15.4			
gi|29610655	hypothetical protein [Streptomyces avermitilis MA-4680]	1	1.4	12.8			
gi|29609637	hypothetical protein [Streptomyces avermitilis MA-4680]	1	1.4	6.9	0.9259		
gi|120610660	hypothetical protein Aave_1980 [Acidovorax avenae subsp. citrulli AAC00-1]	1	1.4	4.8			
gi|149912076	hypothetical protein PE36_12287 [Moritella sp. PE36]	1	1.4	26.5	0.9682		
gi|124268268	hypothetical protein Mpe_A3084 [Methylibium petroleiphilum PM1]	1	1.33	29.6	1.8227	0.0754	1.9466
Unknown funtion							

Accession no.	Name	Number of peptides	Total score	Seq Coverage (%)	D30:930918-3	*p* value	Error factor
gi|87161686	putative lipoprotein	51	32.02	52.2	0.5638	0	0
gi|82751366	Probable transaldolase	8	13.17	67.9	0.6997	0.0006	1.1679
gi|87161661	putative lipoprotein	7	13.51	43.8	0.4656	0.0004	1.1939
gi|87161314	putative lipoprotein [USA300]	4	6.01	29.5	0.6518	0.3505	1.4789
gi|49484622	putative solute binding lipoprotein [MRSA252]	3	6.91	24.3	1.8307	0.0116	EF > 2
gi|87160546	putative cell-division initiation protein [USA300]	3	6	40.5	1.7071	0.082	1.4924
gi|87161260	phiSLT ORF144-like protein, putative lipoprotein [USA300]	2	4.05	36.1	0.5132	0.0011	EF > 2
gi|87161351	putative lipoprotein [USA300]	2	4.01	17.5	1.4335	0.1135	1.3614
gi|87161825	putative lipoprotein [USA300]	2	4	26.9	0.5028	0.2762	1.6214
gi|153005206	protein of unknown function DUF849 [Anaeromyxobacter sp. Fw109-5]	2	2	22.1	4.1702		EF > 2
gi|124010323	lipoprotein, putative [Microscilla marina ATCC 23134]	1	3.36	7.1	1.2868	0.7142	
gi|87161720	putative arsenate reductase [USA300]	1	2.8	26.3	0.7002	0.7028	EF > 2
gi|117164639	putative modular polyketide synthase [ATCC 23877]	1	2.2	12.3	1.7159	0.0172	EF > 2
gi|121583546	protein of unknown function DUF262 [Polaromonas naphthalenivorans CJ2]	1	2	11.4	1.1489	0.1227	1.5354
gi|81693746	Uncharacterized lipoprotein SACOL2497 precursor	1	2	18.4	10.6267		1.2057
gi|120609276	uncharacterized protein UPF0065 [Acidovorax avenae subsp. citrulli AAC00-1]	1	2	18.6	1.7374	0.2738	
gi|149910937	Uncharacterized protein conserved in bacteria [Moritella sp. PE36]	1	2	17.2	0.9901	0.7765	EF > 2
gi|148869366	putative patatin [Vibrio harveyi HY01]	1	1.7	20.5	1.0616	0.0931	EF > 2
gi|116250012	putative methyltransferase [Rhizobium leguminosarum bv. viciae 3841]	1	1.52	12.4			1.0725

Accession no.	Name	Number of peptides	Total score	Seq Coverage (%)	D30:930918-3	*p* value	Error factor
gi|146306168	protein of unknown function DUF1302 [Pseudomonas mendocina ymp]	1	1.52	6.9	2.2487		
gi|51894011	putative cadmium-transporting ATPase [Symbiobacterium thermophilum IAM 14863]	1	1.41	28.7	1.0075		
gi|25027269	putative urea carboxylase [Corynebacterium efficiens YS-314]	1	1.4	6.3	1.0061	0.9669	
gi|29608736	putative integral membrane protein [Streptomyces avermitilis MA-4680]	0	1.41	21.3	0.9063	0.1005	1.7525

Table 13: Functional classification of the total 488 exoproteome proteins of nasal carrier strain (D30) in planktonic and biofilm growth conditions identified by iTRAQ analysis in three independent experiments

D30 planktonic: D30 biofilm is the ratio of protein expression levels between the planktonic and biofilm growth conditions of D30. The p values and the error factor associated with the protein expression levels are also indicated here.

Accession no.	Name	Number of peptides	Total score	Sequence Coverage (%)	D30 planktonic: D30 biofilm	*p* value	Error factor
Amino Acid & Protein Synthesis							
gi|88194310	translation elongation factor Tu	109	63.62	85.8	0.5935	0.0053	1.4324
gi|87161362	50S ribosomal protein L15	47	48.25	83.6	0.7047	0	1.1329
gi|14586725	translation elongation factor Tu	35	26.26	70.4			
gi|87160058	cysteine synthase A	25	40.61	84.8	1.6513	0	1.2339
gi|73919121	30S ribosomal protein S7	25	18.57	68.6	0.2482	0.0001	1.9256
gi|87161596	30S ribosomal protein S16	23	22.1	52.7	1.2803	0.0236	1.2359
gi|87160271	30S ribosomal protein S20	23	14	22.9	0.9639	0.8864	1.6811
gi|87161732	30S ribosomal protein S9	20	24.3	58.3	1.3604	0.1011	1.447
gi|87160361	50S ribosomal protein L5	20	20.23	53.6	1.22	0.2287	1.3869
gi|87160513	50S ribosomal protein L22	20	13.82	54.7	0.7482	0.2366	1.6294
gi|56961930	elongation factor Tu [Bacillus clausii KSM-K16]	20	23.05	57.3			
gi|90110058	50S ribosomal protein L3	19	4.01	18.4	0.2327	0	1.0318
gi|87161210	translation elongation factor Ts	18	26.16	73.4	1.0637	0.7845	1.581
gi|87161455	ribosomal protein L7/L12	17	19.7	78.7	1.6151	0	1.246
gi|87160153	ribosome recycling factor	17	14.48	64.1	1.1476	0.6539	1.8627
gi|87161079	translation initiation factor IF-1	17	10.02	77.8	0.8221	0.1116	1.2702
gi|87162219	30S ribosomal protein S1	16	26.03	57.3	1.2969	0.4009	1.873
gi|87161718	50S ribosomal protein L9	15	21.91	63.5	0.9782	0.8161	1.2061
gi|87160155	50S ribosomal protein L4	15	17.22	77.8	0.4465	0.0751	EF > 2
gi|70725821	50S ribosomal protein L30	15	17.07	79.7	1.0036	0.9879	1.6157
gi|87162334	50S ribosomal protein L2	13	19.76	41.5	0.552	0	1.2905
gi|87161133	ribosomal protein L11	13	8.83	67.9	1.5494	0.0733	1.622

Accession no.	Name	Number of peptides	Total score	Sequence Coverage (%)	D30 planktonic: D30 biofilm	*p* value	Error factor
gi|87161952	50S ribosomal protein L32	13	7.36	57.9	1.3774	0.2461	1.7414
gi|11612404	elongation factor Tu [Enterococcus dispar]	13	21.05	74.5	1.2278	0.7976	EF > 2
gi|82581599	50S ribosomal protein L7/L12	13	7.44	84.4			
gi|88909112	50S ribosomal protein L17	11	12.79	35.8	0.3434	0	1.1362
gi|90101744	30S ribosomal protein S8	10	16.55	89.4	0.8202	0.6385	EF > 2
gi|91207380	50S ribosomal protein L1	9	11.57	47	1.2369	0.2505	1.4463
gi|151220721	translation elongation factor G (EF-G)	8	15.92	37.8	1.1213	0.7264	EF > 2
gi|87161329	50S ribosomal protein L21	8	13.4	55.9	1.2524	0.6012	EF > 2
gi|91207792	30S ribosomal protein S6	8	10.34	60.2	1.0042	0.9899	1.9838
gi|97181999	50S ribosomal protein L10	7	12.54	66.9	1.6519	0.1542	EF > 2
gi|87161988	50S ribosomal protein L3	7	9	46.4	1.1273	0.6057	1.6072
gi|87161367	threonyl-tRNA synthetase	6	13.25	28.2	0.5856	0.3288	EF > 2
gi|91207680	30S ribosomal protein S11	6	10.43	41.9	1.2143	0.6708	EF > 2
gi|87160873	50S ribosomal protein L23	6	9.18	45.1	0.6365	0.0053	1.3686
gi|87161591	30S ribosomal protein S15	6	8.82	51.7	1.3098	0.1072	1.4247
gi|87160559	aspartyl/glutamyl-tRNA amidotransferase subunit C	6	8.68	67	0.9329	0.9588	EF > 2
gi|56749400	Seryl-tRNA synthetase (Seryl-tRNA(Ser/Sec) synthetase) (Serine--tRNA ligase) (SerRS)	6	8	29.9	1.3812	0.362	EF > 2
gi|87161370	50S ribosomal protein L31 type B	6	6.22	59.5	1.1487	0.7321	EF > 2
gi|87161038	hypothetical protein SAUSA300_0916 [USA300]	5	10.92	60.9	1.0217	0.938	1.8773
gi|87160935	50S ribosomal protein L6	5	7.97	50.6	0.6564	0.5014	EF > 2
gi|73917907	30S ribosomal protein S10	5	6.9	62.7	0.86	0.7556	EF > 2
gi|91207889	30S ribosomal protein S5	4	8.59	58.4	0.9539	0.9144	EF > 2
gi|87161481	50S ribosomal protein L29	4	8.2	47.9	1.1427	0.6818	EF > 2
gi|88195373	glycyl-tRNA synthetase	4	6.23	15.6	0.9964	0.9956	EF > 2
gi|71153662	50S ribosomal protein L25 (General stress protein CTC)	4	6.13	36.4	3.1543	0.0067	EF > 2
gi|59797753	Glutamine synthetase (Glutamate--ammonia ligase) (GS)	4	6.12	16.6	3.2059	0.2443	EF > 2

Accession no.	Name	Number of peptides	Total score	Sequence Coverage (%)	D30 planktonic: D30 biofilm	*p* value	Error factor
gi|90101727	30S ribosomal protein S4	3	6	36	1.1093	0.8768	EF > 2
gi|87161271	chorismate mutase/phospho-2-dehydro-3-deoxyheptonate aldolase	3	6	19.6	3.2938	0.0406	EF > 2
gi|87160953	translation initiation factor IF-3	3	6	21.1	2.4551	0.051	EF > 2
gi|87162332	50S ribosomal protein L16	3	5.44	42.4	0.2155	0.041	EF > 2
gi|153202305	ribosomal protein S21 [HPB2262]	3	5.3	38.2	0.18	0.0774	EF > 2
gi|87161395	50S ribosomal protein L24 [USA300]	3	4.54	41	1.165	0.7682	EF > 2
gi|87161828	50S ribosomal protein L27	3	4.09	35.1	1.0654	0.9425	EF > 2
gi|152937150	translation elongation factor Tu [Clostridium botulinum F str. Langeland]	3	5.28	30.7			
gi|38372424	30S ribosomal protein S8	3	6.04	55.3	0.2343		
gi|87161168	50S ribosomal protein L13	2	5.21	36.6	1.2251	0.6859	EF > 2
gi|91207727	30S ribosomal protein S13	2	5.03	52.1	1.3499	0.4334	EF > 2
gi|87162298	30S ribosomal protein S19 [USA300]	2	4.6	51.1	0.9502	0.9248	EF > 2
gi|87160596	50S ribosomal protein L18 [USA300]	2	4.58	46.2	0.1403	0.1439	EF > 2
gi|151220702	glutamyl-tRNA synthetase	2	4	22.1	0.6181	0.1033	EF > 2
gi|87161400	phenylalanyl-tRNA synthetase (beta subunit)	2	3.7	33.3	1.1207	0.9365	EF > 2
gi|87162294	phosphoribosylaminoimidazole carboxylase, catalytic subunit	2	3.7	48.9			
gi|90101380	Translation initiation factor IF-2	2	3.48	35.2	0.617	0.4178	EF > 2
gi|90101385	Translation initiation factor IF-2	1	3.56	14.3	0.1044	0.0105	EF > 2
gi|87162006	tetrahydrodipicolinate acetyltransferase	1	3.05	33.1	0.9433		
gi|87160672	30S ribosomal protein S2	1	2.29	11	6.0952		
gi|87162222	translation elongation factor P	1	2.19	12.4	1.9077	0.0089	1.3029
gi|149122046	(Glutamate--ammonia-ligase) adenylyltransferase [Methylobacterium sp. 4-46]	1	2.15	38.3	2.4004	0.5889	EF > 2
gi|138896204	Valyl-tRNA synthetase [Geobacillus thermodenitrificans NG80-2]	1	2.13	9.1			

Accession no.	Name	Number of peptides	Total score	Sequence Coverage (%)	D30 planktonic: D30 biofilm	*p* value	Error factor
gi|73662075	peptide chain release factor 1 [ATCC 15305]	1	2.11	13.1	0.0294	0.2435	EF > 2
gi|91207843	30S ribosomal protein S3	1	2.06	35.5	0.0165		
gi|113476121	RNA binding S1 [Trichodesmium erythraeum IMS101]	1	2.05	22.7	0.0634	0.3808	EF > 2
gi|149376055	imidazole glycerol phosphate synthase subunit HisF [Marinobacter algicola DG893]	1	2.03	32.7			
gi|73918993	Dihydrodipicolinate synthase (DHDPS)	1	2.02	26.4	0.3638	0.3594	EF > 2
gi|92090969	Arginine biosynthesis bifunctional protein argJ [Includes: Glutamate N-acetyltransferase (Ornithine acetyltransferase) (Ornithine transacetylase) (OATase); Amino-acid acetyltransferase (N-acetylglutamate synthase) (AGS)] [Contains: Arginine biosynthesis b	1	2.01	21.1	8.2239		
gi|97051447	Serine hydroxymethyltransferase (Serine methylase) (SHMT)	1	2.01	14.1	0.5065		
gi|21284173	2-hydroxyacid dehydrogenase [MW2]	1	2.01	7.7	2.115		
gi|90108439	Valyl-tRNA synthetase (Valine--tRNA ligase) (ValRS)	1	2.01	13.8	0.4091		
gi|87161786	1-pyrroline-5-carboxylate dehydrogenase	1	2	12.5	0.2202		
gi|145588242	ribosomal protein L3 [Polynucleobacter sp. QLW-P1DMWA-1]	1	2	39	0.2122		
gi|90101261	Dihydrodipicolinate reductase (DHPR)	1	2	16.7	0.4375		
gi|87160676	threonine synthase	1	2	15.9	1.2543		
gi|87161544	branched-chain amino acid aminotransferase	1	2	21.5	0.9127		
gi|87162399	50S ribosomal protein L20	1	1.8	16.1	0.2449	0.0015	EF > 2
gi|38605460	50S ribosomal protein L11	1	2.84	23.4			
gi|121534747	ribosomal protein L11[Thermosinus carboxydivoransNor1]	1	2.01	22			
gi|116491401	Ribosomal protein L11 [Oenococcus oeni PSU-1]	1	2	15.3			
gi|126635115	non-ribosomal peptide synthetase A [Actinoplanes	1	1.54	22.7	0.5948	0.6304	EF > 2

Accession no.	Name	Number of peptides	Total score	Sequence Coverage (%)	D30 planktonic: D30 biofilm	*p* value	Error factor
	friuliensis]						
gi|115502775	50S ribosomal protein L16	1	1.54	42.5	0.2859	0.0025	1.52
gi|15672583	serine hydroxymethyltransferase [Lactococcus lactis subsp. lactis Il1403]	1	1.52	16.4	0.2847	0.0005	1.4125
gi|148242083	L-asparaginase II [Synechococcus sp. RCC307]	1	1.52	15.9			
gi|58761240	elongation factor [Mycoplasma fermentans]	1	2.51	28.9	1.0522		
gi|89052742	Glutamate synthase (ferredoxin) [Jannaschia sp. CCS1]	1	1.31	13.4	0.265	0	1.1126
Energy Metabolism							
gi|87161989	quinol oxidase, subunit II	92	88.88	50.8	2.0034	0	1.1792
gi|87161213	hypothetical protein SAUSA300_1720 [USA300]	19	21.88	35.6	0.8644	0.6624	1.9628
gi|70726902	hypothetical protein SH1901 [JCSC1435]	15	25.23	38.2	0.7721	0.7636	EF > 2
gi|87162272	triosephosphate isomerase	15	16.92	64.8	1.2911	0.3299	1.6961
gi|88196553	fructose-bisphosphate aldolase class-I, putative	14	24.51	64.2	0.7455	0.4438	EF > 2
gi|87160110	phosphopyruvate hydratase	14	22.02	50	1.0613	0.7798	1.5436
gi|87162014	fructose bisphosphate aldolase	13	14.13	55.9	2.2576	0	1.1896
gi|87161115	glyceraldehyde-3-phosphate dehydrogenase, type I	11	16.49	53.3	2.2266	0.2818	EF > 2
gi|87162120	formate acetyltransferase	11	16.45	22.2	1.2969	0.3535	1.7802
gi|87160940	phosphate acetyltransferase	10	17.3	59.8	1.2194	0.6172	EF > 2
gi|87162024	pyruvate kinase	9	14.37	45	0.3151	0.1398	EF > 2
gi|87161439	hypothetical protein SAUSA300_0871 [USA300]	9	11.01	40.3	0.472	0.2802	EF > 2
gi|81782064	3-hexulose-6-phosphate synthase (HPS) (D-arabino-3-hexulose-6-phosphate formaldehyde lyase)	8	11.53	64.8	0.3201	0.0279	EF > 2
gi|91206698	Glucose-6-phosphate isomerase (GPI) (Phosphoglucose isomerase) (PGI) (Phosphohexose isomerase) (PHI)	6	10.18	37.2	1.1617	0.7751	EF > 2
gi|87159954	pyruvate dehydrogenase E1 component, beta subunit	5	10.84	41.5	0.8038	0.6895	EF > 2
gi|87160408	phosphoglycerate kinase	5	9.9	30.1	0.7872	0.5093	EF > 2

Accession no.	Name	Number of peptides	Total score	Sequence Coverage (%)	D30 planktonic: D30 biofilm	*p* value	Error factor
gi|87161599	malate:quinone-oxidoreductase	5	9.38	26.9	0.4397	0.4782	EF > 2
gi|73663225	glyceraldehyde-3-phosphate dehydrogenase [ATCC 15305]	5	9.64	44.2	0.1652		
gi|87161833	putative lipase/esterase [USA300]	5	8	30	0.7626	0.3571	1.896
gi|87162313	5'-nucleotidase, lipoprotein e(P4) family	4	8.82	16.2	1.9033	0.0782	EF > 2
gi|87161068	formate-tetrahydrofolate ligase	4	8.03	32.4	1.6538	0.2908	EF > 2
gi|87162359	aconitate hydratase [USA300]	4	8.01	18.1	0.4778	0.2174	EF > 2
gi|87161490	alcohol dehydrogenase	4	8	33.6	2.0921	0.0699	EF > 2
gi|87161543	2,3-bisphosphoglycerate-independent phosphoglycerate mutase	4	8	17.4	1.1148	0.8688	EF > 2
gi|87161186	deoxyribose-phosphate aldolase	4	8	54.1	3.6127	0.0094	EF > 2
gi|87160632	hypothetical protein SAUSA300_1804 [USA300]	4	7.9	65.8	0.4563	0.5071	EF > 2
gi|81694562	Transketolase	4	7.84	21	1.2441	0.5831	EF > 2
gi|90102247	6-phosphogluconate dehydrogenase, decarboxylating	4	6.32	19	2.0107	0.3038	EF > 2
gi|87161569	methylenetetrahydrofolate dehydrogenase/methenyltetrahydrofolate cyclohydrolase	4	6.2	44.4	1.041	0.9333	EF > 2
gi|87162047	Ornithine aminotransferase	4	6.01	23.7	0.7286	0.7881	EF > 2
gi|87160754	pyruvate dehydrogenase E1 component, alpha subunit	4	6	17	1.2496	0.657	EF > 2
gi|151221843	hypothetical protein NWMN_1631 [Newman]	3	6.34	45.1	1.2844	0.66	EF > 2
gi|87161332	succinyl-CoA synthetase, alpha subunit	3	6.09	39.7	2.9055	0.1072	EF > 2
gi|91206786	2,3-bisphosphoglycerate-dependent phosphoglycerate mutase (Phosphoglyceromutase) (PGAM) (BPG-dependent PGAM) (dPGM)	3	6	23.2	2.8206	0.1302	EF > 2
gi|81695276	Probable acetyl-CoA acyltransferase (Acetoacetyl-CoA thiolase)	3	6	32.3			
gi|70727178	hypothetical protein SH2179 [JCSC1435]	3	5.74	15.7	1.1119	0.7969	EF > 2
gi|73920841	L-lactate dehydrogenase 1 (L-LDH 1)	3	4.35	17.4	0.3571	0.4121	EF > 2

Accession no.	Name	Number of peptides	Total score	Sequence Coverage (%)	D30 planktonic: D30 biofilm	*p* value	Error factor
gi|87162164	Acetoin(diacetyl) reductase [USA300]	3	4	21.7	1.0084	0.9932	EF > 2
gi|87161124	citrate synthase II [USA300]	2	4.62	11	0.7236	0.5519	EF > 2
gi|61214622	Phosphoenolpyruvate-protein phosphotransferase (Phosphotransferase system, enzyme I)	2	4.23	22.9	0.0862	0	1.4532
gi|87161326	putative NADP-dependent malic enzyme [USA300]	2	4.08	23	1.6469	0.4668	EF > 2
gi|77417488	Succinyl-CoA synthetase beta chain (SCS-beta)	2	4.02	18.6	0.9444	0.682	EF > 2
gi|87161670	isocitrate dehydrogenase, NADP-dependent	2	4	19.7	0.4506		
gi|73663003	dihydrolipoamide S-acetyltransferase component of pyruvate dehydrogenase complex E2	2	4	16.6	0.8021	0.5291	EF > 2
gi|87162156	phosphoenolpyruvate carboxykinase (ATP)	2	4	11.3	0.3495	0.6481	EF > 2
gi|87161885	transglycosylase [USA300]	2	4	11.3	2.1487	0.389	EF > 2
gi|87160719	hypothetical protein SAUSA300_0844 [USA300]	2	2.02	14.9	1.2217	0.7089	EF > 2
gi|78101526	Chain A, Crystal Structure Of 3',5"-Aminoglycoside Phosphotransferase Type Iiia Adp Neomycin B Complex	1	2.5	18.6	0.0746		
gi|123548254	Putative aldehyde dehydrogenase SAB2006c	1	2.24	9.9	0.9588		
gi|87161665	L-lactate dehydrogenase	1	2.18	25.1	0		
gi|87161078	4-oxalocrotonate tautomerase	1	2.03	37.7	0.8706	0.8305	EF > 2
gi|23465821	polyphosphate kinase [Bifidobacterium longum NCC2705]	1	2.04	12.8	1.0581	0.9743	EF > 2
gi|87162105	glycerate dehydrogenase-like protein	1	2.01	20.5	1.2463	0.6539	EF > 2
gi|152976979	pyruvate kinase [Bacillus cereus subsp. cytotoxis NVH 391-98]	1	2.22	11.8			
gi|56748589	Acetate kinase (Acetokinase)	1	2	12.8	2.1261		
gi|87160338	6-phosphofructokinase [USA300]	1	2	31.9	3.3581		
gi|119717219	UDP-glucose/GDP-mannose dehydrogenase [Nocardioides sp. JS614]	1	2	13	1.3533		
gi|87161715	hypothetical protein SAUSA300_1902 [USA300]	1	2	7.6	1.3104		
gi|87160639	hypothetical protein SAUSA300_0843 [USA300]	1	2	20.2	0.6078		

Accession no.	Name	Number of peptides	Total score	Sequence Coverage (%)	D30 planktonic: D30 biofilm	*p* value	Error factor
gi|152933808	L-serine dehydratase, iron-sulfur-dependent, beta subunit [Clostridium botulinum F str. Langeland]	1	1.72	19.2	0.1046	0.0006	1.8701
gi|110637666	urea amidohydrolase (urease) alpha subunit [Cytophaga hutchinsonii ATCC 33406]	1	1.52	18.6			
gi|78223411	Short-chain dehydrogenase/reductase SDR [Geobacter metallireducens GS-15]	1	1.52	15.4	0.2848		
gi|87161617	chaperone protein DnaK	30	32.79	60.5	1.225	0.3121	1.4883
gi|87160551	trigger factor	17	21.26	58.2	1.6286	0.0751	1.7163
gi|88195151	hypothetical protein SAOUHSC_01427 [NCTC 8325]	16	30.82	54.2	1.7453	0.1671	EF > 2
gi|87162356	foldase protein PrsA precursor	15	22.35	49.4	1.7512	0.0389	1.699
gi|87161296	putative serine protease HtrA [USA300]	9	17.52	28.5	1.0613	0.9034	EF > 2
gi|87161831	putative ATP-dependent Clp proteinase	7	12.11	37.5	0.2175	0.0598	EF > 2
gi|87160799	ornithine carbamoyltransferase	7	11.82	30.3	1.3897	0.5629	EF > 2
gi|87159917	urocanate hydratase	5	9.57	31.6	0.4147	0.2731	EF > 2
gi|87161225	copper chaperone copZ	5	2.04	64.7	0.4044	0.0219	EF > 2
gi|87161349	dihydrolipoamide dehydrogenase	4	7.4	24.6	1.5271	0.2427	EF > 2
gi|87161339	glycine cleavage system H protein	4	4.1	46	1.8493	0	1.2776
gi|87160352	hypothetical protein SAUSA300_0857 [USA300]	3	7.61	50.3	1.8911	0.3026	EF > 2
gi|87161328	hydrolase family protein	3	6.41	51.1	0.7896	0.6196	EF > 2
gi|116248102	Serine protease htrA-like	3	5.76	26.3	0.6326	0.5623	EF > 2
gi|87161390	DJ-1/PfpI family protein	2	4.13	23.3	0.2629	0.345	EF > 2
gi|87160700	60 kDa chaperonin	2	4.09	22.9			
gi|87162424	putative membrane-associated zinc metalloprotease [USA300]	2	4	25.4	2.7816	0.0399	EF > 2
gi|87161475	NAD-specific glutamate dehydrogenase	2	4	15.7	1.7125	0.3645	EF > 2
gi|87160107	signal peptidase IB	2	4	43.9	0.84	0.6979	EF > 2
gi|87161613	co-chaperone GrpE	2	4	23.6	0.2342	0.5439	EF > 2
gi|87160848	peptidase, rhomboid family	2	2.03	9.4	0.3986	0.451	EF > 2
gi|87162079	putative pyridoxal phosphate-dependent	1	2.17	10.6	0.0223		

Accession no.	Name	Number of peptides	Total score	Sequence Coverage (%)	D30 planktonic: D30 biofilm	*p* value	Error factor
	acyltransferase [USA300]						
gi|87161347	Peptidase family M20/M25/M40	1	2	19.6	0.0506		
gi|90183185	ATP-dependent Clp protease proteolytic subunit (Endopeptidase Clp)	1	2	34.9	1.2575	0.6154	EF > 2
gi|87161219	hypothetical protein SAUSA300_0207 [USA300]	1	2	12	2.9775		
gi|15672533	trigger factor [Lactococcus lactis subsp. lactis Il1403]	1	1.7	12.9	0.1057		
gi|152975536	amino acid adenylation domain [Bacillus cereus subsp. cytotoxis NVH 391-98]	1	1.31	6.8	6.2429		
Stress							
gi|87162409	CsbD-like superfamily	34	23.94	90.6	1.3708	0.0058	1.249
gi|87162200	Alkyl hydroperoxide reductase subunit C	27	17.18	51.9	1.6239	0.0128	1.4606
gi|87160786	hypothetical protein SAUSA300_1652 [USA300]	24	31.43	68.6	0.8978	0.2323	1.1928
gi|894289	alkaline shock protein 23; ASP23	20	19.57	69.8	1.1024	0.6569	1.5506
gi|87162087	universal stress protein family	18	22.55	71.7	3.0664	0	1.5719
gi|87162159	hypothetical protein SAUSA300_1582 [USA300]	13	8.33	75	2.0123	0.0135	1.7222
gi|87161236	thioredoxin	12	15.51	83.7	0.7305	0.0387	1.3421
gi|87160079	peptide methionine sulfoxide reductase regulator MsrR	10	10.51	33.9	1.7545	0.0863	1.9197
gi|87161001	thioredoxin-disulfide reductase	9	10	36	1.1776	0.6298	EF > 2
gi|87161687	thiol peroxidase	8	8	55.5	1.4239	0.2404	1.8458
gi|70726220	hypothetical protein SH1219 [JCSC1435]	7	13.15	54.7			
gi|87160477	putative thioredoxin [USA300]	5	10.3	58.3	1.2503	0.6608	EF > 2
gi|87160511	catalase	5	7.43	20.2	4.7999	0.0241	EF > 2
gi|87161707	superoxide dismutase (Mn/Fe family)	5	6.01	40.2	0.7623	0.7832	EF > 2
gi|21282513	hypothetical protein MW0784 [MW2]	5	4	41.5	1.2352	0.3626	1.5996
gi|88195790	ferritin, putative [NCTC 8325]	4	6.67	51.8	0.4058	0.1265	EF > 2
gi|87160405	hypothetical protein SAUSA300_1909 [USA300]	4	4.21	27.8	0.7007	0.628	EF > 2
gi|87161642	alkyl hydroperoxide reductase subunit F	1	2.72	12.8	0.3723	0.188	EF > 2

Accession no.	Name	Number of peptides	Total score	Sequence Coverage (%)	D30 planktonic: D30 biofilm	*p* value	Error factor
gi|87161086	methionine-R-sulfoxide reductase	1	2.33	16.2	15.0177	0.4261	EF > 2
gi|87162273	OsmC/Ohr family protein	1	2	34.3	2.8528	0.3618	EF > 2
gi|87160980	hypothetical protein SAUSA300_0725 [USA300]	1	2	17.9	1.3866		
gi|87160505	DNA-binding protein HU	36	20	75.6	0.6834	0	1.1104
gi|87161697	transcription elongation factor GreA [USA300]	9	12	60.1	0.5201	0.0799	EF > 2
gi|87160906	putative transcriptional regulator [USA300]	9	12	39.7	0.8645	0.8012	EF > 2
gi|90110870	DNA-directed RNA polymerase alpha chain (RNAP alpha subunit) (Transcriptase alpha chain) (RNA polymerase subunit alpha)	5	6.37	27.7	0.5049	0.4065	EF > 2
gi|87161137	DNA-directed RNA polymerase, beta' subunit	3	6.01	23.4	3.642	0.0601	EF > 2
gi|87159899	transcriptional regulator, MarR family	3	6	46.3	0.6518	0.5505	EF > 2
gi|81695152	DNA-directed RNA polymerase beta chain (RNAP beta subunit) (Transcriptase beta chain) (RNA polymerase subunit beta)	3	4.04	25.2	0.6254	0.3628	EF > 2
gi|81651715	Putative septation protein spoVG	2	3.1	47	1.6545	0.0649	1.9237
gi|148556982	Hydantoinase/oxoprolinase [Sphingomonas wittichii RW1]	1	2.23	29.2	0.3135		
gi|87161403	DNA-directed RNA polymerase, omega subunit	2	2.3	62.5	1.2342	0.6411	EF > 2
gi|87161266	anti-sigma-B factor, antagonist	2	2	23.1	0.4855		
gi|87160104	hypothetical protein SAUSA300_2547 [USA300]	1	2.15	20.9	0.2937		
gi|87160250	hypothetical protein SAUSA300_0003 [USA300]	1	2.01	58	0.3488	0.3713	EF > 2
gi|87159916	DNA-directed RNA polymerase, delta subunit	1	2	22.2	3.8401		
gi|87162043	lytic regulatory protein	1	2	8.8	4.19		
gi|153095029	DeoR family transcriptional regulator [PHL213]	1	2	12.5	0.1222	0.002	1.9304
gi|126433686	transcriptional regulator, MarR family [JLS]	1	2	25.7			
gi|88193109	Chain B, Crystal Structure Of Sara, A Transcription Regulator From Staphylococcus Aureus	1	1.94	21.3	0.2275	0.0169	1.6478
gi|149186684	transcription-repair coupling factor [Erythrobacter sp. SD-21]	1	1.62	19.3			

Accession no.	Name	Number of peptides	Total score	Sequence Coverage (%)	D30 planktonic: D30 biofilm	*p* value	Error factor
gi|94968840	response regulator receiver protein [Acidobacteria bacterium Ellin345]	1	1.52	21.8			
gi|87162130	triacylglycerol lipase precursor [USA300]	3	4.01	20.6	1.4921	0.4387	EF > 2
gi|87162021	acyl carrier protein	2	5.7	77.9	0.3941	0.2074	EF > 2
gi|87161805	3-oxoacyl-(acyl-carrier-protein) reductase	2	4	53.7	0.5969	0.8853	EF > 2
gi|87161662	hypothetical protein SAUSA300_1856 [USA300]	2	4	39.8	1.4886	0.2819	EF > 2
gi|99032669	Chain B, The Crystal Structure Of B-Ketoacyl-Acp Synthase Ii (Fabf) From Staphylococcus Aureus	1	2.18	17.2	2.6989	0.3598	EF > 2
gi|87161082	acetyl-CoA carboxylase, biotin carboxyl carrier protein	1	2.02	33.1	2.144	0.0858	EF > 2
gi|70726948	enoyl-(acyl carrier protein) reductase [JCSC1435]	1	2.02	14.8	0.9001	0.9378	EF > 2
gi|87160287	fatty acid/phospholipid synthesis protein PlsX	1	2	10.4	1.5645		
gi|119502734	acetyl-CoA carboxylase [marine gamma proteobacterium HTCC2080]	1	1.7	15.2	0.2246	0	1.0826
gi|148821476	PE-PGRS family protein [Mycobacterium tuberculosis F11]	1	1.4	34.8	3.0713	0.1735	EF > 2
gi|38604919	Inosine-5'-monophosphate dehydrogenase (IMP dehydrogenase) (IMPDH) (IMPD)	13	20	55.9	1.9091	0.0421	1.8591
gi|87161595	phosphoribosylformylglycinamidine synthase	5	6.32	59.8	0.5524	0.4703	EF > 2
gi|87161373	adenylate kinase [USA300]	4	8.04	53	1.3267	0.6999	EF > 2
gi|87161059	uracil phosphoribosyltransferase	3	6.37	31.6	1.1876	0.4306	1.6122
gi|81650637	Pyrimidine-nucleoside phosphorylase (PYNP)	3	6.05	24	0.8242	0.7042	EF > 2
gi|87161310	dihydroorotase [USA300]	3	6.02	22.2	0.9461	0.9381	EF > 2
gi|987497	nucleoside diphosphate kinase	3	6	53	0.2176	0.0267	EF > 2
gi|87160143	purine nucleoside phosphorylase	3	3.55	30.5	2.3949	0.081	EF > 2
gi|87160876	adenylosuccinate synthetase	2	4.01	15.5	3.9573	0.0264	EF > 2
gi|87162294	phosphoribosylaminoimidazole carboxylase, catalytic subunit	2	3.7	48.9			
gi|87160186	polyribonucleotide nucleotidyltransferase	1	2.69	48.9	0.3073	0.461	EF > 2

Accession no.	Name	Number of peptides	Total score	Sequence Coverage (%)	D30 planktonic: D30 biofilm	*p* value	Error factor
gi|91206761	[Protein-PII] uridylyltransferase (PII uridylyl-transferase) (Uridylyl-removing enzyme) (UTase)	1	2.38	15.4	2.7259	0.3048	EF > 2
gi|84366297	ATP-dependent RNA helicase [Xanthomonas oryzae pv. oryzae MAFF 311018]	1	2.22	33.5			
gi|87161299	hypoxanthine phosphoribosyltransferase	1	2.02	20.8	0.1858	0.4644	EF > 2
gi|87160831	dihydroorotate dehydrogenase	1	2	11.6	0.3178		
gi|70726884	phosphoribosylamine--glycine ligase [JCSC1435]	1	2	8.7	2.4564		
gi|91206832	GMP synthase [glutamine-hydrolyzing] (Glutamine amidotransferase) (GMP synthetase)	1	2	10.3	0.8514		
gi|150385859	carbamoyl-phosphate synthase, large subunit [Victivallis vadensis ATCC BAA-548]	1	1.42	17.7			
DNA Metabolism: replication, recombination and repair							
gi|88195046	hypothetical protein SAOUHSC_01316 [NCTC 8325]	6	10	23.7	1.4239	0.4191	EF > 2
gi|134296873	DEAD/DEAH box helicase domain protein	3	7.7	21.2	0.5856	0.5282	EF > 2
gi|149125815	LigA [Methylobacterium sp. 4-46]	1	2.96	49.2	0.7602	0.6531	EF > 2
gi|87160839	recombinase A protein	1	2.01	9.3	1.1215	0.7964	EF > 2
gi|88193844	hypothetical protein SAOUHSC_00023 [NCTC 8325]	1	2.01	26.7	0.8205		
gi|70725957	hypothetical protein SH0956 [JCSC1435]	1	2	15.5	1.8224		
gi|88193825	DNA polymerase III, beta subunit	1	2	10.1	1.3451		
gi|150005913	ATP-dependent exonuclease V, alpha subunit - helicase superfamily I member [Bacteroides vulgatus ATCC 8482]	1	2	6.8	1.0835		
gi|98311102	thermostable nuclease	1	2	6.9	6.5589		
gi|149189072	MshA, mannose-sensitive haemaglutinin [AK1]	1	2	10.8	0.0288		
gi|149913440	NAD-dependent deacetylase [Roseobacter sp. AzwK-3b]	1	2	7.7	0.0046		
gi|109946687	ComB3 protein [Sheeba]	1	2	15.9	0.2194	0	1.2431

Accession no.	Name	Number of peptides	Total score	Sequence Coverage (%)	D30 planktonic: D30 biofilm	*p* value	Error factor
gi|121611662	DEAD/DEAH box helicase domain protein [Verminephrobacter eiseniae EF01-2]	1	1.91	21.5	0	0	
gi|153006953	LigA [Anaeromyxobacter sp. Fw109-5]	1	1.82	44.1	0.0302	0.251	EF > 2
gi|147676398	DNA polymerase III, gamma/tau subunits [Pelotomaculum thermopropionicum SI]	1	1.7	31.6	0.2573	0.0001	1.2668
gi|41409059	hypothetical protein MAP2961c [Mycobacterium avium subsp. paratuberculosis K-10]	1	1.54	46.9	1.4137	0.4906	EF > 2
gi|61215122	DNA repair protein recO (Recombination protein O)	1	1.52	17.7			
Pathogenesis and Immunomodulation							
gi|87160749	cell surface elastin binding protein	200	45.07	43.4	1.3029	0.0961	1.3624
gi|133853458	immunoglobulin G binding protein A precursor	138	58.7	78.8	1.0756	0.3757	1.1747
gi|56749001	Immunodominant staphylococcal antigen A precursor	57	18.55	49.8	0.9476	0.656	1.2667
gi|15926764	penicillin-binding protein 1	43	61.62	38.4	1.4429	0.0048	1.2868
gi|87161577	cold shock protein, CSD family	36	16.74	65.2	0.7602	0.0001	1.1446
gi|87162077	penicillin binding protein 2	32	52.49	66.6	0.6655	0.1167	1.669
gi|87160015	staphylococcal tandem lipoprotein	14	21.24	48.9	1.1702	0.4995	1.6198
gi|47169194	Chain A, Staphylococcal Protein A, B-Domain, Y15w Mutant, Nmr, 25 Structures	12	12.14	82.3			
gi|70726765	beta-lactamase	10	16.53	40.6	0.1207	0.0022	EF > 2
gi|87160380	alpha-hemolysin precursor	10	14.14	36.7	1.1949	0.4484	1.6137
gi|87160982	Leukocidin/Hemolysin toxin family protein	10	13.16	49.7	0.7128	0.2953	1.9623
gi|87162162	hypothetical protein SAUSA300_1018 [USA300]	8	16.29	24.9	0.6697	0.3322	EF > 2
gi|87161881	antibacterial protein	7	4.08	50	0.8559	0.5626	1.7379
gi|87161157	penicillin-binding protein 4	6	7.74	23.4	2.7796	0.013	EF > 2
gi|15927581	hypothetical protein SA1813 [N315]	5	11.45	39.9	1.1987	0.519	1.8296
gi|87162347	hypothetical protein SAUSA300_2164 [USA300]	4	6.34	48.2	0.1106	0.0494	EF > 2
gi|87160217	secretory antigen precursor SsaA	4	6.25	25.5	0.5127	0.069	EF > 2

Accession no.	Name	Number of peptides	Total score	Sequence Coverage (%)	D30 planktonic: D30 biofilm	*p* value	Error factor
gi|88194063	hypothetical protein SAOUHSC_00257 [NCTC 8325] - ESAT6 family virulence protein	4	6.01	53.6	2.158	0.2965	EF > 2
gi|87160365	antibacterial protein [USA300]	4	2	50	0.2771	0	1.1218
gi|87160520	acetyltransferase family protein	3	4.09	51.1	0.8063	0.7857	EF > 2
gi|87161173	teicoplanin resistance associated membrane protein TcaA protein [USA300]	3	4.02	11.3	1.4697	0.7023	EF > 2
gi|88195687	hypothetical protein SAOUHSC_01999 [NCTC 8325]	3	3.52	15.2	1.9644	0.0359	1.8518
gi|68565538	Protein esaA	2	4.01	23.2	0.197	0.2859	EF > 2
gi|87162375	hypothetical protein SAUSA300_1323 [USA300]	2	2.01	38.6	0.1985	0.3431	EF > 2
gi|87161897	IgG-binding protein SBI	1	2.7	10.6	5.4157	0.0616	EF > 2
gi|87160565	immunodominant antigen B	1	2.61	28	2.0875		
gi|87160905	hypothetical protein SAUSA300_0282 [USA300]- similar to essB,	1	2	12.6	0.4179		
gi|87162379	ferredoxin	1	2	18.9	1.8553		
gi|62391257	secreted penicillin binding protein [Corynebacterium glutamicum ATCC 13032]	1	1.7	7	2.2857		
Cell Division and Cycle							
gi|87162194	cell division protein ftsZ	18	20.02	43.6	0.6616	0.0412	1.4853
gi|87161534	putative cell division protein FtsH [USA300]	7	15.83	34.3	1.141	0.778	EF > 2
gi|87161782	cell division protein	7	7.81	30.8	1.8474	0.0095	1.5272
gi|87162117	hypothetical protein SAUSA300_1337 [USA300]	5	9.29	58.8	0.512	0.5782	EF > 2
gi|73662607	putative cell division initiation protein [ATCC 15305]	3	6.99	46.2	15.8442		
gi|87160736	cell-division initiation protein	3	3.16	51.5	3.2325	0.0211	EF > 2
gi|87161457	HIT family protein	2	3.58	29.3	2.9177		
gi|24374683	hypothetical protein SO_3170 [MR-1]	1	2.01	17.1	2.6296	0.3792	EF > 2
gi|151591524	cell divisionFtsK/SpoIIIE [Methylobacterium extorquens PA1]	1	1.7	22.1			

Accession no.	Name	Number of peptides	Total score	Sequence Coverage (%)	D30 planktonic: D30 biofilm	*p* value	Error factor
Cell Adhesion							
gi|87160939	cell wall surface anchor family protein	57	42.04	60.2	1.2777	0.0838	1.3182
gi|151222604	hypothetical protein NWMN_2392 [Newman]	40	59.98	69.5	0.2444	0	1.5991
gi|87162026	autolysin	31	42.59	49.3	0.7695	0.2717	1.6067
gi|87160697	D-alanine-activating enzyme/D-alanine-D-alanyl, dltD protein	18	24.96	49.4	1.9912	0.0001	1.3862
gi|87162315	putative lipoprotein [USA300]	16	14.26	40.4	1.1145	0.7887	EF > 2
gi|61213890	77 kDa outer membrane protein precursor	11	22.71	36.1	0.6572	0.1167	1.6996
gi|81781509	UPF0365 protein SAV1573	8	14.02	46.2	2.9173	0.0019	1.7732
gi|87160285	rod shape-determining protein MreC	8	11.59	51.8	2.9577	0	1.4552
gi|87160775	N-acetylmuramoyl-L-alanine amidase	8	11.4	29.9	2.0519	0.0096	1.6427
gi|87161887	N-acetylmuramoyl-L-alanine amidase domain protein	7	14.01	25.4	1.3838	0.4234	EF > 2
gi|88196468	sortase, putative [NCTC 8325]	5	10.01	25.7	1.2683	0.5337	EF > 2
gi|87161790	5'-nucleotidase family protein [USA300]	3	2.04	10.4	1.5688	0.1773	EF > 2
gi|87160715	fmt protein [USA300]	2	4.86	20.4	1.1849	0.6709	EF > 2
gi|81673756	Phosphoglucosamine mutase	1	2.8	20.4	3.3119	0.2556	EF > 2
gi|87160798	serine-aspartate repeat family protein, SdrH	1	2.21	17.5	1.3251	0.4213	EF > 2
gi|116694144	flp pilus assembly protein TadC [Ralstonia eutropha H16]	1	2.19	22.9	2.585		
gi|81781921	Extracellular matrix protein-binding protein emp precursor	1	2.12	12.9	1.4533	0.5086	EF > 2
gi|87160121	D-alanine-activating enzyme/D-alanine-D-alanyl, dltC protein	1	1.7	38.5	16.1543		
gi|91211353	AsmA suppressor of OmpF assembly mutants [Escherichia coli UTI89]	1	1.7	19.9			
Transport proteins							
gi|87160674	putative lipoprotein [USA300]	41	30.7	68.4	0.7197	0.0011	1.2149

Accession no.	Name	Number of peptides	Total score	Sequence Coverage (%)	D30 planktonic: D30 biofilm	*p* value	Error factor
gi|87162197	amino acid ABC transporter, amino acid-binding protein	34	41.25	63.3	1.3001	0.0518	1.3007
gi|87162140	oligopeptide ABC transporter, substrate-binding protein	30	41.53	48.3	1.3918	0.0533	1.3984
gi|87161315	hypothetical protein SAUSA300_2378 [USA300]	21	21.34	58	1.6492	0.0873	1.7803
gi|87160588	molybdenum ABC transporter, molybdenum-binding protein ModA	17	26.41	46.5	1.8056	0.0558	1.8336
gi|87161352	ABC transporter, substrate-binding protein	12	18.38	38.7	0.4137	0.092	EF > 2
gi|87160965	phosphocarrier protein HPr	11	17	89.8	0.4598	0	1.4007
gi|87162382	PTS system, glucose-specific IIA component	11	12	54.2	2.9434	0.004	1.9242
gi|87162442	transferrin receptor	8	12.69	31.9	3.5596	0.0002	1.7112
gi|87160279	AcrB/AcrD/AcrF family protein	7	13.76	34	1.0728	0.9096	EF > 2
gi|87161641	amino acid ABC transporter, permease/substrate-binding protein	7	10.49	30.7	2.5162	0.0341	EF > 2
gi|21284120	oligopeptide transporter putative substrate binding domain [MW2]	6	12.01	29.1	1.9632	0.1937	EF > 2
gi|87160515	protein-export membrane protein SecF	6	10.63	16.2	0.7504	0.4761	EF > 2
gi|21282147	hypothetical protein MW0418 [MW2]	6	8.69	49.3	1.2602	0.507	EF > 2
gi|87161764	putative iron compound ABC transporter, iron compound-binding protein [USA300]	5	10.17	36	0.7301	0.561	EF > 2
gi|87160849	iron compound ABC transporter, iron compound-binding protein	4	8	28.5	0.6344	0.5184	EF > 2
gi|87161518	glycine betaine/carnitine/choline ABC transporter [USA300]	4	8	14.4	1.0605	0.8404	1.9436
gi|87161864	ABC transporter, substrate-binding protein	3	8.12	25.2	2.1079	0.0742	EF > 2
gi|87160369	hypothetical protein SAUSA300_0833 [USA300]	3	6.1	20.5	0.4642	0.5479	EF > 2
gi|15925912	RGD-containing lipoprotein [N315]	3	6.02	17.4	1.0422	0.9709	EF > 2
gi|87161142	ferric hydroxamate receptor	3	4	8.9	0.4321	0.2314	EF > 2
gi|87162224	osmoprotectant ABC transporter, permease	2	4	35.1	3.9979		

Accession no.	Name	Number of peptides	Total score	Sequence Coverage (%)	D30 planktonic: D30 biofilm	*p* value	Error factor
gi|87161872	putative lipoprotein [USA300]	2	4	16.4	2.4403	0.1588	EF > 2
gi|87160414	multidrug resistance protein A, drug resistance transporter	1	3.16	15.3	0.7756	0.7943	EF > 2
gi|87162284	putative ferrichrome ABC transporter [USA300]	1	3.05	22.3	0.5068	0.6105	EF > 2
gi|149201149	nitrate transport ATP-binding subunits C and D [TM1035]	1	2.4	16.3	7.9917	0.1401	EF > 2
gi|151575108	outer membrane efflux protein [Ralstonia pickettii 12D]	1	2.22	15.6	3.8451	0.3525	EF > 2
gi|87161139	iron transport associated domain protein [USA300]	1	2.09	21.1	0.1596		
gi|149910101	Hypothetical transport protein [Moritella sp. PE36]	1	2.02	6.8	4.2379	0	1.1745
gi|87161389	putative iron compound A C transporter, iron compound-binding protein [USA300]	1	2.01	9.9	1.4787	0.3341	EF > 2
gi|35211526	gll0963 [Gloeobacter violaceus PCC 7421]	1	2	14			
gi|87162212	amino acid ABC transporter, ATP-binding protein	1	2	25.6	0.571		
gi|127512243	efflux transporter, RND family, MFP subunit [Shewanella loihica PV-4]	1	2	11.1			
gi|126355053	ABC transporter related [Pseudomonas putida GB-1]	1	1.71	6.4	6.929	0.0699	EF > 2
gi|17131745	all2652 [Nostoc sp. PCC 7120]	1	1.7	37.6	0.8275		
gi|149194563	ABC transporter-related protein [Caminibacter mediatlanticus TB-2]	1	1.7	8.4	0.0083		
gi|87162344	phosphonate ABC transporter, phosphonate-binding protein	1	1.7	4.4	6.3883	0.0356	EF > 2
gi|51595518	molybdenum transport regulatory (repressor) protein ModE [Yersinia pseudotuberculosis IP 32953]	1	1.55	33.5	1.1322	0.9636	EF > 2
gi|23005821	COG1131: ABC-type multidrug transport system, ATPase component [Magnetospirillum magnetotacticum MS-1]	1	1.52	17.5	0.6174		
gi|152936446	flagellar motor switch protein fliG [Clostridium botulinum F str. Langeland]	1	1.52	7.7			

Accession no.	Name	Number of peptides	Total score	Sequence Coverage (%)	D30 planktonic: D30 biofilm	*p* value	Error factor
gi|146301866	RND efflux system, outer membrane lipoprotein, NodT family [Flavobacterium johnsoniae UW101]	1	1.46	14.1	0.4187		
Other functions							
gi|21283573	hypothetical protein MW1844 [MW2]	4	6.1	29.1	0.4337	0.1254	EF > 2
gi|15928229	hypothetical protein SA2436 [N315]	2	4.14	12	1.3409	0.624	EF > 2
gi|87161880	manganese-dependent inorganic pyrophosphatase	2	4	18.4	0.8997	0.7506	EF > 2
gi|87161327	S-ribosylhomocysteinase	1	2.16	21.8			
gi|116696021	signal transduction histidine kinase containing a receiver domain (hybrid) [Ralstonia eutropha H16]	1	2.01	23.6	0.4873	0.6468	EF > 2
gi|62900222	HAM1 protein homolog	1	2	25.1	1.6669		
gi|56749556	6,7-dimethyl-8-ribityllumazine synthase (DMRL synthase) (Lumazine synthase) (Riboflavin synthase beta chain)	1	2	30.5			
gi|87161407	hypothetical protein SAUSA300_1160 [USA300]	1	2	21.3	8.5821		
gi|29347076	hydrolase, haloacid dehalogenase-like hydrolase [Bacteroides thetaiotaomicron VPI-5482]	1	1.74	17.1	0.1912	0.4991	EF > 2
gi|146292939	TonB-dependent siderophore receptor [Shewanella putrefaciens CN-32]	1	1.7	9.8	3.3337		
Hypothetical proteins							
gi|87160135	hypothetical protein SAUSA300_1581 [USA300]	23	8.04	72.9	1.6716	0.0292	1.5836
gi|87159943	hypothetical protein SAUSA300_1908 [USA300]	21	17.48	29.3	1.0866	0.5504	1.3214
gi|87160606	hypothetical protein SAUSA300_1698 [USA300]	20	14.73	64.3	0.5379	0.0027	1.4823
gi|87161419	hypothetical protein SAUSA300_1795 [USA300]	18	10.24	86	0.5763	0.1351	EF > 2
gi|15926079	Hypotheticall protein SA0363 [N315]	13	21.12	47.6	2.1698	0.0016	1.5797
gi|87161713	hypothetical protein SAUSA300_0385 [USA300]	8	8	41.5	2.2422	0.0096	1.7718
gi|88195776	hypothetical protein SAOUHSC_02093 [NCTC 8325]	8	6	71.2	0.361	0.0015	1.7818
gi|87160537	hypothetical protein SAUSA300_2132 [USA300]	7	11.27	80.2	1.6246	0.0855	1.746

Accession no.	Name	Number of peptides	Total score	Sequence Coverage (%)	D30 planktonic: D30 biofilm	*p* value	Error factor
gi|87161087	hypothetical protein SAUSA300_2144 [USA300]	7	8.59	28	0.6785	0.2674	EF > 2
gi|87160300	hypothetical protein SAUSA300_1440 [USA300]	6	10.54	27.7	0.1828	0.0226	EF > 2
gi|87160039	hypothetical protein SAUSA300_2330 [USA300]	5	10.04	32.2	0.9286	0.8918	EF > 2
gi|87160421	hypothetical protein SAUSA300_0172 [USA300]	5	8	68.7	0.2115	0.0234	EF > 2
gi|87162221	hypothetical protein SAUSA300_0664 [USA300]	5	8	66.7	0.7676	0.8232	EF > 2
gi|88196395	hypothetical protein SAOUHSC_02759 [NCTC 8325]	5	4.01	23.2	0.9368	0.9304	EF > 2
gi|87161527	hypothetical protein SAUSA300_1572 [USA300]	5	2	34.3	0.9818	0.9803	EF > 2
gi|88195426	hypothetical protein SAOUHSC_01721 [NCTC 8325]	4	5	53.5	0.5708	0.1071	EF > 2
gi|87161381	hypothetical protein SAUSA300_1857 [USA300]	2	4.03	50.9	0.3602	0.4048	EF > 2
gi|15926825	hypothetical protein SA1085 [N315]	2	4.02	13.1	1.7915	0.1137	EF > 2
gi|87160698	hypothetical protein SAUSA300_1906 [USA300]	2	4	13.6	0.339	0.1035	EF > 2
gi|87159919	hypothetical protein SAUSA300_2527 [USA300]	2	4	49.5	0.4974		
gi|87161111	hypothetical protein SAUSA300_2212 [USA300]	2	4	61.1	2.4645	0.2051	EF > 2
gi|87161468	hypothetical protein SAUSA300_1215 [USA300]	2	4	41.5	0.4229	0	1.3891
gi|88195065	hypothetical protein SAOUHSC_01336 [NCTC 8325]	2	2.32	41.8	1.7896	0.2728	EF > 2
gi|87160907	hypothetical protein SAUSA300_0602 [USA300]	2	2.1	17.9	4.5784	0.0414	EF > 2
gi|87161979	hypothetical protein SAUSA300_2560 [USA300]	2	2	47	0.0879		
gi|87162360	hypothetical protein SAUSA300_1685 [USA300]	2	2	9.2	0.4863	0.3742	EF > 2
gi|150393509	hypothetical protein SaurJH1_1041 [JH1]	2	2	25			
gi|21284001	hypothetical protein MW2272 [MW2]	1	3.17	16.5	0.2983	0.3902	EF > 2
gi|87162045	hypothetical protein SAUSA300_1788 [USA300]	1	2.68	47.9	0.8105	0.657	EF > 2
gi|77465081	hypothetical protein RSP_3067 [Rhodobacter sphaeroides 2.4.1]	1	2.52	26	830%	1%	EF > 2
gi|87160235	hypothetical protein SAUSA300_1904 [USA300]	1	2.26	28.1	0.4476	0.1437	EF > 2
gi|87161000	hypothetical protein SAUSA300_1606 [USA300]	1	2.24	47.1	3.2155	0.0595	EF > 2
gi|93140725	Uncharacterized N-acetyltransferase SAB1040c	1	2.19	19.2	2.1143	0.0585	EF > 2
gi|87161220	hypothetical protein SAUSA300_0383 [USA300]	1	2.14	23.3	0.1962		
gi|87161658	hypothetical protein SAUSA300_2148 [USA300]	1	2.1	21.5	1.4355		
gi|87159886	hypothetical protein SAUSA300_2493 [USA300]	1	2.08	34.9	0.4565	0.4986	EF > 2

Accession no.	Name	Number of peptides	Total score	Sequence Coverage (%)	D30 planktonic: D30 biofilm	*p* value	Error factor
gi|55773538	conserved hypothetical protein [HB8]	1	2.06	8.4	0.1597	0.1348	EF > 2
gi|119386105	hypothetical protein Pden_3391 [PD1222]	1	2.04	30.6	0.9539	0.9356	EF > 2
gi|87160533	hypothetical protein SAUSA300_1321 [USA300]	1	2.01	17.2	6.2229		
gi|30262516	hypothetical protein BA2524 [Bacillus anthracis str. Ames]	1	2.01	30.1	0.4684		
gi|87160245	hypothetical protein SAUSA300_1864 [USA300]	1	2.01	6.9	94.4809		
gi|87160914	hypothetical protein SAUSA300_1223 [USA300]	1	2	18.3	3.0338		
gi|70726727	hypothetical protein SH1726 [JCSC1435]	1	2	8.6	4.4216	0.3643	EF > 2
gi|21283169	hypothetical protein MW1440 [MW2]	1	2	52.9	0.5239		
gi|87162265	hypothetical protein SAUSA300_1057 [USA300]	1	2	18.2	1.4172		
gi|87160560	hypothetical protein SAUSA300_1335 [USA300]	1	2	9.1	3.9586		
gi|87160349	hypothetical protein SAUSA300_0982 [USA300]	1	2	6.1	0.7242		
gi|87160886	hypothetical protein SAUSA300_0990 [USA300]	1	1.84	40.3	0.4073	0.1543	EF > 2
gi|116618724	hypothetical protein LEUM_1630 [ATCC 8293]	1	1.71	22	2.3737	0.3812	EF > 2
gi|15595185	Hypothetical protein BB0840 [B31]	1	1.7	7.8	0.0524	0.0518	EF > 2
gi|145299288	hypothetical protein ASA_2332 [Aeromonas salmonicida subsp. salmonicida A449]	1	1.7	18.2	2.0155		
gi|148556846	hypothetical protein Swit_3945 [RW1]	1	1.7	31.8	0.2165	0	1.2074
gi|118602465	hypothetical protein Rmag_0450 [Candidatus Ruthia magnifica str. Cm (Calyptogena magnifica)]	1	1.7	10.1	0.1032	0.0386	EF > 2
gi|83647697	hypothetical protein HCH_05022 [Hahella chejuensis KCTC 2396]	1	1.53	8.4	2.734		
gi|89070338	hypothetical protein OG2516_12764 [Oceanicola granulosus HTCC2516]	1	1.53	23.8			
gi|86136324	hypothetical protein MED193_19414 [Roseobacter sp. MED193]	1	1.53	38.3	0.0658		
gi|88194234	hypothetical protein SAOUHSC_00444 [NCTC 8325]	1	1.52	41.9	0.3885		
gi|149191551	hypothetical protein VSAK1_15442 [Vibrio shilonii	1	1.52	11.9	0.014		

Accession no.	Name	Number of peptides	Total score	Sequence Coverage (%)	D30 planktonic: D30 biofilm	*p* value	Error factor
	AK1]						
gi|145220937	hypothetical protein Mflv_0333 [Mycobacterium gilvum PYR-GCK]	1	1.52	5.8			
gi|88194796	hypothetical protein SAOUHSC_01044 [NCTC 8325]	1	1.52	15.4			
gi|29610655	hypothetical protein [Streptomyces avermitilis MA-4680]	1	1.4	12.8	0.0136		
gi|29609637	hypothetical protein [Streptomyces avermitilis MA-4680]	1	1.4	6.9	0.3196		
gi|120610660	hypothetical protein Aave_1980 [Acidovorax avenae subsp. citrulli AAC00-1]	1	1.4	4.8	0		
gi|149912076	hypothetical protein PE36_12287 [Moritella sp. PE36]	1	1.4	26.5	0.3601		
gi|124268268	hypothetical protein Mpe_A3084 [Methylibium petroleiphilum PM1]	1	1.33	29.6	2.5243	0.0241	EF > 2
Unknown funtion							
gi|87161686	putative lipoprotein	51	32.02	52.2	0.7716	0.0528	1.297
gi|82751366	probable transaldolase	8	13.17	67.9	0.9884	0.9746	EF > 2
gi|87161661	putative lipoprotein	7	13.51	43.8	0.7766	0.5033	EF > 2
gi|87161314	putative lipoprotein [USA300]	4	6.01	29.5	2.1337	0.4052	EF > 2
gi|49484622	putative solute binding lipoprotein [MRSA252]	3	6.91	24.3	0.728	0.7599	EF > 2
gi|87160546	putative cell-division initiation protein [USA300]	3	6	40.5	1.408	0.8736	EF > 2
gi|87161260	phiSLT ORF144-like protein, putative lipoprotein [USA300]	2	4.05	36.1	0.3313	0.0857	EF > 2
gi|87161351	putative lipoprotein [USA300]	2	4.01	17.5	1.6355	0.4519	EF > 2
gi|87161825	putative lipoprotein [USA300]	2	4	26.9	0.4877	0.3342	EF > 2
gi|153005206	protein of unknown function DUF849 [Anaeromyxobacter sp. Fw109-5]	2	2	22.1	18.383		
gi|124010323	lipoprotein, putative [Microscilla marina ATCC 23134]	1	3.36	7.1	0.2374	0.085	EF > 2
gi|87161720	putative arsenate reductase [USA300]	1	2.8	26.3	243%	0%	120%

Accession no.	Name	Number of peptides	Total score	Sequence Coverage (%)	D30 planktonic: D30 biofilm	*p* value	Error factor
gi|117164639	putative modular polyketide synthase [ATCC 23877]	1	2.2	12.3	0.0313	0	EF > 2
gi|121583546	protein of unknown function DUF262 [Polaromonas naphthalenivorans CJ2]	1	2	11.4	0.2361	0	1.1909
gi|81693746	Uncharacterized lipoprotein SACOL2497 precursor	1	2	18.4	1.2088		
gi|120609276	uncharacterized protein UPF0065 [Acidovorax avenae subsp. citrulli AAC00-1]	1	2	18.6	2.3592	0.6088	EF > 2
gi|149910937	Uncharacterized protein conserved in bacteria [Moritella sp. PE36]	1	2	17.2	0.2327	0	1.0888
gi|148869366	putative patatin [Vibrio harveyi HY01]	1	1.7	20.5	0.2573	0	1.1117
gi|116250012	putative methyltransferase [Rhizobium leguminosarum bv. viciae 3841]	1	1.52	12.4			
gi|146306168	protein of unknown function DUF1302 [Pseudomonas mendocina ymp]	1	1.52	6.9	0.4866		
gi|51894011	putative cadmium-transporting ATPase [Symbiobacterium thermophilum IAM 14863]	1	1.41	28.7	0.042	0.5037	EF > 2
gi|25027269	putative urea carboxylase [Corynebacterium efficiens YS-314]	1	1.4	6.3	0.2722	0.0031	1.3676
gi|29608736	putative integral membrane protein [Streptomyces avermitilis MA-4680]	0	1.41	21.3	0.4418		

APPENDIX C: CHAPTER FOUR SUPPLEMENT

Table 14: Oligonucleotides utilized in this study

Oligonucleotides	Description and Sequence (5' to 3')	Restriction site
D30spatgtF	Sequence *spa*; GACGACGTCCAGCTAATAAC	
D30spatgtR	Sequence *spa*; AAAGCGGATAACAAATTCAA	
755|756s-IBS	D20 *spa*-pNL9164 cloning; AAAAAAGCTTATAATTATCCTTAT TGCCTTGTTCGTGCGCCCAGATAGGGTG	HindIII
755|756s-EBS1d	D20 *spa*-pNL9164 cloning; CAGATTGTACAAATGTGG TGATAACAGATAAGTCTTGTTCTTTAACTTACCTTTCTTTGT	BsrGI
755|756s-EBS2	D20 *spa*-pNL9164 cloning; TGAACGCAAGTTTCT AATTTCGGTTGCAATCCGATAGAGGAAAGTGTCT	
147|148s-IBS	D547 *spa*-pNL9164 cloning; AAAAAAGCTTATAATTATCCTTATT TATCAGCTAAGTGCGCCCAGATAGGGTG	HindIII
147|148s-EBS1d	D547 *spa*-pNL9164 cloning; CAGATTGTACAAATGTGGTGATAA CAGATAAGTCAGCTAATTTAACTTACCTTTCTTTGT	BsrGI
147|148s-EBS2	D547 *spa*-pNL9164 cloning; TGAACGCAAGTTTCTAATTTCGGTT ATAAATCGATAGAGGAAAGTGTCT	
D20spatgtF	Identify intron insertion in *spa* in D20 *SA*; TTCTTTGCTCACTGAAGGAT	
D20spatgtR	Identify intron insertion in *spa* in D20 *SA*; AAAATGCTTTCTATGAAATCTTACA	
pNLmcsF	Amplify region around MCS in pNL9164; TTGTGTGTTTGTGATATAG	
pNLmcsR	Amplify region around MCS in pNL9164; GATTTTCAAGCTCTAGTG	
D547spatgtF	Identify intron insertion in *spa* in D547-14, D20-24, D830 *SA*; ATGGTTTGCTGGTTGCTTCT	
D547spatgtR	Identify intron insertion in *spa* in D547-14, D20-24, D830 *SA*; GCTCAAGCACCAAAAGAGGA	
ESPF[#]	Identify the presence of epidermidis serine protease gene *in S. epidermidis* TTTGGAGGTTATCATATGAAAAAGAG	
ESPR[#]	CTGAATATTTATATCAGGTATATTGTTTC	

[#] Primer sequence obtained from Iwase and colleagues [145]

Table 15: Detection of epidermidis serine protease (esp) gene in *S. epidermidis* isolated from participants undergoing *SA* recolonization

Participant	Type of *SA* recolonization performed	Days *esp* gene containing *S. epidermidis* detected[#]	Days *esp* gene containing *S. epidermidis* not detected
D528	WT	Day 1 (D1), D3, D6, D8, D15, D17, D24, D28, D32	None
D757	WT	D1, D3, D6, D8, D10	D13, D15, D17, D20, D24, D27, D31
D756	WT	D10, D15, D20	D1, D3, D6, D8, D17, D24, D28, D32
D637	WT	D1, D3, D6, D8, D10, D13, D15, D17, D20, D24, D30	None
D502	WT	D1, D3, D6, D8, D10, D13, D15, D17, D20, D24, D30	D1, D3, D6, D8
D20	D20 WT and *Δspa*	D1, D3, D6, D8, D10, D19, D21	None
D20	D20-24 WT and *Δspa*	D1, D3, D6, D8, D10, D13, D15, D17, D21, D24, D27, D35	None
D20	D20-24 WT and *Δspa*	D1, D3, D6, D8, D10, D13, D15, D20, D23, D27, D31	None
D547	WT and *Δspa*	D1, D3, D6, D8, D10, D13, D15, D20, D23, D27, D31	
D547	WT and *Δspa*	D1, D3, D6, D8, D10, D13, D15, D17, D20, D24, D27	None
D830	WT and *Δspa*	D1, D6, D10, D13, D15, D17, D20, D24, D27, D31	D3, D8
D713	WT	ND*	ND
D720	WT	ND	ND
D831	WT	ND	ND

[#] PCR-based identification of *esp* gene in *S. epidermidis* isolated throughout the duration of *SA* recolonization in a subset of participants.

* Not determined

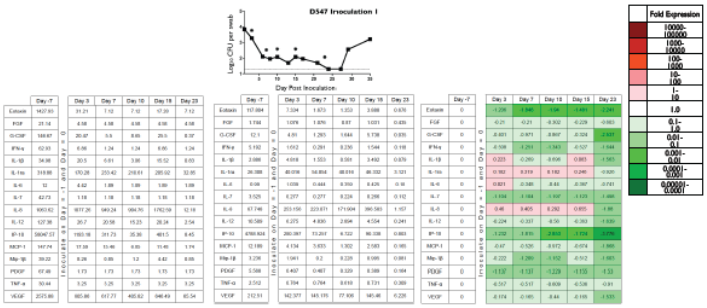
D547 Inoculation I
Log10 CFU per swab
Day Post Inoculation
Fold Expression
10000-100000
1000-10000
100-1000
10-100
1-10
1.0
0.1-1.0
0.01-0.1
0.001-0.01
0.0001-0.001
0.00001-0.0001

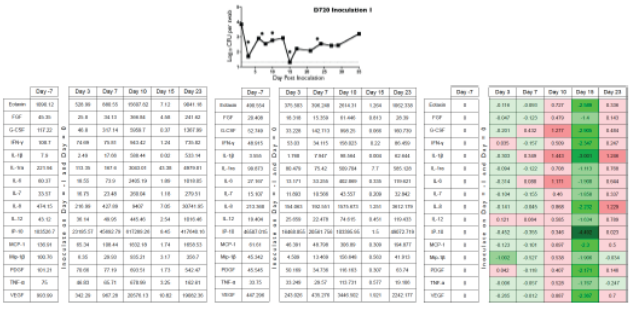
D720 Inoculation I
Log10 CFU per swab
Day Post Inoculation

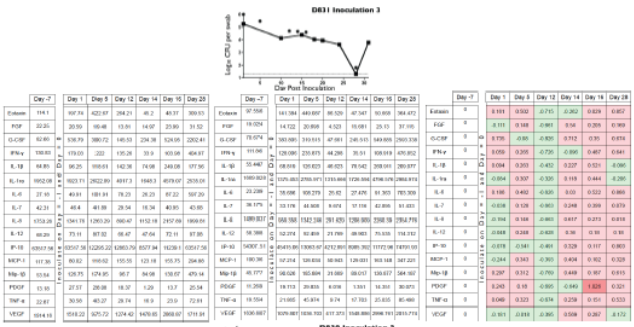
D831 Inoculation 3
Log10 CFU per swab
Day Post Inoculation

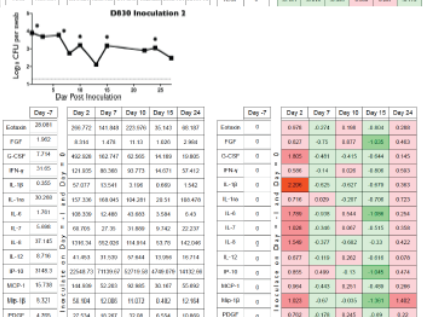
D830 Inoculation 3
Log10 CFU per swab
Day Post Inoculation

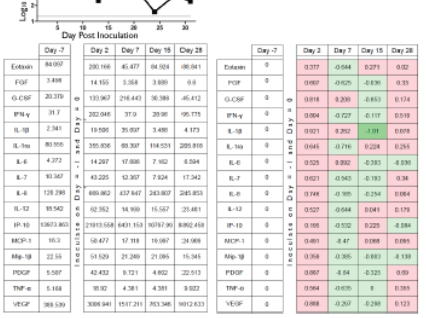
D502 Inoculation I
Log10 CFU per swab
Day Post Inoculation

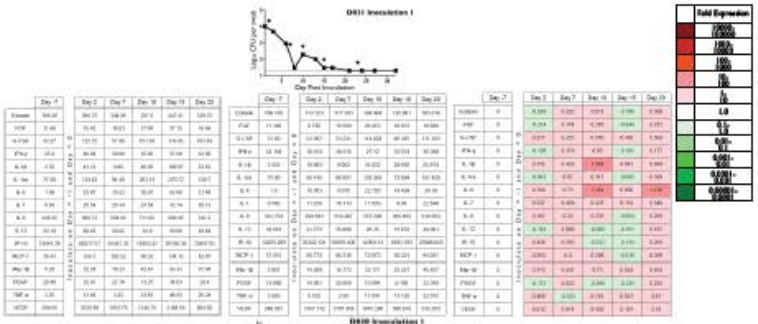
D511 Inoculation 1
Log10 CFU per swab
Day Post Inoculation
Fold Expression

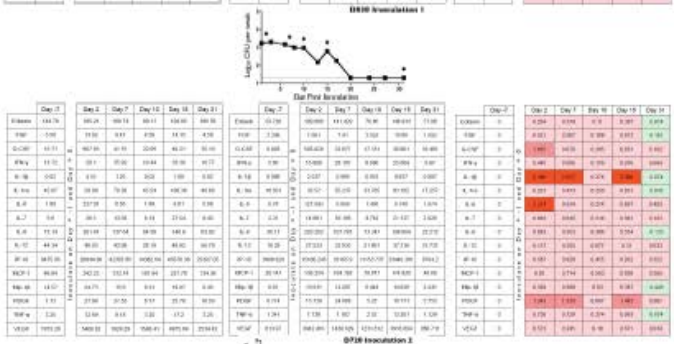
D930 Inoculation 1
Log10 CFU per swab
Day Post Inoculation

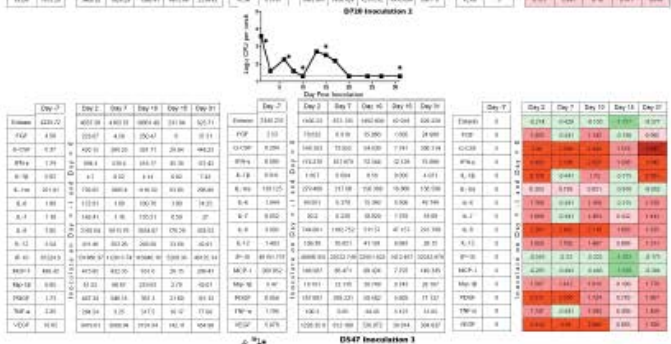
D710 Inoculation 2
Log10 CFU per swab
Day Post Inoculation

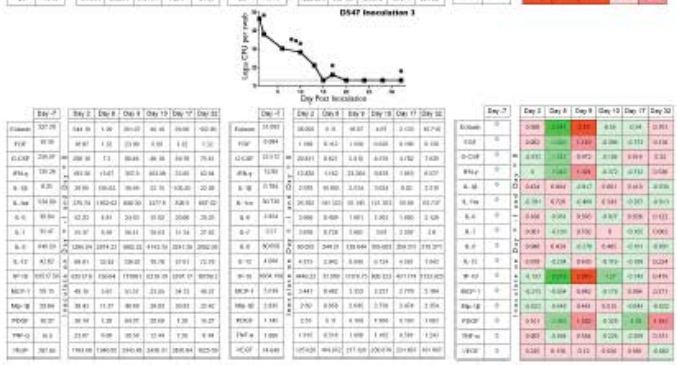
D547 Inoculation 3
Log10 CFU per swab
Day Post Inoculation

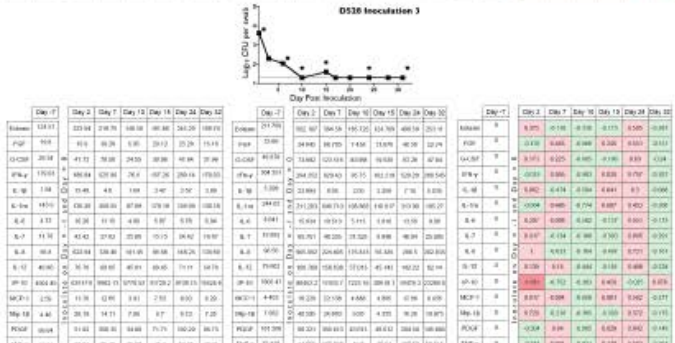
D538 Inoculation 3
Log10 CFU per swab
Day Post Inoculation

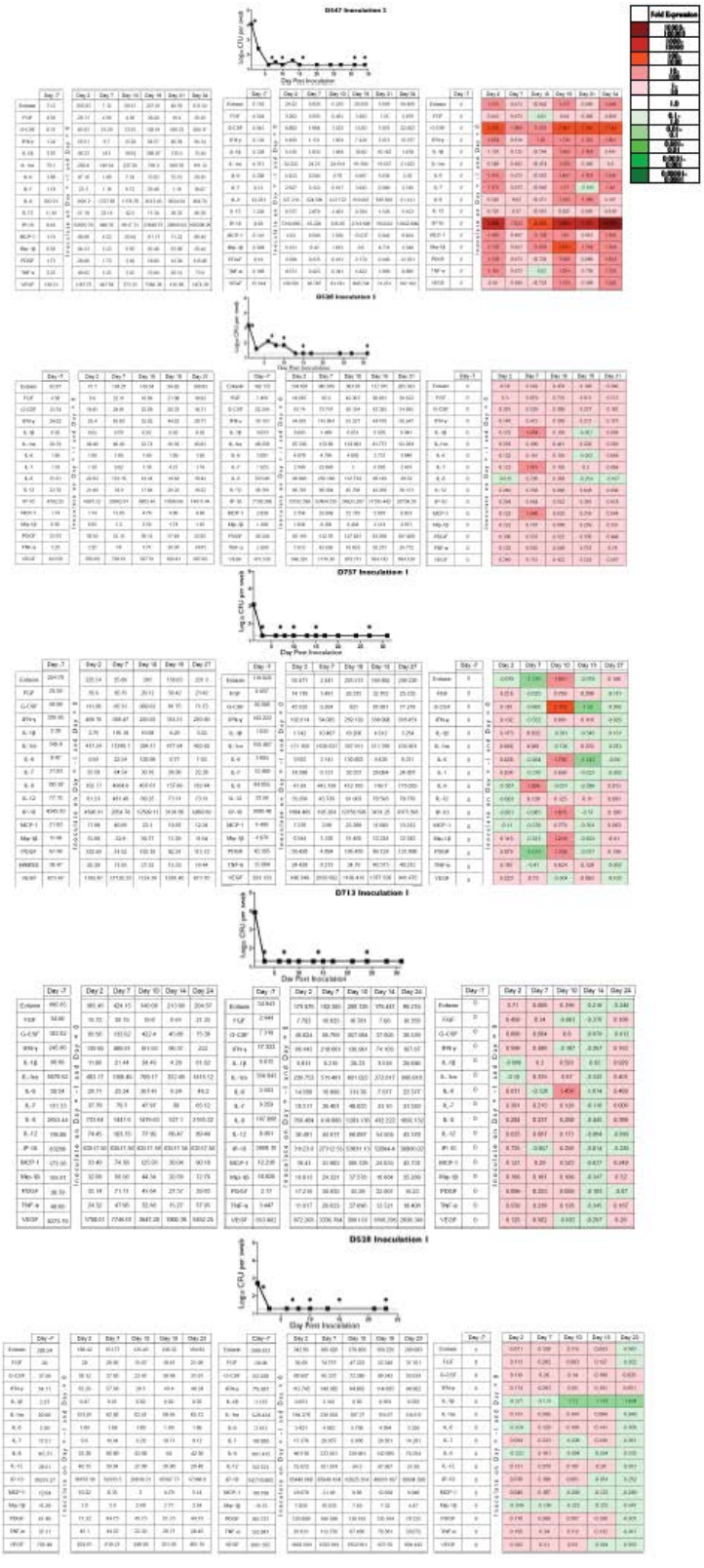

Figure 22: Inflammatory host response to *SA* nasal carriage corresponds to clearance

Shown are matched *SA* carriage levels with each point reflecting the CFUs recovered and cytokine data for all autologous colonization studies that were performed for greater than 22 days. Dotted line in the top panel indicates the limit of *SA* CFU detection and (*) indicates nasal fluid collection days. The first tow cytokine panels represent cytokine quantification in pg/ml, pg/donor at indicated days. The third cytokine pane with color assignment reflects the fold change in each cytokine level compared to day -7 as shown in the legend. Note that within host differences in *SA* nasal carriage pattern was observed due to altered host immune response.

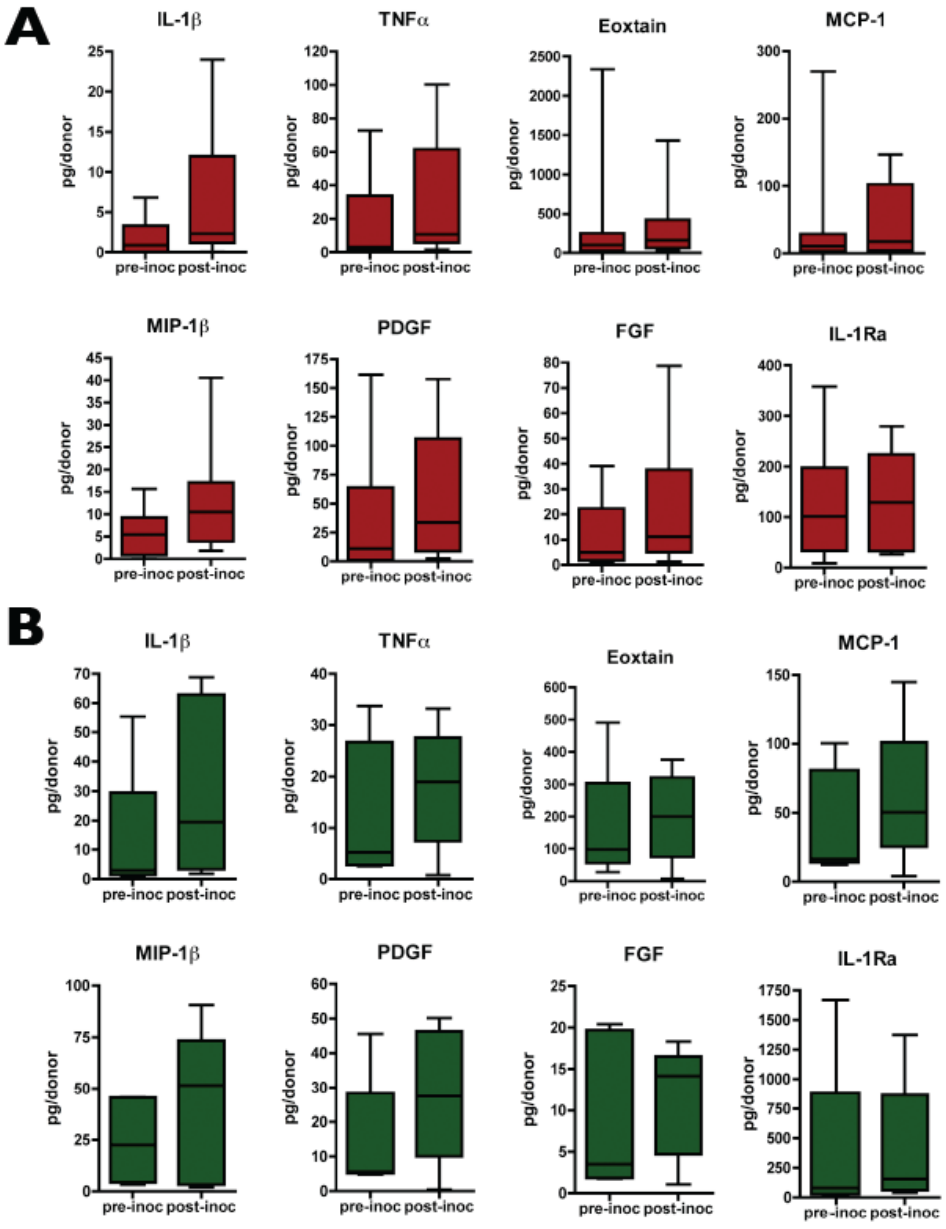

Figure 23: Supporting multiplex cytokine panel

Analytes that did not show any trend in either nasal carriage patterns are represented here. (A) *SA* nasal clearance (B) *SA* nasal survival.

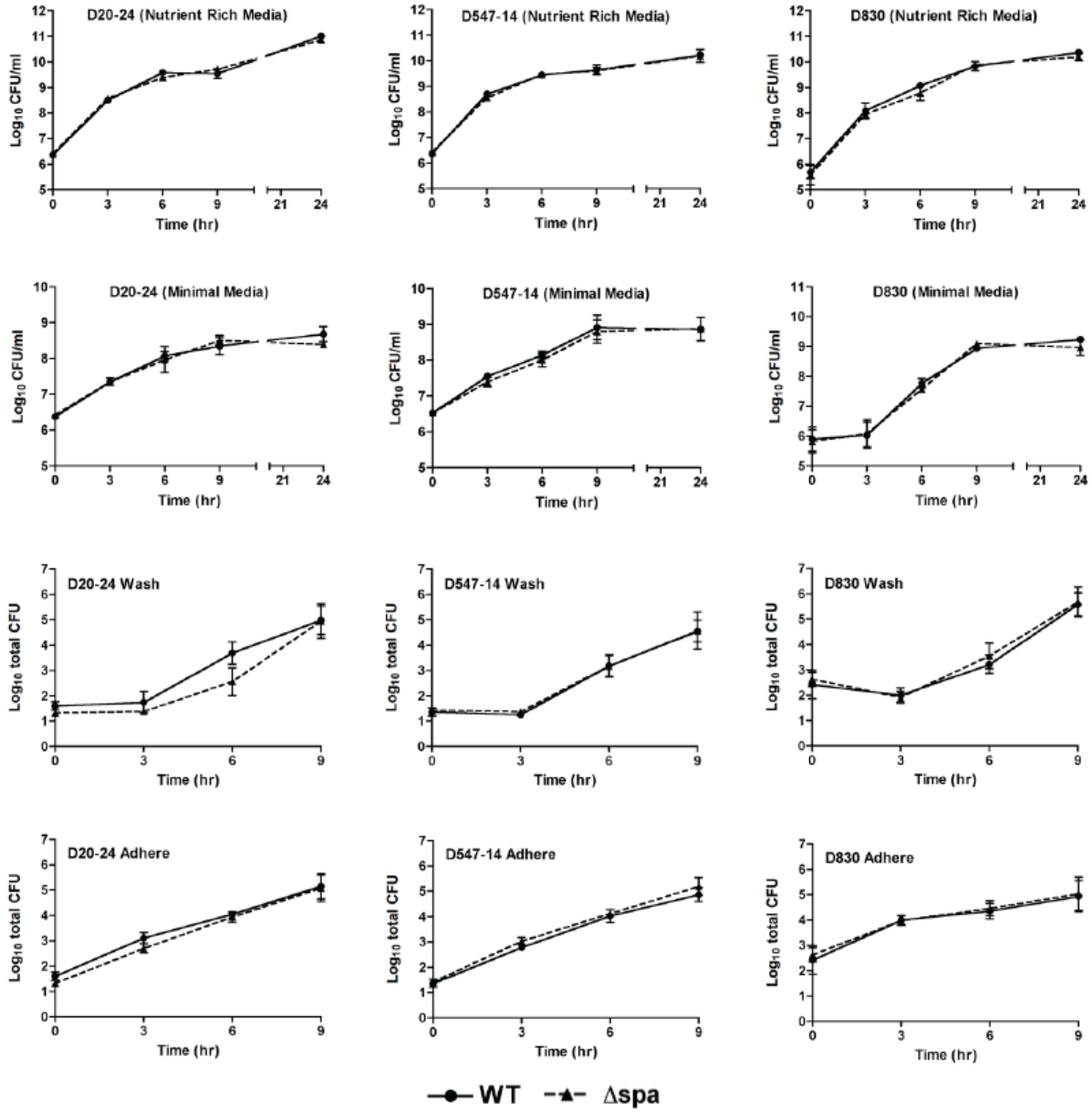

Figure 24: Supporting growth kinetics data of WT and Δspa strains

In vitro growth kinetics and *ex vivo* growth on nasal epithelial cells of the remaining WT and *Δspa* strains are illustrated here (N=3-4). No significant difference in fitness was observed.

APPENDIX D: HUMAN RESEARCH IRB APPROVAL LETTER

University of Central Florida Institutional Review I
Office of Research & Commercialization
12201 Research Parkway, Suite 501
Orlando, Florida 32826-3246
Telephone: 407-823-2901 or 407-882-2276
www.research.ucf.edu/compliance/irb.html

Approval of Human Research

From: **UCF Institutional Review Board #1**
FWA00000351, IRB00001138

To: **Alexander M. Cole** and Co-PIs: **Amy L. Cole, Christopher Parkinson, Gowrishankar Muthukrishnan, Michael G. Deichen, M.D.**

Date: **October 02, 2013**

Dear Researcher:

On 10/2/2013, the IRB approved the following minor modification to human participant research until 02/11/2014 inclusive:

Type of Review:	IRB Addendum and Modification Request Form
Modification Type:	This research study has a new funding source and this information has been added in iRIS. A revised Informed Consent that includes the name of the sponsor has been approved for use.
Project Title:	Nasal Innate Host Defense
Investigator:	Alexander M Cole, Ph.D.
IRB Number:	BIO-06-03582
Funding Agency:	FL Department of Health, James and Esther King Biomedical Research Program
Grant Title:	"Utilizing a smoking cessation program to understand how cigarette smoke exacerbates nasal carriage of Staphylococcus aureus"
Research ID:	1056064

The scientific merit of the research was considered during the IRB review. The Continuing Review Application must be submitted 30days prior to the expiration date for studies that were previously expedited, and 60 days prior to the expiration date for research that was previously reviewed at a convened meeting. Do not make changes to the study (i.e., protocol, methodology, consent form, personnel, site, etc.) before obtaining IRB approval. A Modification Form **cannot** be used to extend the approval period of a study. All forms may be completed and submitted online at https://iris.research.ucf.edu .

If continuing review approval is not granted before the expiration date of 02/11/2014, approval of this research expires on that date. When you have completed your research, please submit a Study Closure request in iRIS so that IRB records will be accurate.

Use of the approved, stamped consent document(s) is required. The new form supersedes all previous versions, which are now invalid for further use. Only approved investigators (or other approved key study personnel) may solicit consent for research participation. Participants or their representatives must receive a copy of the consent form(s).

In the conduct of this research, you are responsible to follow the requirements of the Investigator Manual.

On behalf of Sophia Dziegielewski, Ph.D., L.C.S.W., UCF IRB Chair, this letter is signed by:

Joanne Muratori

IRB Coordinator

REFERENCES

1. (1984) Classics in infectious diseases. "On abscesses". Alexander Ogston (1844-1929). Rev Infect Dis 6: 122-128.

2. Wertheim HF, Melles DC, Vos MC, van Leeuwen W, van Belkum A, et al. (2005) The role of nasal carriage in Staphylococcus aureus infections. The Lancet infectious diseases 5: 751-762.

3. Kluytmans J, van Belkum A, Verbrugh H (1997) Nasal carriage of Staphylococcus aureus: epidemiology, underlying mechanisms, and associated risks. Clin Microbiol Rev 10: 505-520.

4. Klevens RM, Morrison MA, Nadle J, Petit S, Gershman K, et al. (2007) Invasive methicillin-resistant Staphylococcus aureus infections in the United States. Jama 298: 1763-1771.

5. Dantes R, Mu Y, Belflower R, Aragon D, Dumyati G, et al. (2013) National Burden of Invasive Methicillin-Resistant Staphylococcus aureus Infections, United States, 2011. JAMA Intern Med.

6. Williams RE (1963) Healthy carriage of Staphylococcus aureus: its prevalence and importance. Bacteriol Rev 27: 56-71.

7. Cole AM, Tahk S, Oren A, Yoshioka D, Kim YH, et al. (2001) Determinants of Staphylococcus aureus nasal carriage. Clin Diagn Lab Immunol 8: 1064-1069.

8. Hu L, Umeda A, Kondo S, Amako K (1995) Typing of Staphylococcus aureus colonising human nasal carriers by pulsed-field gel electrophoresis. J Med Microbiol 42: 127-132.

9. Eriksen NH, Espersen F, Rosdahl VT, Jensen K (1995) Carriage of Staphylococcus aureus among 104 healthy persons during a 19-month period. Epidemiol Infect 115: 51-60.

10. van Belkum A, Verkaik NJ, de Vogel CP, Boelens HA, Verveer J, et al. (2009) Reclassification of Staphylococcus aureus nasal carriage types. J Infect Dis 199: 1820-1826.

11. Burian M, Wolz C, Goerke C (2010) Regulatory adaptation of Staphylococcus aureus during nasal colonization of humans. PLoS One 5: e10040.

12. Wertheim HF, Vos MC, Ott A, van Belkum A, Voss A, et al. (2004) Risk and outcome of nosocomial Staphylococcus aureus bacteraemia in nasal carriers versus non-carriers. Lancet 364: 703-705.

13. von Eiff C, Becker K, Machka K, Stammer H, Peters G (2001) Nasal carriage as a source of Staphylococcus aureus bacteremia. Study Group. N Engl J Med 344: 11-16.

14. Tulloch LG (1954) Nasal carriage in staphylococcal skin infections. Br Med J (Clin Res Ed) 2: 912-913.

15. Honda H, Krauss MJ, Coopersmith CM, Kollef MH, Richmond AM, et al. (2010) Staphylococcus aureus nasal colonization and subsequent infection in intensive care unit patients: does methicillin resistance matter? Infect Control Hosp Epidemiol 31: 584-591.

16. Ellis MW, Hospenthal DR, Dooley DP, Gray PJ, Murray CK (2004) Natural history of community-acquired methicillin-resistant Staphylococcus aureus colonization and infection in soldiers. Clinical infectious diseases : an official publication of the Infectious Diseases Society of America 39: 971-979.

17. Kazakova SV, Hageman JC, Matava M, Srinivasan A, Phelan L, et al. (2005) A clone of methicillin-resistant Staphylococcus aureus among professional football players. N Engl J Med 352: 468-475.

18. Breuer K, S HA, Kapp A, Werfel T (2002) Staphylococcus aureus: colonizing features and influence of an antibacterial treatment in adults with atopic dermatitis. Br J Dermatol 147: 55-61.

19. Laudien M, Gadola SD, Podschun R, Hedderich J, Paulsen J, et al. (2010) Nasal carriage of Staphylococcus aureus and endonasal activity in Wegener s granulomatosis as compared to rheumatoid arthritis and chronic Rhinosinusitis with nasal polyps. Clin Exp Rheumatol 28: 51-55.

20. Weinke T, Schiller R, Fehrenbach FJ, Pohle HD (1992) Association between Staphylococcus aureus nasopharyngeal colonization and septicemia in patients infected with the human immunodeficiency virus. Eur J Clin Microbiol Infect Dis 11: 985-989.

21. Miller M, Cespedes C, Bhat M, Vavagiakis P, Klein RS, et al. (2007) Incidence and persistence of Staphylococcus aureus nasal colonization in a community sample of HIV-infected and -uninfected drug users. Clinical infectious diseases : an official publication of the Infectious Diseases Society of America 45: 343-346.

22. Feil EJ, Enright MC (2004) Analyses of clonality and the evolution of bacterial pathogens. Curr Opin Microbiol 7: 308-313.

23. Feng Y, Chen CJ, Su LH, Hu S, Yu J, et al. (2008) Evolution and pathogenesis of Staphylococcus aureus: lessons learned from genotyping and comparative genomics. FEMS Microbiol Rev 32: 23-37.

24. Weller TM (2000) Methicillin-resistant Staphylococcus aureus typing methods: which should be the international standard? J Hosp Infect 44: 160-172.

25. Maiden MC, Bygraves JA, Feil E, Morelli G, Russell JE, et al. (1998) Multilocus sequence typing: a portable approach to the identification of clones within populations of pathogenic microorganisms. Proceedings of the National Academy of Sciences of the United States of America 95: 3140-3145.

26. Enright MC, Day NP, Davies CE, Peacock SJ, Spratt BG (2000) Multilocus sequence typing for characterization of methicillin-resistant and methicillin-susceptible clones of Staphylococcus aureus. J Clin Microbiol 38: 1008-1015.

27. Robinson DA, Enright MC (2004) Multilocus sequence typing and the evolution of methicillin-resistant Staphylococcus aureus. Clin Microbiol Infect 10: 92-97.

28. Feil EJ, Li BC, Aanensen DM, Hanage WP, Spratt BG (2004) eBURST: inferring patterns of evolutionary descent among clusters of related bacterial genotypes from multilocus sequence typing data. J Bacteriol 186: 1518-1530.

29. Enright MC, Robinson DA, Randle G, Feil EJ, Grundmann H, et al. (2002) The evolutionary history of methicillin-resistant Staphylococcus aureus (MRSA). Proceedings of the National Academy of Sciences of the United States of America 99: 7687-7692.

30. Tenover FC, Goering RV (2009) Methicillin-resistant Staphylococcus aureus strain USA300: origin and epidemiology. J Antimicrob Chemother 64: 441-446.

31. Milheirico C, Oliveira DC, de Lencastre H (2007) Update to the multiplex PCR strategy for assignment of mec element types in Staphylococcus aureus. Antimicrob Agents Chemother 51: 3374-3377.

32. Ma XX, Ito T, Tiensasitorn C, Jamklang M, Chongtrakool P, et al. (2002) Novel type of staphylococcal cassette chromosome mec identified in community-acquired methicillin-resistant Staphylococcus aureus strains. Antimicrob Agents Chemother 46: 1147-1152.

33. Daum RS, Ito T, Hiramatsu K, Hussain F, Mongkolrattanothai K, et al. (2002) A novel methicillin-resistance cassette in community-acquired methicillin-resistant Staphylococcus aureus isolates of diverse genetic backgrounds. J Infect Dis 186: 1344-1347.

34. Oliveira DC, de Lencastre H (2002) Multiplex PCR strategy for rapid identification of structural types and variants of the mec element in methicillin-resistant Staphylococcus aureus. Antimicrob Agents Chemother 46: 2155-2161.

35. Gomes AR, Vinga S, Zavolan M, de Lencastre H (2005) Analysis of the genetic variability of virulence-related loci in epidemic clones of methicillin-resistant Staphylococcus aureus. Antimicrob Agents Chemother 49: 366-379.

36. Lamers RP, Stinnett JW, Muthukrishnan G, Parkinson CL, Cole AM (2011) Evolutionary analyses of Staphylococcus aureus identify genetic relationships between nasal carriage and clinical isolates. PLoS One 6: e16426.

37. Shopsin B, Gomez M, Montgomery SO, Smith DH, Waddington M, et al. (1999) Evaluation of protein A gene polymorphic region DNA sequencing for typing of Staphylococcus aureus strains. J Clin Microbiol 37: 3556-3563.

38. Harmsen D, Claus H, Witte W, Rothganger J, Claus H, et al. (2003) Typing of methicillin-resistant Staphylococcus aureus in a university hospital setting by using novel software for spa repeat determination and database management. J Clin Microbiol 41: 5442-5448.

39. Weidenmaier C, Goerke C, Wolz C (2012) Staphylococcus aureus determinants for nasal colonization. Trends Microbiol 20: 243-250.

40. Johannessen M, Sollid JE, Hanssen AM (2012) Host- and microbe determinants that may influence the success of S. aureus colonization. Front Cell Infect Microbiol 2: 56.

41. Ruimy R, Angebault C, Djossou F, Dupont C, Epelboin L, et al. (2010) Are host genetics the predominant determinant of persistent nasal Staphylococcus aureus carriage in humans? J Infect Dis 202: 924-934.

42. Emonts M, Uitterlinden AG, Nouwen JL, Kardys I, Maat MP, et al. (2008) Host polymorphisms in interleukin 4, complement factor H, and C-reactive protein associated with nasal carriage of Staphylococcus aureus and occurrence of boils. J Infect Dis 197: 1244-1253.

43. van Belkum A, Emonts M, Wertheim H, de Jongh C, Nouwen J, et al. (2007) The role of human innate immune factors in nasal colonization by Staphylococcus aureus. Microbes Infect 9: 1471-1477.

44. Panierakis C, Goulielmos G, Mamoulakis D, Maraki S, Papavasiliou E, et al. (2009) Staphylococcus aureus nasal carriage might be associated with vitamin D receptor polymorphisms in type 1 diabetes. International journal of infectious diseases : IJID : official publication of the International Society for Infectious Diseases 13: e437-443.

45. van den Akker EL, Nouwen JL, Melles DC, van Rossum EF, Koper JW, et al. (2006) Staphylococcus aureus nasal carriage is associated with glucocorticoid receptor gene polymorphisms. J Infect Dis 194: 814-818.

46. Vuononvirta J, Toivonen L, Grondahl-Yli-Hannuksela K, Barkoff AM, Lindholm L, et al. (2011) Nasopharyngeal bacterial colonization and gene polymorphisms of mannose-binding lectin and toll-like receptors 2 and 4 in infants. PLoS One 6: e26198.

47. Schauber J, Gallo RL (2009) Antimicrobial peptides and the skin immune defense system. J Allergy Clin Immunol 124: R13-18.

48. Hancock RE, Sahl HG (2006) Antimicrobial and host-defense peptides as new anti-infective therapeutic strategies. Nat Biotechnol 24: 1551-1557.

49. Cole AM, Dewan P, Ganz T (1999) Innate antimicrobial activity of nasal secretions. Infect Immun 67: 3267-3275.

50. Pynnonen M, Stephenson RE, Schwartz K, Hernandez M, Boles BR (2011) Hemoglobin promotes Staphylococcus aureus nasal colonization. PLoS Pathog 7: e1002104.

51. Cole AM, Liao HI, Stuchlik O, Tilan J, Pohl J, et al. (2002) Cationic polypeptides are required for antibacterial activity of human airway fluid. J Immunol 169: 6985-6991.

52. Harder J, Bartels J, Christophers E, Schroder JM (2001) Isolation and characterization of human beta -defensin-3, a novel human inducible peptide antibiotic. J Biol Chem 276: 5707-5713.

53. Midorikawa K, Ouhara K, Komatsuzawa H, Kawai T, Yamada S, et al. (2003) Staphylococcus aureus susceptibility to innate antimicrobial peptides, beta-defensins and CAP18, expressed by human keratinocytes. Infect Immun 71: 3730-3739.

54. Menzies BE, Kenoyer A (2006) Signal transduction and nuclear responses in Staphylococcus aureus-induced expression of human beta-defensin 3 in skin keratinocytes. Infect Immun 74: 6847-6854.

55. Zanger P, Nurjadi D, Vath B, Kremsner PG (2011) Persistent nasal carriage of Staphylococcus aureus is associated with deficient induction of human beta-defensin 3 after sterile wounding of healthy skin in vivo. Infect Immun 79: 2658-2662.

56. Nurjadi D, Herrmann E, Hinderberger I, Zanger P (2013) Impaired beta-defensin expression in human skin links DEFB1 promoter polymorphisms with persistent Staphylococcus aureus nasal carriage. J Infect Dis 207: 666-674.

57. Quinn GA, Cole AM (2007) Suppression of innate immunity by a nasal carriage strain of Staphylococcus aureus increases its colonization on nasal epithelium. Immunology 122: 80-89.

58. Quinn GA, Tarwater PM, Cole AM (2008) Subversion of IL-1-mediated host defense by a nasal carrier strain of Staphylococcus aureus. Immunology.

59. Fournier B, Philpott DJ (2005) Recognition of Staphylococcus aureus by the innate immune system. Clin Microbiol Rev 18: 521-540.

60. Nilsen NJ, Deininger S, Nonstad U, Skjeldal F, Husebye H, et al. (2008) Cellular trafficking of lipoteichoic acid and Toll-like receptor 2 in relation to signaling: role of CD14 and CD36. J Leukoc Biol 84: 280-291.

61. Craven RR, Gao X, Allen IC, Gris D, Bubeck Wardenburg J, et al. (2009) Staphylococcus aureus alpha-hemolysin activates the NLRP3-inflammasome in human and mouse monocytic cells. PLoS One 4: e7446.

62. Voss E, Wehkamp J, Wehkamp K, Stange EF, Schroder JM, et al. (2006) NOD2/CARD15 mediates induction of the antimicrobial peptide human beta-defensin-2. J Biol Chem 281: 2005-2011.

63. Martinon F, Mayor A, Tschopp J (2009) The inflammasomes: guardians of the body. Annu Rev Immunol 27: 229-265.

64. Hruz P, Zinkernagel AS, Jenikova G, Botwin GJ, Hugot JP, et al. (2009) NOD2 contributes to cutaneous defense against Staphylococcus aureus through alpha-toxin-dependent innate immune

activation. Proceedings of the National Academy of Sciences of the United States of America 106: 12873-12878.

65. Deshmukh HS, Hamburger JB, Ahn SH, McCafferty DG, Yang SR, et al. (2009) Critical role of NOD2 in regulating the immune response to Staphylococcus aureus. Infect Immun 77: 1376-1382.

66. Casanova JL, Abel L (2004) Human Mannose-binding Lectin in Immunity: Friend, Foe, or Both? J Exp Med 199: 1295-1299.

67. Holtfreter S, Roschack K, Eichler P, Eske K, Holtfreter B, et al. (2006) Staphylococcus aureus carriers neutralize superantigens by antibodies specific for their colonizing strain: a potential explanation for their improved prognosis in severe sepsis. J Infect Dis 193: 1275-1278.

68. Verkaik NJ, de Vogel CP, Boelens HA, Grumann D, Hoogenboezem T, et al. (2009) Anti-staphylococcal humoral immune response in persistent nasal carriers and noncarriers of Staphylococcus aureus. J Infect Dis 199: 625-632.

69. Colque-Navarro P, Jacobsson G, Andersson R, Flock JI, Mollby R (2010) Levels of antibody against 11 Staphylococcus aureus antigens in a healthy population. Clin Vaccine Immunol 17: 1117-1123.

70. Burian M, Grumann D, Holtfreter S, Wolz C, Goerke C, et al. (2012) Expression of staphylococcal superantigens during nasal colonization is not sufficient to induce a systemic neutralizing antibody response in humans. Eur J Clin Microbiol Infect Dis 31: 251-256.

71. Broker BM, van Belkum A (2011) Immune proteomics of Staphylococcus aureus. Proteomics 11: 3221-3231.

72. Holtfreter S, Nguyen TT, Wertheim H, Steil L, Kusch H, et al. (2009) Human immune proteome in experimental colonization with Staphylococcus aureus. Clin Vaccine Immunol 16: 1607-1614.

73. Patti JM, Allen BL, McGavin MJ, Hook M (1994) MSCRAMM-mediated adherence of microorganisms to host tissues. Annu Rev Microbiol 48: 585-617.

74. Weidenmaier C, Kokai-Kun JF, Kulauzovic E, Kohler T, Thumm G, et al. (2008) Differential roles of sortase-anchored surface proteins and wall teichoic acid in Staphylococcus aureus nasal colonization. Int J Med Microbiol 298: 505-513.

75. Burian M, Rautenberg M, Kohler T, Fritz M, Krismer B, et al. (2010) Temporal expression of adhesion factors and activity of global regulators during establishment of Staphylococcus aureus nasal colonization. J Infect Dis 201: 1414-1421.

76. Clarke SR, Andre G, Walsh EJ, Dufrene YF, Foster TJ, et al. (2009) Iron-regulated surface determinant protein A mediates adhesion of Staphylococcus aureus to human corneocyte envelope proteins. Infect Immun 77: 2408-2416.

77. Wertheim HF, Walsh E, Choudhurry R, Melles DC, Boelens HA, et al. (2008) Key role for clumping factor B in Staphylococcus aureus nasal colonization of humans. PLoS Med 5: e17.

78. O'Brien LM, Walsh EJ, Massey RC, Peacock SJ, Foster TJ (2002) Staphylococcus aureus clumping factor B (ClfB) promotes adherence to human type I cytokeratin 10: implications for nasal colonization. Cell Microbiol 4: 759-770.

79. Haim M, Trost A, Maier CJ, Achatz G, Feichtner S, et al. (2010) Cytokeratin 8 interacts with clumping factor B: a new possible virulence factor target. Microbiology 156: 3710-3721.

80. Grundmeier M, Hussain M, Becker P, Heilmann C, Peters G, et al. (2004) Truncation of fibronectin-binding proteins in Staphylococcus aureus strain Newman leads to deficient adherence and host cell invasion due to loss of the cell wall anchor function. Infect Immun 72: 7155-7163.

81. Sinha B, Francois PP, Nusse O, Foti M, Hartford OM, et al. (1999) Fibronectin-binding protein acts as Staphylococcus aureus invasin via fibronectin bridging to integrin alpha5beta1. Cell Microbiol 1: 101-117.

82. Clarke SR, Brummell KJ, Horsburgh MJ, McDowell PW, Mohamad SA, et al. (2006) Identification of in vivo-expressed antigens of Staphylococcus aureus and their use in vaccinations for protection against nasal carriage. J Infect Dis 193: 1098-1108.

83. Corrigan RM, Miajlovic H, Foster TJ (2009) Surface proteins that promote adherence of Staphylococcus aureus to human desquamated nasal epithelial cells. BMC Microbiol 9: 22.

84. Foster TJ (2005) Immune evasion by staphylococci. Nat Rev Microbiol 3: 948-958.

85. Haas PJ, de Haas CJ, Poppelier MJ, van Kessel KP, van Strijp JA, et al. (2005) The structure of the C5a receptor-blocking domain of chemotaxis inhibitory protein of Staphylococcus aureus is related to a group of immune evasive molecules. J Mol Biol 353: 859-872.

86. Postma B, Kleibeuker W, Poppelier MJ, Boonstra M, Van Kessel KP, et al. (2005) Residues 10-18 within the C5a receptor N terminus compose a binding domain for chemotaxis inhibitory protein of Staphylococcus aureus. J Biol Chem 280: 2020-2027.

87. Haas PJ, de Haas CJ, Kleibeuker W, Poppelier MJ, van Kessel KP, et al. (2004) N-terminal residues of the chemotaxis inhibitory protein of Staphylococcus aureus are essential for blocking formylated peptide receptor but not C5a receptor. J Immunol 173: 5704-5711.

88. Postma B, Poppelier MJ, van Galen JC, Prossnitz ER, van Strijp JA, et al. (2004) Chemotaxis inhibitory protein of Staphylococcus aureus binds specifically to the C5a and formylated peptide receptor. J Immunol 172: 6994-7001.

89. de Haas CJ, Veldkamp KE, Peschel A, Weerkamp F, Van Wamel WJ, et al. (2004) Chemotaxis inhibitory protein of Staphylococcus aureus, a bacterial antiinflammatory agent. J Exp Med 199: 687-695.

90. Higgins J, Loughman A, van Kessel KP, van Strijp JA, Foster TJ (2006) Clumping factor A of Staphylococcus aureus inhibits phagocytosis by human polymorphonuclear leucocytes. FEMS Microbiol Lett 258: 290-296.

91. Palmqvist N, Foster T, Fitzgerald JR, Josefsson E, Tarkowski A (2005) Fibronectin-binding proteins and fibrinogen-binding clumping factors play distinct roles in staphylococcal arthritis and systemic inflammation. J Infect Dis 191: 791-798.

92. Rooijakkers SH, van Wamel WJ, Ruyken M, van Kessel KP, van Strijp JA (2005) Anti-opsonic properties of staphylokinase. Microbes Infect 7: 476-484.

93. Lee LY, Liang X, Hook M, Brown EL (2004) Identification and characterization of the C3 binding domain of the Staphylococcus aureus extracellular fibrinogen-binding protein (Efb). J Biol Chem 279: 50710-50716.

94. Schneewind O, Model P, Fischetti VA (1992) Sorting of protein A to the staphylococcal cell wall. Cell 70: 267-281.

95. Moks T, Abrahmsen L, Nilsson B, Hellman U, Sjoquist J, et al. (1986) Staphylococcal protein A consists of five IgG-binding domains. Eur J Biochem 156: 637-643.

96. Cedergren L, Andersson R, Jansson B, Uhlen M, Nilsson B (1993) Mutational analysis of the interaction between staphylococcal protein A and human IgG1. Protein Eng 6: 441-448.

97. Romagnani S, Giudizi MG, del Prete G, Maggi E, Biagiotti R, et al. (1982) Demonstration on protein A of two distinct immunoglobulin-binding sites and their role in the mitogenic activity of Staphylococcus aureus Cowan I on human B cells. J Immunol 129: 596-602.

98. Graille M, Stura EA, Corper AL, Sutton BJ, Taussig MJ, et al. (2000) Crystal structure of a Staphylococcus aureus protein A domain complexed with the Fab fragment of a human IgM antibody: structural basis for recognition of B-cell receptors and superantigen activity. Proceedings of the National Academy of Sciences of the United States of America 97: 5399-5404.

99. Gomez MI, O'Seaghdha M, Magargee M, Foster TJ, Prince AS (2006) Staphylococcus aureus protein A activates TNFR1 signaling through conserved IgG binding domains. J Biol Chem 281: 20190-20196.

100. Gomez MI, Lee A, Reddy B, Muir A, Soong G, et al. (2004) Staphylococcus aureus protein A induces airway epithelial inflammatory responses by activating TNFR1. Nat Med 10: 842-848.

101. Gomez MI, Seaghdha MO, Prince AS (2007) Staphylococcus aureus protein A activates TACE through EGFR-dependent signaling. Embo J 26: 701-709.

102. Labandeira-Rey M, Couzon F, Boisset S, Brown EL, Bes M, et al. (2007) Staphylococcus aureus Panton-Valentine leukocidin causes necrotizing pneumonia. Science 315: 1130-1133.

103. Merino N, Toledo-Arana A, Vergara-Irigaray M, Valle J, Solano C, et al. (2009) Protein A-mediated multicellular behavior in Staphylococcus aureus. J Bacteriol 191: 832-843.

104. Kokai-Kun JF (2008) The Cotton Rat as a Model for Staphylococcus aureus nasal colonization in humans: cotton rat S. aureus nasal colonization model. Methods Mol Biol 431: 241-254.

105. Weidenmaier C, Kokai-Kun JF, Kristian SA, Chanturiya T, Kalbacher H, et al. (2004) Role of teichoic acids in Staphylococcus aureus nasal colonization, a major risk factor in nosocomial infections. Nat Med 10: 243-245.

106. Kiser KB, Cantey-Kiser JM, Lee JC (1999) Development and characterization of a Staphylococcus aureus nasal colonization model in mice. Infect Immun 67: 5001-5006.

107. Gonzalez-Zorn B, Senna JP, Fiette L, Shorte S, Testard A, et al. (2005) Bacterial and host factors implicated in nasal carriage of methicillin-resistant Staphylococcus aureus in mice. Infect Immun 73: 1847-1851.

108. Archer NK, Harro JM, Shirtliff ME (2013) Clearance of Staphylococcus aureus nasal carriage is T cell dependent and mediated through interleukin-17A expression and neutrophil influx. Infect Immun 81: 2070-2075.

109. Chambers HF, Deleo FR (2009) Waves of resistance: Staphylococcus aureus in the antibiotic era. Nat Rev Microbiol 7: 629-641.

110. Kuehnert MJ, Kruszon-Moran D, Hill HA, McQuillan G, McAllister SK, et al. (2006) Prevalence of Staphylococcus aureus nasal colonization in the United States, 2001-2002. J Infect Dis 193: 172-179.

111. Lazo ND, Downing DT (1999) A mixture of alpha-helical and 3(10)-helical conformations for involucrin in the human epidermal corneocyte envelope provides a scaffold for the attachment of both lipids and proteins. J Biol Chem 274: 37340-37344.

112. Steven AC, Steinert PM (1994) Protein composition of cornified cell envelopes of epidermal keratinocytes. J Cell Sci 107 (Pt 2): 693-700.

113. Williams RE (1963) Healthy carriage of Staphylococcus aureus: its prevalence and importance. Bacteriol Rev 27: 56-71.

114. Miller M, Cook HA, Furuya EY, Bhat M, Lee MH, et al. (2009) Staphylococcus aureus in the community: colonization versus infection. PLoS One 4: e6708.

115. Nouwen JL, Fieren MW, Snijders S, Verbrugh HA, van Belkum A (2005) Persistent (not intermittent) nasal carriage of Staphylococcus aureus is the determinant of CPD-related infections. Kidney Int 67: 1084-1092.

116. Koreen L, Ramaswamy SV, Naidich S, Koreen IV, Graff GR, et al. (2005) Comparative sequencing of the serine-aspartate repeat-encoding region of the clumping factor B gene (*clfB*) for resolution within clonal groups of *Staphylococcus aureus*. J Clin Microbiol 43: 3985-3994.

117. Naas T, Fortineau N, Spicq C, Robert J, Jarlier V, et al. (2005) Three-year survey of community-acquired methicillin-resistant Staphylococcus aureus producing Panton-Valentine leukocidin in a French university hospital. J Hosp Infect 61: 321-329.

118. Suggs AH, Maranan MC, Boyle-Vavra S, Daum RS (1999) Methicillin-resistant and borderline methicillin-resistant asymptomatic Staphylococcus aureus colonization in children without identifiable risk factors. Pediatr Infect Dis J 18: 410-414.

119. Naimi TS, LeDell KH, Como-Sabetti K, Borchardt SM, Boxrud DJ, et al. (2003) Comparison of community- and health care-associated methicillin-resistant Staphylococcus aureus infection. Jama 290: 2976-2984.

120. Muthukrishnan G, Quinn GA, Lamers RP, Diaz C, Cole AL, et al. (2011) Exoproteome of Staphylococcus aureus reveals putative determinants of nasal carriage. J Proteome Res 10: 2064-2078.

121. Nashev D, Toshkova K, Salasia SI, Hassan AA, Lammler C, et al. (2004) Distribution of virulence genes of Staphylococcus aureus isolated from stable nasal carriers. FEMS Microbiol Lett 233: 45-52.

122. Ferry T, Perpoint T, Vandenesch F, Etienne J (2005) Virulence determinants in Staphylococcus aureus and their involvement in clinical syndromes. Curr Infect Dis Rep 7: 420-428.

123. VandenBergh MF, Yzerman EP, van Belkum A, Boelens HA, Sijmons M, et al. (1999) Follow-up of Staphylococcus aureus nasal carriage after 8 years: redefining the persistent carrier state. J Clin Microbiol 37: 3133-3140.

124. Huelsenbeck JP, Ronquist F (2001) MRBAYES: Bayesian inference of phylogenetic trees. Bioinformatics 17: 754-755.

125. Huelsenbeck JP, Ronquist F, Nielsen R, Bollback JP (2001) Bayesian inference of phylogeny and its impact on evolutionary biology. Science 294: 2310-2314.

126. Ronquist F, Huelsenbeck JP (2003) MrBayes 3: Bayesian phylogenetic inference under mixed models. Bioinformatics 19: 1572-1574.

127. Posada D (2008) jModelTest: phylogenetic model averaging. Mol Biol Evol 25: 1253-1256.

128. Hasegawa M, Iida Y, Yano T, Takaiwa F, Iwabuchi M (1985) Phylogenetic relationships among eukaryotic kingdoms inferred from ribosomal RNA sequences. J Mol Evol 22: 32-38.

129. Spratt BG, Hanage WP, Li B, Aanensen DM, Feil EJ (2004) Displaying the relatedness among isolates of bacterial species -- the eBURST approach. FEMS Microbiol Lett 241: 129-134.

130. Sanger F, Nicklen S, Coulson AR (1977) DNA sequencing with chain-terminating inhibitors. Proc Natl Acad Sci U S A 74: 5463-5467.

131. Gotelli NJ, Ellison AM (2004) A Primer Of Ecological Statistics: Sinauer Associates.

132. Ni Eidhin D, Perkins S, Francois P, Vaudaux P, Hook M, et al. (1998) Clumping factor B (ClfB), a new surface-located fibrinogen-binding adhesin of Staphylococcus aureus. Mol Microbiol 30: 245-257.

133. Nouwen J, Boelens H, van Belkum A, Verbrugh H (2004) Human factor in Staphylococcus aureus nasal carriage. Infect Immun 72: 6685-6688.

134. Goslings WR, Buchli K (1958) Nasal carrier rate of antibiotic-resistant staphylococci; influence of hospitalization on carrier rate in patients, and their household contacts. AMA Arch Intern Med 102: 691-715.

135. Nouwen JL, Ott A, Kluytmans-Vandenbergh MF, Boelens HA, Hofman A, et al. (2004) Predicting the Staphylococcus aureus nasal carrier state: derivation and validation of a "culture rule". Clinical infectious diseases : an official publication of the Infectious Diseases Society of America 39: 806-811.

136. Hidron AI, Low CE, Honig EG, Blumberg HM (2009) Emergence of community-acquired meticillin-resistant Staphylococcus aureus strain USA300 as a cause of necrotising community-onset pneumonia. The Lancet infectious diseases 9: 384-392.

137. King MD, Humphrey BJ, Wang YF, Kourbatova EV, Ray SM, et al. (2006) Emergence of community-acquired methicillin-resistant Staphylococcus aureus USA 300 clone as the predominant cause of skin and soft-tissue infections. Annals of internal medicine 144: 309-317.

138. Hofman A, Boerlage PA, Bots ML, den Breeijen JH, de Bruijn AM, et al. (1995) [Prevalence of chronic diseases in the elderly; the ERGO study (Erasmus Rotterdam Health and the Elderly)]. Ned Tijdschr Geneeskd 139: 1975-1978.

139. Chen K, Pachter L (2005) Bioinformatics for whole-genome shotgun sequencing of microbial communities. PLoS Comput Biol 1: 106-112.

140. Nashev D, Toshkova K, Bizeva L, Akineden O, Lammler C, et al. (2007) Distribution of enterotoxin genes among carriage- and infection-associated isolates of Staphylococcus aureus. Lett Appl Microbiol 45: 681-685.

141. Van Belkum A, Riewarts Eriksen NH, Sijmons M, Van Leeuwen W, Van den Bergh M, et al. (1997) Coagulase and protein A polymorphisms do not contribute to persistence of nasal colonisation by Staphylococcus aureus. J Med Microbiol 46: 222-232.

142. Nouwen J, Ott A, Boelens H, van Belkum A, de Marie S, et al. (2004) Smoking pattern and fasting glucose levels determine Staphylococcus aureus nasal carriage. Ph.D. Thesis. Rotterdam, The Netherlands: Erasmus University Medical Center.

143. Bogaert D, van Belkum A, Sluijter M, Luijendijk A, de Groot R, et al. (2004) Colonisation by Streptococcus pneumoniae and Staphylococcus aureus in healthy children. Lancet 363: 1871-1872.

144. Shinefield HR, Wilsey JD, Ribble JC, Boris M, Eichenwald HF, et al. (1966) Interactions of staphylococcal colonization. Influence of normal nasal flora and antimicrobials on inoculated Staphylococcus aureus strain 502A. Am J Dis Child 111: 11-21.

145. Iwase T, Uehara Y, Shinji H, Tajima A, Seo H, et al. (2010) Staphylococcus epidermidis Esp inhibits Staphylococcus aureus biofilm formation and nasal colonization. Nature 465: 346-349.

146. Regev-Yochay G, Dagan R, Raz M, Carmeli Y, Shainberg B, et al. (2004) Association between carriage of Streptococcus pneumoniae and Staphylococcus aureus in Children. Jama 292: 716-720.

147. van Belkum A, Melles DC, Nouwen J, van Leeuwen WB, van Wamel W, et al. (2009) Co-evolutionary aspects of human colonisation and infection by Staphylococcus aureus. Infect Genet Evol 9: 32-47.

148. Cole AM, Kim YH, Tahk S, Hong T, Weis P, et al. (2001) Calcitermin, a novel antimicrobial peptide isolated from human airway secretions. FEBS Lett 504: 5-10.

149. Schaffer AC, Solinga RM, Cocchiaro J, Portoles M, Kiser KB, et al. (2006) Immunization with Staphylococcus aureus clumping factor B, a major determinant in nasal carriage, reduces nasal colonization in a murine model. Infect Immun 74: 2145-2153.

150. Lindsay JA, Moore CE, Day NP, Peacock SJ, Witney AA, et al. (2006) Microarrays reveal that each of the ten dominant lineages of Staphylococcus aureus has a unique combination of surface-associated and regulatory genes. J Bacteriol 188: 669-676.

151. Becker K, Friedrich AW, Peters G, von Eiff C (2004) Systematic survey on the prevalence of genes coding for staphylococcal enterotoxins SElM, SElO, and SElN. Mol Nutr Food Res 48: 488-495.

152. Sivaraman K, Venkataraman N, Tsai J, Dewell S, Cole AM (2008) Genome sequencing and analysis reveals possible determinants of Staphylococcus aureus nasal carriage. BMC Genomics 9: 433.

153. Quinn GA, Tarwater PM, Cole AM (2009) Subversion of interleukin-1-mediated host defence by a nasal carrier strain of Staphylococcus aureus. Immunology 128: e222-229.

154. Kostenko V, Ceri H, Martinuzzi RJ (2007) Increased tolerance of Staphylococcus aureus to vancomycin in viscous media. FEMS Immunol Med Microbiol 51: 277-288.

155. Ross PL, Huang YN, Marchese JN, Williamson B, Parker K, et al. (2004) Multiplexed protein quantitation in Saccharomyces cerevisiae using amine-reactive isobaric tagging reagents. Mol Cell Proteomics 3: 1154-1169.

156. Forsgren A (1970) Significance of protein a production by staphylococci. Infect Immun 2: 672-673.

157. Dreisbach A, Hempel K, Buist G, Hecker M, Becher D, et al. Profiling the surfacome of Staphylococcus aureus. Proteomics 10: 3082-3096.

158. Brown RE, Jarvis KL, Hyland KJ (1989) Protein measurement using bicinchoninic acid: elimination of interfering substances. Anal Biochem 180: 136-139.

159. Smith PK, Krohn RI, Hermanson GT, Mallia AK, Gartner FH, et al. (1985) Measurement of protein using bicinchoninic acid. Anal Biochem 150: 76-85.

160. Kessler RJ, Fanestil DD (1986) Interference by lipids in the determination of protein using bicinchoninic acid. Anal Biochem 159: 138-142.

161. Wiechelman KJ, Braun RD, Fitzpatrick JD (1988) Investigation of the bicinchoninic acid protein assay: identification of the groups responsible for color formation. Anal Biochem 175: 231-237.

162. Zhu M, Dai S, McClung S, Yan X, Chen S (2009) Functional differentiation of Brassica napus guard cells and mesophyll cells revealed by comparative proteomics. Mol Cell Proteomics 8: 752-766.

163. Unwin RD, Pierce A, Watson RB, Sternberg DW, Whetton AD (2005) Quantitative proteomic analysis using isobaric protein tags enables rapid comparison of changes in transcript and protein levels in transformed cells. Mol Cell Proteomics 4: 924-935.

164. Shilov IV, Seymour SL, Patel AA, Loboda A, Tang WH, et al. (2007) The Paragon Algorithm, a next generation search engine that uses sequence temperature values and feature probabilities to identify peptides from tandem mass spectra. Mol Cell Proteomics 6: 1638-1655.

165. Griffiths SD, Burthem J, Unwin RD, Holyoake TL, Melo JV, et al. (2007) The use of isobaric tag peptide labeling (iTRAQ) and mass spectrometry to examine rare, primitive hematopoietic cells from patients with chronic myeloid leukemia. Mol Biotechnol 36: 81-89.

166. Donowitz M, Singh S, Salahuddin FF, Hogema BM, Chen Y, et al. (2007) Proteome of murine jejunal brush border membrane vesicles. J Proteome Res 6: 4068-4079.

167. Guo Y, Singleton PA, Rowshan A, Gucek M, Cole RN, et al. (2007) Quantitative proteomics analysis of human endothelial cell membrane rafts: evidence of MARCKS and MRP regulation in the sphingosine 1-phosphate-induced barrier enhancement. Mol Cell Proteomics 6: 689-696.

168. Kassie F, Anderson LB, Higgins L, Pan Y, Matise I, et al. (2008) Chemopreventive agents modulate the protein expression profile of 4-(methylnitrosamino)-1-(3-pyridyl)-1-butanone plus benzo[a]pyrene-induced lung tumors in A/J mice. Carcinogenesis 29: 610-619.

169. Graham RL, Sharma MK, Ternan NG, Weatherly DB, Tarleton RL, et al. (2007) A semi-quantitative GeLC-MS analysis of temporal proteome expression in the emerging nosocomial pathogen Ochrobactrum anthropi. Genome Biol 8: R110.

170. Martin B, Brenneman R, Becker KG, Gucek M, Cole RN, et al. (2008) iTRAQ analysis of complex proteome alterations in 3xTgAD Alzheimer's mice: understanding the interface between physiology and disease. PLoS One 3: e2750.

171. Keshamouni VG, Jagtap P, Michailidis G, Strahler JR, Kuick R, et al. (2009) Temporal quantitative proteomics by iTRAQ 2D-LC-MS/MS and corresponding mRNA expression analysis identify post-transcriptional modulation of actin-cytoskeleton regulators during TGF-beta-Induced epithelial-mesenchymal transition. J Proteome Res 8: 35-47.

172. Drummelsmith J, Winstall E, Bergeron MG, Poirier GG, Ouellette M (2007) Comparative proteomics analyses reveal a potential biomarker for the detection of vancomycin-intermediate Staphylococcus aureus strains. J Proteome Res 6: 4690-4702.

173. Foster TJ, Hook M (1998) Surface protein adhesins of Staphylococcus aureus. Trends Microbiol 6: 484-488.

174. Leski TA, Tomasz A (2005) Role of penicillin-binding protein 2 (PBP2) in the antibiotic susceptibility and cell wall cross-linking of Staphylococcus aureus: evidence for the cooperative functioning of PBP2, PBP4, and PBP2A. J Bacteriol 187: 1815-1824.

175. Katzif S, Danavall D, Bowers S, Balthazar JT, Shafer WM (2003) The major cold shock gene, cspA, is involved in the susceptibility of Staphylococcus aureus to an antimicrobial peptide of human cathepsin G. Infect Immun 71: 4304-4312.

176. Ravipaty S, Reilly JP Comprehensive characterization of methicillin-resistant Staphylococcus aureus subsp. aureus COL secretome by two-dimensional liquid chromatography and mass spectrometry. Mol Cell Proteomics 9: 1898-1919.

177. Kohler C, Wolff S, Albrecht D, Fuchs S, Becher D, et al. (2005) Proteome analyses of Staphylococcus aureus in growing and non-growing cells: a physiological approach. Int J Med Microbiol 295: 547-565.

178. Sibbald MJ, Ziebandt AK, Engelmann S, Hecker M, de Jong A, et al. (2006) Mapping the pathways to staphylococcal pathogenesis by comparative secretomics. Microbiol Mol Biol Rev 70: 755-788.

179. Hassan KA, Skurray RA, Brown MH (2007) Active export proteins mediating drug resistance in staphylococci. J Mol Microbiol Biotechnol 12: 180-196.

180. Clements MO, Foster SJ (1999) Stress resistance in Staphylococcus aureus. Trends Microbiol 7: 458-462.

181. Andre G, Leenhouts K, Hols P, Dufrene YF (2008) Detection and localization of single LysM-peptidoglycan interactions. J Bacteriol 190: 7079-7086.

182. Perego M, Glaser P, Minutello A, Strauch MA, Leopold K, et al. (1995) Incorporation of D-alanine into lipoteichoic acid and wall teichoic acid in Bacillus subtilis. Identification of genes and regulation. J Biol Chem 270: 15598-15606.

183. Hall-Stoodley L, Costerton JW, Stoodley P (2004) Bacterial biofilms: from the natural environment to infectious diseases. Nat Rev Microbiol 2: 95-108.

184. Hall-Stoodley L, Stoodley P (2009) Evolving concepts in biofilm infections. Cell Microbiol 11: 1034-1043.

185. Stewart PS, Costerton JW (2001) Antibiotic resistance of bacteria in biofilms. Lancet 358: 135-138.

186. Buist G, Steen A, Kok J, Kuipers OP (2008) LysM, a widely distributed protein motif for binding to (peptido)glycans. Mol Microbiol 68: 838-847.

187. Foster TJ (2009) Colonization and infection of the human host by staphylococci: adhesion, survival and immune evasion. Vet Dermatol 20: 456-470.

188. Rooijakkers SH, van Kessel KP, van Strijp JA (2005) Staphylococcal innate immune evasion. Trends Microbiol 13: 596-601.

189. Burlak C, Hammer CH, Robinson MA, Whitney AR, McGavin MJ, et al. (2007) Global analysis of community-associated methicillin-resistant Staphylococcus aureus exoproteins reveals molecules produced in vitro and during infection. Cell Microbiol 9: 1172-1190.

190. Burian M, Rautenberg M, Kohler T, Fritz M, Krismer B, et al. Temporal expression of adhesion factors and activity of global regulators during establishment of Staphylococcus aureus nasal colonization. J Infect Dis 201: 1414-1421.

191. Jones RC, Deck J, Edmondson RD, Hart ME (2008) Relative quantitative comparisons of the extracellular protein profiles of Staphylococcus aureus UAMS-1 and its sarA, agr, and sarA agr regulatory mutants using one-dimensional polyacrylamide gel electrophoresis and nanocapillary liquid chromatography coupled with tandem mass spectrometry. J Bacteriol 190: 5265-5278.

192. Peschel A, Otto M, Jack RW, Kalbacher H, Jung G, et al. (1999) Inactivation of the dlt operon in Staphylococcus aureus confers sensitivity to defensins, protegrins, and other antimicrobial peptides. J Biol Chem 274: 8405-8410.

193. Blumel P, Uecker W, Giesbrecht P (1979) Zero order kinetics of cell wall turnover in Staphylococcus aureus. Arch Microbiol 121: 103-110.

194. Pearce EJ, Sher A (1987) Mechanisms of immune evasion in schistosomiasis. Contrib Microbiol Immunol 8: 219-232.

195. Cole AM, Ganz T, Liese AM, Burdick MD, Liu L, et al. (2001) Cutting edge: IFN-inducible ELR- CXC chemokines display defensin-like antimicrobial activity. J Immunol 167: 623-627.

196. Yung SC, Parenti D, Keiser J, Murphy PM Host chemokines bind to Staphylococcus aureus and stimulate protein A release. J Biol Chem.

197. Rivinoja A, Hassinen A, Kokkonen N, Kauppila A, Kellokumpu S (2009) Elevated Golgi pH impairs terminal N-glycosylation by inducing mislocalization of Golgi glycosyltransferases. J Cell Physiol 220: 144-154.

198. Schmidt MA, Riley LW, Benz I (2003) Sweet new world: glycoproteins in bacterial pathogens. Trends Microbiol 11: 554-561.

199. Costerton JW, Stewart PS, Greenberg EP (1999) Bacterial biofilms: a common cause of persistent infections. Science 284: 1318-1322.

200. Boles BR, Horswill AR (2008) Agr-mediated dispersal of Staphylococcus aureus biofilms. PLoS Pathog 4: e1000052.

201. van Belkum A (2011) Novel Technology to study co-evolution of humans and Staphylococcus aureus: consequences for interpreting the biology of colonisation and infection. Adv Exp Med Biol 697: 273-288.

202. Jacobsson G, Colque-Navarro P, Gustafsson E, Andersson R, Mollby R (2010) Antibody responses in patients with invasive Staphylococcus aureus infections. Eur J Clin Microbiol Infect Dis 29: 715-725.

203. Muthukrishnan G, Lamers RP, Ellis A, Paramanandam V, Persaud AB, et al. (2013) Longitudinal genetic analyses of Staphylococcus aureus nasal carriage dynamics in a diverse population. BMC infectious diseases 13: 221.

204. Lamers RP, Stinnett JW, Muthukrishnan G, Parkinson CL, Cole AM Evolutionary analyses of Staphylococcus aureus identify genetic relationships between nasal carriage and clinical isolates. PLoS One 6: e16426.

205. Lamers RP, Eade CR, Waring AJ, Cole AL, Cole AM (2011) Characterization of the retrocyclin analogue RC-101 as a preventative of Staphylococcus aureus nasal colonization. Antimicrob Agents Chemother 55: 5338-5346.

206. Bai S, Yang T, Abbruscato TJ, Ahsan F (2008) Evaluation of human nasal RPMI 2650 cells grown at an air-liquid interface as a model for nasal drug transport studies. J Pharm Sci 97: 1165-1178.

207. Yao J, Zhong J, Fang Y, Geisinger E, Novick RP, et al. (2006) Use of targetrons to disrupt essential and nonessential genes in Staphylococcus aureus reveals temperature sensitivity of Ll.LtrB group II intron splicing. Rna 12: 1271-1281.

208. Monk IR, Shah IM, Xu M, Tan MW, Foster TJ (2012) Transforming the untransformable: application of direct transformation to manipulate genetically Staphylococcus aureus and Staphylococcus epidermidis. MBio 3.

209. Shinji H, Yosizawa Y, Tajima A, Iwase T, Sugimoto S, et al. (2011) Role of fibronectin-binding proteins A and B in in vitro cellular infections and in vivo septic infections by Staphylococcus aureus. Infect Immun 79: 2215-2223.

210. Shinji H, Sakurada J, Seki K, Murai M, Masuda S (1998) Different effects of fibronectin on the phagocytosis of Staphylococcus aureus and coagulase-negative staphylococci by murine peritoneal macrophages. Microbiol Immunol 42: 851-861.

211. Eade CR, Diaz C, Wood MP, Anastos K, Patterson BK, et al. (2012) Identification and characterization of bacterial vaginosis-associated pathogens using a comprehensive cervical-vaginal epithelial coculture assay. PLoS One 7: e50106.

212. Cole AM, Wu M, Kim YH, Ganz T (2000) Microanalysis of antimicrobial properties of human fluids. Journal of microbiological methods 41: 135-143.

213. Falugi F, Kim HK, Missiakas DM, Schneewind O (2013) Role of Protein A in the Evasion of Host Adaptive Immune Responses by Staphylococcus aureus. MBio 4.

214. Garofalo A, Giai C, Lattar S, Gardella N, Mollerach M, et al. (2012) The length of the Staphylococcus aureus protein A polymorphic region regulates inflammation: impact on acute and chronic infection. J Infect Dis 206: 81-90.

215. Miller LS, O'Connell RM, Gutierrez MA, Pietras EM, Shahangian A, et al. (2006) MyD88 mediates neutrophil recruitment initiated by IL-1R but not TLR2 activation in immunity against Staphylococcus aureus. Immunity 24: 79-91.

216. Kolls JK, McCray PB, Jr., Chan YR (2008) Cytokine-mediated regulation of antimicrobial proteins. Nat Rev Immunol 8: 829-835.

217. McLoughlin RM, Lee JC, Kasper DL, Tzianabos AO (2008) IFN-gamma regulated chemokine production determines the outcome of Staphylococcus aureus infection. J Immunol 181: 1323-1332.

218. Dubin PJ, Kolls JK (2008) Th17 cytokines and mucosal immunity. Immunol Rev 226: 160-171.

219. Ong PY, Ohtake T, Brandt C, Strickland I, Boguniewicz M, et al. (2002) Endogenous antimicrobial peptides and skin infections in atopic dermatitis. N Engl J Med 347: 1151-1160.

220. Askarian F, Sangvik M, Hanssen AM, Snipen L, Sollid JU, et al. (2013) Staphylococcus aureus nasal isolates from healthy individuals cause highly variable host cell responses in vitro: The Tromso Staph and Skin Study. Pathog Dis.

221. Perl TM, Cullen JJ, Wenzel RP, Zimmerman MB, Pfaller MA, et al. (2002) Intranasal mupirocin to prevent postoperative Staphylococcus aureus infections. N Engl J Med 346: 1871-1877.

222. Kalmeijer MD, Coertjens H, van Nieuwland-Bollen PM, Bogaers-Hofman D, de Baere GA, et al. (2002) Surgical site infections in orthopedic surgery: the effect of mupirocin nasal ointment in a double-blind, randomized, placebo-controlled study. Clinical infectious diseases : an official publication of the Infectious Diseases Society of America 35: 353-358.

223. Caffrey AR, Quilliam BJ, LaPlante KL (2010) Risk factors associated with mupirocin resistance in meticillin-resistant Staphylococcus aureus. J Hosp Infect 76: 206-210.

224. Fei Y, Wang W, Kwiecinski J, Josefsson E, Pullerits R, et al. (2011) The combination of a tumor necrosis factor inhibitor and antibiotic alleviates staphylococcal arthritis and sepsis in mice. J Infect Dis 204: 348-357.

225. Gaar E, Naziri W, Cheadle WG, Pietsch JD, Johnson M, et al. (1994) Improved survival in simulated surgical infection with combined cytokine, antibiotic and immunostimulant therapy. Br J Surg 81: 1309-1311.

226. van den Berg S, van Wamel WJ, Snijders SV, Ouwerling B, de Vogel CP, et al. (2011) Rhesus macaques (Macaca mulatta) are natural hosts of specific Staphylococcus aureus lineages. PLoS One 6: e26170.